Chromatographic Selectivity and Hyper-Crosslinked Liquid Chromatography Stationary Phases

A DISSERTATION
SUBMITTED TO THE FACULTY OF THE GRADUATE SCHOOL
OF THE UNIVERSITY OF MINNESOTA
BY

Yu Zhang

IN PARTIAL FULFILLMENT OF THE REQUIREMENTS
FOR THE DEGREE OF
DOCTOR OF PHILOSOPHY

Professor Peter W. Carr, Adviser
Professor Philippe Buhlmann, Co-Adviser

December, 2009

ACKNOWLEDGEMENTS

I would like to express my deepest appreciation to my advisors and mentors, Professor Peter W. Carr and Professor Philippe Buhlmann. I thank Pete for his tireless guidance, support and encouragement throughout the course of my Ph.D. study. His passion about chemistry and dedication to research has been a tremendous inspiration for me as well as many others. More importantly, He is compassionate and considerate for students; he is always willing to talk with us about science as well as life. I felt blessed to have him as my advisor and mentor. I would also like to thank Phil, who has generously given his time and expertise to better my work. His prolific knowledge and guidance have been essential to my success. I learned a great deal from him and the Buhlmann group.

I am also grateful for the friendship, helpful discussions and enjoyable working environment provided by all the former and present Carr group members: Dr. Hao Luo, Dr. Xiaoli Wang, Dr. Dwight Stoll, Dr. Lianjia Ma, Dr. Brian Trammell, Dr. Adam Schellinger, Dr. Jun Dai, Dr. Xiaoping Li, Dr. Wenzhe Fan, Dr. Yuan Huang, Dr. Haiwei Gu, Dr. Ayse Beyaz and Chang-Yub Paek. I specially thank Dr. Hao Luo, Chang-Yub Paek, Dr. Xiaoli Wang, Dr. Yuan Huang and Dr. Dwight Stoll who have contributed to the progress of my work in numerous ways.

Lastly, I would like to take this opportunity to thank my graduate committee members Dr. Mike Bowser and Dr. Alon McCormick for their support and useful feedback.

DEDICATION

I dedicate this thesis to my most loving parents, Lemin Zhang and Ping Zhou, for their tremendous love, support and sacrifice they have made for me over the years. They always believe in me, encourage me to pursue my dreams, and more importantly unconditionally love and support me during the highs and lows through the college, graduate school and forever. I honestly feel that I have the best parents in the world. I just want to say: I love you both very much! I miss you so much! As usual, I will do my best to make you proud of me.

I also dedicate this thesis to my best friend and soul mate, Hai Bo Ma, for his endless love, support and encouragement. I feel so fortunate to be able to go through the most important journey of graduate school with him by my side. Without him, I could not achieve what I have accomplished.

ABSTRACT

The development of new stationary phases have always been of great interest in HPLC and has become increasingly important in recent years mainly driven by rapidly evolving industrial need as well as the quest for higher throughput HPLC analyses for better resolution and higher sensitivity. In this thesis, we developed a family of silica based RPLC stationary phases based on a novel *hyper-crosslinked* (HC) platform, prepared through a multi-layer, two-dimensional, orthogonal polymerization reaction. The resulting stationary phases showed better stability, higher efficiency and novel selectivities, which are the three essentials properties of the stationary phase that users are looking for and column developers strive to achieve.

We first studied the synthesis and full characterization of a novel mixed-mode reversed-phase/*weak cation exchange* (RP/WCE) phase by introducing a small amount of carboxylate functionality into a hydrophobic hyper-crosslinked (HC) platform. The phase thus prepared shows a mixed-mode retention mechanism, allowing for both neutral organic compounds and charged bases to be separated simultaneously on the same phase under the same conditions. More importantly, the inherent weak cation exchange groups allow simple mobile phases to be used thereby avoiding the mass spectrometric ionization suppression problems concomitant to the use of non-volatile additives such as strong amine modifiers (e.g. triethylamine) to elute basic solutes from the strong cation exchange phases or ion pairing reagents (e.g. trifluoroacetic acid, ClO_4^-) to retain these solutes on conventional ODS phases. We next studied the development of a highly hydrophilic HC-OH phase prepared by hydrolyzing residual benzyl chloride groups on

the hydrophobic platform. This phase is potentially useful as a candidate for use as the first dimension phase of comprehensive two-dimensional LC where column stability and low retentivity are greatly desired. We also developed a novel graphical method, the phase selectivity triangle plots, for visualizing the effect of surface chemistry (e.g. C18 vs. Phenyl vs. Fluoro) on stationary phase selectivities. The use of the new plots assists the selection of appropriate stationary phases for method development in both isocratic and gradient elution.

TABLE OF CONTENTS

LIST OF FIGURES

LIST OF TABLES

PREFACE

Part of Chapter 4 and Chapter 5 have been published in the manuscripts cited below:

(1) Yu Zhang and Peter W. Carr, "A Visual Approach to Stationary Phase Selectivity Classification Based on the Snyder-Dolan Hydrophobic-Subtraction Model", *Journal of Chromatography A*, **2009**, *1216*, 6685-6694.

(2) Yu Zhang, Xiaoli Wang, Partha Mukherjee and Patrik Petersson, "Critical Comparison of Performances of Superficially Porous Particles and Sub-2 μm Particles under Optimized Ultra-high Pressure Conditions", *Journal of Chromatography A*, **2009**, *1216*, 4597-4605.

Chapter 1

Introduction to Stationary Phase in Reversed-Phased Liquid Chromatography

1.1. INTRODUCTION

The development of stationary phases over the past fifty years has had a tremendous impact on the way much of chromatography is done today. The existence of these column packings makes it possible to tackle more difficult separation problems or to improve the overall productivity and sample throughput. For example, naturally occurring mixtures, especially in the field of bio-chemical analysis, typically contain hundreds of components present over a wide range of concentrations. Analysis of these complex samples would not have been possible without the development of microparticulate silicas of well defined particle shape and size, surface area, porosity, and pore size[1-3]. The applications of such columns led to enormous improvement in chromatographic resolution and analysis speed, which started modern/high performance liquid chromatography (HPLC). The most remarkable progress, however, was the development and manufacture of chemically bonded silicas, in particular those with hydrophobic groups, called reversed phase (RP)[3,4]. It allows the separation of non-polar, polar non-ionic, and ionic analytes. The result of such stationary phases was the successful transformation of HPLC into one of the most powerful analytical techniques in many fields including chemical, bio-processing and pharmaceutical industry.

Even though tremendous progresses have been achieved, there is still need for new stationary phases as driven by rapidly evolving industry and concomitantly quest for

HPLC analyses of higher throughput, better resolution and higher sensitivity. Particularly, *better stability*, *higher efficiency* and *novel selectivity* are the three essentials that users are looking for and column developers strive to improve with new stationary phases. The objective of this work is to develop a new family of RPLC stationary phases based on novel aromatic polymer-coated silica particles, aimed at two of the most important characteristics: *stability* and *novel selectivity*. First, the importance of stationary phase stability and the improvements made over the last two decades is reviewed. We then introduce the concept of the hyper-crosslinked platform and its superior stability and efficiency over conventional silica based bonded phases. Following that, a polar embedded phase HC-OH and a hydrophobic weak cation exchange phase HC-COOH were prepared based on this novel platform by attaching various organic moieties onto silica's surface. Thus the significance of stationary phase selectivity that inspired our work here is discussed next. In addition, we will also introduce major chemical classes of common reversed phases and strategies used to characterize their phase selectivity. Finally, the scope of this dissertation is presented.

1.2. STATIONARY PHASE STABILITY IN LIQIUID CHROMATOGRAPHY

As one of the most popular separation modes in pharmaceutical, environment and biotechnology industries, liquid chromatography (LC) has been used extensively for sample identification, method development and the establishment of a reliable database for fast screening. As a result, the stability of stationary phases has become extremely important. In particular, once the desired separation is achieved, column characteristics

should remain unchanged for as long as possible so that we can obtain reproducible retention factors and peak shapes from run to run under the same separation conditions. Thus it is clear that a physically and chemically stable column is essential in developing a rugged HPLC method.

By far, organosilane-bonded silica phases are the most commonly used stationary phase in Reversed Phase Liquid Chromatography (RPLC). They are typically prepared by attaching a monofunctional silane such as dimethyl octadecylchlorosilane (ODS or C_{18}) to silica surface's; the resulted structure is shown in Figure 1.1. This type of reactions is widely used by column manufactures and often referred to as "conventional silanization". Stationary phases prepared by this method usually have excellent kinetic properties (mass transfer) and highly reproducible properties (retention, efficiency) from column to column and batch to batch [5-8]. Thus they have been used extensively in RPLC separations and often treated as the standards against which all improvements in column technology are measured.

One major limitation of these mono-functional conventional phases is that they are chemically stable only when the pH of the mobile phase is between about 2 and 8. Recently, McCalley has stated that the long term stability is even limited to pH values between 3 and 7[9,10]. This is mainly due to the limited accessibility of surface silanol groups during the conventional silanization; at best only 40-50% of the silanols reacted with organosilane, [6,11], leaving a significant fraction of residual silanol groups on silica surface. Consequently, there are three major problems (see Figure 1.2) associated with the application of conventional bonded phases:

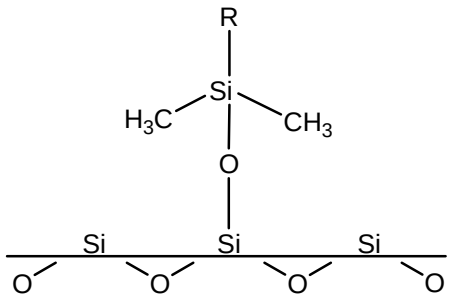

Figure 1.1 General structure of a conventional, monomeric organosilane bonded to silica

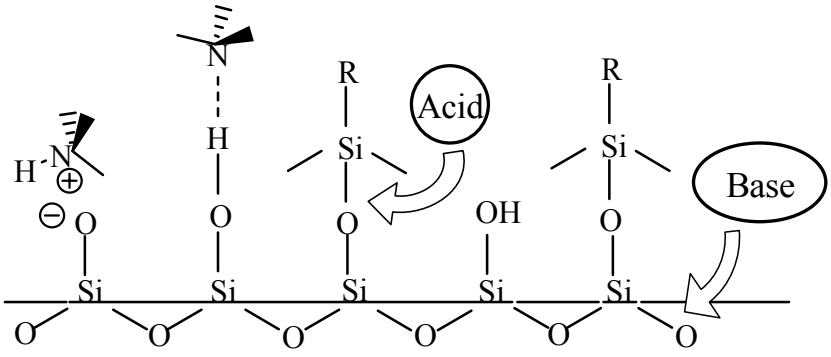

Figure 1.2 Problems in monofunctional stationary phase

1) Instability at high pH (>8): Exposed unshielded silica areas are easily attacked by base, which causes the rapid dissolution of silica, developing a high backpressure and eventually collapse of the column bed

2) Instability at low pH (<2): Easy access to the siloxane bond of the silane facilitates the hydrolysis of the bonded phase, resulting in continuous loss of the bonded phases and concomitant drifting in retention [12]..

3) Poor HPLC performance characteristics of basic analytes: acidic silanols strongly interact with basic analytes through electrostatic forces or H-bonding [11,13,14], often resulting in severe peak tailing and poor separation efficiency.

It should be stressed that the rate of degradation is also strongly influenced by the mobile phases used (i.e. % organic, buffer) and the operating temperature [15-17]. For example, the data in Fig. 3 [15] shows the effect of buffer type and concentration on the stability of Zorbax Rx-C18 column measured at two temperatures. It is clear that at pH = 7, phosphate buffer is much more aggressive than organic-based glycine buffers; In addition, a small temperature increase from 40 °C and 60 °C cause a dramatic increase in the rate of column deterioration, even at much lower buffer concentrations. The use of elevated temperature can also accentuate the hydrolysis of bonded phase at low pHs. Thus, operating at temperature lower than 40 °C is highly recommended, especially at "extreme" pHs or when using particularly aggressive buffers[15,18]

The simplest solution of the stability problem is to avoid using both mobile phases with pH values outside the range of 2-8 and elevated temperatures. However, this severely limits the use of these two parameters as variables for optimizing separations of many classes of solutes. For example, the RPLC separation of silanophilic solutes such as

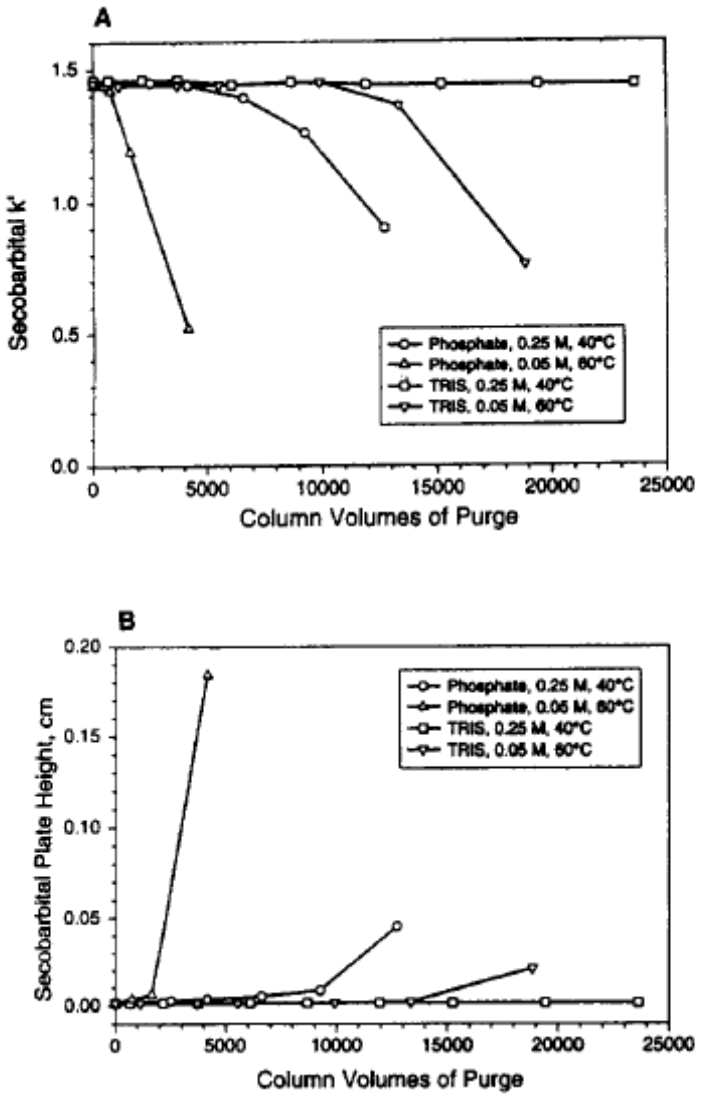

Figure 1.3 Buffer type, concentration and temperature effects: Columns: Zorbax Rx-C18, 15×0.46 cm; purge: 20% methanol-80% sodium phosphate/Tris buffer (pHs^{w} 8) at 40°C / 60°C, respectively. F=1.0 ml/min; chromatographic test: 40% acetonitrile-60% TRIS, 0.0l M, 40°C, 1.0 ml/min; solute: secobarbital. (A) k' values. (B) Plate height values. (Adapted from ref. [15])

basic drugs and many biologically solutes (e.g. proteins, peptides) often benefits from the use of either highly acidic or highly basic eluents [19]. Lowering the pH can suppress deleterious interactions between positive charged solutes and the surface by protonating the surface silanol groups. Therefore, greatly improved peak shapes and efficiencies can be achieved for the separation of small organic bases, while the enhanced solubility and recovery can be obtained for the larger bi-molecules such as proteins and peptides. Conversely, raising mobile phase pH can also "turn off" these electrostatic interactions by deprotonating the solutes, leading to significant improvement in both peak shape and efficiency. Meanwhile, temperature is another important variable and has been proved to be very powerful for optimizing selectivity in thermally tuned tandem column chromatography [20-23]. Perhaps more importantly, the use of high temperature can decrease the mobile phase viscosity and increase analyte diffusion. The reduced backpressure and improved mass transfer resulting from the elevated temperature can then allow one to achieve fast analysis without compromising separation efficiency[24,25]. A good example of the Ultra Fast High Temperature LC (UFHTLC) was the successful separation of maize extracts by comprehensive two-dimensional LC (2D-LC)[26], where a record high peak capacity of over 2000 in 30 minutes and rates of peak capacity production of nearly 1 peak/sec have been achieved mainly by the use of the high temperatures (100- 150 ^{o}C), which is the key to speed up the second dimension LC to do a separation in less than 30 seconds for a full gradient elution run. In general, there are many advantages to the use of highly acidic (pH < 2) or highly basic eluent (pH > 8) and elevated temperatures (> 50°C). These are summarized in Fig. 4 and the details can be found in the literatures [27,28].

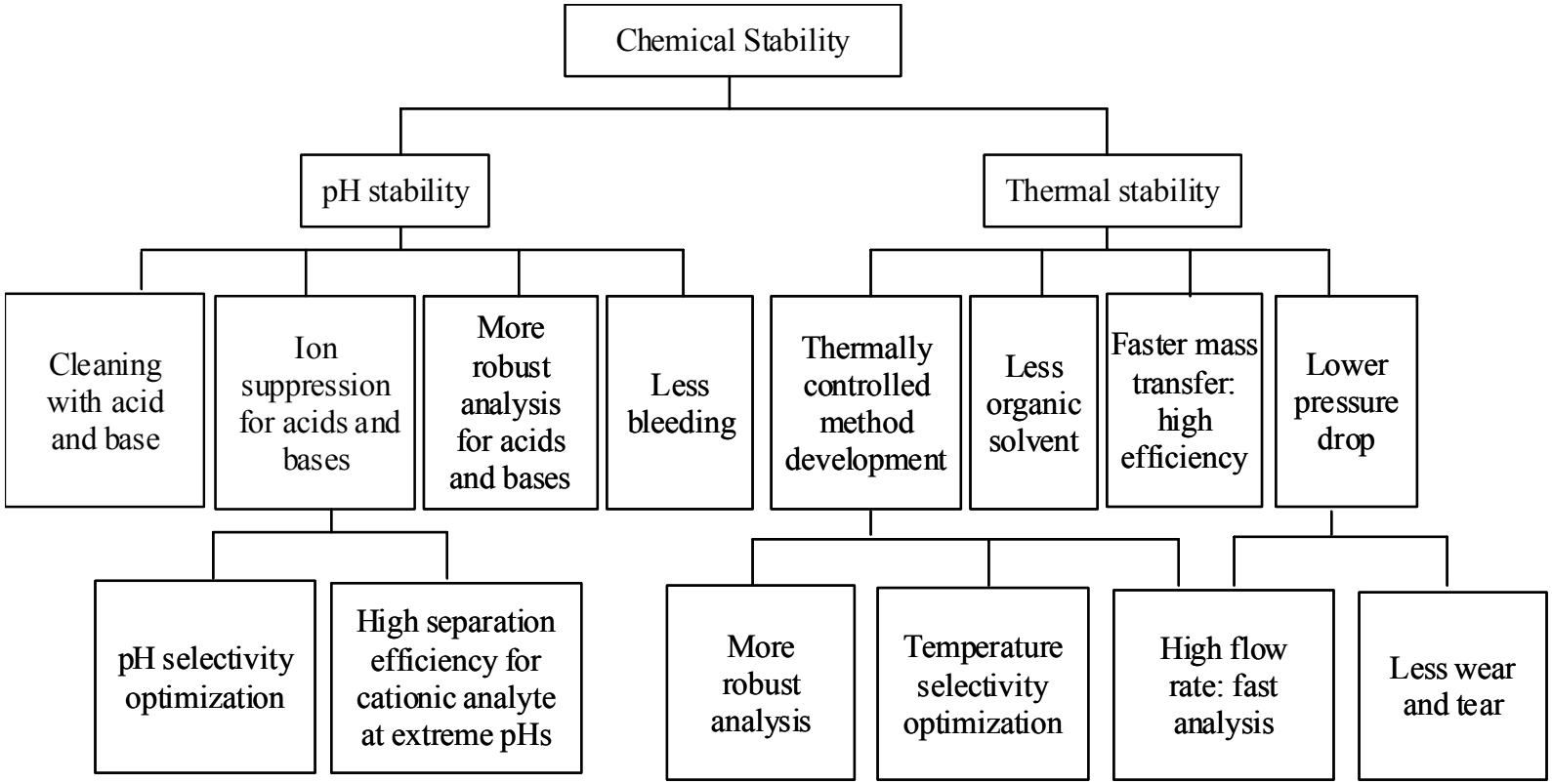

Figure 1.4 Summary of the advantages of highly stable packings in HPLC (Adapted from reference [27,28]).

1.3. GENERAL METHODS TO IMPROVE ACID STABILITY OF SILICA-BASED STATIONARY PHASE FOR RPLC

Over the years, extensive work [6,29-42] has been done to enhance chemical stability of silica based stationary phases. Since the primary focus of this study is to improve the acid stability, the most prominent approaches to extend column lifetime at low pH conditions and their advantages and disadvantages are summarized in Table 1.1. In general, these methods can be categorized into three strategies: 1) to better shield the underlying siloxane bond from hydrolysis by steric protection, such as the use of bulky silane (i.e. C18 vs. C8 vs. C4[29], or isobutyl side groups[30,31]) or by coating silica with polymers (i.e. self assemble monolayer[32-36]); 2) to decrease the rate of phase loss by formation of multiple bonds between the stationary phase and the silica substrates[6,30,35,37]; 3) to change the chemistry of the surface bonding by replacing the surface Si-O-Si bonds with chemically more stable Si-C bonds[38,39], or use pH inert materials such as metal oxides [40-42] and polymers instead of silica[19,43]. As these efforts have been comprehensively studied and compared in several excellent books and reviews [8,19,28], we will not elaborate them in detail but rather focus on two of the approaches most relevant to our work in the following sections.

1.3.1. Polymer Coated Phases

One of the strategies to improve the low pH stability of silica based stationary phase is to coat the silica substrate with an acid-inert polymers. The extensive crosslinked polymer coatings can then shield the surface of the support from interactions with aggressive eluents, which provide these types of materials with greatly enhanced pH stability and decreased silanophilicity compared to the conventional monomeric phases

[44]. As a result, many polymer coated stationary phases were developed some years ago as packing materials for RPLC [2,45,46].

In this area, styrene-divnylbenzene copolymers coated silica particles were first introduced by Horvath and Lispsky in 1966[45]. After polymerizing a mixture of styrene and divinylbenzene on the surface of silica, a completely insoluble cross-linked polymer layer is formed with a thickness of 1-2 μm [44]. For this type of phase, a serious decrease in specific surface area and specific pore volume were observed. Further, the phase shows significantly lower mass-transfer kinetics which is due to "pore blockage" resulted from the bulk polymer in the pores [44].

In 1973, a novel "chemical binding" approach was developed by pretreating the silica surface with unsaturated reagent (e.g. vinyltrichlorosilanes), and subsequent polymerizing the surface monomers [46]. Stationary phases prepared in this way have polymer layers chemically bound to the surface; after synthesis, the non-bonded polymers in the pores have to be removed by extensive extraction. However, for this type of stationary phases, even after thorough extraction, a large amount of polymers still remain to cause pore blockage and thus slow intra-particle mass transfer of analytes [44].

In 1991, Schomburg et al. [2] developed one type of silica stationary phases coated with physically adsorbed polymer. The procedure involves the fixation of the polymer layer by evaporation of the solvent from a polymer solution in the presence of the support. This technique has also been used by Carr et al. to produced polymer coated zirconia particles[47-52]. It turns out that these type of stationary phases have inhomogeneous distribution of polymers on the surface of the substrate[44]. In addition, the efficiency of mass transfer resistance in the "film" of polymeric stationary phase is

strongly dependent on the amount of polymer loaded [47,52]. Serious pore blockage could happen with excess loading of these organic moieties [47,52].

In general, great enhanced acid stability has generally been achieved for polymer coated stationary phase. However, one of the major limitations associated with this type of stationary phase is clearly slow mass transfer kinetics. Due to uncontrolled polymerization, either thick polymer layers on the surface [44,53] or the undesirable polymer accumulation in the micropores [44,47,53] can happen during the modifications; both lead to the restricted pore accessibility and thus slow intraparticle mass transfer of analytes.

1.3.2. Steric Protection

So far the most successful approach to improve the low pH stability of silica based stationary phase is to use the "sterically protected" silanes developed by Kirkland [30,31,54]. The general structure of a sterically protected silane is shown in Figure 1.5. With two bulky isopropyl or isobutyl side groups, this type of silane can provide significant steric protection to the siloxane bond on the silica surface against acid hydrolysis even under low pH (1% trifluoroacetic acid, T = 90℃, pH = 0.9)[19]. More importantly, column efficiency, reproducibility, and selectivity are equivalent to those of conventional monofunctional silane bonded-phases. So they can be routinely used at ambient and slightly super-ambient temperature at pH = 1 for thousands of column volumes without significant loss in bonded phase[55]. Because of the superior performance in terms of both stability and efficiency, the sterically protected stationary phases have been widely used in RPLC separations and were chosen as the standard in our study against which hyper-crosslinked phases were compared.

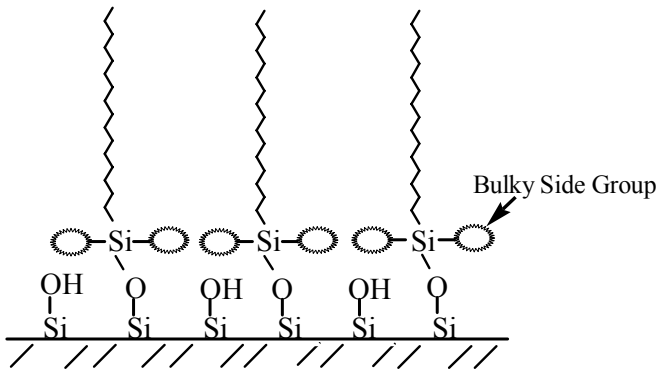

Figure 1.5 Silica sterically protected by silane with bulky side groups

Table 1.1 General Methods to Improve Acid Stability of Silica-Based Stationary Phases for RPLC

Strategies	Chemistry	Key advantage(s)	Major Limitation(s)	References
Steric protection	Silanes with long alkyl chain (e.g. C_8 vs. C_{18})	Reproducible synthesis, good mass transfer kinetics ease of modification	insufficient stability especially at elevated temperatures	[29]
	Silanes with bulky side groups (e.g. isopropyl vs. isobutyl)	Reproducible synthesis, greatly enhanced pH stability, good mass transfer kinetics, ease of modification		[30,31]
	Polymer coating on silica surface (e.g. styrene-divnylbenzene, vinyltrichlorosilanes)	Greatly enhanced pH stability, decreased silanolphilicity	Inferior mass transfer due to pore blockage from uncontrolled polymerization	[2,45,46]
Multivalent	Bi-functional(CH_3RSiX_2), tri-functional ($RSiX_3$) organosilanes (e.g. X = Cl, OR)	Greatly enhanced pH stability	High silanolphilicity induced by a large number of residual silanol groups, inferior mass transfer due to pore blockage from oligomers.	[46]
	Self assembled monolayer (SAM) (e.g. octadecyltrichlorosilane, methyltrichlorosilane)	Greatly enhanced pH stability	High silanolphilicity induced by a large number of residual silanol groups	[32-36]
	Multi-dentate (e.g. a bidentate C_{18}/C_{18} silane with a propylene bridge)	Reproducible synthesis, greatly enhanced pH stability, good mass transfer kinetics		[6,30,35,37]
Bonding chemistry	Si-C	Greatly enhanced pH stability, good mass transfer kinetics	Multi-step of synthesis, residual Si-H groups can limit the application of this phase at	[38,39]

			intermediate and high pH	
	Metal oxide vs. Silica (e.g. ZrO_2)	Superb pH stability (pH 1~14), good mass transfer kinetics	More difficult surface modification, complex surface chemistry, limited range of commercially available stationary phase-functionality	[40-42]
	Polymer vs. silica (e.g. polystyrene (PRP))	Superb pH stability (pH 1~14)	Inferior separation efficiency, slow equilibration upon a change in solvent due to polymer swelling	[19,43]

1.3.3. HYPER-CROSSLINKED PLATFORM

Recently, a novel hyper-crosslinked silica based platform was developed in our lab [17,56-58]and the structure is shown in Figure 1.6. In particular, orthogonal polymerization reactions are used to prepare a *very thin layer* of hyper-crosslinked (HC) aromatic network that is entirely confined to the silica surface. Outstanding stability has been achieved due to the formation of extensively *networked* polymers. At the same time, the excellent mass transfer properties of monomeric bonded phases were preserved and none of the adverse kinetic effects [17,56-58] of depositing a polymer have been observed. The superior stability and efficiency afforded by this novel hyper-crosslinked platform over conventional silica based stationary phases are discussed in detailed below. It is also worth notice that Davankov et al. used similar chemistry to synthesize hyper-crosslinked divinylbenzene-styrene copolymers with good mechanic strength for solid phase extraction, inverse size exclusion chromatography and ion-exchange chromatography [59]

1.3.3.1. Extensive crosslinked polymer network

The hyper-crosslinked platform is prepared by using monomeric silanization and "orthogonal (see next section)" Friedel-Crafts reactions [17,57]. A conventional monolayer of silane is first formed by covalently bonding dimethyl-(p-chloromethylphenylethyl) chlorosilane (DM-CMPES) to the silica surface. Then by reacting the surface benzyl chloride groups with first a multi-valent aromatic reagent (e.g. styrene heptamer) and secondly with a bi-functional alkylation reagent (e.g. chloro-methyl-methylether(CMME)), a hyper-crosslinked network is formed on the silica surface.

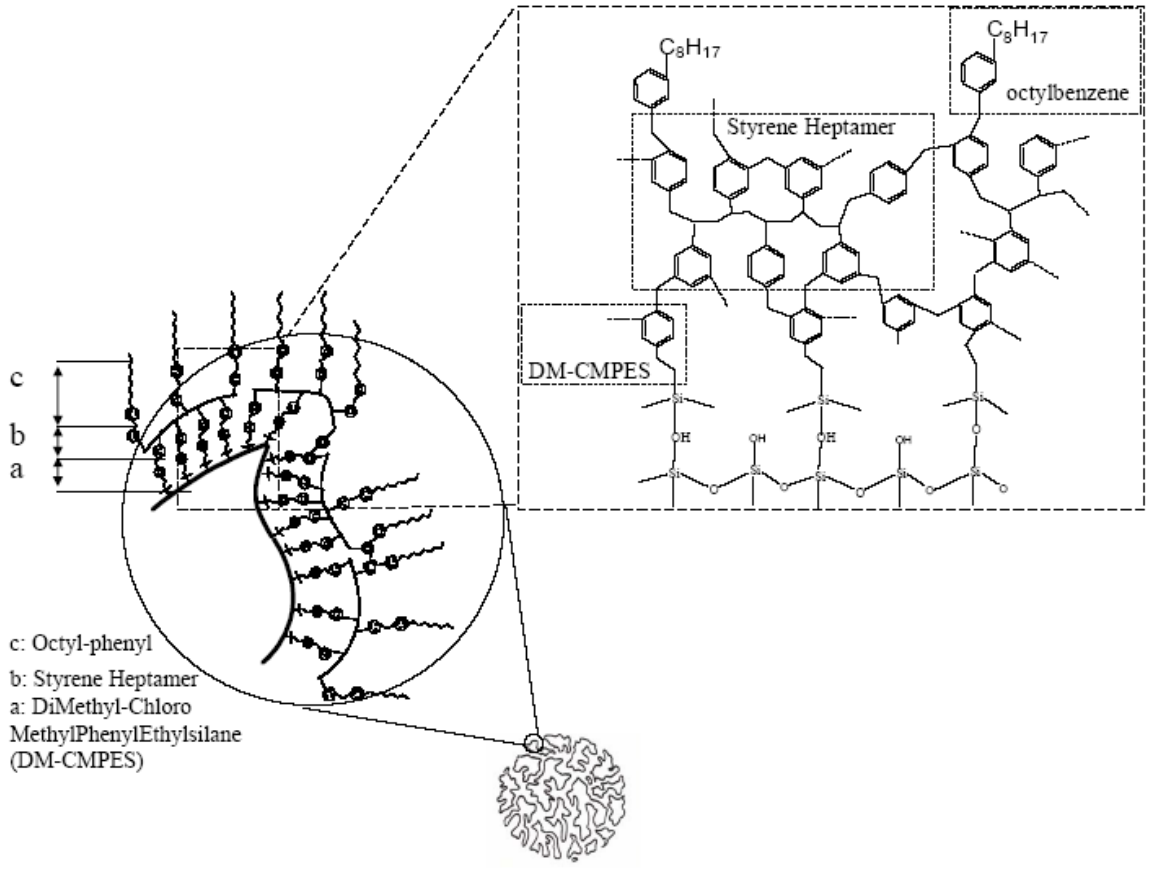

Figure 1.6 Chemical structure of a particle coated with an HC-C8 phase (Adapted from reference [27]).

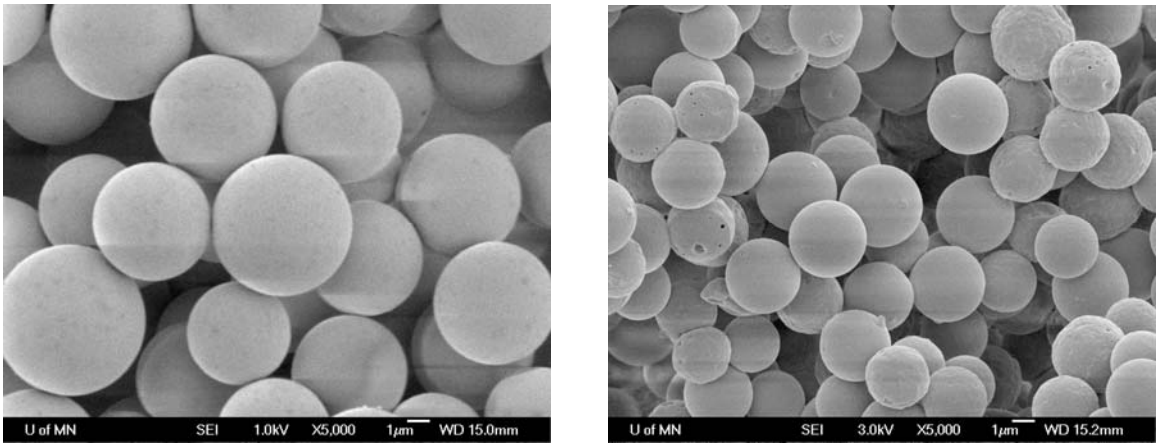

A B

Figure 1.7 SEM images of the HC-C8-HiChrom phases before and after removal of the silica substrate by HF digestion.
A. The HC-C8-HiChrom coated silica particles before HF treatment.
B. The HC-C8-HiChrom coated silica particles after HF removal of the silica substrate (Adapted from ref.[57]).

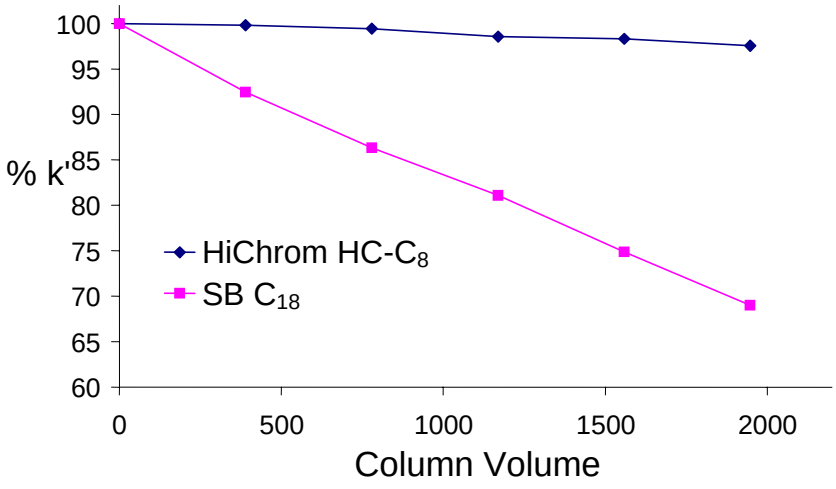

Figure 1.8 Dynamic acid stability comparison of sterically protected C18 phase and Hyper-Crosslinked stationary phase. Columns: 3.3×0.21 cm; Eluent:50/50 ACN/H2O with 0.1%TFA; T = 150℃; Flow Rate = 0.5 ml/min; Solute = Hexanodecanophenone (Adapted from ref. [57]).

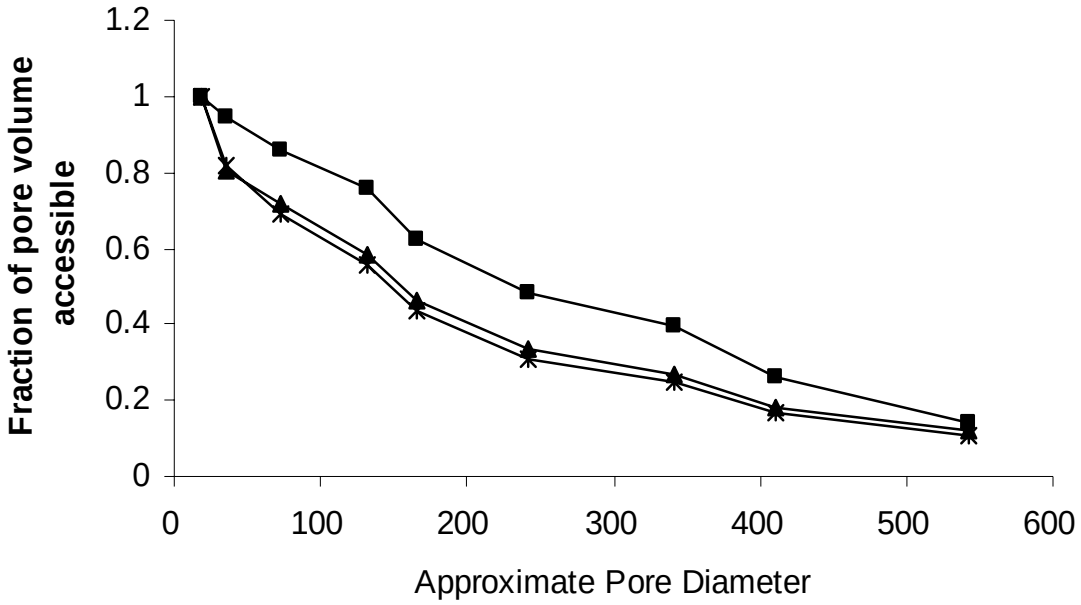

Figure 1.9 Pore accessibility study by inverse size exclusion chromatography. Mobile phase: 100% THF; T= 40 ºC; F = 1.0 mL/min, λ = 254 nm. ■ Bare HiChrom silica; ▲ Ace C18; * HC-C8-HiChrom (Adapted from ref. [57]).

The formation of a polymer network on the interior surface of the silica particle was verified by SEM of the coated silica particles before and after removal of the silica skeleton by exhaustive dissolution of the silica substrate by treatment with hydrofluoric acid [56,57]. Since silica can be totally dissolved in hydrofluoric acid, there was nothing left when the bare silica was treated. However, the result is clearly different for the hyper-crosslinked particles as indicated by the residual micro-sphere of polymer beads shown in Figure 1.7. This is because, even after the silica substrate was fully removed by HF digestion, the polymer network remains intact due to the extensive crosslinking and network formation. These results confirmed the formation of hyper-crosslinked network polymers on silica surface. The existence of such a network can prevent phase loss even under very aggressive conditions [56,57]; As a result, when the acid stability of the stationary phase developed based on HC platform (HC-C_8) was challenged by 5% trifluoroacetic acid (pH =0.5) at 150 °C, the HC phase showed excellent acid stability as indicated by the minimum drifting in retention, whereas the decrease of retention is clearly more rapidly on the sterically protected C_{18}, one of the best acid stable commercial phases (see Figure 1.8).

1.3.3.2. Surface confined orthogonal chemistry

It is very important to point out that, the improvement in acid stability was not achieved at the price of losing separation efficiency. As discussed above, a major problem of many polymer coated stationary phases is the slow mass transfer kinetics due to the pore blockage caused by uncontrolled polymerization [8,47,53]. However, during the hyper-crosslinking modification of silica particles, the two sequential F-C coupling reactions were carefully designed so that all polymerization processes are well confined

on surface. Consequently, the excellent mass transfer properties of monomeric bonded phases were preserved and none of the adverse kinetic effects [56,57] of depositing a polymer have been observed.

This was confirmed by inverse size exclusion chromatography (ISEC), where the mesopore structure of the hyper-crosslinked stationary phase were tested and compared to a monomeric bonded ACE C_{18} phase. As shown in Figure 1.9, the pore accessibility of the hyper-crosslinked phase (HC-C_8) is almost the same as the ACE C_{18} phase. Both materials are built on the same silica provided by HiChrom. This indicates that there is no or little pore blockage during the hyper-crosslinking process [56,57]. As a result, previous work from this laboratory demonstrated that the separation efficiency of both neutral and small basic analytes on this type of newly developed phase was comparable or even better than a number of very high quality mono-functional conventional phases [56,57]. Overall, the superior stability and efficiency of this hyper-crosslinked platform over conventional silica based stationary phases make it a nearly ideal candidate for use as platform to develop new stationary phases.

All the techniques we discussed above focus on the optimization of stability. There is another essential characteristic of stationary phase which is critical in terms of separation power in RPLC: selectivity. An understanding of this concept is crucial to achieve the best separation performance in method development. Thus the concept and the significance of selectivity will be reviewed in the following sections.

1.4. CONCEPTS OF RESOLUTION AND SELECTIVITY

The ultimate goal of any separation is to achieve acceptable resolution (Rs) in a reasonable time. As the most essential metric of separation power in chromatography, Rs in HPLC can be expressed in terms of three parameters (N, α, and k').

$$R_s = \frac{\sqrt{N}}{4}\frac{\alpha\text{-}1}{\alpha}\frac{k'}{k'+1} \qquad (1.1)$$

N: the number of theoretical plates

k': retention factor, which is determined by distribution coefficient K and the phase ratio β ($k' \equiv K\beta$)

α: selectivity factor, defined as the ratio of the retention factors of two adjacent peaks ($\alpha \equiv \frac{k'_2}{k'_1}$)

The three parameters are treated as independent variables to illustrate their influence on resolution in Figure 1.10.

As can be seen from Figure 1.10, the retention factor (k') has the least effect on resolution. Resolution improvement with k' increase will only occur for solutes with very low retention factors (k' < 2). Plate count N plays a more important role in resolution, although the influence from N is reduced by the square root relationship. Therefore, narrow symmetric peak shapes are *always* preferred in any separation. However, it is clear that the most significant impact on resolution comes from selectivity. A small change in selectivity leads to a big change in resolution. For example, a change in α from 1.1 to 1.2 nearly doubles the resolution, whereas it is necessary to increase the plate count four-fold for the same improvement in resolution. Thus for typical analytical samples (e.g. synthetic intermediate with number of solutes < 10~15), how to effectively change selectivity becomes a key to achieve better separations in liquid chromatography.

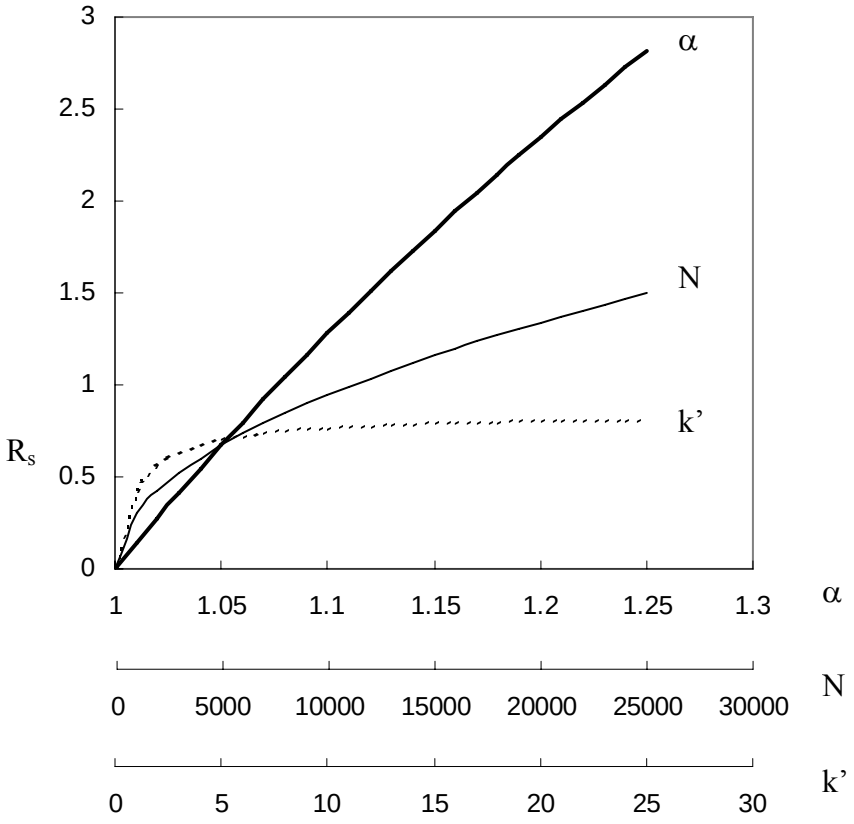

Figure 1.10 Influence of α, N, k' on resolution
(α=1.05, N=5000, k'=3.9 if the parameter is not varied)

To answer this question, we have to first understand the separation process in chromatography. Ultimately chromatography is a thermodynamically based method of separation, where each component in the sample is dynamically distributed between the mobile phase and the stationary phase[60].

$$A_{mobile} \Leftrightarrow A_{stationary}$$

The distribution of compound A is governed by the partition coefficient, *Ki*

$$K_i = \frac{[A_{stationary}]}{[A_{mobile}]} \tag{1.2}$$

where $[A_{mobile}]$ and $[A_{stationary}]$are the concentration of analyte *i* in the mobile phase and stationary phase, respectively. Thus the retention factor k', defined as the time solute *i* resides in the stationary phase relative to the time it resides in the mobile phase, can be measured by the ratio of total amount of solutes in each phase [60]:

$$k' = \frac{N_{A,stationary}}{N_{A,mobile}} = \frac{[A_{stationary}]}{[A_{mobile}]}\frac{V_S}{V_M} = K_i\frac{V_S}{V_M} \tag{1.3}$$

where V_S is the volume of the stationary phase and V_M is the volume of the mobile phase.

Since the selectivity factor α is defined as the ratio of the retention factors of two adjacent peaks:

$$\alpha = \frac{k'_1}{k'_2} \tag{1.4}$$

Combing equations (3) and (4) gives

$$\alpha = \frac{k'_1}{k'_2} = \frac{K_1\frac{V_S}{V_M}}{K_2\frac{V_S}{V_M}} = \frac{K_1}{K_2} \tag{1.5}$$

In equation 5, k_1' and k_2' are the retention factors of two adjacent solutes (1 and 2) eluting out of column, respectively; K_1 and K_2 are the distribution coefficients of these two compounds between stationary phase and mobile phase. When α equals unity, the two solutes will be co-eluting from the column. The ability of a column to separate them clearly lies on the differential distributions/affinity of these compounds between stationary phase and mobile phase. Particularly, at equilibrium, the distribution coefficient K_i can be described as:

$$K_{i,eq} = \frac{[A_{stationary}]_{eq}}{[A_{mobile}]_{eq}} = \exp(-\Delta\mu_i^{\,0} / RT) \tag{1.6}$$

where $[A_{stationary}]_{eq}$ and $[A_{mobile}]_{eq}$ are the equilibrium concentration of *i* in stationary phase and mobile phase, respectively; R is the gas constant and T is the temperature. $-\Delta\mu_i^{\,0}$ is the free energy change during the process of transferring the solute molecules from the mobile phase to the stationary phase, which can be calculated by:

$$-\Delta\mu_i^{\,0} = \mu_i^{\,S} - \mu_i^{\,M} \tag{1.7}$$

where $\mu_i^{\,S}$ and $\mu_i^{\,M}$ are the standard chemical potentials of compound *i* in stationary phase and mobile phase, and

$$\Delta\mu_i^{\,0} = \Delta H_i^{\,0} - T\Delta S_i^{\,0} \tag{1.8}$$

where $\Delta H_i^{\,0}$ and $\Delta S_i^{\,0}$ are the partial molar enthalpy and entropy under standard conditions [60].

Combining equations (5), (6), (7) and (8) gives

$$\alpha = \frac{\exp(-\Delta\mu_1^{\,0} / RT)}{\exp(-\Delta\mu_2^{\,0} / RT)} = \exp(\Delta\mu_2^{\,0} - \Delta\mu_1^{\,0} / RT)$$

$$= \exp\{[(\Delta H_2^0 - \Delta H_1^0) - T(\Delta S_2^0 - \Delta S_1^0)]/RT\} \quad (1.9)$$

Equation (9) indicates that the selectivity factor α is ultimately governed by two distinct terms: an enthalpy term and an entropy term. For most RPLC separation system involving a partition of components between phases as discussed above, $\Delta H_i^0 >> T\Delta S_i^0$; consequently, the separation is largely controlled by enthalpy factors [60], wherein intermolecular interactions (e.g., dipole-dipole, hydrogen bonding, and dispersion) between solutes and two phases dominate the changes in ΔH_i^0. This led to the conclusion that, *all chromatographic separations are ultimately based on a blend of intermolecular interactions between solutes, mobile phase and stationary phase*. As a result, it became clear that the identification of various solute-column interactions and an assessment of their relative importance in affecting both retention and selectivity are absolutely necessary for chromatographers to achieve the separation of different samples.

1.5. STATIONARY PHASE AND SELECTIVITY

There are various solute-column interactions involved in RPLC separations. The nature and the magnitude of these intermolecular interactions are strongly dependent on the physicochemical properties of the stationary phases [61-69]. Consequently, selectivity of silica based stationary phase relies on many factors [19] including: the nature of silica support (e.g. Type A silica or Type B silica), the silane used for bonding (e.g., C18 or phenyl or fluoro), the completeness of bonding, the presence or absence of endcapping, and the surface area of the support. The differences in these factors can have significant impact on stationary phase selectivity and thus affecting the operation of RPLC. For example, Figure 1.11 shows that there are multiple changes in elution order when the C18

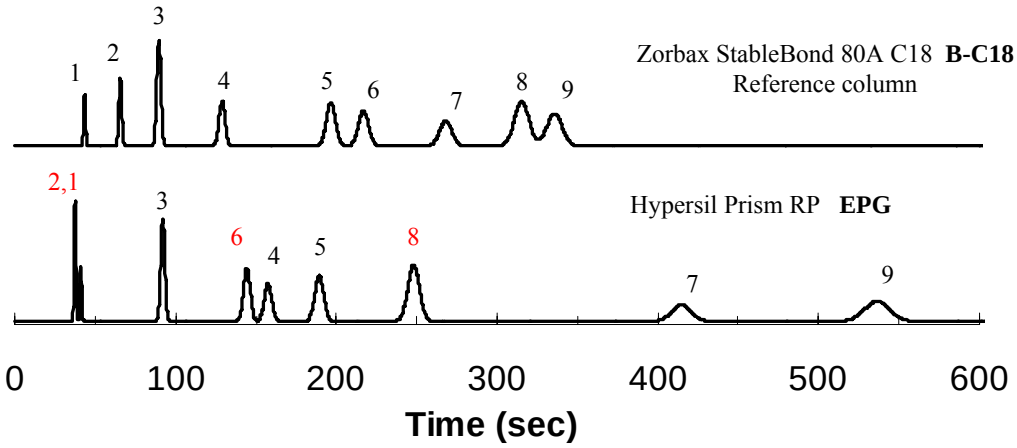

Figure 1.11 Chromatograms of selected drugs on two columns (Zorbax StableBond 80A C18 (B-C18) and Hypersil Prism RP (EPG)) under isocratic conditions. Chromatographic conditions: 50% ACN/buffer (30 mM, pH 2.8); 35 ^{o}C; 1.0mL/min. Sample solutes: 1) N, N-dimethylaccetamide; 2) Amitriptyline; 3) Acetophenone; 4) 5-phenylpentanol; 5) 4-n-butylbenzoic acid; 6) Toluene; 7) Cis-chalcone; 8) Trans-chalcone; 9) Mefenamic acid.

phase is replaced with the EPG phase (i.e. Hypersil Prism RP), wherein the poorly separated pairs 8/9 are well separated on the EPG phase; On the other hand, solutes 1/2 and 4/6 which are closely eluted on the EPG phase are well resolved on the C18 column. It is evident that the ability of a phase to discriminate among certain types of samples varies with the physicochemical properties of the stationary phases. Thus *the choice of the stationary phase that has the largest resolving power on the analytes of interest is critical for method development in HPLC*. In this section, we will discuss the physicochemical nature of the major type of stationary phases for RPLC separations. These properties are at the heart of an understanding of their differences in selectivity and of the ways in which the chromatographer can select the "right" column to achieve desired analysis.

Currently, there are more than 400 reversed phases commercially available. Among them, stationary phases in which organic moieties (i.e. alkyl chains, phenol groups, cyano, amide etc.) are grafted onto a silica surface are the most popular choices due to many reasons [8,19]. For example, the silica substrate is mechanically strong to withstand the high pressure required by LC; In addition, it has a high surface area and an easily tailored pore size to ensure sufficient retention and sample capacity; Perhaps most importantly, the rich chemistry of silanol groups on silica surface can allow one to attach a great variety of organic moieties to produce stationary phases with a diverse set of chromatographic selectivities. Among many features affecting retention and selectivity on these silica-based stationary phases[19], the most important factors are the nature of particle packing in the column bed and the chemistry of bonded phases on the silica surface. Accordingly, the most common silica based RPLC phases can be classified into

several chemical classes based on these two characteristics and the result is summarized in Table 1.2.

1.5.1. Type A alkyl bonded phases

Reversed phase columns packed with micro-particulate silica modified by hydrocarbon chains first became commercially available in early 1970s; since then it had been widely applied for RPLC separations in the next twenty years. This generation of alkylsilica columns is now commonly referred as "Type-A" alkylsilica phases and the general structure is shown is Figure 1.12. One common feature about this type of stationary phases is trace levels of metal impurities on the silica substrate from either organosilicate starting materials or contaminations introduced during manufacturing process[8,70]. Verzele et al [71] have shown that these chromatographic-grade silica gel may contain 0.1-0.3% of metals impurities, with Na, Ca, Al, Mg, Ti and Fe as the prevailing elements. The metals, especially those Lewis acid (e.g. boron or aluminum atom), can interfere with adjacent silanol groups to induce undesired surface acidity. Thus the stationary phases based upon these silica tend to show unusual high silanol activity, which can act as strong adsorption sites and cause deleterious secondary interactions during separations [72]. Thus for compounds containing a protonated amino group, a chelating group or a group capable of forming an hydrogen bond, this group of stationary phases suffered from severe peak tailings and irreproducible retentions from run to run and from batch to batch[73].

1.5.2. Type-B alkyl bonded phases vs. Columns with embedded polar groups (EPG)

Since then a great deal of effort [6,14,74,75] has been made to optimize the performance of silica based stationary phases by eliminating undesirable secondary

interactions. One of the most important approaches was the development of highly-purified "type-B" silica in early 1990s [73]; the alkylsilica phases based upon this new generation of silica is so-called "type-B alkylsilica" phase. As shown in Figure 1.12, these stationary phases are also prepared by using monofunctional organosilane and thus have a surface structure similar to "type-A alkylsilica" phase. However, due to the more efficient production procedure of the silica particles (i.e. less metal contents) and surface modifications (i.e. better surface coverage), the silanol activity on the newly-introduced "type-B alkylsilica" phases (i.e. better surface coverage) is greatly reduced. Thus the stationary phases based upon the new generation of silica packings showed not only substantially improved separation efficiency for these charged analytes, but also excellent run-to-run reproducibility and batch-to-batch uniformity [73]. Consequently, they have become the phase of choice and have been widely used for a large portion of RPLC separations.

Another alternative for improving the above-mentioned separation is the application of the columns modified with embedded or end-capping polar groups (EPG). The basic concept of this type of stationary phases is to suppress the adverse silanol reactivity by attaching chemically competing nucleophilic groups close to the silica surface[74,76-80]. This led to significant improvement in peak symmetry and separation efficiency for these ionized basic or acidic analytes [74,76-78,80]. As a result, the analysis of these polar solutes can be performed at low ionic strength and/or without amino modifiers, which makes these phases especially attractive for LC-MS separations of pharmaceutical or biological samples. In addition, many studies [74,76-78,80] show that the selectivity of EPG columns varies with nature of the polar groups and whether

that group is embedded or used to end-cap the column. For example, columns with embedded polar groups are generally less hydrophobic than non-EPG columns due to the introduction of the polar groups [74,81]. Thus weaker mobile phase (i.e. less organic) has to be used to ensure sufficient retention of neutral compounds. On the other hand, the presence of the polar groups often induces a pronounced hydrogen-bond basicity of EPG column, resulting in selective retention of phenols when compared to the retention on non-EPG phases as noted by several groups [74,81,82]. In general, the unique selectivity, coupled with the excellent separation efficiency of the material, make it a very good candidate for use in pharmaceutical and biological analysis.

1.5.3. Phenyl phases and Cyano phases

Phenyl phases are a group of silica packings consisting of phenyl group chemically bonded to silica gel through a short alkyl chain. Many studies [83-86] have shown that this type of packing often exhibits a highly specific selectivity for aromatic compounds due to π–π interactions that can take place between the solute and stationary phase. For example, in a study where the retention characteristics of a C8 phase was compared to a phenylethyl phase, Tanaka et al.[87] found the preferential retentions of aromatic compounds versus alkanes and alicyclics on the phenyl bonded silica. Likewise, Hanai et. al. [85] studied the retention of alkylbenzenes and polyaromatic hydrocarbons (PAH) on a series of phenylalkyl bonded phases. They observed that the relative retention of these solutes when compared to a C18 column followed the order: aliphatics < benzene derivatives < polycyclic aromatic, which are consistent with the order of increasing π–activity (i.e. aromaticity) of the solute. Such preferential π–π interactions of π–active solutes (e.g. benzene derivatives, PAHs and nitro-substituted aromatics) with phenyl

columns versus alkylsilica columns were also recognized in a more recent study by Marchand et. al. [65]. The presence of the π–π interaction facilitates the application of the phenyl phases as a useful selectivity alternative for compounds which can not be separated on alkyl-bonded phases [88].

A similar trend between retention order and π–active solutes was also noted for cyano phases, with the silica surface modified by nitrile group (i.e. –C≡N) chemically bonded at the end of a short alkyl chain. In an early investigation of retention mechanisms among different stationary phases [89], Tchapla et al. observed a closer correlation between the behavior of a phenyl bonded phase and a multifunctional phase (silica grafted simultaneously with C18 and cyanopropyl chains) when compared to a monofunctional C18 phase, wherein both of the functionalized stationary phases showed preferential retention towards aromatic solute. This study was further extended by Snyder and coworkers [64], in which 44 solutes including aliphatics, substituted benzenes and π–active solutes were used to study and compare the retention characteristics of a C8, a phenyl and a cyano phases using either (a) 40% ACN or (b)60% MeOH as mobile phase. For 40% ACN as mobile phase, very good linear correlations (i.e. r^2=0.99) were seen for the cyano versus the phenyl columns, suggesting these two phases are very similar in their solute-column interactions; with π–π interactions contributed on both the cyano and the phenyl columns. Alternatively, the use of methanol as organic solvent seems to result in more pronounced differences in retention and selectivity between the two columns (i.e. r^2=0.87); this could be attributed to the presence of dipole-dipole interaction on cyano column, which was suppressed previously by the use of acetonitrile-containing mobile phase [64]. This solvent effect has also been noted in the past [85]. Thus a change from

one solvent to the other will result in changes in stationary phase behavior, especially for the dipole-dipole interactions [64].

1.5.4. Fluoro-substituted phases

Since the introduction in the early 1980s[90], perfluorinated stationary phases are becoming more widely used as an alternative to traditional C18 and C8 phases in RPLC due to their potential for providing unique selectivity. The general structure of the phases is shown in Fig.??, with surface ligands (e.g. alkyl, phenyl) heavily substituted by fluorine atoms. One common characteristic of these stationary phases is that they often exhibit a reduced sensitivity for a methylene unit; while the retention and selectivity for fluoro-substituted and polar compounds are enhanced instead when compared to retention on corresponding alkyl or phenyl phases [90-95]. This unusual selectivity has been variously rationalized by the large dipole moment of the C-F bond [96,97], and/or the very low polarizability of fluorinated ligands [95,96], both of which can lead to the differential retention behavior of perfluorinated phase versus C18 and C8 phases. However, a recent study of Marchand and Snyder [65] suggested that the large differences in bonded-phase polarizability may be more important in contributing to the special selectivity of the fluoro phases while the dipole-dipole interactions of solute and stationary phase appears to be less significant in RPLC separations.

1.6. GENERAL STRATEGIES TO CHARACTERIZE STATIONARY PHASE SELECTIVITIES

Table 1.2 Summaries of Major Chemical Classes of Silica-Based Stationary Phases for RPLC

Chemical classes	Surface chemistry	Major Contributors from Intermolecular Interactions	Number of commercially available phases	References
Type-B alkylsilica	Type-B silica modified by silanes with different alkyl chain length (e.g. C_4 vs. C_8 vs. C_{18})	dispersion interaction	>220	[8,61,73]
Type-A alkylsilica	Type-A silica modified by silanes with different alkyl chain length (e.g. C_4 vs. C_8 vs. C_{18})	dispersion interaction, coulombic interaction	>60	[62,70-73]
Phenyl	Type-B silica modified by silanes with phenyl groups in the end (e.g. phenylpropyl vs. phenylhexyl)	dispersion interaction, π–π interaction, polar-polar interaction	>20	[83-87]
Cyano	Type-B silica modified by silanes consist of a short alkyl linker terminated by a nitrile group (e.g. propyl cyano)	dispersion interaction, π–π interaction, polar-polar interaction	>20	[64,85,89]
Polar Embedded Groups	Type-B silica modified by silanes with polar groups embedded within an alkyl ligand (e.g. amide vs. urea vs. carbamate)	dispersion interaction, hydrogen bonding	>40	[40,63,76,78-80]
Polar Endcapped	Type-B alkylsilica endcapped with polar functional groups	dispersion interaction, hydrogen bonding		
Fluoro substituted	Type-B silica modified by silanes with ligands heavily substituted by fluorine atom (e.g. per-fluorinated alkyl vs. per-fluorinated phenyl)	dispersion interaction, possible polar-polar interaction (?)	>10	[29,90-96]

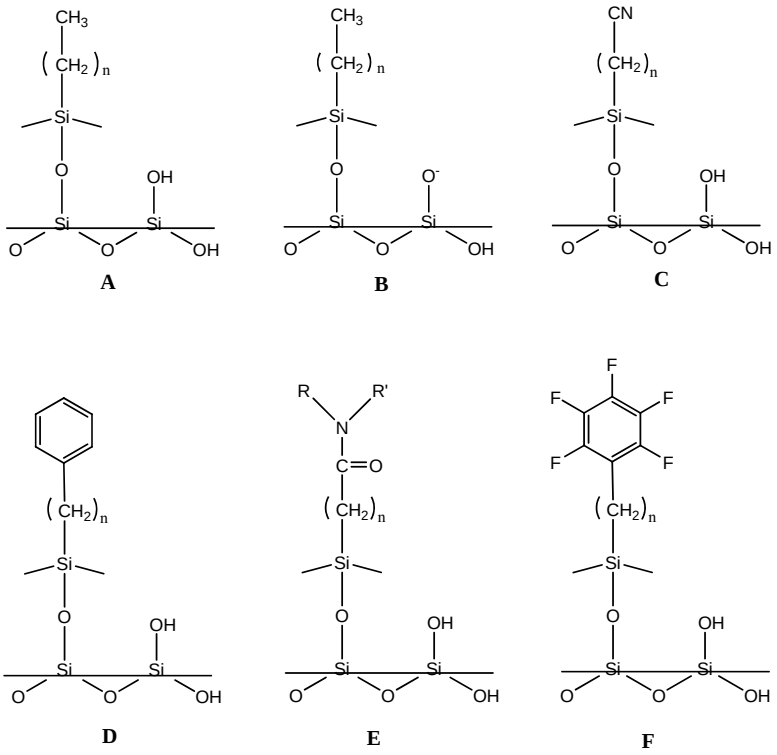

Figure 1.12 General structure of silica-based stationary phases from different chemical classes:
A: Type-B alkylsilica. B: Type-A alylsilica. C: Cyano phase.
D: Phenyl phase. E: EPG phase. F: Fluoro phase

Due to the complexity of physicochemical properties as discussed above, characterization of stationary phase properties is often challenging especially in RPLC. Measurements which can identify various solute-column interactions and assess their relative importance in affecting both retention and selectivity are absolutely necessary to better understand these stationary phases, and more importantly, to guide chromatographic researchers in selecting the appropriate column for practical analysis.

In response, many techniques [6,11,13,14,70,98] have been proposed to characterize stationary phases properties such as: FTIR; cross-polarization magic-angle spinning (MAS) NMR for 29Si and 13C; electron, atomic, and tunneling microscopies; and thermochemical and thermogravimetric methods. Even though these methods are undoubtedly valuable to provide detailed insights into the physicochemical properties of silica particles, they are typically not easy to perform and cannot be carried out on a packed column without destruction. Furthermore, in order to ensure clean surface, in many cases the packings to be measured must be pretreated under ultrahigh-vacuum conditions and high temperatures. Thus results obtained under these conditions (e.g. ultra-vaccum, high temperature) sometimes show poor correlation with the performance of the columns under typical separation conditions. On the other hand, chromatographic tests, based on some simple well–characterized solutes, can allow clear-cut investigation of stationary phase properties under more relevant conditions [8,10]. Thus they have been more widely used over the last twenty years to study and compare RPLC phases.

There are many approaches that can be used for stationary phase characterization. Recently, Lesellier and West have critically compared some of the most prominent strategies in the literature [99]. A thorough comparison of each different approach is far

beyond the scope of this dissertation; a brief summary of their principles, advantages and limitations is given in Table 1.3 to put the merit of the Linear Solvation Energy Relationship (LSER) [100] and Hydrophobic Subtraction Method (HSM)[69], which we have used extensively to characterize our hyper-crosslinked stationary phases.

In general, there are two type of tests commonly performed. One approach is based on several key solutes having well defined properties. The chromatographic response (retention and efficiency) of each solute is then correlated to one specify physico-chemical properties of stationary phases. The result of this method often produces a distribution of stationary phases in simple plots where the differences between the stationary phases are clearly illustrated by their locations in the plot. Various such tests have been developed for almost all major phyisco-chemical properties of stationary phase including hydrophobicity [74,82,101,102], shape selectivity [101-103], hydrogen-bonding capacity [74,82] and silanol activity [74,82,102] These tests are attractive because they are very easy to use, provide a relative high accuracy in measuring specific property of stationary phase, the presentation of the results can be simple and only need relatively small number of exploratory runs. Hundreds of successful applications of these tests have been published, such as Sander and Wise shape test [103] to distinguish monomeric from polymeric phases, Tanaka test [101] to measure hydrophobic selectivity and Neue test [74,82] to investigate both the hydrogen-bonding capacity and silanol activity.

Despite many advantages of the key solutes tests as discussed above, the application of these methods are still challenging especially for real separation problems. This is because, in developing methods for practical separations such as pharmaceutical

Table 1.3 General methods to evaluate stationary phase properties in RPLC

Strategies	Methods	Probes	Elution conditions	Properties studied	Number of column tested
Key solute test	Sander and Wise shape test	1) Phenantrophenanthrene 2) Tetrabenzonaphtalene 3) Benzo[a]pyrene	ACN/H_2O (85/15)	1) Shape selectivity	>40
	Engelhart test	1) Ethylbenzene 2) Toluene 3) Ethylbenzoate 4) Aniline 5) Phenol 6) p-Ethylaniline	MeOH/ H_2O (55/45) T=40 °C	1) Shape selectivity 2) Hydrophobicity 3) Cation exchange ability	>20
	Tanaka test	1) Amylbenzene 2) Butylbenzene 3) Triphenylene 4) o-Terphenyl 5) Caffeine 6) Phenol 7) Benzylamine	Solute 1-6: MeOH/ H_2O (80/20) T=30 °C Solute 7: MeOH/ 0.02M phosphate buffer (pH=2.7 or 7.6) (80/20)	1) Hydrophobicity 2) Hydrophobic selectivity 3) Shape selectivity 4) Hydrogen bonding 5) Cation exchange ability	>20
	Neue's test	1) Acenaphthene 2) Butyl paraben 3) Dipropylphthalate 4) Propranolol 5) Amitriptyline	MeOH/ H_2O (65/35) T=23.4 °C	1) Hydrogen bonding 2) Cation exchange ability	>100

	Sandi test	13 compounds[a]	Linear gradient 5-95% ACN	1) Hydrophobicity 2) Dipolarity/polarizability 3) Hydrogen bonding	>10
	SRM 870 test	1) Uracil 2) Toluene 3) Ethylbenzene 4) Quinizarin 5) Amitriptyline	MeOH/ 0.02M phosphate buffer (80/20) T=23 °C	1) Hydrophobicity 2) Metal impurities 3) Cation exchange ability	>40
QSRR	LSER	22 compounds[b]	ACN/H_2O (85/15) T=30 °C	1) Hydrophobicity /dispersiveness 2) Dipolarity/polarizability 3) Hydrogen bonding	>100
	HSM	16 key solutes out of 67 compounds[c]	ACN/ 0.03M phosphate buffer (50/50) T=35 °C	1) Hydrophobicity 2) Dipolarity/polarizability 3) Steric selectivity 4) Hydrogen bonding 5) Cation exchange ability	>400

[a] Details of 13 test solutes can be found in ref. [104];
[b] Details of 22 test solutes can be found in ref. [105,106];
[c] Details of 16 and 67 test solutes can be found in ref. [69]

analysis, impurity profiling, and in forensic analysis of intoxicants, the sample solutes are usually compounds with very different structures and properties. Therefore, it is an open question as to whether the conclusion obtained by the limited number of rather simple solutes can be applicable to the samples consisting of highly variegated compounds. In addition, a complete comparison is not always available when the conclusions of these tests are often drawn under different analytical conditions with different solute sets [107].

Alternatively, more complex methods such as quantitative structure-retention relationships (QSRR) are proposed to study stationary phase properties. The basic concept is to correlate retentions to the chemical structure of analytes and physicochemical properties of both the mobile and the stationary phase. In particular, the first step is to test stationary phase with a set of structurally diverse solutes including non-polar, polar, acidic and basic solutes spanning a reasonable range in shape and size. The retention time or retention factor of all the solutes are then correlated to the solute-column interactions via a linear equation. Since the solute parameters used in the equation are usually known, either measured or derived from thermodynamically valid models, or estimated from large amounts of experimental results and fully empirical, these methods can produce a set of coefficients for each stationary phase to quantitatively measure all the major solute-column interactions by multi-linear regression. For a fixed mobile phase composition, differences in the interaction coefficients indicate that there are differences in the chemical properties of the stationary phase at equilibrium. Thus QSRR can be applied [108] to 1) investigate and assess the relative importance of the separation mechanisms involved in a given chromatographic system; 2) identify and evaluate complex physicochemical properties of analytes; 3) identify and evaluate

physicochemical properties of stationary phases; 4) get insight into the effect of different chemical nature (i.e. organic ligand, silica substrate) on stationary phase selectivity; 5) predict retention for a new analyte.

One of the most studied QSRR model is so-called linear solvation energy relationships (LSER) based upon solvophobic theory. This approach was first developed by Kamlet and Taft [105,106]. In principle, the free energy of retention is related to five fundamental molecular parameters of twenty-two probe solutes through the following equation:

$$\log k' = \log k'_0 + vV_2 + s\pi_2^* + a\Sigma\alpha_2^H + b\Sigma\beta_2^H + rR_2 \qquad (1.10)$$

where $\log k'_0$ is the regression intercept. The solute molecular descriptors are V_2, π_2^*, $\Sigma\alpha_2^H$, $\Sigma\beta_2^H$, and R_2. V_2 stands for the solute's molecular volume computed[109]; π_2^* is its dipolarity/polarizability; $\Sigma\alpha_2^H$ and $\Sigma\beta_2^H$ are the measure of solute's overall hydrogen-bond acidity, respectively, and R_2 is its excess molar refraction. Thus the coefficients v, s, a, b, and r correspond to the complementary properties of stationary phase, that is cohesiveness/dispersiveness, dipolarity/polarizability, hydrogen-bond acceptor basicities, and hydrogen-bond donor acidities under the fixed mobile phase conditions. The major virtue of this model is that it is a comprehensive model which can be applied for almost all types of chromatography (e.g. GC, RPLC, NPLC and micellar electrophoretic capillary chromatography) to distinguish different stationary phases and also help elucidating retention mechanisms. However, this method does not take into account the contributions to retention from either electrostatic interaction associated with surface ionized silanols or shape selectivity. Thus it is not accurate or precise enough to be used to predict retention for purposes of method development.

Inspired by the LSER model as discussed above, Snyder and coworkers [69] have developed a new scheme to characterize stationary phase properties, especially for reversed phase separations. This scheme entails a quantitative description of column properties in terms of five predominant solute-column interactions through the following equation:

$$\log (k / k_{EB}) \equiv \log \alpha = \eta'H - \sigma'S^* + \beta'A + \alpha'B + \kappa'C \qquad (1.11)$$

where k' is the retention factor of a given solute and k'_{EB} is the retention factor of a non-polar reference solute (ethylbenzene) on the same column under the same conditions. The relative retention factor, α, is related to five solute-column interactions widely recognized as significant contributors to RPLC retention[69]: hydrophobicity (η'H), shape selectivity (σ'S*), hydrogen bonding of acidic solutes with a basic column group (α'B) or basic solutes with an acidic column group (β'A), and cation exchange with ionized silanol groups (κ'C). The coefficients thus inform on the interactive capabilities of the phases: H refers to column hydrophobicity, S* refers to steric resistance, A refers to hydrogen-bond acidity, B refers to hydrogen-bond basicity, and C refers to cation-exchange activity. The corresponding complementary solute properties are denoted as η', σ', β', α', and κ'. This model has been applied for 150 solutes of widely different molecular structure and for several hundreds RPLC columns of various surface chemistry. For a given column type, it can predict values of α with an average accuracy of ±1-3%. These results indicate that all significant solute-column interactions have been included under RPLC conditions. Thus the greatest advantage of this model is that it is a more reliable, complete characterization for RPLC stationary phases. In addition, application of this model can give a better understanding of the nature and relative importance of different

solute–column interactions. For example, the practical importance of these five contributions to column selectivity for type-B alkylsilica columns increases in the order: H < B < S* < A << C [61]. Therefore, for basic (cationic) solutes, the silanol acidity (A) and charge charge (C) interactions are of major importance in determining column selectivity, while H makes a lesser contribution to column selectivity.

Another very useful application of the hydrophobic-subtraction approach is that a single parameter called the "column selectivity function F_s" has been defined[69], and can be used to quantitatively compare the selectivity of any two phases:

$$F_s = \{12.5(H_2 - H_1)^2 + 100(S^*_2 - S^*_1)^2 + 30(A_2 - A_1)^2 + 143(B_2 - B_1)^2 + 83(C_2 - C_1)^2\}^{1/2} \quad (2)$$

This equation is based upon the assumption that the differences in phase selectivity for any two columns can be measured by the Euclidean distance between the two phases in the five dimensional space defined by the five phase coefficients. Each term of Eq. (2) is weighted differently because the column parameters (H, S*, etc.) vary in their relative contribution to the overall selectivity [61,69]. Clearly, the smaller is the weighted distance (i.e., Fs), the more similar are the two columns. In the extreme case when two columns are sufficiently close (Fs ≤ 3), two columns can be considered essentially "equivalent"[61,69]. On the other hand, columns with bigger Fs values are more widely separated in 5-D space; correspondingly they are more different in terms of H, S*, etc., and therefore in terms of selectivity. This turns out to be very useful for method development since not only it allows an easy identification of equivalent replacement column for routine assay procedures[69], but it also enable selection of maximally different phases to improve the resolution so that "hidden" peaks are revealed,

and/or impurities are separated from the main product. Both attributes are very important for pharmaceutical analysis, impurity profiling, and in forensic analysis of intoxicants [69,110].

1.7. THE SCOPE OF THIS DISSERTATION

The major objective of this work is to develop a new family of RPLC stationary phases based on novel aromatic polymer-coated silica particles, aimed at the most important characteristics: *stability, novel selectivity* and *efficiency*.

In Chapter 2, we focus on the synthesis and characterization of a new stationary phases based on the hyper-crosslinked platform. Specifically, it describes the development of a hydrophobically assisted weak cation exchange HC-COOH phase by introducing a small amount of cation exchange sites into the hydrophobic platform. The new phase was extensively characterized at different stages. Column performance was evaluated with various solutes in terms of retention, efficiency, and selectivity.

In Chapter 3, we focus on stationary phase selectivity characterization in RPLC. Specifically, we develop a novel graphical method for investigating the effect of surface chemistry of stationary phases and utilize our understandings to guide the column selection for method development (i.e. columns with the same selectivity, columns with radically different selectivity).

Chapter 4 presents our efforts in optimizing the hyper-crosslinked platform in terms of separation efficiency, wherein a series of kinetic studies were conducted to investigate the effect of reaction time and crosslinking reagents used in preparing HC phases.

In Chapter 5, we make critical comparison of two types of commercial stationary phases (i.e. 2.7 μm superficially porous silica versus 1.8 μm fully porous silica), which are both commonly used to achieve fast analysis, in terms of their separation speed and separation efficiency for both isocratic and gradient elution RPLC separations.

Finally, we summarize the results from above studies in Chapter 6 and discuss the future research directions.

Chapter 2

Synthesis and Characterization of Silica-Based Hydrophobic Weak Cation Exchange Phase

2.1 Introduction

The ultimate goal of any separation is to achieve acceptable resolution (Rs) in a reasonable time. As the most essential metric of separation power in chromatography, Rs can be expressed in terms of three parameters efficiency (N), chromatographic selectivity (α) and retention (k'), where for simple mixtures the most significant impact comes from selectivity [1-3]. Useful method development strategies for optimizing selectivity are based on manipulating the experiment conditions, such as the mobile phase compositions (%B) or mobile phase type [4-9], stationary phase type [4,5] and sometimes the temperature [3]. Previously, because of the long-held belief that retention and selectivity in RPLC are dominated by the mobile phase (i.e. the solvophobic theory [10]), major emphasis is usually given to optimizing mobile phases (e.g. %B, type of organic modifier) while the effect of the type of stationary phase on selectivity has been very much underestimated. However, with the further elucidation of retention mechanisms in RPLC, more and more reports indicate that the stationary phase also plays an important role [11-14]. Recently, it has been suggested by several studies [4,5,15] that varying the type of stationary phases is in fact one of the most effective ways to change chromatographic selectivity.

In response, many types of chemically bonded novel phases have been developed [16-20]. Among them, a novel type of mixed-mode stationary phases has recently drawn

increasing attention [21-24]. In principle, this group of stationary phases is designed by combining two or more orthogonal separation mechanisms such as non-specific hydrophobic interaction and specific electrostatic interactions. The resulting materials often tends to offer radically different selectivity from conventional ODS columns where the separation and selectivity are dominated by hydrophobic interaction only [25-29]. As a result, the use of these phases, often referred as "orthogonal" phases, can provide an alternative and complementary separation for many analyses performed on the most frequently used conventional C8 or C18 columns [26-29]. This is very important for method development in both analytical and preparative HPLC where dramatically different selectivity is required or advantageous. For example, for compounds that are very difficult on traditional ODS phase, the elution order of solutes often differs on the "orthogonal" phases thus providing enhanced selectivity for difficult-to-separate compounds [30]. This can aid in identification, proof of purity and quantitation. Hence many have found them extremely useful when incorporated into a method development screening process in the pharmaceutical industry [4,5,30-34]. One the other hand, the change of elution order can also be useful in preparative HPLC. It may enable the elution of a minor component in front of a major component upon using a unique phase, thereby making collection and/or quantitation considerably easier. Also in two dimensional chromatographic separations, the column in the second dimension must be very different from the column in the first dimension to achieve high peak capacities [35].

In fact, mixed-mode phases are not a new concept. It has been well established in solid phase extraction materials [36]] and capillary electrochromatography [25,37-42] where reversed phase is usually coupled with ion exchange phase. In LC, mixed-mode

RP/ion-exchange phases have previously been developed mainly based on organic polymer, such as on poly(styrenedivinylbenzene) or polymethacrylate developed by Huber et. al. [43]. However, these purely organic polymeric phases generally have low plate count compared to silica based stationary phases [44] and equilibration upon a change in solvent can be slow [44,45]. More recently, several examples of silica based mixed-mode RP/ion-exchange phases have also been reported [21-24,26,28,29,46,47]. For example, Nogueira and Lindner synthesized a reversed-phase/weak anion exchange (RP/WAX) material by grafting N-(10-undecenoyl) -3-aminoquinuclidine onto thiol-functionalised silica particles [22-24] or monoliths [21]. It has several distinct interaction sites including a hydrophobic alkyl chain (hydrophobic domain), embedded polar functional groups (hydrophilic domains), and a terminal bicyclic quinuclidine ring as anion exchange site on silica surface. Thus it offers very unique selectivity and concurrently enhanced mass loading capacity compared to traditional C8 or C18 phases [22-24]. However, the hydrolytic stability of the material can be very challenging. The hydrophobic organic layer on the silica surface was mainly bridged by amide and sulfide groups. The rather readily hydrolysis of these polar groups, especially at elevated temperatures, can lead to continuous loss of the bonded phases and thus limit the application of the phase under acidic conditions.

In the present study, we developed a novel type of ultra stable highly efficient mixed-mode reversed-phase/weak cation exchange (RP/WCE) phase by introducing a small amount of carboxylate functionality into a hydrophobic *hyper-crosslinked* (HC) platform. This silica based HC-platform was recently developed in this lab [48-52], which has an extensive aromatic network completely confined to the particle's surface.

The fully connected polymer network can prevent the loss of bonded phase, which leads to a superior hydrolytic stability of the new phase when compared to conventional silica based phases [48-52]. In addition, the added carboxylic groups provided unique weak cation exchange selectivity to the hydrophobic HC platform. The phase thus prepared showed a mixed-mode retention mechanism, allowing for both neutral organic compounds and charged bases simultaneously separated on the same phase under the same conditions. In addition, the new phase offers the flexibility that gradients in either organic modifier, pH or ionic competitors can be used to effect the separation of a wide range in solutes. Moreover, the inherited weak cation exchange groups allow simple mobile phases to be used thereby avoiding the mass spectrometric ionization suppression problems concomitant to the use of non-volatile additives such as strong amine modifiers (e.g. Triethylamine) or salt (e.g. NaCl) to elute basic solutes from the strong cation exchange phases which was previously developed in this lab [27,53]. In this paper, we describe the preparation, characterization, and surface chemistry of a new packing material. Its chromatographic properties were also thoroughly evaluated.

2.2 Experimental Section

2.2.1 Chemicals

Reaction reagents: dimethyl chloromethylphenylethylchlorosilane (DM-CMPES) was obtained from Gelest Inc. (Tullytown, PA). Styrene heptamer (SH) is a polystyrene standard (number average molecular weight Mn: 800) purchased from Scientific Polymer Products Inc. (Ontario, NY). Diisopropylethylamine (≥ 99%), Chloromethylmethyl ether

(CMME, CH_3OCH_2Cl), $SnCl_4$ (99%) and ethyl phenyl acetate were obtained from Aldrich (Milwaukee, WI)

Reaction solvents: Dichloromethane was obtained from Mallinkrodt (HPLC grade, Phillipsburg, NJ) and dried by MB-SPS (Solvent Purification System from MBRAUN, Stratham, NH) before use. ACS grade tetrahydrofuran (THF), acetone, 37.6% HCl and HPLC grade methanol (MeOH), isopropanol (IPA) were also obtained from Mallinkrodt (Phillipsburg, NJ). Anhydrous 1,2-dichloroethane (99+%, ACS grade) was obtained from Aldrich (Milwaukee, WI).

HPLC buffers and solvents: ACS grade lithium chloride and potassium chloride were obtained from Aldrich, 50% formic acid, acetic acid and ammonium acetate are HPLC grade reagents from Fluka (Allentown, PA). HPLC acetonitrile (MeCN) was obtained from Sigma-Aldrich (St. Louis, MO). HPLC water was prepared by purifying house deionized water with a Barnstead Nanopure II deionizing system with an organic-free cartridge and run through an "organic-free" cartridge followed by a 0.45 μm Mini Capsule filter from PALL (East Hills, NY).

HPLC solutes: Ephedrine, methamphetamine, methylenedioxymethamphetamine (MDMA), methylenedioxyamphetamine (MDA), MDEA, methcathinone, cathinone were purchased from Cerilliant (Round Rock, TX) as 1 mg/mL solutions of drug in methanol. All other chromatographic solutes were obtained from Aldrich or Sigma.

Silica substrate: Type-B HiChrom silica particles and ACE C_{18} particles were gifts from Mac-Mod, Inc (Chadds Ford, PA). The particle diameter, surface area, and pore diameter of the particles are 5.0 microns, 250 m^2/g, and 150 Å respectively.

2.2.2 Synthesis of HC-COOH Phases

2.3.2.1 Silanization

All glassware was rigorously cleaned, rinsed thoroughly with HPLC water, dried at 150 °C overnight and cooled under nitrogen prior to use. 10 grams of type-B HiChrom silica were dried under vacuum at 160 °C for 12 hours prior to use. After cooling to room temperature under vacuum, the dried silica was slurried in fresh dichloromethane at a ratio of 5ml/g (of silica). The slurry was sonicated under vacuum in a 250 mL roundbottom flask for 15 minutes to fully wet the pores. After sonication, diisopropylethylamine was added to the slurry as the "acid scavenger" and silanization catalyst at a concentration of 3.2 μmoles/m^2 (of silica). Then, 16 μmoles/m^2 (of silica) of DM-CMPES was added to the stirring slurry. An activated alumina column was used to cap the condenser to prevent water contamination. The reaction mixture was refluxed at 50 °C for 4 hours. Next, the silica particles were washed sequentially with 350 mL aliquots of dichloromethane, THF, MeOH, MeOH/water, and acetone. After washing, the silica was air dried overnight at room temperature before the next step was performed.

2.3.2.2 Synthesis of Hyper-Crosslinked Platform

Hyper-crosslinked platform was prepared by a series of two $SnCl_4$ catalyzed Friedel-Crafts alkylations on type-B HiChrom silica that has been silylated with DMCMPES. The detailed reaction conditions are listed in Table 2.1 and can be found in our previous publications [48,49].

2.3.2.3 Derivatization of HC-COOH phase

10 grams of alkylated type-B HiChrom silica were put into a 250 mL two-neck round-bottom flask and sonicated under vacuum with 100 mL of anhydrous 1,2-

Table 2.1 The F-C Reaction Conditions Used in the Preparation of HC-COOH

Reaction	Phase Designation	Reagents Used	Catalyst Type	Reaction Temperature (°C)	Reaction Time (hours)
Primary Crosslinking	SH-DMCMPES	SH[a] (2 ×)	$SnCl_4$[d] (10 ×)	80	3
Secondary Crosslinking	Hyper-Crosslinked platform	CMME[b] (10 ×)	$SnCl_4$[d] (10 ×)	50	1.5
Derivatization	HC-COOH	Ethyl phenyl acetate[c] (10 ×)	$SnCl_4$[d] (10 ×)	80	1.0

[a] SH: styrene heptamer. The mole ratio of styrene heptamer to chloromethyl group on DMCMPES is 2.

[b] CMME: chloromethylmethyl ether. The mole ratio of CMME to chloromethyl group on DMCMPES is 10.

[c] The mole ratio of CMME to chloromethyl group on DMCMPES is 10.

[d] The mole ratio of $SnCl_4$ to chloromethyl group on DMCMPES is 10.

Other detailed procedures are described in Section 2.2.2

dichloroethane for 10 minutes, followed by the addition of a 10-fold excess of ethyl phenyl acetate, relative to the molar amount of surface chloromethyl groups. Next, the catalyst $SnCl_4$ dissolved in 8 mL of anhydrous 1,2-dichloroethane is injected into the heated stirred slurry through a rubber septum seal on one neck of the flask. The reaction mixture was refluxed at 80 °C for 1 hour**.** After reaction, the particles were filtered and washed sequentially with 350 mL of 1,2-dichloroethane, THF, THF with 10% (v/v) concentrated hydrochloride, MeOH, and acetone.

2.3.2.4 Gradient Acid Washing

After synthesis, the hyper-crosslinked phase HC-COOH, was pre-conditioned by gradient acid washing at 150°C as described in our previous publications [48,49]. The purpose of this aggressive gradient acid washing is to: 1) introduce ion exchange sites by hydrolyzing the acetate into the corresponding carboxylic acid, 2) remove tin contamination introduced during the F-C reactions, 3) hydrolyze residual chloromethyl groups and the labile Si-O-Si bonds to prevent their slow hydrolysis over time during use. After gradient washing, the column was flushed with 50/50 IPA/H_2O thoroughly and then unpacked to dry the particles inside.

2.2.3 Elemental Analysis

A small amount of stationary phases after each step was sent for carbon, hydrogen, and chlorine analysis conducted by Atlantic Microlabs, Inc. (Norcross, GA).

2.2.4 Column packing

HC particles were packed into a 5.0 × 0.46 cm column for further characterization. The particles were slurried in a mixture of n-BuOH/DMSO/THF (v/v/v) 7.5/7.5/85 (1.0 g/22.5 mL) and sonicated for 20 minutes prior to packing. Columns were packed by the

downward slurry technique using a Haskel 16501 high-pressure pump to drive methanol through the column. The packing pressure was slowly increased from 500 psi to 7000 psi during the first 2 minutes of packing, and maintained at high pressure until about 150 mL of solvent were collected before the pressure was released.

2.2.5 Characterization of the cation-exchange capacity

The cation exchange capacity of the HC-COOH phase was assessed by frontal uptake method [54], wherein the amount of surface cation-exchange sites on the HC-COOH phase were measured at different pHs. In order to keep the conditions consistent with the chromatographic conditions in the study of the retention of basic compounds, the column was first washed with 60ml of 24/76 ACN/water with 10mM potassium acetate at pH of 4.0, 5.0 or 6.0 (buffered by acetic acid) at 1ml/min to saturate the cation exchange sites with potassium ions. The column was then detached and the pumping system was purged with 24/76 ACN/water with 10mM lithium acetate at the same pH. After the system was thoroughly flushed, the flow was stopped and column reattached. The potassium ions were then eluted and collected in a 25-ml graduated cylinder. The concentration of potassium ions was determined by quantitative cation chromatography, using a Dionex ICS-2000 system equipped with a CS16 analytical column and a CMMS III suppressor. The cation exchange capacity Λ ($\mu mol/m^2$) can be then calculated through Eq. (1):

$$\Lambda = \frac{N_{K^+} - C_{K^+} V_0}{\omega A} \qquad (2.1)$$

where N_{K^+} is the amount of potassium ions eluted out of the column. The measured number of potassium ions was corrected for the amount of free ions in the void volume of

the column represented by $C_{K^+}V_0$, where C_{K^+} is the concentration of potassium ion in the eluent, V_0 is the void volume measured by uracil. The term *A* represents the specific area of the silica particles (250m^2/g) and ω is the weight of the particles in a 5.0×0.46cm column, which is assumed to be 0.5g.

2.2.6 Characterization of the overloading capacity

The overloading studies were performed on a 5.0 cm × 0.46 cm HC-COOH column and a 5.0 cm × 0.46 cm Ace C_{18} column. Both columns were brand new. Column efficiency (i.e. plate count) was measured at a series of different amount of samples injected between 0.05 to 10 ug. The columns were thermostated at 40 °C and the detection was at 210 nm. The mobile phases were 5 mM ammonium acetate ($^{S}_{W}$ pH = 6.08, $^{S}_{S}$ pH = 6.14) in 10/90 ACN/H_2O (v/v) for the Ace C_{18} column and 5 mM ammonium acetate ($^{S}_{W}$ pH = 5. 96, $^{S}_{S}$ pH = 6.13) in 40/60 ACN/H_2O (v/v) for the HC-COOH column. These mobile phases gave a similar range of retention factors for the basic solutes on both phases. Note that in this study, buffers were prepared and adjusted to the desired pH after addition of organic solvent ($^{S}_{w}$pH values), where the meter calibrated in aqueous buffer. The measured pHs were then corrected by a δ parameter to convert pH scales from $^{S}_{W}$ pH to $^{S}_{S}$ pH by eliminate the differences in residual liquid junction potential of the electrode between the aqueous calibration buffer and the target solutions [55].

2.2.7 Characterization of the stability

Dynamic stability tests were performed on a brand new 5.0 cm × 0.21 cm HC-COOH column. A 24/76(v/v) ACN/H_2O with 5mM ammonium acetate (pH=5.0) mobile phase was first flowed through the column at 60 °C for a thousand column volume,

wherein the retentions of a neutral compound and a basic probe were recorded over time. The eluent was then switched to 24/76(v/v) ACN/ H_2O with 10 mM ammonium acetate (pH=6.0) to further test the stability of the HC-COOH phase under more aggressive conditions. The same procedure was repeated and the result is shown in Fig. 2.14.

2.2.8 Chromatographic Conditions

All chromatographic experiments were carried out on a Hewlett-Packard 1090 chromatography system, equipped with a binary pump, an autosampler a temperature controller and a diode array detector (Hewlett Packard S.A., Wilmington, DE). Data were collected and processed using Hewlett Packard Chemstation software. The solutes were prepared in ca. 1 mM 24/76 MeCN/H_2O solutions and the injection volume was 10 μL. Acetate buffer was prepared from ammonium acetate, adjusting to the required pH with acetic acid. Formate buffer was prepared from ammonium formate, adjusting to the required pH by adding formic acid. pH was measured before addition of organic solvent unless otherwise noted.

2.3 Result and Discussion

2.3.1 Elemental analysis

The synthesis scheme from the previous described HC-platform to the final HC-COOH phase and the phase structure at each step are shown in Figure 2.1. The product at each stage in the preparation was characterized by elemental analysis (see Table 2.2).

As shown in Figure 2.1, the HC platform has an extensive aromatic network completely confined to the particle's surface; the network was formed by a multi-layer, two-dimensional, orthogonal polymerization method using Friedel-Crafts chemistry with

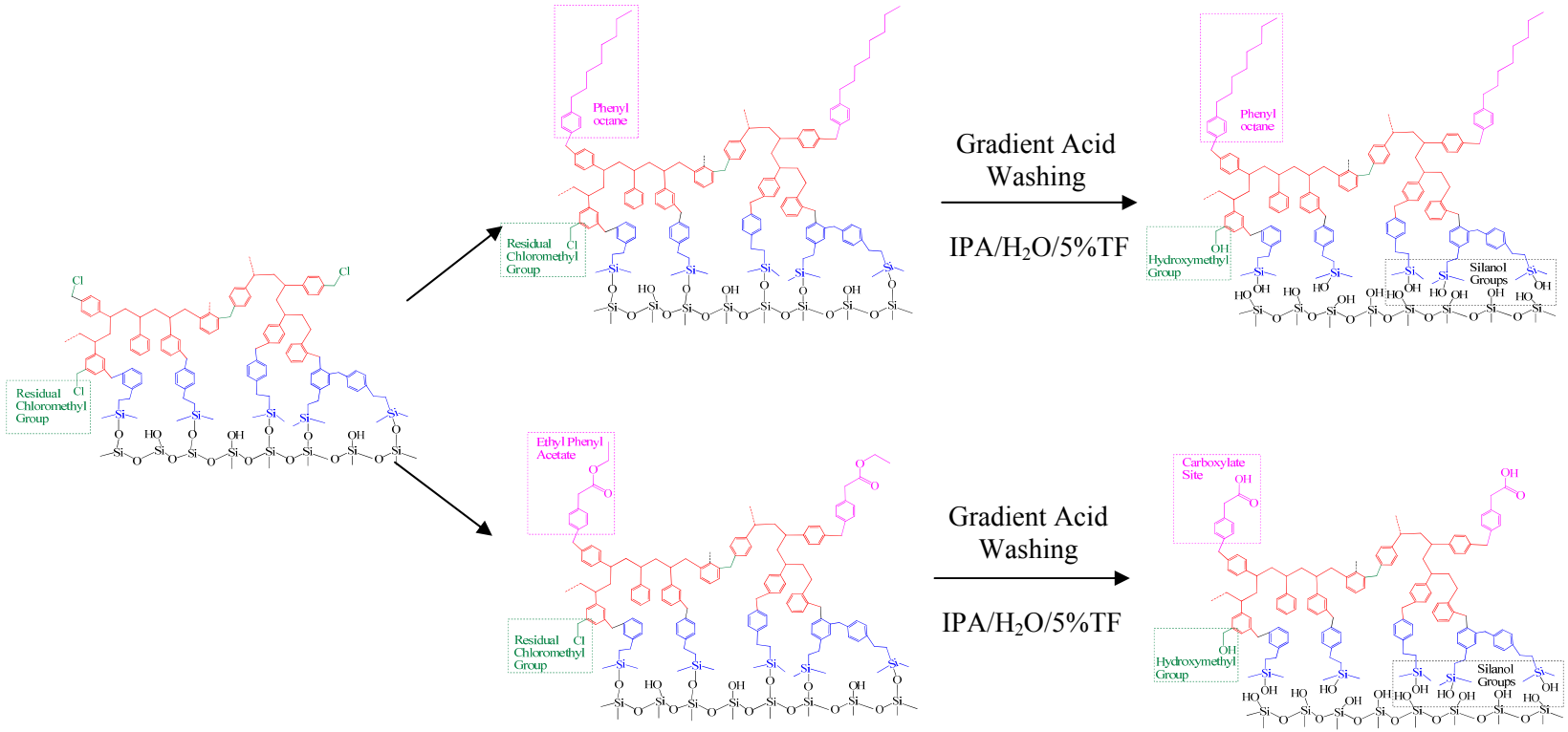

Figure 2.1 Synthesis scheme for the HC-COOH phase and HC-C_8 phase

multifunctional alkylating reagents such as styrene heptamer as the primary cross linker and (chloro-methyl)methylether as the secondary cross linker[48,50]. The resulting monolayer surface polymer shows dramatically enhanced acid stability and can be used at quite high temperatures [56].

Previously, a reversed HC-C_8 phase [50] and a strong cation exchange phase $^-SO_3$-HC-C_8 phase [27,53] was developed based on this platform. In particular, the HC-C_8 phase was synthesized through a third Friedel-Crafts alkylation, wherein a 10-fold molar excess of 1-phenyloctane, relative to number of initial surface chloromethylphenyl groups, were used to react with the surface chloromethyl groups at 80 °C for 0.5 hours. After the reaction, there are approximately 1.0 ± 0.1 μmol/m^2 of octyl groups attached to the aromatic network, with 1.0 ± 0.1 μmol/m^2 of residual chloromethyl groups left [50]. The $^-SO_3$-HC-C_8 phase was prepared by quite briefly treating the HC-C_8 phase with chlorosulfonic acid at -61°C, to introduce only a very small amount of sulfonyl groups (i.e. ~0.1 μmol/m^2) into the hydrophobic aromatic network [53]. The phase thus prepared demonstrated very strong cation exchange ability as shown in the separation of many highly hydrophilic basic compounds [53]. Note that residual chloromethyl on both of these phases are ultimately converted to hydroxymethyl groups in the final phase pretreatment step, that is, gradient hot acid washing [50].

In the development of the cation exchange HC-COOH phase, we decided to choose the F-C alkylation as our synthetic method after careful study of many derivatization methods and in view of our experiences with Friedel-Crafts chemistry. Specifically, a 10-fold molar excess of ethyl phenyl acetate, relative to amount of initial surface chloromethylphenyl groups, were used to introduce the cation exchange sites.

During control reactions (data not shown) carried out in solution where benzyl chloride was used instead of complex silica matrix but otherwise under identical conditions, different reactivity was observed for ethyl phenyl acetate when compared to 1-phenyloctane. This result is not surprising and can be explained by the well known "substituent effect" [57]. In particular, the electron-donating octyl chains facilitated the reaction by increasing the electron density and thus activated the aromatic rings of phenyl octane; whereas the electron-withdrawing acetate groups inhibited the reaction by decreasing the electron density and thus deactivated the aromatic rings of ethyl phenyl acetate. As a result, after an hour of reaction with the surface chloromethyl groups at 80 °C, only 0.5 ± 0.1 μmol/m^2 of phenyl acetate groups were attached to the aromatic network based on carbon content analysis, which is 50% less than the loading density of the phenyl octyl groups. Nevertheless, the amount of carboxylate groups on the HC-COOH is still five times higher than that of sulfonyl groups on the $^{-}SO_3$-HC-C_8 phase. Previous work [27,53] in this lab demonstrated the strong cation exchange ability due to the presence of 0.1 μmol/m^2 sulfonyl groups. Thus we believe the amount of carboxylate sites on the HC-COOH phase should provide sufficient weak cation exchange selectivity to the hydrophobic hyper-crosslinked substrate

After the synthesis was complete, the HC-COOH phase was extensively pre-treated by "gradient" washing at pH 0.5 and 150 °C to (1) remove tin (IV) catalyst that was left after the Friedel-Crafts reactions, (2) eliminate incompletely crosslinked organic moieties, (3) hydrolyze the siloxane bonds under the extensively crosslinked networks, (4) convert residual chloromethyl groups to hydroxymethyl groups, and (5) break the labile O=C-O bond to generate the carboxylic acid groups which will serve as the weak

cation exchange sites. We believe that almost all the labile bonds and groups will be broken or reacted after the aggressive acid treatment. For example, nearly all chlorine was removed on both phases as shown in Table 2.2, which suggests that the chloromethyl groups were almost completely converted to hydroxylmethyl groups during the treatment. Based on the change in the carbon content of the HC-C_8 phase, there was essentially no loss in the amount of bonded phase, which confirms the existence of hyper-crosslinked network on silica surface. This indicates that the 2% decrease in the carbon content of the HC-COOH phase is mainly due to the hydrolysis of the O=C-O bond and the subsequent loss of ethyl groups.

2.3.2 Characterization of cation-exchange capacity at different pH

2.3.2.1 Ion chromatography

The ion exchange capacity was first assessed by ion chromatography as described in our previous publication [53]. Table 2.3 shows the ion exchange capacity for potassium on the HC-COOH and HC-C8 phases measured at three different pHs respectively. As can be seen, at pH = 4, only a slight increase in cation exchange capacity were observed on HC-COOH phase when compared to HC-C8. This is because, the carboxyl groups are weak acids with pKa ~ 5, suggesting only half of the groups should be ionized at pH 5 and even less than 10% at pH 4. Therefore, at this pH (i.e. 4.0) when the ionization of carboxylic groups are greatly suppressed, the small number of ion exchanges sites found on the HC-COOH phase are mainly due to the surface silanol groups generated from siloxane bonds, which is the same as the HC-C_8 phase. However, as we started to increase pH of the eluent, the two phases began to behave differently and

Table 2.2 Summary of elemental analysis at each step in the synthesis of the HC-COOH phase and the HC-C8 phase

	Elemental analysis (wt/wt)		Surface coverage (μmol/m^2)		
Phase designation	%C [a]	%Cl [b]	Chloromethyl group [c]	Octyl group [d]	Carboxylic group [e]
HC-platform[f]	10.95	2.23	2.9	N/A	N/A
HC-$COOC_2H_5$	12.54	0.89	1.2	N/A	0.5
HC-COOH	12.29	<0.25	<0.3	N/A	0.5
HC-platform[f]	11.00	2.09	2.8	N/A	N/A
HC-C_8	14.43	0.71	1.0	1.0	N/A
HC-C_8 after acid washing	14.84	0.26	0.4	1.1	N/A

a. Detection limit is 0.10% (wt/wt).
b. Detection limit is 0.25% (wt/wt).
c. Surface coverage of chloromethyl groups based on chlorine analysis.
d. Surface coverage of octyl groups based on carbon analysis.
e. Surface coverage of carboxyl groups based on carbon analysis.
f. HC platform prepared on HiChrom silica using $SnCl_4$ as the Friedel-Crafts catalyst in the synthesis [Leo's JCA].

Table 2.3 The cation exchange capacity of the HC-COOH phase and HC-C_8 phases

Stationary phases	Void volume (ml)	Total amount of K^+ eluted from column (mmol)			Cation-exchange capacity (mmol/m^2)[a]		
		pH = 4.0	pH = 5.0	pH = 6.0	pH = 4.0	pH = 5.0	pH = 6.0
HC-COOH[b,c]	0.608	58.96	77.95	130.95	0.42	0.57	1.00
HC-C_8[b,d]	0.572	52.69	57.70	62.73	0.38	0.42	0.46
[-COOH]=L(HC-COOH)-L(HC-C_8)[e]		6.27	20.25	68.21	0.05	0.16	0.54
$^-SO_3$-HC-C_8[b,f]	0.476		11.99			0.11	

[a]. The cation exchange capacity was calculated based on Eq. (2.1) assuming that each column was packed with 0.5 g of particles.
[b]. Phase designation is the same as in Table 2.2.
[c]. For HC-COOH phase, $\Lambda(HC-COOH) = \Lambda(-SiOH) + \Lambda(-COOH)$.
[d]. For HC-C_8 phase, $\Lambda(HC-C_8) = \Lambda(-SiOH)$.
[e]. The number of ionized carboxylic groups on the HC-COOH at different pH.
[f]. The data was obtained from ref. [Hao, JCA, 2009]. The cation exchange capacity of the -SO3-HC-C8 was measured in 50/50 ACN/water containing 0.1% formic acid (pH=2.8).

increasingly more potassium ions could be loaded on the HC-COOH column. At pH = 6 where almost all of the carboxylic acids are ionized (i.e. pH > pK_a+1), more than twice as many cation exchange sites were measured on HC-COOH phase than were on the HC-C8. Overall, the results here confirm the significant increase in cation exchange capacity on the HC-COOH phase due to the introduction of the carboxylic acid groups after acid treatment. The amount of ionized carboxylic groups, at different pH, can be estimated by taking the differences of the number of ion exchange sites between the HC-COOH and the HC-C8 phases and are summarized in Table 2.3. It is clear that at pH = 4, only a minimum number of ionized carboxylate groups (~10%) are available for ionic interaction; whereas almost all of the carboxylic acids are fully ionized at pH = 6. The total amount of carboxylic acid groups, as measured under pH = 6, is roughly 0.54 μmol/m^2. This agrees very well with the results based upon the elemental analysis as discussed above.

2.3.2.2 Effect of pH on the retention of basic compounds on HC-COOH phase

We next examined the cation exchange capacity of the HC-COOH phase by measuring the retention of basic solutes at different pHs. The probes used in this study were a number of highly hydrophilic basic compounds including catecholamines and amphetamine related drugs (see Fig.2.2 for the compounds structure). Fig 2.3 shows the retention changes of the test solutes as a function of the pH. As expected, all the basic solutes became substantially more retained as the pH was increased while the retention of neutral compounds stayed the same. If we compare the two HC phases, it is clear that the two curves essentially converge on the left side of the plot at pH = 4, suggesting the

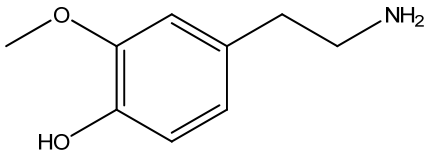

3-methoxytyramine (9.54)

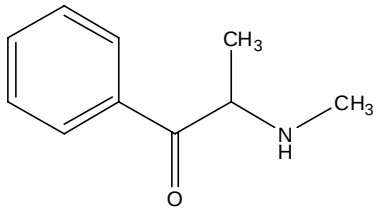

Methcathinone (~10)

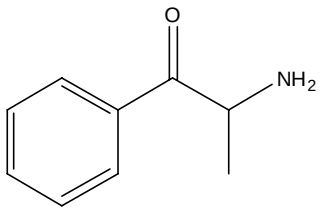

Cathinone (~10)

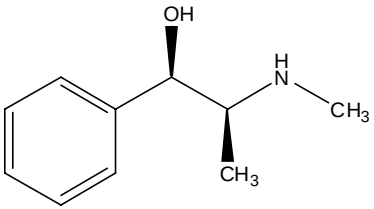

Ephedrine (9.6)

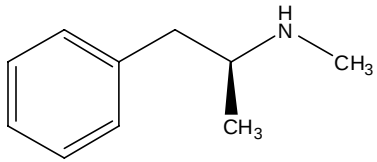

Methamphetamine (10.1)

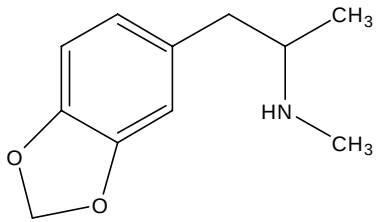

Methylenedioxymethamphetamine (MDMA) (10.38)

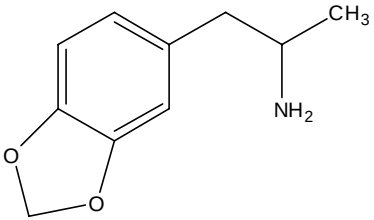

Methylenedioxyamphetamine (MDA) (10.04)

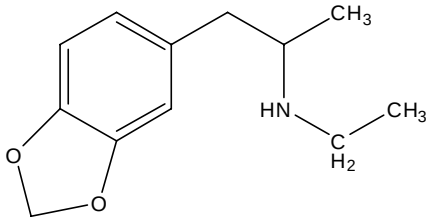

MDEA (~10)

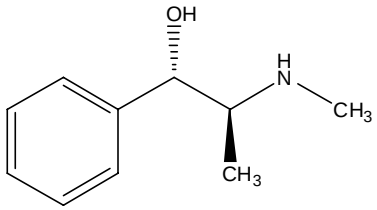

PseudoEphedrine (9.6)

Figure 2.2. The structures and pKas of the basic solutes used in the ion-exchange and overloading study

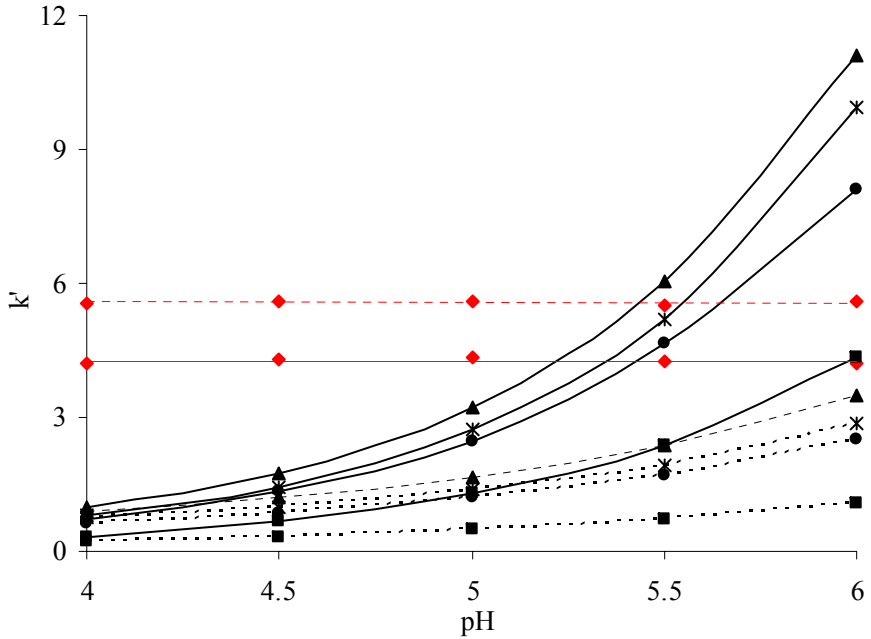

Figure 2.3 Plots of k' vs. pH on HC-COOH phase and HC-C_8 phase. Chromatographic conditions: 24/76 ACN/water with 10mM NH_4Ac at pH 4.0, 4.5, 5.0, 5.5 or 6.0 buffered by acetic acid. 5.0 cm × 0.46 cm column, T = 40 °C, F = 1.0 ml/min. Cationic solutes: (♦) Acetopheone; (▲) Methcathione; (*) Epherine; (●) Cathione; (■) 3-methoxytyramine. The solid lines are the retentions measured on HC-COOH phase; The dotted lines are the retentions measured on HC-C_8 phase.

similar numbers of ion exchange sites as discussed above. As we move toward higher pH where the carboxylic acid groups start to ionize, the two curves begin to separate where increasingly more and more retention of the basic compounds was obtained on the HC-COOH column. At pH = 6 where the carboxylic acids should be fully charged (i.e. pH > pK_a+1) and maximum ionic retention should occur, more than 10 fold increases in retention can be achieved on the HC-COOH phase relative to retention at pH =4.

Based on the retentions of basic solutes on HC-COOH phase and HC-C8 phase, the percent contributions of the –COOH groups to the total retention at different pH were estimated using the following equation:

$$\%k'_{IEX,[-COOH]} = \frac{k'_{IEX,[-COOH]}}{k'_{total}(HC-COOH)} \times 100\% = \frac{[k'_{IEX}(HC-COOH) - k'_{IEX}(HC-C8)]}{k'_{total}(HC-COOH)}$$

(2.2)

where the ion exchange contribution from silanol groups can be estimated and calibrated based on the HC-C_8 phase. As shown in Table 2.4, clearly the HC-COOH phases showed a mixed-mode retention mechanism with the presence of both cation exchange sites and hydrophobic interaction sites. When the pH is below 5.0, retention on HC-COOH is dominated by the hydrophobic hyper-crosslinked substrate; when the pH is above 5.0, the added carboxylate groups start to play a more important role in determining the overall retention of basic analytes. What this suggests is that the new HC-COOH phase can function as an ordinary RPLC phase for polar and non-polar but non-electrolyte analytes. At the same time, polar cationic compounds which could not be separated on typical reversed phases due to very low retention are now much more retained and thus better separated on the new weak cation exchange phase. As a result, one of the most interesting

Table 2.4 The total retention and the percent cation exchange contributions on HC-COOH phase as a function of pH[a]

pH	Stationary phase	Retention	Solutes: Acetophenone	3-methoxy tyramine	Methcathione	Cathione	Epherine
4.0	HC-COOH	$k'_{total}=k'_{RP}+k'_{IEX,[SiOH]}+k'_{IEX,[COOH]}$	4.21	0.33	0.97	0.73	0.82
	HC-C8	$k'_{total}=k'_{RP}+k'_{IEX,[SiOH]}$	5.57	0.22	0.90	0.65	0.74
		$\%k'_{IEX,[COOH]}$ [b]		0	0	0	0
4.5	HC-COOH	$k'_{total}=k'_{RP}+k'_{IEX,[SiOH]}+k'_{IEX,[COOH]}$	4.30	0.68	1.74	1.33	1.45
	HC-C8	$k'_{total}=k'_{RP}+k'_{IEX,[SiOH]}$	5.59	0.34	1.21	0.87	1.00
		$\%k'_{IEX,[COOH]}$ [b]		35	27	29	26
5.0	HC-COOH	$k'_{total}=k'_{RP}+k'_{IEX,[SiOH]}+k'_{IEX,[COOH]}$	4.32	1.31	3.22	2.48	2.73
	HC-C8	$k'_{total}=k'_{RP}+k'_{IEX,[SiOH]}$	5.61	0.50	1.67	1.22	1.38
		$\%k'_{IEX,[COOH]}$ [b]		53	46	48	47
5.5	HC-COOH	$k'_{total}=k'_{RP}+k'_{IEX,[SiOH]}+k'_{IEX,[COOH]}$	4.26	2.38	6.04	4.64	5.20
	HC-C8	$k'_{total}=k'_{RP}+k'_{IEX,[SiOH]}$	5.51	0.73	2.36	1.70	1.94
		$\%k'_{IEX,[COOH]}$ [b]		65	60	62	61
6.0	HC-COOH	$k'_{total}=k'_{RP}+k'_{IEX,[SiOH]}+k'_{IEX,[COOH]}$	4.23	4.35	11.10	8.11	9.93
	HC-C8	$k'_{total}=k'_{RP}+k'_{IEX,[SiOH]}$	5.59	1.06	3.51	2.50	2.85
		$\%k'_{IEX,[COOH]}$ [b]		73	68	68	71

a. The chromatographic conditions are the same as in Fig. 2.3.

b. The percentage of cation exchange contributions from carboxyl groups to the total retention at different pH calcaulted from Eq. 2.2.

features of this new material is that both neutral organic compounds and charged bases can be simultaneously separated on the same phase under the same conditions, that gradients in either organic modifier, pH or ionic competitors can be used to effect the separation of a wide range in solutes and in contradistinction to what is usually observed on traditional RPC media charged organic bases are more retained than are related but uncharged solutes. This will be discussed in more detail below.

2.3.3 Hydrophobicity of the HC-COOH phase

To better understand the overall retention of the HC-COOH phase, we also evaluated the hydrophobicity of the HC-COOH phases based on the free energy of transfer per methylene group from the stationary phase to the mobile phase. A series of alkyphenone homologs were tested on the HC-COOH phase, HC-C8 phase, a commercial ODS phase (i.e. SB-C18) and a commercial cation exchange phase (i.e. Primesep 200). The free energy can be estimated via the Martin equation:

$$\log k' = A + Bn_{CH_2} \qquad (2.3)$$

Where linear regression analysis of log *k*' versus n_{CH_2} allows the free energy to be calculated from the slope, B from the equation:

$$\Delta G^{\circ}_{CH_2} = -2.3RTB \qquad (2.4)$$

The log *k*' values were then plotted against the n_{CH_2} as shown in Figure 2.4. The slopes, intercepts and free energies of transfer per methylene group for the various phases together with the correlation coefficients and standard errors of the regression are listed in Table 2.5. We see from the result that the hydrophobicity (represented by $\Delta G^{\circ}_{CH_2}$) follows the order: HC-COOH < $^{-}SO_3$-HC-C_8 < HC-C_8 < SB C_{18}. As expected, the new

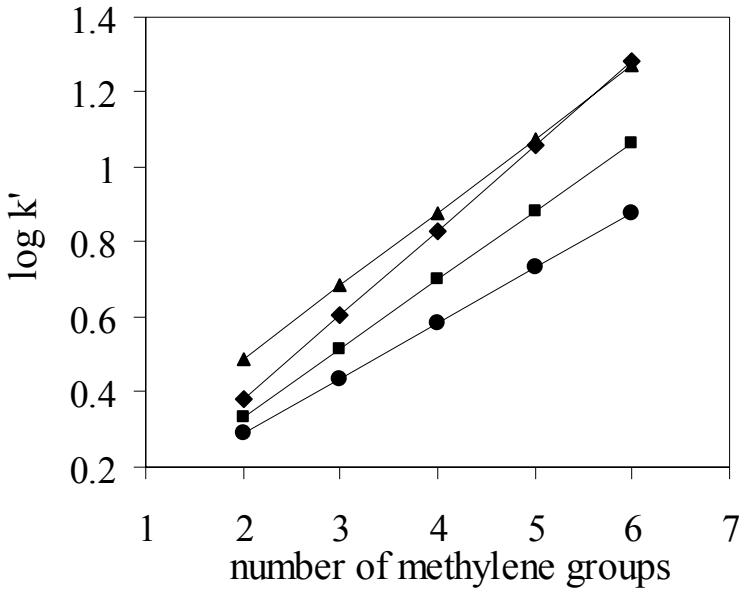

Figure 2.4 Plot of log k' vs. number of methylene groups. Chromatographic conditions: 50/50 ACN/water with 0.1% formic acid and 10mM TEA. HCl, 5.0 cm × 0.46 cm column, T = 40 °C, F = 1.0 ml/min. Alkylphenone homolog solutes: acetophenone, propiophenone, butyrophenone, valerophenone and hexanopheone. (♦) SB C_{18}; (▲) HC-C_8; (●) HC-COOH; (■) $^{-}SO_3$-HC-C_8.

Table 2.5 The slope and intercepts of logk' vs. n_{CH2}, and $\Delta G°_{CH2}$ obtained on different stationary phases

Stationary phases	Slope[a]	Intercept[b]	R^{2c}	S.E.[d]	$G°_{CH2}$[e] (cal mol^{-1})
SB C_{18}[f]	$0.226_{\pm 0.0006}$	$-0.073_{\pm 0.003}$	0.999985	0.0019	$-324_{\pm 0.9}$
HC-C_8[f]	$0.195_{\pm 0.0006}$	$0.100_{\pm 0.003}$	0.999980	0.0014	$-280_{\pm 0.9}$
-SO_3-HC-C_8[f]	$0.183_{\pm 0.0002}$	$-0.033_{\pm 0.001}$	0.999997	0.0007	$-262_{\pm 0.3}$
HC-COOH	$0.147_{\pm 0.0004}$	$-0.003_{\pm 0.002}$	0.999979	0.0012	$-210_{\pm 0.6}$

a. The slope of the linear regression of logk' vs. n_{CH2} based on the data in Fig. 2.4
b. The intercept of the linear regression of logk' vs. n_{CH2} based on the data in Fig. 2.4
c. The squared correlation coefficient of the linear regression of logk' vs. n_{CH2} based on the data in Fig. 2.4
d. The standard error of the linear regression of the linear regression of logk' vs. n_{CH2} based on the data in Fig. 2.4
e. The free energy of transfer per methylene group calculated from Eq. (2.4) using the corresponding slope given in Table 2.5.
f. The data is obtained from ref [Hao, JCA, 2009].

HC-COOH phase shows the lowest hydrophobicity; the less free energies compared to the other two HC phases is mainly due to the absence of the hydrophobic octyl chain. The HC phase's hydrophobicity decreases upon the introduction of polar sulfonyl groups but it is only a very small change as clearly indicated by less than 10% decrease in the $\Delta G°_{CH_2}$ of $^{-}SO_3$-HC-C_8 when compared to HC-C_8. The lower hydrophobicity of the HC-C_8 phases compared to the commercial C18 phases results from a combined effect of shorter alkyl chain (i.e. C8 vs. C18) as well as a lower surface density (i.e. 0.9 μmol/m^2 vs. 2-3 μmol/m^2). Nevertheless, it is important to note that hydrophobic hyper-crosslinked platform ensure the $\Delta G°_{CH_2}$ of the HC-COOH phase to be still around 65% of that of SB C_{18} and 81% of that of HC-C_8. As will be discussed in more detail subsequently, the high hydrophobicity of the HC-COOH phase is very important for the separation of hydrophilic cations.

2.3.4 Retention mechanism on HC-COOH phase

Ion-exchange theory indicates that the ion-exchange contributions to k' must decrease as the eluent concentration of counterion is increased. Specifically, according to the stoichiometric displacement model involving both reversed phase and ion exchange mechanism [58], the total retention factor of k' of a singly charged basic compounds on a hydrophobic ion-exchange phase using a singly charged displacer is given by the following equation, where [59] is the displacer concentration in the mobile phase:

$$k' = k'_{RP} + k'_{IEX} = k'_{RP} + \frac{B_{IEX}}{[C^+]_m} \qquad (2.5)$$

The intercept of a plot of k' versus $1/[C^+]_m$, k'_{RP} represents an "ion-exchange-free" contribution to retention since it corresponds to the k' at infinite displacer

concentration. The slope B_{IEX} is a measure of the strength of the ion-exchange interaction process; it is proportional to the ion-exchange equilibrium constant and to the number of negatively charged sites on the stationary phase surface. Figure 2.5 illustrates the dependence of the retention factors of three single charged analytes on HC-COOH phase as a function of different monoamine displacers. As can be seen, very good linear relationships were observed between k' and the reciprocal of the displacer concentration where the protonated ammonium (NH_4^+), n-butylamine (n-$BuNH_3^+$) and n-octylamine (n-$OctNH_3^+$) were used as the displacers. The slopes B_{IEX} and the intercepts k'_{RP} of the regression are listed in Table 2.6a. The reversed-phase and ion exchange contributions to the total retention at different displacer concentrations (see Table 2.6b) can be further separated using Eq. (2.5) by applying the B_{IEX} and k'_{RP} from Table 2.6a.

First of all, it is quite clear that finites intercepts were obtained in all of the three cases. The finite values of these intercepts unambiguously validated the existence of the hydrophobic interaction mechanism on HC-COOH phase, resulting in retention under conditions where retention by ion-exchange has been eliminated [60].

Secondly, we see from the slopes that changing the cationic modifiers have a significant impact on the magnitude of the ion exchange interaction (represented by B_{IEX}). Specifically, it follows the order: B_{IEX} (NH_4^+) > B_{IEX} (n-$BuNH_3^+$) > B_{IEX} (n-$OctNH_3^+$), suggesting the ion exchange retentions of basic analytes can be suppressed as the length of the alkyl chain on the amine displacers is increased that is as the displacer becomes more hydrophobic. The same trend was reported previously where the effects of various amine mobile phase modifiers were investigated as silanol blocking agents [58,61-63]. Amine modifiers that have higher hydrophobicity but little increases in steric

hinderance [58,63] are found to be more effective in reducing peak tailing and controlling the retention of basic analytes. As pointed out by Nahum and Horvath, and Bij et al. [58,61-63], this results from enhanced binding of these more hydrophobic displacers. Consequently they act as better competitors for surface silanol groups and thus at a given concentration, give lower retention of basic analytes. This is also confirmed by a study in this laboratory on PBD-ZrO_2 [64], a completely different reversed phase having dynamically adsorbed phosphate as the ion exchange sites.

In general, it is clear that the choice of the amine modifier is critical in determining the ion-exchange contribution to the overall retention on HC-COOH phase. For the purpose of this study, most of the work was done using NH_4^+ as the amine modifier, mainly based on its high volatility and considerable cation exchange ability at low concentration, which makes the mobile phase more LC-MS compatible. In addition, as will be discussed in detail later on, NH_4^+ also provided very good peak shape for the basic compounds studied.

Similar to what we reported previously on silica based Alltima ODS, PBD-ZrO2 phase [64] and SO_3^--HC-C_8 phase [53], a good linear relationship is observed between the two parameters k'_{RP} and B_{IEX} with finite intercepts (see Figure 2.6). This indicated the presence of an interesting type of ion exchange sites, which we previously termed "hydrophobic assisted ion exchange sites" [64], in addition to the pure ion exchange interaction site. As we know, for equally charged solutes, the increase in pure ion-exchange retention can not improve selectivity [65], but only contributes to the overall retention. However, the existence of the hydrophobic assisted ion exchange sites allows

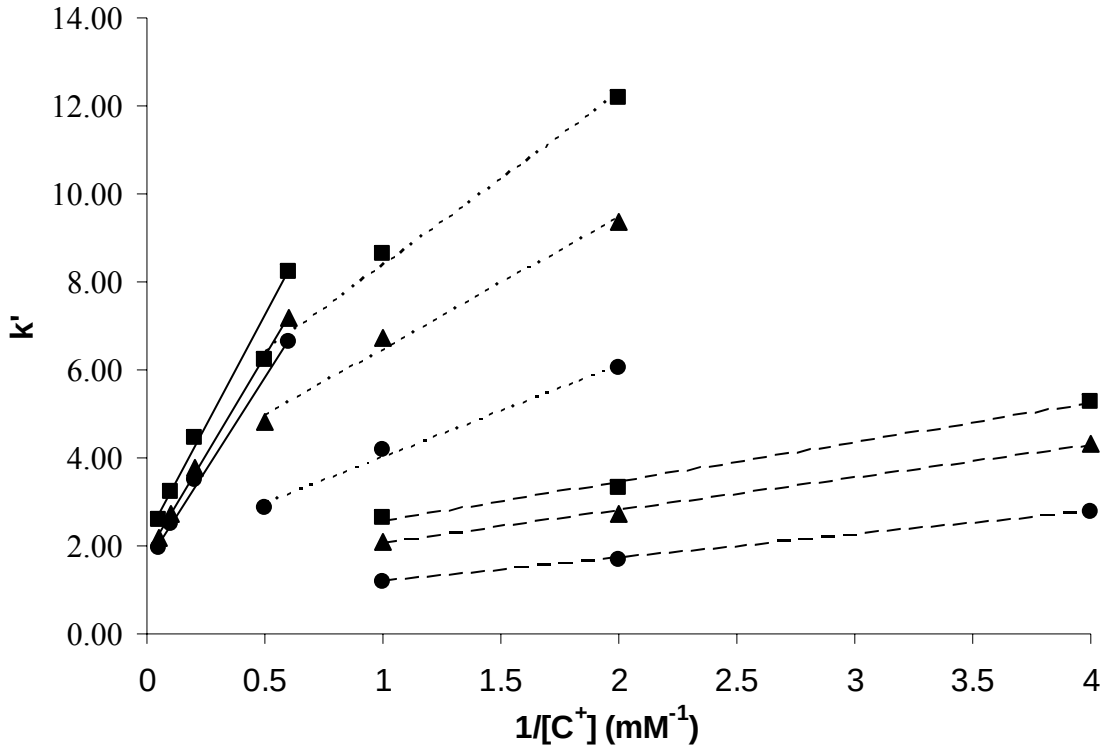

Figure 2.5 Plots of k' vs. $1/[C^+]$ on HC-COOH phase. Chromatographic conditions: 24/76 ACN/water with different amount of cationic displacer buffered by acetic acid (pH=5.0). 5.0 cm × 0.46 cm column, T = 40 °C, F = 1.0 ml/min. Cationic solutes: (■) Methcathione; (▲)Epherine; (●) Cathione. The solid lines are the retentions measured using $[NH_4^+]$; The dotted lines are the retentions measured using $[n\text{-}BuNH_3^+]$; The dashed lines are the retentions measured using $[n\text{-}OctNH_3^+]$;

Table 2.6a The slope and intercepts of k' vs. $1/[C^+]$ obtained on HC-COOH phase with different cationic displacer

Displacer	# of Carbon	B_{IEX}[a]			k'_{RP}[b]		
		Cathione	Methcathione	Epherine	Cathione	Methcathione	Epherine
ammoniun	0	5.58	10.14	8.40	0.76	2.22	1.66
n-butylamine	4	2.08	3.91	2.99	1.93	4.45	3.48
n-octylamine	8	0.53	0.89	0.74	0.64	1.66	1.31

[a] The slope of the linear regression of k' vs. $1/[C^+]$ based on the data in Fig. 2.5

[b] The intercept of the linear regression of k' vs. $1/[C^+]$ based on the data in Fig. 2.5

Table 2.6b The total retention and the percent ion exchange contribution on HC-COOH phase as a function of cationic displacer[a]

Displacer	$[C^+]$ (mM)	Retention	Solutes			
			Acetopheone	Cathione	Methcathione	Epherine
ammoniun	10	k'_{total}	4.32	1.31	3.22	2.48
		$\%k'_{IEX}$[b]	0	42	31	34
	5	k'_{total}	4.36	1.96	4.44	3.49
		$\%k'_{IEX}$[b]	0	59	48	50
	1.67	k'_{total}	4.41	4.09	8.24	6.65
		$\%k'_{IEX}$[b]	0	81	73	75
n-butylamine	2	k'_{total}	4.32	2.87	6.21	4.80
		$\%k'_{IEX}$[b]	0	35	31	30
	1	k'_{total}	4.33	4.17	8.64	6.74
		$\%k'_{IEX}$[b]	0	52	47	46
	0.5	k'_{total}	4.32	6.05	12.17	9.37
		$\%k'_{IEX}$[b]	0	68	64	63
n-octylamine	1	k'_{total}	4.16	1.20	2.62	2.11
		$\%k'_{IEX}$[b]	0	45	35	36
	0.5	k'_{total}	4.16	1.66	3.34	2.71
		$\%k'_{IEX}$[b]	0	62	52	53
	0.25	k'_{total}	4.21	2.79	5.26	4.32
		$\%k'_{IEX}$[b]	0	77	68	69

a. The chromatographic conditions are the same as in Fig. 2.5.

b. The percentage of cation exchange contributions to the total retention at different $[C^+]$ calcaulted from Eq. 2.5 using the B_{IEX} and k'_{RP} as listed in Table 2.6a.

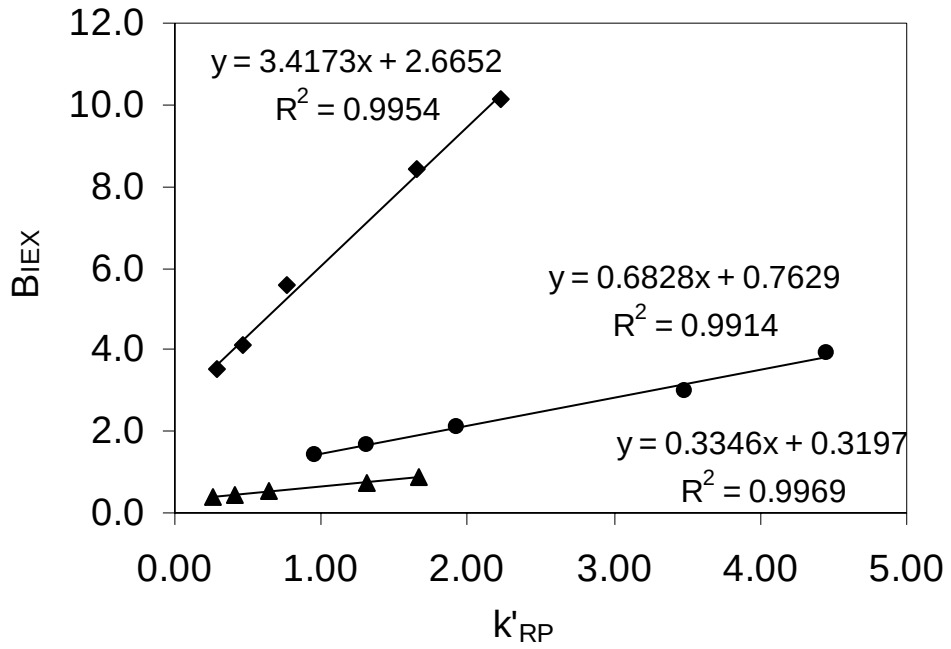

Figure 2.6 Plots of B_{IEX} vs. k'_{RP} on the HC-COOH phase with different cationic displacers. Chromatographic conditions are the same as Figure 5. (■)[NH_4^+]; (●)[n-$BuNH_3^+$]; (▲)[n-$OctNH_3^+$]; The solid lines in each plot are the least square fittings of the corresponding data.

the separation of analytes with similar charge to size ratios provided that they have different hydrophobicitites. As a result, hydrophobic interactions superimposed on ion exchange become one of the key factors to provide high selectivity for different basic compounds on the HC-COOH phase.

2.3.5 The comparison of HC-COOH phases and other RPLC phases by Snyder-Dolan Hydrophobic-Subtraction Method

To more completely investigate the selectivity of the HC-COOH phase, the comprehensive hydrophobic subtraction method (HSM) developed by Snyder and his collaborators [16-20,30,66-68] was used to characterize this weak cation exchange phase and compared it with a few relevant stationary phases for differences in their selectivities. In the HSM a set of 16 very judiciously selected but chemically simple probe solutes are used to study the stationary phases with a set of 5 phase parameters by fitting relative retention data of the 16 probe solutes to the equation [30]:

$$\log (k / k_{EB}) \equiv \log \alpha = \eta'H - \sigma'S^* + \beta'A + \alpha'B + \kappa'C \qquad (2.6)$$

Here, ethylbenzene is a "neutral" reference compound. The five phase coefficients represent the five dominant solute-column interactions as elucidated and explained by the Snyder group; specifically they are: hydrophobicity (H), steric resistance (S*), hydrogen-bond acidity (A), hydrogen-bond basicity (B), and cation-exchange activity (C). The first four stationary phase parameters have been shown to be relatively independent of the mobile phase, although the C-term is very pH dependent and C is available at two pHs (2.8 and 7.0) [30]. This approach has been explored extensively [5,16-20,30,66-69] and found very useful in the classification of more than 350 reversed phases of different types.

The new HC-COOH phase was studied by this method to compare it with a reversed phase HC-C_8 and the strong cation exchange phase $^{-}SO_3$-HC-C_8 derivatized from the same hyper-crosslinked platform. The resulting column parameters together with the average data of a few relevant commercials phases are listed and compared in Fig. 2.7. As indicated by the regression results (see the caption of Fig.2.7), all of the HC-based phases showed excellent fittings using the HSM. The squared correlation coefficients are very close to one and the corresponding standard errors are quite small.

We see from the results in Fig. 2.7, the hydrophobicity (represented by H) follows the order: HC-COOH ~ Phenyl < EPG ~ $^{-}SO_3$-HC-C_8 < HC-C_8 ~ type-B C_8, which agrees very well with the order of hydrophobicity measured by the alkylphenone homolog solutes (see section 3.3). As expected, the H value of the HC-C_8 phase is almost the same as the average of 38 type-B silica-based commercial C_8 phases, both of which showed the highest hydrophobicity among all the phases compared. The hydrophobicity of $^{-}SO_3$-HC-C_8 is reduced upon the introduction of polar sulfonyl groups as previously reported [53]. A bigger decrease as compared to the $^{-}SO_3$-HC-C_8 in H is observed with the HC-COOH phase, which exhibits a hydrophobicity close to the average value of the phenyl phases. This can be attributed to the absence of the hydrophobic octyl chain on the HC-COOH phase as discussed above.

The S* coefficients, are clearly negative and larger in magnitude for all the HC-phases compared to the three general classes of conventional phases given in the figure. This means that the steric repulsion contribution to selectivity is actually retention enhancing on these materials. All HSM coefficients other than the H coefficient are best understood as phase properties relative to a "typical" type-B C18 silica phase. Thus if a

phase has a parameter of zero it means that it behaves in this regard just as does the "typical" phase. Consequently a phase with a negative S* means that a solute with a correspondingly larger σ value (steric impedance) will be more retained on the phase in question as compared to a "typical" phase. . In fact, when we compared the S* values for over 350 reversed phases (data not shown here) derivatized with a wide variety of surface chemistries (e.g. cyano, phenyl, fluoro, EPG), the HC phases showed the most negative value of all phases reported by Snyder [30], suggesting that the two solutes (i.e. trans-chalcone and cis-chalcone), which are major determinants of S*, are much more strongly retained on the HC phases than on conventional RPLC phases. One potential cause of long retention of solutes with large σ values on HC phases is the rather low surface density of C_8 groups (1.0 ± 0.1 μmole/m^2) or the ethyl phenyl acetic groups (0.5 ± 0.1 μmole/m^2) when compared to the typical 2.0 to 3.5 μmole/m^2 of conventional alkylsilica phases. In addition, we also noticed that the two σ marker compounds are highly aromatic. From the phase structures shown in Fig.2.8, we can see that our HC phases are also highly aromatic. Therefore, it is possible that strong π - π interactions might also contribute significantly to the long retention of the two solutes and consequently lead to an apparent highly negative S*.

The A values, which represent the H-bond acidity of stationary phases, are higher for all the HC phases as compared to the averages of the other types of reversed phases (see Fig. 2.7) and are among the top 10% of all the RPLC columns studied by Snyder. This is mainly due to the large number of active hydrogen bond donors released upon hydrolyzing the siloxane bonds and hydrolysis of the chloromethyl groups on the surface of the HC platform upon post-synthesis hot acid washing. A further increase in A was

expected on HC-COOH upon the introduction of the carboxylic acid groups. However, this change was not observed in this study, suggesting the small amount of the weak acid groups don not contribute significantly to the H-bond acidity of the HC-COOH phase.

The B term, which represent the H-bond basicity of stationary phase, are lower on the HC phases than the average of the polar-embedded phases, but higher than the other commercial reversed phases listed in Fig.2.7. Comparing the B value of the three HC phases, the hydrogen-bond basicity of HC-COOH is similar to that of the $^{-}SO_3$-HC-C_8 and essentially the same as that of HC-C_8. According to Snyder, the B coefficient is postulated to be closely related to adsorbed water on the stationary phase [30]. This suggests that the amount of water adsorbed on the HC phases may be mainly controlled by the surface silanol groups and probably the benzyl alcohol groups from the hyper-crosslinked platform while the effect of the ion exchange groups (i.e. sulfonyl, carboxylate) is negligible.

As expected, radically different cation exchange interactions (represented by the C term) were observed between the HC phases derivatized with different functionality. In particular, at pH of 2.8, an extraordinary C coefficient was measured for the strong cation exchange phase $^{-}SO_3$-HC-C_8 ($C_{-SO_3\text{-HC-}C_8}$ = 2.593), followed by the weak cation exchange phase HC-COOH ($C_{HC\text{-}COOH}$ = 0.378); while the C(2.8) coefficient of the HC-C_8 phase ($C_{HC\text{-}C8}$ = 0.215) is not very different from the average of all the commercial phenyl phase(C_{Phenyl} = 0.181)[53]. As discussed above, the strong cation exchange ability of the $^{-}SO_3$-HC-C_8 phase is mainly due to the presence of 0.11 μmole/m^2 sulfonyl groups; while the ionization of carboxylic acid groups are greatly suppressed at this pH, producing only a minimal effect on the C(2.8) value of the HC-COOH phase. On the

other hand, at pH of 7.0, the cation exchange ability of all three HC phases are greatly enhanced as indicated by its C(7.0) coefficient, especially for the reversed phase HC-C_8 ($C_{HC\text{-}C8}$ = 1.032) and the weak cation exchange phase HC-COOH ($C_{HC\text{-}COOH}$ = 1.689). Compared to the average C_8 phase, the HC-C_8 phase has a much higher C(7.0) value. We believe this is due to the silanol groups released during the acid treatment which gives this phase a quite strong cation exchange behavior at pH 7.0. Further it should be noted that the HC phases are not endcapped at all because they are designed to be used in acid media. The presence of such deprontated silanols along with the rather high surface density of carboxylate groups leads to further increases in the C(7.0) value of the HC-COOH phase, which is critical for the separation of polar cationic compounds that can not be retained on typical reversed phases.

It is very important to point out that, the relatively high population of the surface silanol groups of the HC platform does not compromise the separation efficiency of the HC phases for basic analytes. In fact, when we compared the performance of the reversed phase HC-C_8 vs. several of the most widely used commercial ODS phases, it showed the highest plate counts for all three basic compounds as previously reported [50]. This suggests the silanol groups inherent on the silica base of the HC phases do not generate deleterious secondary interactions, which are believed to be the main reason for the bad peak shape and poor plate counts specifically for cationic analytes. This is further confirmed by this study wherein a set of drug compounds were tested on the HC-COOH phase (see below).

Overall, the unique phase coefficients S, A, B, C(2.8), and C(7.0) values of the HC-COOH phase will lead to significant differences in phase selectivity in the

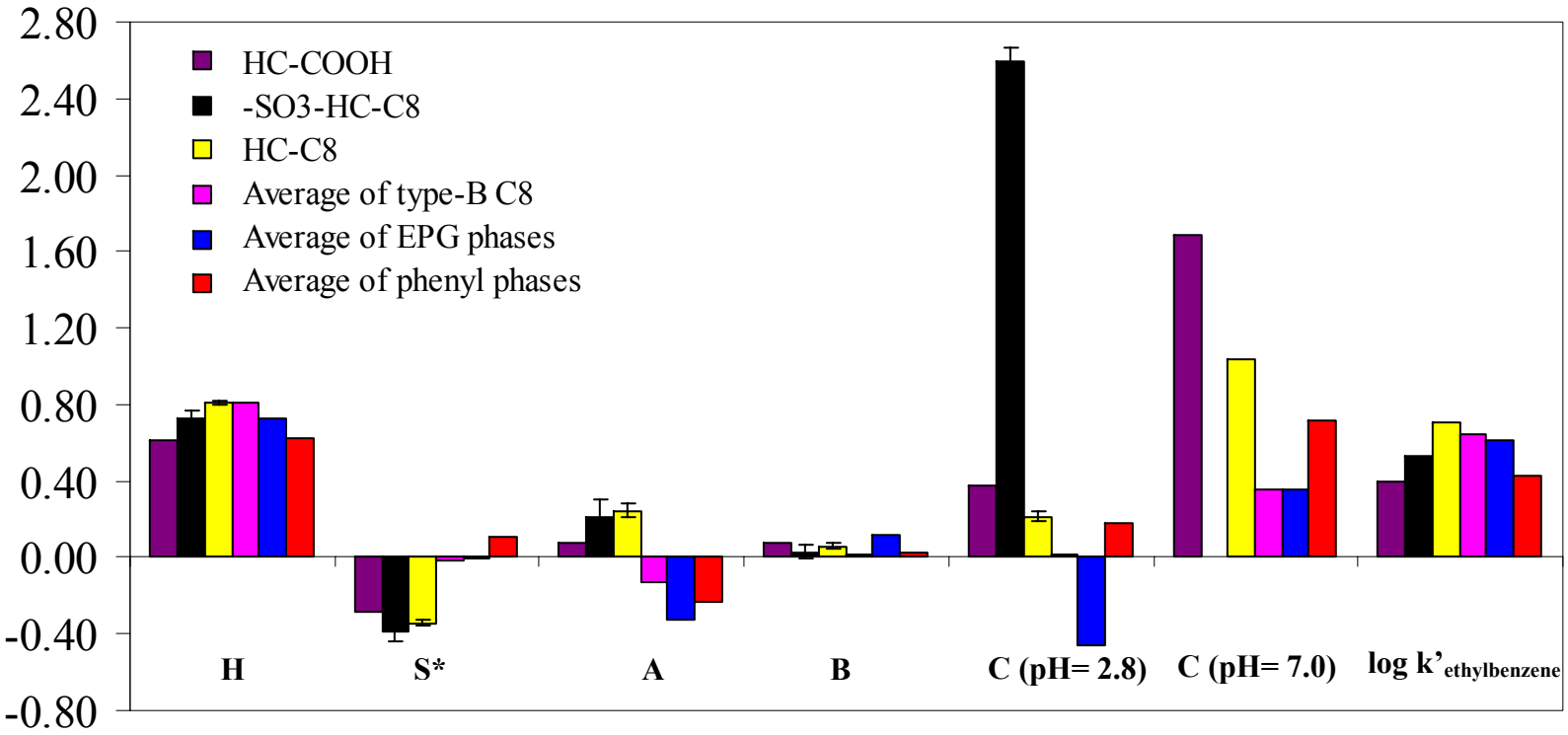

Figure 2.7 The column selectivity parameters of different phases measured by Snyder-Dolan method. Chromatographic conditions: 50/50 ACN/60Mm phosphate buffer (pH=2.8 or 7.0), T = 35 °C, F = 1.0ml/min.
The squared correlation coefficients and the standard errors of the regression of Eq. 2.6 indicate good fits for all three phases: HC-COOH, R^2 = 0.994, S.E. = 0.034 ; HC-C_8, R^2 = 0.999, S.E. = 0.022; $^-SO_3$-HC-C_8, R^2 = 0.995, S.E. = 0.060; The data for HC-C_8, $^-SO_3$-HC-C_8, type-B C_8 phases, EPG phases and phenyl phases were obtained from ref. [Hao, JCA, 2009].

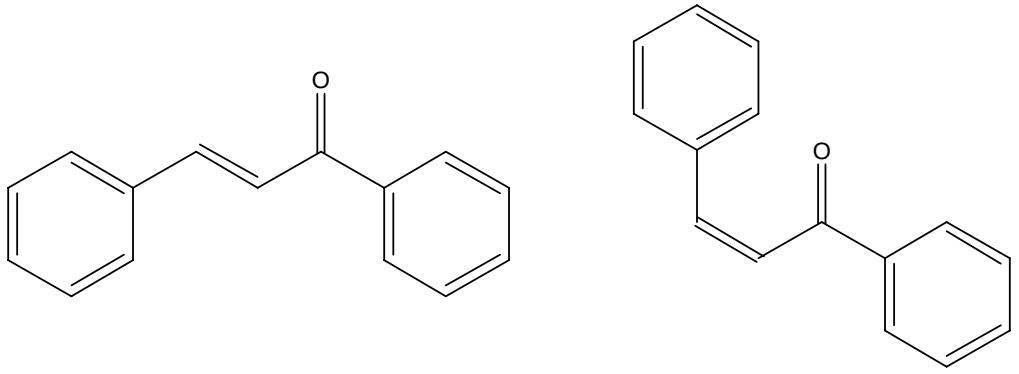

trans-chalcone cis-chalcone

Figure 2.8. The structures of the two marker compounds to determine *S** in Snyder-Dolan Hydrophobic Subtraction Method

separationof a wide variety of analytes. In the next section, we will compare the selectivity of the HC-C_8-Hi-Sn phase with several commercial columns in the separation of non-electrolytes and basic analytes.

2.3.6 Selectivity comparison of the HC-COOH phase vs. other RPLC phases via κ−κ plot

2.3.6.1 Separation of non-electrolyte solutes

The difference in selectivity between two stationary phases can be summarized globally by a κ-κ plot [70]; this is a plot of log k' of a judiciously selected set of solutes on one stationary phase versus the log k' on a second phase. According to Horvath and coworkers [70], a good linear correlation between the two sets of log k' indicates a similar retention mechanism on the columns compared; if the slope is close to 1.0 then the energetics are identical. On the other hand a poor linear correlation implies differences in retention mechanisms and selectivities.

The HC-COOH phase was first studied by twenty two non-electrolyte solutes and compared to Zorbax C_8, Phenyl, PRP, HC-C_8 and $^{-}SO_3$-HC-C_8 phases. The twenty-two solutes were selected to span a wide range in hydrophobicities, polarities and hydrogen bonding characteristics [71-74]. The κ-κ plots of the HC-COOH phase vs. the other four phases are shown in Figure 2.9. As expected, the HC-COOH shows very good correlations with the other two HC phases, which means that the three phases based upon the same hyper-crosslinked platform are very similar in the separation of these non-ionic solutes. For the three commercial phases, the HC-COOH phase exhibits the most different selectivity from the aliphatic phase Zorbax C8 and more closely resembles the two aromatic phases: Phenyl phase and PRP. Moreover, the normalized k' ratios (relative

to the k' of Zorbax C_8) of all twenty two solutes on different phases were plotted to investigate the difference in selectivity towards each solute. As shown in Fig.2.10, the solutes were sorted from left to right in the ascending order of hydrophobicity according to their retentions on Zorbax C_8. Therefore, we should expect a flat line at 1.00 for a phase that has very similar properties to the Zorbax C_8. However, selectivities are clearly different among these stationary phases as illustrated by the diverse retention patterns and many fluctuations. More importantly, the retention pattern of all twenty two solutes on the HC-COOH phase is almost identical to both of the other two HC phases. This indicated that the 0.5 μmol/m^2 of surface carboxylate groups do not significantly change the surface non-ionic properties and the unique reversed phase selectivity from the hyper-crosslinked platform is preserved. This observation is consistent with previous result reported by Hao et. al [53].

The free energy of retention can be related to various fundamental molecular parameters of these twenty-two chromatographic solutes by use of the linear salvation energy relationship (LSER) developed by Kamlet and Taft [75,76]. The RPLC-LSER retention equation is:

$$\log k' = \log k'_0 + \nu V_2 + s\pi_2^* + a\Sigma\alpha_2^H + b\Sigma\beta_2^H + rR_2 \qquad (2.7)$$

where $\log k'_0$ is the regression intercept. The solute molecular descriptors are V_2, π_2^*, $\Sigma\alpha_2^H$, $\Sigma\beta_2^H$, and R_2. V_2 stands for the solute's molecular volume computed [77]; π_2^* is its dipolarity/polarizability; $\Sigma\alpha_2^H$ and $\Sigma\beta_2^H$ reflect solute's overall hydrogen-bond acidity, hydrogen-bond basicity, respectively, and R_2 is its excess molar refraction. The five coefficients of the chromatographic system are complimentary to the above five solute

descriptors: ν represents cohesiveness/dispersiveness; *s* is a measure of dipolarity /polarizability; *a* and *b* is determined by hydrogen bond accepting ability and hydrogen bond donating ability respectively; *r* is related to the π- and n-electron interactions between the system and the solute [18]. The rR_2 term is a correction term that accounts for the inadequacy of lumping dipolarity and polarizability into a single term $s\pi_2^*$ and the regression intercept log k'_0 is associated with the phase ratio. For a fixed mobile phase composition, differences in the interaction coefficients indicate that there are differences in the chemical properties of the stationary phase at equilibrium. Thus LSER has been used over two decades to study the physicochemical properties of stationary phases and assess the relative strength of the chemical interactions involved during the RPLC separations [78].

Twenty two chromatographic probes were judiciously selected from a much larger set of solutes [13] to characterize the HC-COOH phase. The resulting column parameters together with the data of a few commercial phases of interests are listed and compared in Table 2.7. The standard deviations for the regression coefficients and the correlation coefficient, R^2, of the HC-COOH phase are comparable to those obtained for the reversed phase HC-C_8 and the other commercial stationary phases demonstrating the applicability of LSER theory on this special polar embedded phase.

It is clear that changes in surface chemistry have a profound effect on the intermolecular interactions and thus affecting the selectivity of the HC-COOH phase. One of the major differences in seen in the ν-coefficient. When the carboxylic groups are introduced, the HC-COOH phase has a considerably decreased dispersiveness (smaller ν) than the reversed HC-C_8 phase derivatized from the same platform. This is undoubtly due

to the absence of the hydrophobic octyl chain, thereby reducing the hydrophobic interaction between the solutes and the stationary phase. If we further compare the ν-values among different types of stationary phases, it follows the order: Phenyl < HC-COOH < HC-C_8 < PRP < Zorbax C_8, which agrees very well with the order of hydrophobicity measured by the homolog solutes and the HSM (see section 3)

Another significant difference is seen in the hydrogen bonding ability of the HC-COOH phases, as represented by changes in both *a*- and *b*-coefficient when compared to the HC-C_8 phase. Interestingly, increases in both of H-Bond acidity (bigger *b*) and H-Bond basicity (bigger *a*) were seen on the new HC-COOH phase. The enhanced hydrogen bonding basicity is not very surprising since the HC-COOH phase has both the ionized carboxylate functionalities (i.e. 50/50 (v/v) ACN/water, pH~7.0) and more water sorption [30] on silica surface; while the increase in the H-Bond acidity here suggests that there is still a small portion of carboxylate groups that is not ionized and thus can interact with basic solutes through hydrogen bonding.

No significant changes were seen in the *r*-coefficient, which is consistent with the previsou HSM study (see section 3). However, it is worthwhile pointing out that all of the HC phases (r = 0.19~0.22) showed rather high *r*-values, indicating strong π - π compared to conventional aliphatic phases (Zorbax C_8, r = 0.02) and even aromatic phases (Phenyl, r = 0.09). This rather high r coefficients of our HC phases result from the hyper-crosslinked aromatic networks confined on the silica surface, which appears to confirm our belief that π - π does play an important role in determining the selectivity of our hyper-crosslinked phases.

2.3.6.2 Separation of regulated intoxicants.

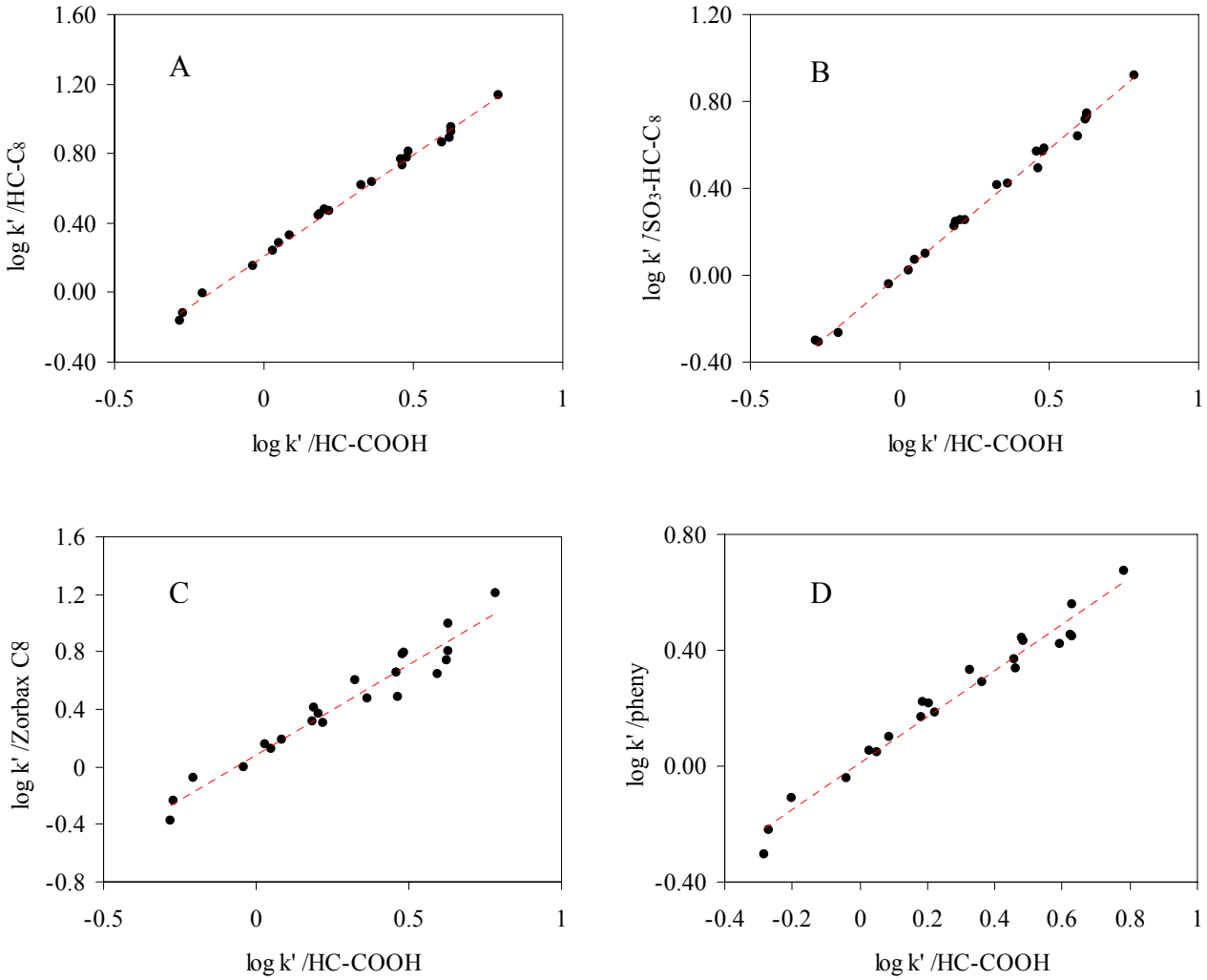
A
log k' /HC-C8
log k' /HC-COOH
1.60
1.20
0.80
0.40
0.00
-0.40
-0.5
0
0.5
1
B
log k' /SO3-HC-C8
log k' /HC-COOH
1.20
0.80
0.40
0.00
-0.40
-0.5
0
0.5
1
C
log k' /Zorbax C8
log k' /HC-COOH
1.6
1.2
0.8
0.4
0
-0.4
-0.8
-0.5
0
0.5
1
D
log k' /pheny
log k' /HC-COOH
0.80
0.40
0.00
-0.40
-0.4
-0.2
0
0.2
0.4
0.6
0.8
1

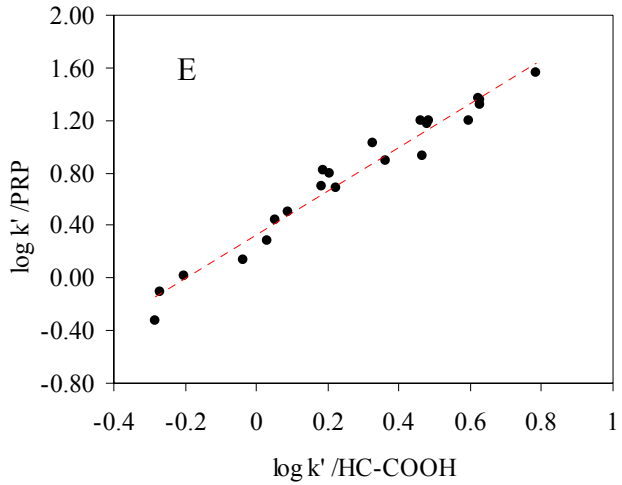

Figure 2.9 Selectivity comparison of different phases via log k' vs. log k' plots based on the retention of the 22 LSER solutes. Chromatographic conditions: 50/50 ACN/water, T = 30 °C, F = 1.0ml/min. Data of $^{-}SO_3$-HC-C_8 is obtained from ref. [Hao, JCA, 2009]; Data of Zorbax C8, Phenyl and PRP phases are obtained from ref. [J. Zhao, Ph.D. thesis,1999]..

A. HC-COOH vs. HC-C_8; R^2 = 0.9954; slope = 1.1654±0.02; S.D. = 0.03;
B. HC-COOH vs. $^{-}SO_3$-HC-C_8; R^2 = 0.9960; slope = 1.1575±0.02; S.D. = 0.02;
C. HC-COOH vs. Zorbax-C_8 phase; R^2 = 0.9432; slope = 1.2573±0.07; S.D. = 0.10;
D. HC-COOH vs. Phenyl phase; R^2 = 0.9686; slope = 0.803±0.03; S.D. = 0.05;
E. HC-COOH vs. PRP phase; R^2 = 0.9643; slope = 1.6693±0.07; S.D. = 0.10;

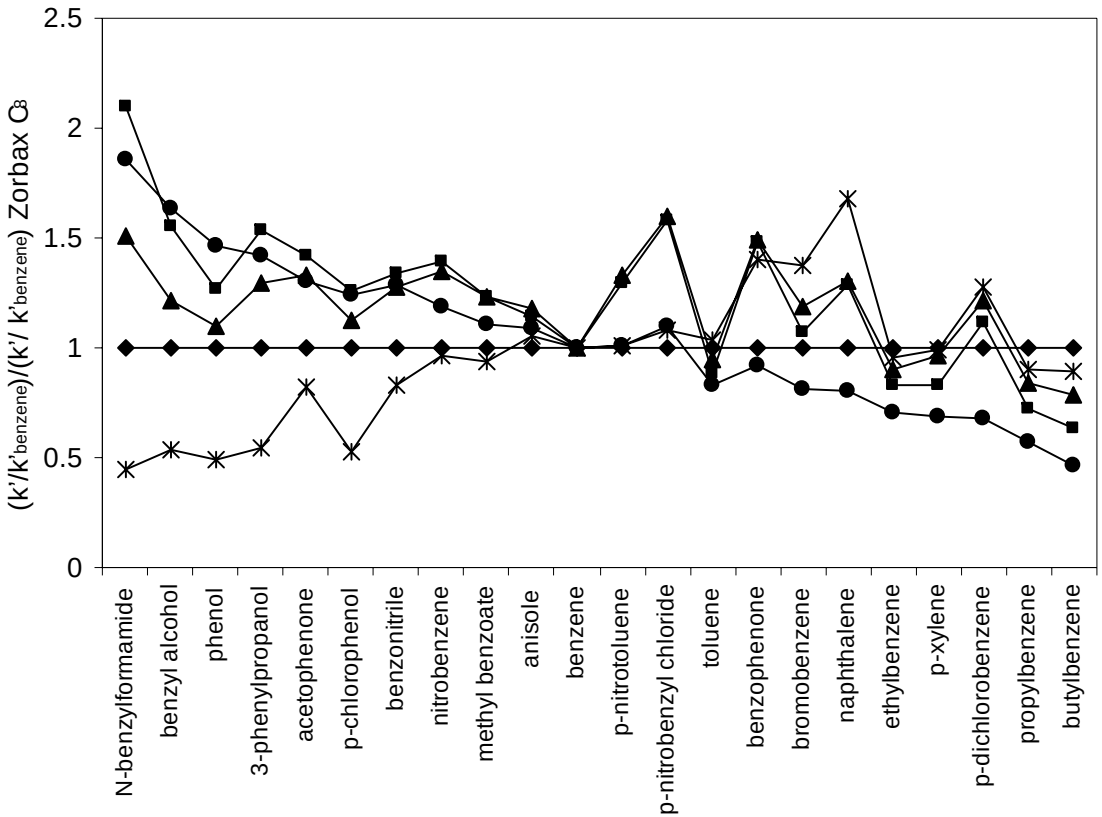

Figure 2.10 Selectivity comparison of different phases based on the retentions of the 22 non-electrolyte LSER solutes via a plot of normalized k' ratio. Chromatographic conditions are the same as Fig. 2.9. (♦) Zorbax C_8; (■) HC-COOH; (▲) HC-C_8; (●) Phenyl; (*) PRP.

Table 2.7 Comparison of LSER coefficients on different stationary phases[a]

Stationary phases	Column coefficients							
	log k'_0	v	s	a	b	r	SE	R^2
HC-COOH	-0.47± 0.05	1.07 ± 0.06	-0.11 ± 0.05	-0.45 ± 0.05	-1.24 ± 0.07	0.22 ± 0.06	0.04	0.989
HC-C_8	-0.24 ± 0.06	1.21 ± 0.08	-0.14 ± 0.06	-0.54 ± 0.06	-1.44 ± 0.08	0.19 ± 0.07	0.05	0.987
$^{-}SO_3$-HC-C_8	-0.47 ± 0.05	1.22 ± 0.06	-0.14 ± 0.04	-0.55 ± 0.04	-1.42 ± 0.06	0.20 ± 0.06	0.04	0.991
Zorbax C_8[b]	-0.25 ± 0.05	1.41 ± 0.06	-0.27 ± 0.05	-0.42 ± 0.05	-1.61 ± 0.07	0.02 ± 0.06	0.04	0.993
PRP[b]	0.03 ± 0.07	1.35 ± 0.08	-0.39 ± 0.06	-0.94 ± 0.06	-1.89 ± 0.08	0.48 ± 0.07	0.05	0.994
Phenyl[b]	-0.22 ± 0.06	0.83 ± 0.07	-0.14 ± 0.05	-0.34 ± 0.05	-0.99 ± 0.07	0.09 ± 0.07	0.04	0.980

[a] All chromatographic separations were performed in 50/50 ACN/water at T = 30 °C with F = 1.0 mL/min.
[b] Data adapted from reference 30.

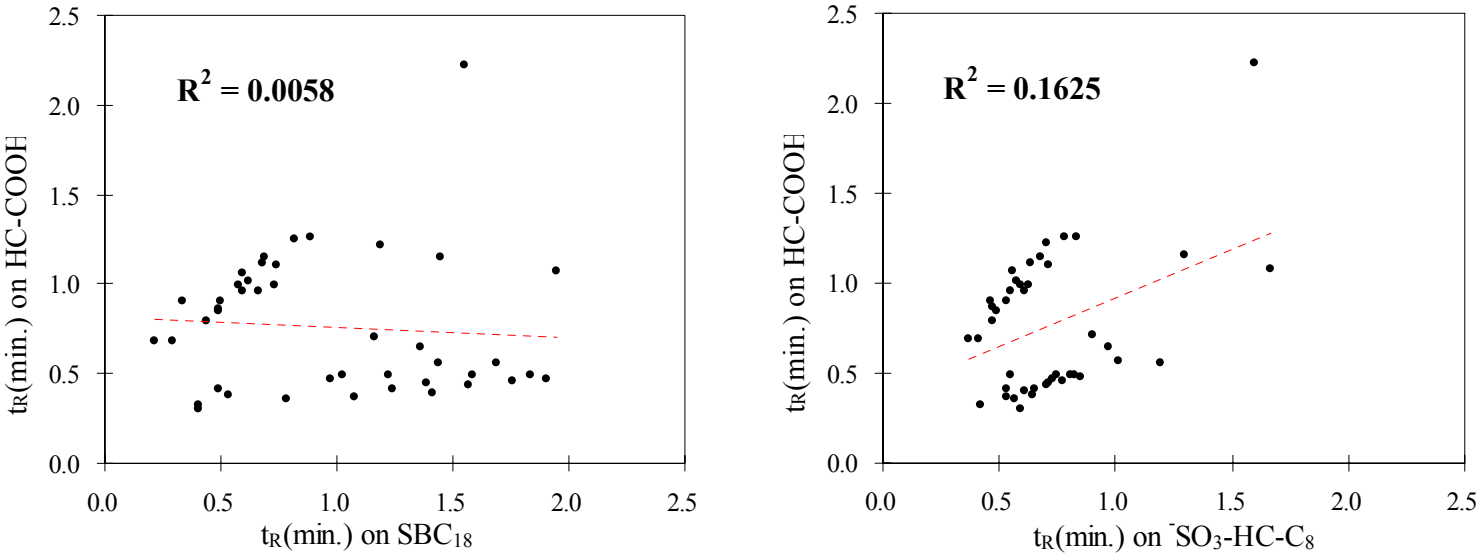

Figure 2.11 Selectivity comparison of different phases via t_R vs. t_R plots based on the retention of the 43 regulated intoxicants. Chromatographic conditions: SB C18: eluent A: 20mM perchloride acid in water; eluent B: 20mM perchloride acid in 80/20 (v/v) ACN/water; gradient profile: 12.5-70% B in 0.00-2.50 min,70-12.5% B in 2.50-2.51 min, and 12.5% B in 2.51-2.80min. $^{-}SO_3$-HC-C_8: eluent A: 20mM perchloride acid in 63/37 (v/v) ACN/water; eluent B: 20mM perchloride acid and 50mM triethylamine.HCl in 63/37 (v/v) ACN/water; gradient profile: 0-100% B in 0.00-2.50 min, 100-0% B in 2.50-2.51 min, and 0% B in 2.51-2.80min; HC-COOH: eluent A: 2mM ammonium acetate in 40/60 (v/v) ACN/water, pH = 5.5; eluent B: 2mM ammonium formate in 40/60 (v/v) ACN/water, pH = 4.0; gradient profile: 0-100% B in 0.00-2.50 min, 100-0% B in 2.50-2.51 min, and 0% B in 2.51-2.80min; Other chromatographic conditions: 5.0 cm × 0.21 cm column, T = 40 °C, F = 1.0ml/min. wavelength =210 nm. Data of $^{-}SO_3$-HC-C_8 and SB C_{18} are obtained from ref. [Dwight, JCA, 2008];

During the HSM reversed phase characterization study, we noticed that the HC-COOH phase showed a very unique cation exchange behavior when compared to the other phases of interest. This suggests that the selectivity of the HC-COOH phase, especially for basic analytes, should be radically different from all the other RP phases, including the two HC phases developed from the same platform.

A set of 43 basic drugs were chosen so that we could compare the selectivity of the HC-COOH phase with both the $^{-}SO_3$-HC-C_8 and a commercial ODS phase SB C18 (see Fig 2.11). It should be point out that because of the fundamental differences in retention mechanisms, different eluent compositions must be applied under gradient elution conditions on the three phases to achieve comparable retention ranges. Specifically, an acetonitrile gradient from 10% to 56% and a salt (i.e. triethylamine) gradient from 0 to 50 mM in 2.50 min were used on SB-C18 and $^{-}SO_3$-HC-C_8 phases, with perchloric acid selected as the buffer for both gradients to increase the retention time or loading capacity of some of the weakly retained cationic drugs through ion pairing (cite Jun and others on perchlorate effect); On the other hand, a weak acid pH gradient using acetic acid from 6.0 to 4.0 was used on the HC-COOH phase, which is much favored for mass spectrometric analysis. The normalized retention times obtained on the three separation systems are plotted in a manner similar to $\kappa - \kappa'$ plot (see Fig. 2.11). The scattered pattern of the data and close to zero correlations in both cases indicate the vast different selectivities among the phases compared, and strongly suggest that the HC-COOH phase is a good candidate for "orthogonal" separations especially when cationic solutes are involved.

2.3.7 The loading capacity and limiting efficiency of bases on HC-COOH phase

The sample loading capacity of the HC-COOH phase was studied together with a commercial Ace C_{18} phase, which was selected for its high separation efficiency and loading capacity of basic analytes [79]. For both of the stationary phases, the plate counts of basic probes (N) were measure at a series of different amounts of samples injected (w) to generate an "overload profile" i.e. plot of N vs. w. The data (N, w) were then fitted into the equation 2.8, which was developed by Dai and Carr [79], based on the kinetic Langmuir model of overload [80,81], to obtain the two key parameters: limiting plate count (N_0) and sample loading capacity ($w_{0.5}$):

$$\frac{N}{N_{0.5}} = \frac{1+1.489\omega'}{1+1.489\omega'+2.489\omega'^2} \qquad (2.8)$$

where $\omega' = w/ w_{0.5}$ is the normalized sample load.

Figure 2.12 shows the "overload profiles" for five basic drugs (structures are shown in Figure 2.2) on the HC-COOH and the ACE C18 phases using 60% of ACN and 10% of ACN as the eluent respectively. Due to the difference in strengths of the reversed-phase and ion-exchange interactions, the retentions for the five testing solutes on the two phases are radically different. On the ODS phases, there is essentially no retention of the basic compounds using polar solvent rich mobile phase. On the other hand, the amines are so strongly retained on the HC-COOH that a high percentage of ACN has to be used to ensure their elution within a reasonable time. To achieve similar retentions of the basic probes, we operated the columns at very different mobile phase conditions with substantially more acetonitrile for the HC-COOH phase. As can be seen from Figure 2.12, both of the plots followed the same pattern with plate counts decreasing as the sample load was increased. However, it is evident that all of the five basic probes on the Ace C18 phase gave rather abruptly dropping profiles; while the change of efficiency on the HC-

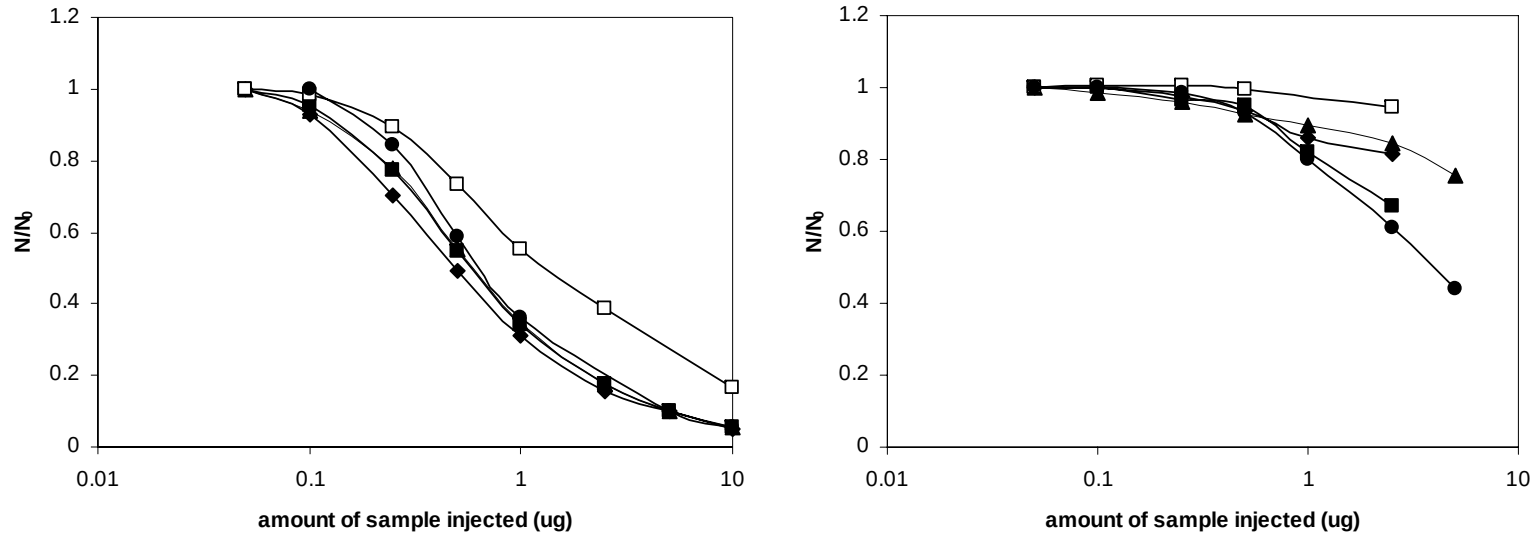

Figure 2.12. Comparison of sample loading capacity of Ace C_{18} vs. HC-COOH phase. Chromatographic conditions: a) Ace C18 column: 5mM ammonium acetate in 10/90 (v/v) ACN/water, pH = 6.08; b) HC-COOH column: 5mM ammonium acetate in 40/60 (v/v) ACN/water, pH = 5.96; Other chromatographic conditions: 5.0 cm × 0.46 cm column, T = 40 °C, F = 1.0ml/min. wavelength =210 nm. Solutes: (□) Methcathinone; (▲) MDA; (■) MDMA; (●) MDEA; (♦) Methamphetamine. The structures of the basic solutes are shown in Fig. 2.2.

Table 2.8 Effect of column type on efficiency, sample loading capacity, and retention of basic drugs.

	HC-COOH[b]				ACE C18[c]					
Solutes[a]	**k'**	**N_0[d]**	**$w_{1/2}$ (nmol)[e]**	**r^{2f}**	**k'**	**N_0[d]**	**$w_{1/2}$ (nmol)[e]**	**r^{2f}**	N_0(HC-COOH) / N_0(ACE C18)	$w_{1/2}$(HC-COOH) / $w_{1/2}$(ACE C18)
Methamphetamine	5.12	3680	77.4	0.885	3.90	2950	3.4	0.997	1.25	22.7
MDMA	5.58	3450	26.9	0.987	4.19	2980	3.0	1.000	1.16	9.1
MDA	4.21	3430	89.7	0.968	3.38	2960	3.0	0.999	1.16	30.2
Methcathinone	3.79	3490	190.0	0.978	2.21	2730	9.9	0.992	1.28	19.2
MDEA	6.56	3310	34.9	0.998	6.56	3110	5.0	1.000	1.06	7.0

a. Structures of the basic solutes are shown in Fig. 2.2.
b. The chromatographic conditions are the same as in Fig. 2.12.
c. The chromatographic conditions are the same as in Fig. 2.12.
d. The limiting plate count calculated from Eq. (2.8) using the corresponding data given in Fig. 2.12.
e. The sample loading capacity calculated from Eq. (2.8) using the corresponding data given in Fig. 2.12.
f. The squared correlation coefficient of the fits based on the data in Fig. 2.12.

COOH phase showed only moderate curvature suggesting much less tendency to overload.

To quantitative explore the overload behavior of the two phases, Table 2.8 shows the limiting efficiency N_0, i.e. the efficiency under conditions of linear chromatography, and $\omega_{0.5}$ the sample loading capacity (the amount of sample (nmol)) that can be injected which causes a decrease in efficiency of analytes by 50% from N_0, and the limiting retention factor (defined as k'_0) on both columns. As can be seen, both loading capacity and the limiting efficiency are found to be much better on HC-COOH compared to the ACE C_{18}. In particular, the average column capacities on HC-COOH are more than an order of magnitude higher than that of the commercial ODS phase. This observation agrees with similar results reported by McCalley et al [82] and can be attributed to the presence of additional retention sites (i.e. the ionized COOH sites) or to the neutralization of solute charge and reduction in mutual repulsion effects (note that the silica particles used for both columns have approximately the same surface area: 225 m^2/g). In addition, very good column efficiency was obtained on the HC-COOH phase for all basic analytes using ammonium acetate buffer, with N_0 in some cases almost 30% higher than the ACE C_{18} phase. We believe that this mainly results from the open pore structure of the HC platform even after the extensive "orthogonal polymerization" and thus the phase maintains the fast mass transfer as previously described[50,53]. Note that these are 5 um diameter particles and the column packing has not been fully optimized ($N_{acetophenone}$ = 4100 for a 0.46 cm × 5.0 cm column), the separation efficiency of the HC-COOH phase in the low ionic strength buffer is clearly superior to the vast majority of classical ion exchangers based on organic polymers [83-85].

It has been shown in many reports [86-88] that, due to the presence of detrimental ionic interactions, separations of basic compounds on conventional RP columns can easily suffer from peak tailing and overloading; both of which can get even worse when low ionic strength buffers (e.g. formic acid), suitable for mass spectrometric detection, are used as suggested by McCalley et al [89]. We believe the application of the new HC-COOH phase, with the appreciable increases in both loading capacity and limiting efficiency, can be beneficial to the separation of basic compounds including many pharmaceuticals and biomedical samples under Mass Spectrometric favored conditions.

2.3.8 Stability of HC-COOH phase

As one of the most essential metrics in chromatography, stability of stationary phase is required to maintain peak shape and to obtain good long term run-to-run repeatability and day-to-day reproducibility. Previous studies in this lab have proven the extreme acid stability of the underlying HC platform even at high temperature (>100 °C). The stability of the HC-COOH phase was further tested at relatively higher pH (i.e. pH =5.0, pH = 6.0) to pave the way for routine applications of basic drugs where the ionization of the surface carboxylic acid groups are desired. In particular, the HC-COOH phase was first tested with 5 mM ammonium acetate (pH = 5.0) in 24/76 (v/v) ACN/water at 60 °C. The pH was deliberately chosen to ensure partially ionization of the surface carboxylate groups. The results are shown in Fig. 2.13. After flushing the column for 1000 column volumes of mobile phase, there was essentially no change of retentions for both of the neutral and basic probes on the HC-COOH phase. The column was then subjected to a second stability test where the pH of the mobile phase was further

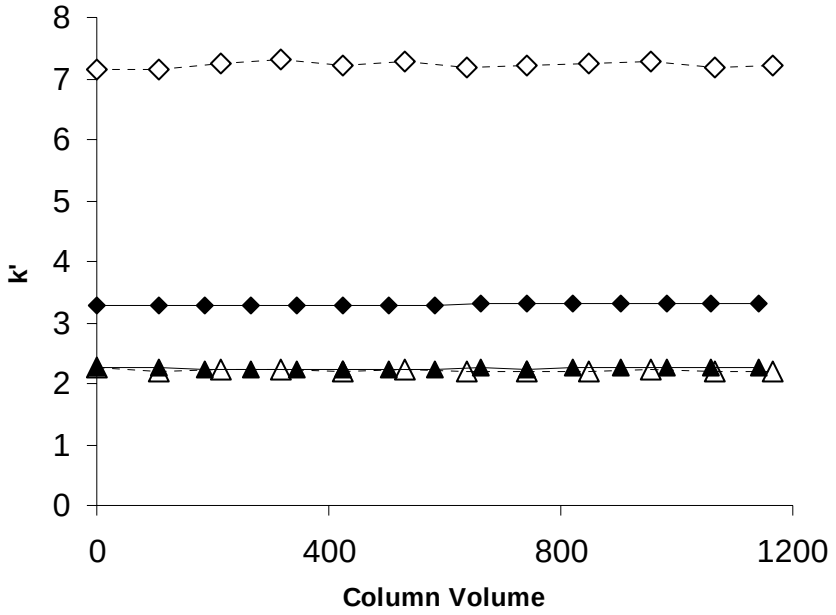

Figure 2.13. Stability test of the HC-COOH phase. Testing conditions: a). 24/76 ACN/H_2O with 5mM ammonium acetate (pH=5.0); (-♦-) methcathione; (-▲-) acetophenone. b). 24/76 ACN/ H_2O with 10 mM ammonium acetate (pH=6.0); (-◊-) methcathione; (-Δ-) acetophenone; Other chromatographic conditions: 5.0 cm × 0.21 cm column, T = 60 °C, F = 1.0ml/min. wavelength =210 nm.

increased from 5.0 to 6.0. Note that 10 mM of ammonium acetate was used instead of 5 mM but otherwise under identical conditions to ensure the reasonable retention of the basic compound at this higher pH. As can be seen from Fig. 2.13, the changes in pH and ionic strength clearly did not affect the stability of the HC-COOH phase. The plots of % k' versus column volume for the two testing probes showed almost no loss in retention and confirmed the stability of the hyper-crosslinked phases even under the higher pH conditions.

Chapter 3

A Visual Approach to Stationary Phase Selectivity Classification Based on Snyder-Dolan Hydrophobic-Subtraction Model (HSM)

3.1 Introduction

The ultimate goal of any separation is to achieve acceptable resolution (Rs) in a reasonable time. As the most essential metric of separation power in chromatography, Rs can be expressed in terms of three parameters: efficiency (N), chromatographic selectivity (α) and retention (k'), where for simple mixtures the most significant impact comes from selectivity [1-3]. Small changes in chromatographic selectivity lead to big changes in resolution. However, there are currently a very large number of phases available for reversed-phase chromatography (RPC) and many show selectivities different from that of a "typical" reversed phase. Extensive work has been done by many research groups, including: Martin, Horvath, Martire, Snyder, Guiochon, Dorsey and Carr [4-22] to understand and rationalize mechanism of retention. Consequently quite a few approaches have been proposed to assess differences in phase selectivity of RPC materials [15,16,18,23-54]. One of the most widely used methods [35,36,55,56] is a comprehensive scheme developed by Snyder and his collaborators [15,16,46-52], specifically for the purpose of classifying reversed phases for differences in their selectivities. The work was initiated by examining a few phases using a large set of some 60 probe solutes including non-polar, polar, acidic and basic solutes spanning a

reasonable range in shape and size in a fixed eluent [15]. This led to the use of a more manageable set of 16 very judiciously selected but chemically simple probe solutes which were then used to study over 350 different commercial RPLC materials and characterize them with a set of 5 phase parameters by fitting relative retention data of the 16 probe solutes to the equation [15]:

$$\log (k' / k'_{EB}) \equiv \log \alpha = \eta'H - \sigma'S^* + \beta'A + \alpha'B + \kappa'C \qquad (3.1)$$

Here, ethylbenzene is a "neutral" reference compound. The five phase coefficients represent the five dominant solute-column interactions elucidated by the Snyder group, specifically: hydrophobicity (H), steric resistance (S*), hydrogen-bond acidity (A), hydrogen-bond basicity (B), and cation-exchange activity (C). The first four stationary phase parameters have been shown to be relatively independent of the mobile phase, although the C-term is very pH dependent and C is available at two pHs (2.8 and 7.0) [15,51]. What is important to understand is that a large fraction of all commercial phases have been studied and almost every reversed phase of every major producer is well fitted by this scheme (±3% S.D).

In this classification scheme two columns are compared by looking at the scatter in a plot of log k' vs. log k' for the above 16 solutes. The scatter is measured by the standard error (s.e.) in a linear least square fit of one column vs. the other. The values of the phase coefficients are then deduced based on the scatter in such plots. Note that Snyder's use of the term "selectivity" in this context is different from what is normally meant by "chromatographic selectivity (α)". The chromatographic selectivity factor is defined as the ratio of retention factors for two solutes. Two phases or columns would

have identical *phase selectivity* when a plot of log k' vs. log k' has no scatter even if all species were perfectly well separated.

A very useful feature of the hydrophobic-subtraction approach is that a single parameter called the "column selectivity function F_s" has been defined [15], and can be used to quantitatively compare the selectivity of any two phases:

$$F_s = \{12.5(H_2 - H_1)^2 + 100(S^*_2 - S^*_1)^2 + 30(A_2 - A_1)^2 + 143(B_2 - B_1)^2 + 83(C_2 - C_1)^2\}^{1/2} \quad (3.2)$$

This equation is based upon the assumption that the differences in phase selectivity for any two columns can be measured by the Euclidean distance between the two phases in the five dimensional space defined by the five phase coefficients. Therefore, the smaller is the distance as measured by F_s, the more similar are the two phases. In the extreme case when two phases are very close ($F_s \leq 3$), the two can be considered to be chromatographically "equivalent" in terms of phase selectivity. On the other hand, two columns with a big F_s are more widely separated; correspondingly they are more different in terms of phase selectivity. This turns out to be the most important application of this model since it allows an easy selection of two phases which are nearly interchangeable and conversely two phases that are dramatically different. Both attributes are very useful in developing new analytical methods as has been demonstrated for a dozen different routine analyses [57].

While the F_s value is undoubtedly useful for identifying columns with *similar phase selectivity*, it application in selecting "orthogonal" phases is still challenging due to some theoretical and practical limitations:

1) Theoretically, it is calculated based upon the *difference* between the five individual column coefficients for two phases. However, in previous work [58] what we at that time called the "effective selectivity", which is actually the "phase selectivity" as used by Snyder, was mathematically proven to be given by the *ratios* of the system (phase) dependent interaction coefficients and not by their *absolute* values. This is precisely in the same spirit as the studies of Abraham and Poole [25,43,59], and Sandi and Szepesy [60,61] on the classification of reversed phases selectivity, where ratios of system coefficients were used.

The validity of this concept becomes evident when we compare three hypothetical columns having the coefficients given in Table 3.1. *These three phases have different absolute values but the same ratios of phase coefficients.* Values of F_s from eq. 3.2 are shown for phases B and C, each of which is compared with column A. As indicated by Snyder [15], a F_s value of 38 ought to be very different. On this basis the values of F_s=40 for column B and F_s=80 for column C ought to produce very different selectivities. However, when we plot the retention data for the 16 standard probes, for all three columns, we observe an exactly linear relationship (r^2 =1.000, se = 0.000) between the data sets which indicates that the two pairs have exactly the same phase selectivity. In the context of the Snyder-Dolan Hydrophobic-Subtraction model it is the scatter that indicates that the phases have different phase selectivities [8,15]. Thus the example of Figure 3.1 confirms that *the differences in phase selectivity only exist when the ratios of phase coefficients differ, not when their absolute values differ.* This showed us that differences in phase selectivity ought to be compared based on the *ratios* of the system dependent interaction coefficients but not on their *absolute values.* The significance of

this conclusion is that it reduces the number of phase characteristics needed to define phase selectivity. In turn this allows us to represent the properties of all stationary phases in terms of a set of four "triangle plots" similar to the very well known solvent classification triangle of Snyder's [4,31,62]. The four phase characteristics in sets of three can thus be displayed in two dimensional graphs.

2) Clearly F_s is a composite parameter as it depends on all the column characteristics and therefore it will indicate that two phases will behave differently even when the solute set of interest does not contain solutes which differ in the selectivity characteristic chiefly responsible for the differences in two phases. The importance of this concept were first noted by Gilar et al.[63] and was further illustrated in a recent study by Marchand et al. [35]. As an example, suppose we were to choose a pair of columns having a big F_s value due mainly to differences in the phases hydrogen-bond acidity and examine them with a set of solutes all having similar hydrogen-bonding basicity (B), but differing in hydrophobicities. It is very likely that the separation on these two columns will not be different because the relative retention factors will be dominated by the solute hydrophobicity. The foregoing example challenges the use of F_s alone for the selection of orthogonal columns. To solve this problem, a modified approach was recently proposed by Snyder and coworkers; they now use a solute set dependent correction factor [15]. The corrected F_s can be adjusted for use with a specific solute set; this greatly improved the practical utility of the method. Another limitation associated with any single-parameter measure of phase selectivity is that, as previously concluded by Lesellier [64], it does not tell us the chemical cause of the difference. It simply says the two phases are different.

Table 3.1 Phase parameters for the three hypothetical phases shown in Figure 3.1.

Phase	Column selectivity parameters					Relative column selectivity parameters [a]				
	H	S	A	B	C	H/H	S/H	A/H	B/H	C/H
A	0.5	0.2	-0.2	0.2	0.2					
B	1	0.4	-0.4	0.4	0.4	1	0.4	-0.4	0.4	0.4
C	1.5	0.6	-0.6	0.6	0.6					

a. Calculated by taking the ratio of column selectivity parameters by dividing by H.

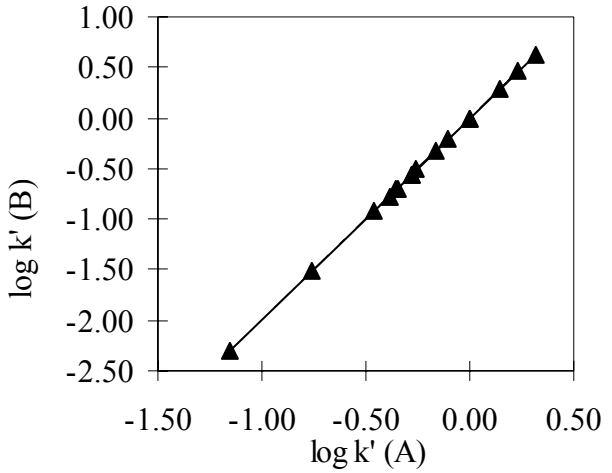

(a)

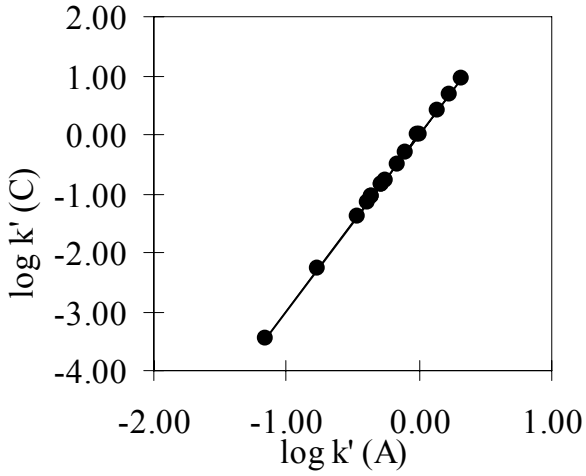

(b)

Figure 3.1 Hypothetical plots of log k' vs. log k' to illustrate the ratio concept. (a) column A vs. column B; (b) column A vs. column C. The retention data for the 16 standard probes is calculated based upon Eq. 3.1 assuming k'(ethylbenzene) =1 on for phases A, B and C.

3) A single table of F_s values relative to a fixed reference column does not allow two or more test columns to be compared to one another. It is evident that two test columns could have exactly the same F_s value relative to a fixed reference yet be quite different from one another [64]. This makes the application of the approach somewhat difficult, especially when columns have to be chosen from over 350 commercial phases. Recently, this problem was greatly reduced when the "Column Match" software developed by Snyder et al.[65], became available. However, there remains a need to develop a method which allows a global view of all stationary phases.

In this work we describe a simple transformation of column parameters based upon the "effective phase selectivity" concept. The data can then be presented as a set of four "selectivity triangles", which we feel is a convenient and useful way to visualize and compare all phases simultaneously. We caution the reader that the triangle scheme thus derived is mainly for classifying stationary phase selectivities. It does not indicate the absolute retention time, a very important parameter to consider when choosing a column for separations. However, it is our understanding that changes in %B do not substantially effect the S-D method [15,51]. Thus when two phases have the same selectivity, which is based on relative retentivity, but show rather different absolute retentivities, what can be done to make column A have the same absolute retentivity as column B is simply to appropriately adjust the volume fraction of the strong component of the eluent; This will have only a small effect on the phase selectivity but will have a large effect on absolute retention.

3.2 Development of the Stationary Phase Triangle Concept

The first step in our approach is to calculate the ratios of Snyder's column parameters. As discussed above, the "effective selectivity" is related to the ratio of the system dependent interaction coefficients. Thus, to compare the selectivities of different stationary phases, we used their S*/H, A/H, B/H, C/H ratios rather than their absolute H, S*, A, B and C values. Mathematically we are free to use any of the five parameters as the denominator to calculate the ratios. For convenience and to avoid large ratios, we decided to take the ratio by dividing by H; its average is close to unity and it has minimal dispersion compared to the other parameters as clearly shown in Figure 3.2.

After obtaining S*/H, etc. the second step was the normalization of these ratios. As defined by eq. 3.3, we arbitrarily adjusted the ratios by first subtracting the minimum value and then rescaling using a set of weighting factors for each term.

$$X_i = (I - I_{\min}) * \phi_i \qquad (3.3)$$

$$i = \frac{S}{H} \text{ or } \frac{A}{H} \text{ or } \frac{B}{H} \text{ or } \frac{C}{H}$$

The last step in developing the new coordinate, to be denoted as three χ values, is normalization to a scale of 0 to 1.000. This is done as follows:

For the S*-B-C triangle, the three scales (χ_j) are defined as:

$$\chi_j = \frac{j}{X_S + X_B + X_C} \qquad (3.4)$$

$$j = X_S \text{ or } X_B \text{ or } X_C$$

For the S*-A-C triangle, the three scales (χ_j) are defined as:

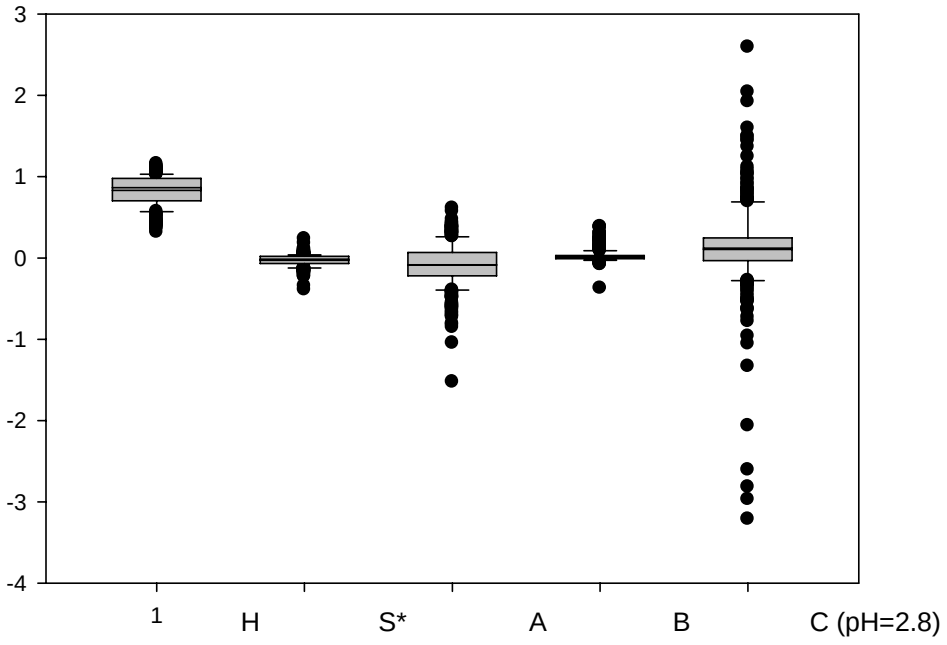

Figure 3. 2 Statistics of the phase coefficients for 366 reversed phases. Data provided by L. R. Snyder. The boundary of the box closest to zero indicates the 25th percentile, a line within the box marks the median, and the boundary of the box farthest from zero indicates the 75th percentile. Whiskers (error bars) above and below the box indicate the 90th and 10th percentiles. Dots above or below whiskers are outlying points.

$$\chi_j = \frac{j}{X_S + X_A + X_C} \qquad (3.5)$$

$$j = X_S \text{ or } X_A \text{ or } X_C$$

For the S*-A-B triangle, the three scales (χ_j) are defined as:

$$\chi_j = \frac{j}{X_S + X_A + X_B} \qquad (3.6)$$

$$j = X_S \text{ or } X_A \text{ or } X_B$$

Finally for the A-B-C triangle, the three scales (χ_j) are defined as:

$$\chi_j = \frac{j}{X_A + X_B + X_C} \qquad (3.7)$$

$$j = X_A \text{ or } X_B \text{ or } X_C$$

It must be stressed that the selection of the weighting factors is important. Initially, we tested the use of a set of weighting factors chosen so that the same numerical change in two different normalized phase properties had the same size effect on phase selectivity as measured by the s.e. values described above. These weighting factors were obtained as described in Appendix I and are summarized in 3.2. The triangles thus derived can be used directly to measure the phase selectivity differences between stationary phases, wherein the distance between two axis (e.g. $\Delta\chi_C$ =0.1 vs $\Delta\chi_A$ =0.1) in the triangle give the same effect on phase selectivity as indicated by equal standard errors in linear correlations of log k' vs. log k'. Unfortunately, as clearly shown in Figure 3.3, this approach to weighting results in a very "tight" clustering of all but the most extreme

phases over a rather small fraction of the plot. One major reason for this is centainly the dominant effect of ionized silanols (C), which has been previously noted by Cruz and Euerby through their principle component analysis of over 30 stationary phases [40] and by Marchant and Dolan where the average contribution of individual parameters H, S*, etc to column selectivity were calculated and compared for over 350 phases [35,36]. In our experience, in those triangles which include the coulombic interaction (i.e. all but the S*-A-B triangle), the C term always far outweighs the other parameters and thus dominates the denominator leading to small χ_S, χ_A and χ_B value. This renders the characterization and comparison of phase selectivity very difficult due to the superimposition of so many data points given the large number of stationary phases to be compared.

Consequently an alternative approach to the choice of weighting factors (see eq. 3.8) was developed to standardize each individual parameter by rescaling over the range of the phases of interest. As shown in eq. 3.8 and listed in Table 3.2, the application of the new set of normalized parameters maximizes the spread of the data points over the triangle. This facilitates visual differentiation of the phases. The resulting triangles are shown in Figure 3.4. Comparison of the two approaches to the weighting issue discussed above (see Figures 3.3 and 3.4) clearly shows that there is very tight clustering of many phases in both cases but there is a significant increase in the number of phases that are not in the cluster when the second approach is used. Consider the S*-B-C triangle as an example, the number of phases that can be clearly differentiated by the first approach is no more than 12; whereas for the second approach, at least 18 extreme phases can be

easily identified and the results are summarized in Table 3.4 and Figure 3.5. Since the triangles calculated with the second set of scaling factors provide a better view of the overall phase selectivity distribution as more individual phases can be recognized, we chose to use this approach to futher classify the selectivity of the reversed phases. However, it should be noted that this approach does not allow quantitative comparisons of the effect of differences in different phase parameters on phase selectivity as does the Snyder-Dolan F_s metric.

$$\phi_i = \frac{1}{I_{\max} - I_{\min}} \qquad (3.8)$$

$$i = \frac{S}{H} \text{ or } \frac{A}{H} \text{ or } \frac{B}{H} \text{ or } \frac{C}{H}$$

In this study, we included 366 reversed phases in toto. Among them, 209 are type-B silica based alkyl silica phases, 58 are type-A silica based alkyl silica phases, 44 are EPG (i.e. polar embedded or polar endcapped) phases, 20 are phenyl phases, 21 are cyano phases, 7 are fluoro phases, 3 are zirconia based stationary phases and 4 are a specialized type of polymer coated silica phases recently developed in our lab [66-69]. All these stationary phases were evaluated under acidic conditions, where the mobile phase pH is 2.8 controlled by a 30 mM phosphate buffer as described by Snyder et al. [50].

3.3 Results and Discussion:

The value of the triangle plots is self-evident. It is all too clear that a very large number of phases are clustered quite tightly in all four triangles. To put it another way *a*

huge fraction of the available space is under populated and certain regions are extremely over populated. A large number of similar pairs of phases exist.

3.3.1 Chemical Interpretation of the Triangles

The new set of selectivity parameters (χ_S, χ_A, χ_B, χ_C) reflect the relative ability of the stationary phases to separate solutes based upon steric hindrance, hydrogen bonding acidity/basicity and coulombic interactions. Thus within the same triangle, phases with large χ_C value will interact strongly with positive charged solutes through coulombic interactions. Similarly, phases with large χ_A, χ_B will interact relatively more strongly with proton acceptors, proton donors via hydrogen bonding. However, as discussed above, the selectivity parameters are normalized (eq. 3.8) to the range of the respective non-normalized parameters. Thus we must not think that the same numerical change in two different normalized parameters will have the same quantitative effect on selectivity.

Since the intermolecular interactions are primarily determined by the nature of the functional groups present on the stationary phases, we expected to find phases with the same chemical functionality in the same region of the selectivity triangle. As seen in Figure 3.6(a), this is generally the case for type-B alkyl silica phases. The majority of type-B alkyl silicas, with the exceptions of Platinum EPS C8 and Purospher C18 [70] (see Figure 3.6a), are very tightly clustered in the center of the triangle. This is consistent with many previous studies [50,71] and the common belief that many alkyl silica phases based on high purity silica are not very different and nearly interchangeable. However, for those types of phases derivatized with different surface chemistry (e.g. cyano, phenyl, fluoro, embedded polar groups) or based upon different substrates (e.g. Type-A silicas),

Table 3.2a Statistics of the relative selectivity parameters based on 366 RPLC stationary phases .

	S/H	A/H	B/H	C/H
Min	-0.391	-1.525	-0.373	-3.213
Max	0.235	0.611	0.384	2.593
Range	0.626	2.136	0.757	5.806

Table 3.2b Weighting factors to normalize the selectivity parameters in the selectivity triangles

	ϕ_S	ϕ_A	ϕ_B	ϕ_C
Snyder-Dolan's[a]	100	30	143	83
1st [b]	100	62	141	96
2nd [c]	100	29	83	11

[a] Coefficients reported by Snyder et al. [9];

[b] Weighting factors are calculated based upon the method of Appendix 1.

[c] Weighting factors are calculated based upon eq. 3.8 where the range of selectivity ratios was further normalized to ϕ_s =100.

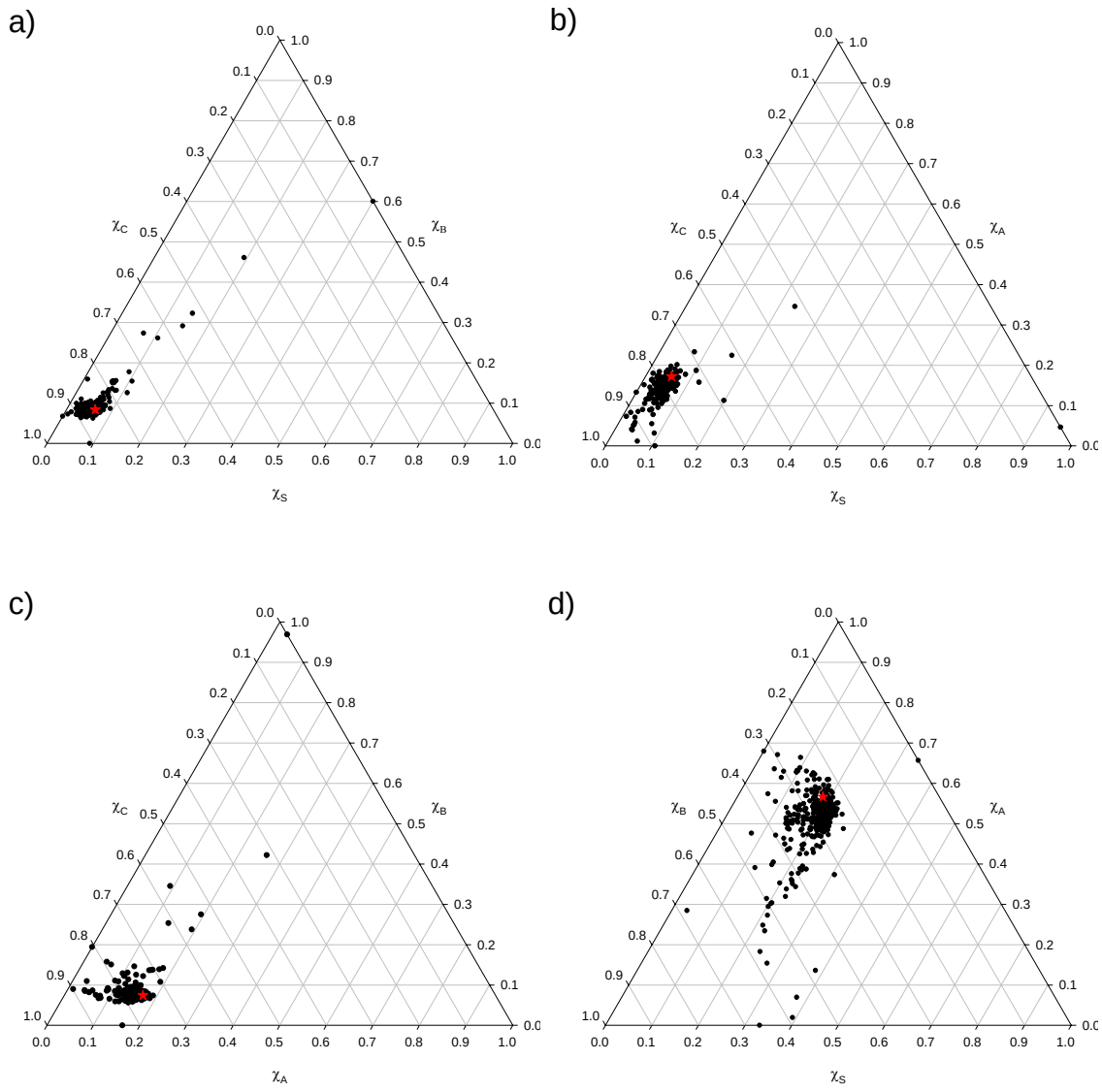

Figure 3.3 Selectivity classifications of 366 reversed stationary phases based upon the 1st set of weighting factor defined by standard error of linear regression. a) S*-B-C triangle; b) S*-A-C triangle; c) A-B-C triangle; d) S*-A-B triangle.

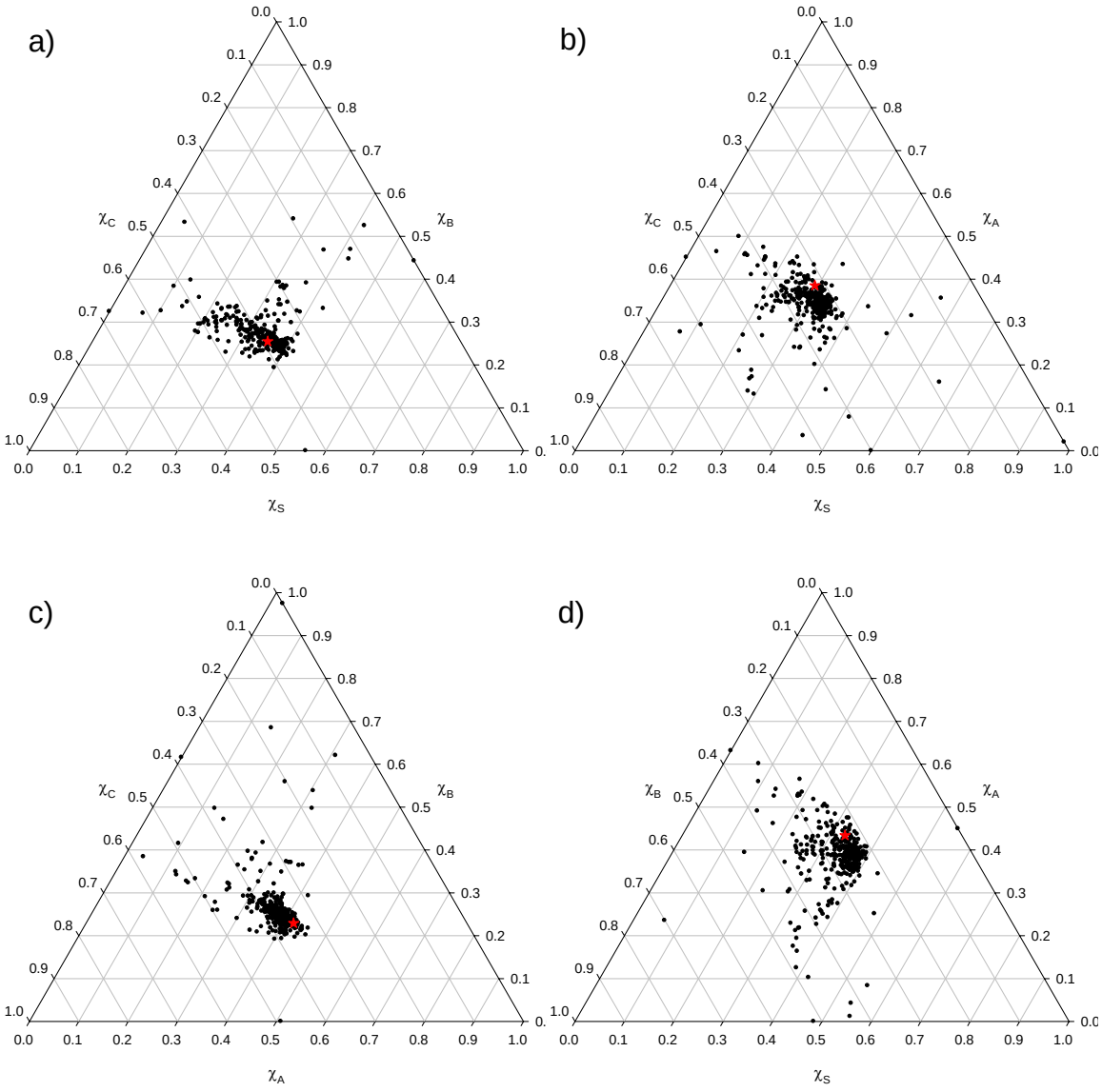

Figure 3.4 Selectivity classifications of 366 reversed stationary phases based upon the 1st set of weighting factor defined by range of stationary phases interested. a) S*-B-C triangle; b) S*-A-C triangle; c) A-B-C triangle; d) S*-A-B triangle.

differences in coefficients are generally quite large. Examples of cyano, phenyl and EPG phases are shown in Figure 3.6(b), where significant variability is seen between the individual data points for all three groups of stationary phases.

For EPG phases, this can be rationalized, at least in part by the fact that a wide variety of chemistries (e.g. amide, urea, carbamate) have been used to make these phases and thus the selectivity of EPG-columns is expected to vary with the nature of the polar group and whether that group is embedded in the chain or used to end-cap the column [15,41]. Nevertheless, upon choosing three EPG phases derivatized with the same group (an amide), we see that they are widely distributed over the triangle plot (see Figure 3.6(b)). Also there are significant differences in the example chromatograms shown in Figure 3.7. It is commonly believed that stationary phases with the same surface chemistry should have similar selectivity. However, the marked diversity observed here strongly suggests that the same surface chemistry does not guarantee the same phase selectivity. This is especially true for stationary phases with novel surface chemistries, as reported by many groups including Snyder and Marchand [46-49], Euerby and Petersson [72], and Neue and et al. [71].

We next compared stationary phases prepared with different chemical functionalities. More particularly type-B alkyl silica phases were compared with non-alkyl silica phases (e.g. cyano, phenyl, EPG, fluoro, Type-A), in this case, EPG phases (see Figure 3.8). Similarly, we expected to see different chemical types of columns occupying different positions in the triangles, reflecting their different chemical selectivities. However, it is surprsingly to see that some stationary phases from different

chemical groups actually lie close to one another and some occupy nearly the same space. Similar results have been shown by Layne wherein the retention of acidic and basic solutes on EPG and ODS columns were compared [41]. This suggests that *different surface chemistries of stationary phasse do not necessarily lead to different selectivity.* Clearly we must be cautious in using inferences based not on data but merely on differences in chemical functionality. This is well illustrated in Figure 3.9, where three columns, from very different chemical classes (i.e. an ACE AQ, an EPG phase; a Betasil Phenyl-Hexyl, a Phenyl phase; Bondclone C18, a Type-A alkysilica phase,) were selected based on their proximity to one another as indicated by the similarity of their coordinates (χ_S, χ_B, χ_C) in Table 3.3. As anticipated, the separation of a sample mixture on these three columns are all very similar as suggested by their near unity r^2 values and small s.e. values and also in agreement with their F_s values.

Even though many stationary phases are strikingly similar, there are nonetheless a reasonable number of phases that do spread over a fairly wide area that offer the possibility of very big differences in selectivities. The virtue of the triangle approach is that it allows the easy visualization of these extreme phases. The most "extreme" phases in all four triangles are summarized in Table 3.4 and examples are labeled in the S-B-C triangle as shown in Figure 3.5. The results here agree very well with conclusions obtained by Dolan et al. in a recent study [36]. It is clear that most of the extreme phases are non-type B alkyl silica columns. *For the purpose of finding "orthogonal" separations this set of phases are probably the best candidates.* It should be understood that this is a complex issue and is still understudy by us.

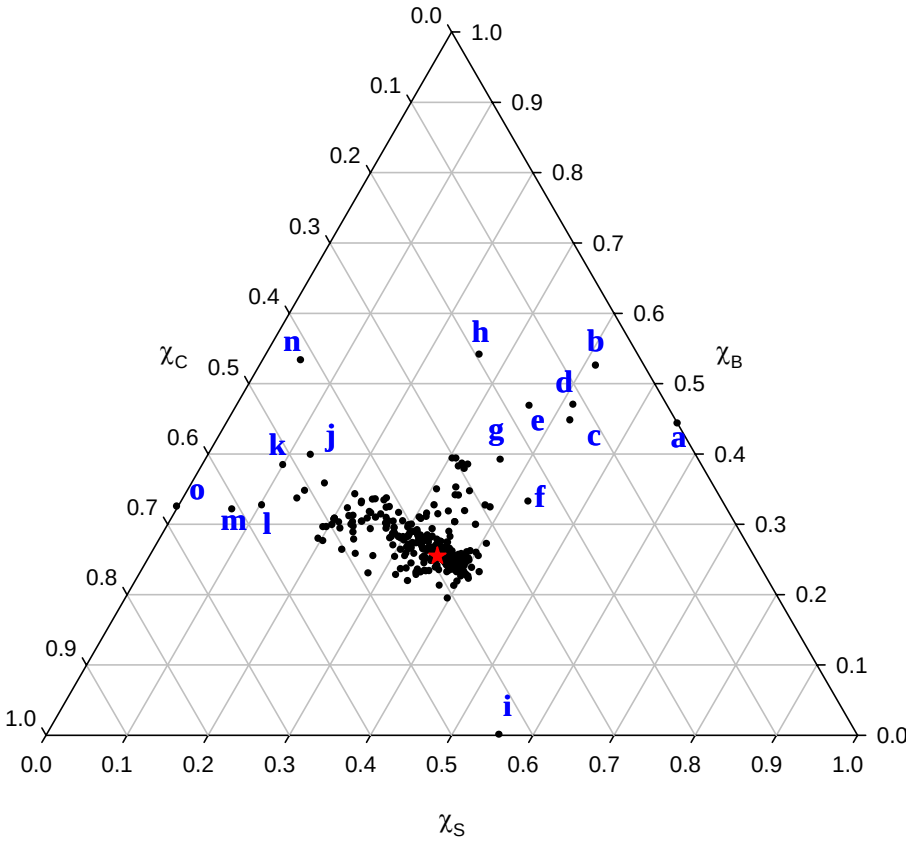

Figure 3.5 Placement of the extreme phases based on the S*-B-C triangle.

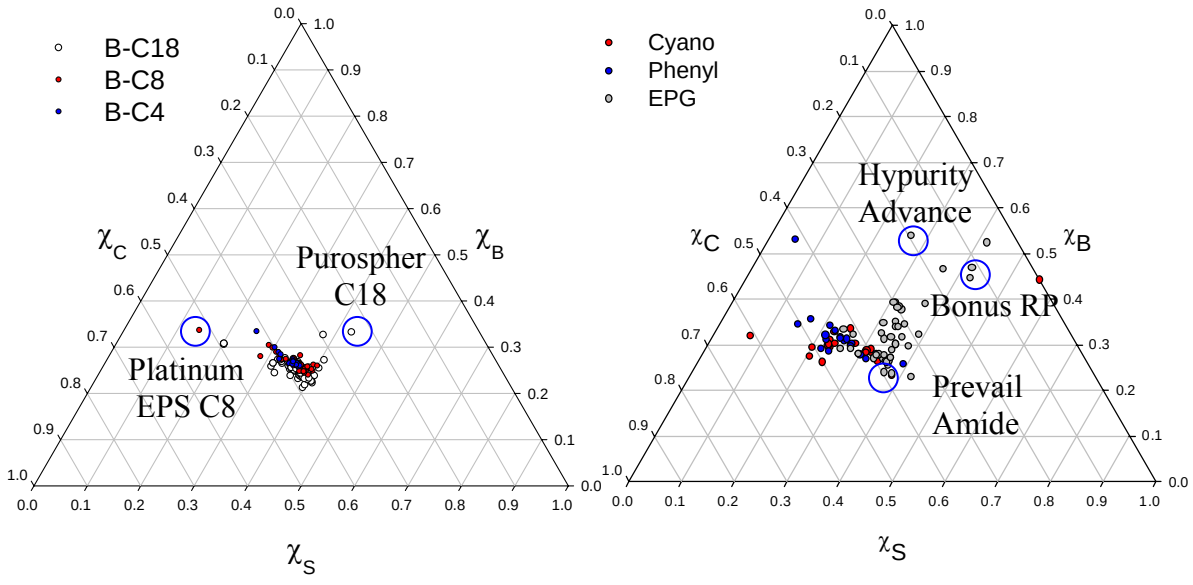

Figure 3.6 Selectivity classification of selected reversed stationary phases in the S*-B-C triangle.
(a) type-B alkylsilica phases;
(b) Embedded Polar Group phases, Cyano phases and Phenyl Phases.

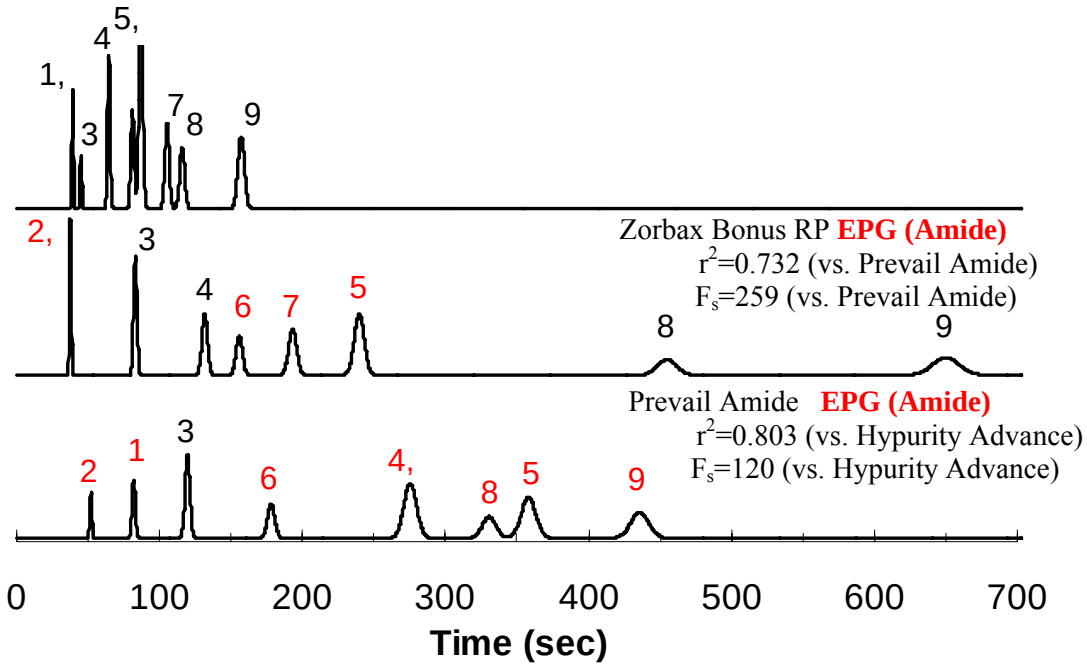

Figure 3.7 Comparison of selectivity for a given sample on three EPG phases of the same chemical type. Solutes: 1) amitriptyline; 2)N,N-dimethylacetamide; 3) acetophenone; 4) toluene; 5) trans-chalcone; 6) 5-phenylpentanol; 7) 4-n-butylbenzoic acid; 8) cis-chalcone; 9) mefenamic acid.
Experimental conditions: 50% acetonitrile/pH 2.8 buffer; 35 ◦C; 1.0 ml/min. r^2 value is compared with Hypurity Advance C18 column.

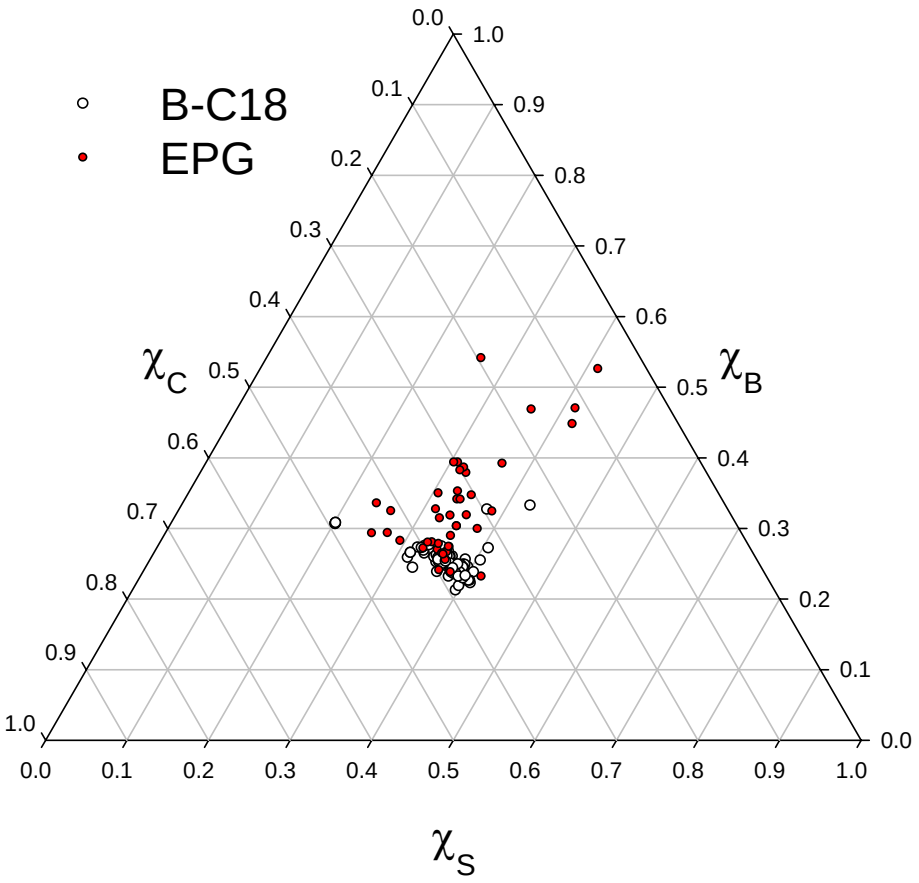

Figure 3.8 Selectivity comparison of type-B alkylsilica phases vs. EPG phases in the S*-B-C triangle.

3.3.2 Applications

3.3.2.1 Selection of "Equivalent" and "Orthogonal" columns;

The "triangle approach" developed here can be used in various ways. Basically, it classifies the selectivity of stationary phases based on their positions in these traingle plots. In other words, stationary phases with similar selectivity will be located close to one another; while stationary phases with "orthogonal" selectivity will be very far apart. Thus selection of an "equivalent" or "orthogonal" column is readily achievable by comparing the coordinates of the columns in the triangles. An example of choosing "equivalent" columns is shown in Figure 3.9 and summarized in Table 3.3; the result is consistent with the prediction from this approach. An example of the selection of "orthogonal" columns is given in Figure 3.10 using Zorbax StableBond C18 as the initial column. As noted above, "extreme" phases should be very good candidates for orthogonal separations due to their markedly different selectivity. Here we picked two extreme phases -- Hypersil Prism C18 RP and Purospher C18 to compare to the StableBond C18 phase. As expected there are significant differences in selectivity between the three columns; these differences are supported by the low r^2 value (see Figure 3.10). The results also agree well with the F_s factors of the S-D approach.

3.3.2.2 Potential Applications of the Stationary Phase Triangle

We believe that the visual display of information inherent in the set of triangle plots will prove to be useful for method development in HPLC. However this is a broad subject and a detailed presentation is beyond the scope of the present work which focuses on the basic development of the concept. At present we merely wish to suggest that these

phase selectivity triangles will be useful for picking phases that should be included in an initial column screening to make sure that columns with maximally different selectivities are included.

A second area of application is in the selection of the proper "orthogonal" pairs of columns to be used in two-dimensional liquid chromatography (2DLC) [73,74]. As Giddings has pointed out not only must the two separation mechanisms used differ but these differences must be complementary to the inherent dimensionality and differences in the properties of the analytes in the mixture [75]. As an example in the separation of complex mixtures of peptides, an ion exchange first dimension is coupled with a reversed phase second dimension separation [71-78]. Similarly if one had a sample whose analytes differed principally in hydrophobicity and in hydrogen bond basicity then one could based on the triangle locate a phase with average properties and pair it with a phase with high phase χ_A.

3.4 Conclusions

A set of four phase selectivity classification "triangle" plots have been developed based on the Snyder-Dolan Hydrophobic-Subtraction Model, wherein the apices of the triangles represent the relative contributions of steric hindrance (χS), hydrogen bonding acidity (χA), hydrogen bonding basicity (χB), coulombic interactions (χC) to phase selectivity. The real benefit of the triangle plots over previous approaches is that it allows the visualization of column selectivity for a large number of phases by plotting three-

Table 3.3 Candidate phases for orthogonal and equivalent separations.

	Column	H	S	A	B	C(2.8)	k'_{ref}	F_s	χ_S	χ_B	χ_C	R^{2a}	Type
Equivalent[b]	**ACE AQ**	0.804	-0.051	-0.129	0.034	0.009	5.0	0	0.335	0.279	0.386	1.000	EPG
	Betasil Phenyl-Hexyl	0.707	-0.053	-0.294	0.028	0.054	4.3	6.4	0.329	0.280	0.392	0.999	Phenyl
	Bondclone C18	0.824	-0.056	-0.125	0.044	0.078	4.5	6.0	0.329	0.283	0.387	0.998	C18-A
Orthogonal[c]	**Zorbax StableBond 80A C18**	0.996	-0.032	0.264	-0.001	0.136	7.6	0	0.355	0.255	0.390	1.000	C18-B
	Purospher RP-18	0.841	0.235	0.155	0.300	-0.964	4.9	104	0.429	0.331	0.239	0.798	C18-B
	Hypersil Prism C18 RP	0.645	0.089	-0.459	0.301	-2.817	4.8	250	0.423	0.447	0.130	0.752	EPG

[a] Chromatographic conditions: 50% acetonitrile/pH 2.8 buffer; 35 °C; 1.0 ml/min. Solutes: 1) 5-phenylpentanol; 2) amitriptyline; 3) acetophenone; 4) N, N-dimethylacetamide; 5) anisole; 6) 4-n-butylbenzoic acid; 7) cis-chalcone; 8) trans-chalcone; 9) mefenamic acid;

[b] F_s and R^2 are obtained by comparing with ACE AQ as reference.

[c] F_s and R^2 are obtained by comparing with Zorbax StableBond C18 as reference.

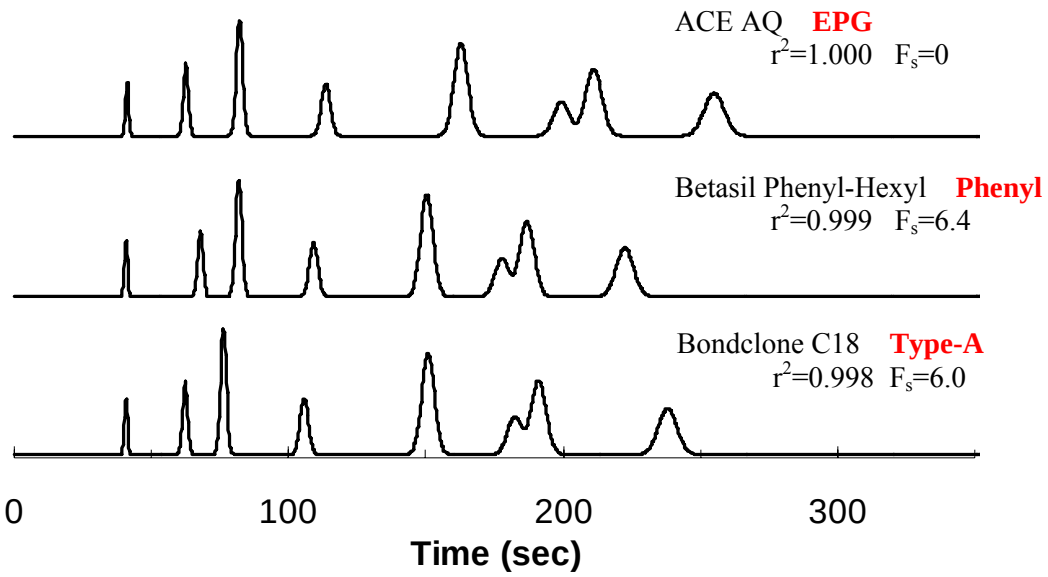

Figure 3.9 Comparison of selectivity for a given sample on three stationary phases of different chemical types. Chromatographic conditions are the same as in Fig. 6. The same set of solutes were used but the elution order is different as follows: 1) N,N-dimethylacetamide; 2) amitriptyline; 3) acetophenone; 4) 5-phenylpentanol; 5) 4-n-butylbenzoic acid; 6) toluene; 7) cis-chalcone; 8) trans-chalcone; 9) mefenamic acid. r^2 value is compared to the ACE AQ column. Note that components 5 and 6 overlapped and thus show as a single peak in all of the three chromatograms.

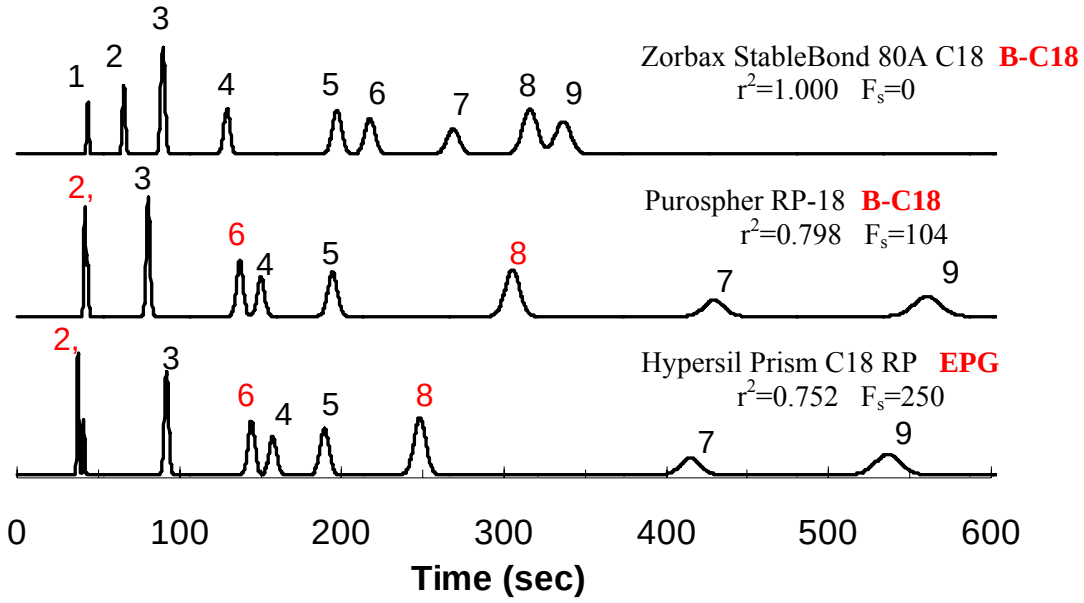

Figure 3.10 Comparison of column selectivity on two extreme phases vs. Zorbax StableBond C18 phase. Chromatographic conditions are the same as in Fig. 6. The same set of solutes were used but the elution order is different as follows: 1) N,N-dimethylacetamide; 2) amitriptyline; 3) acetophenone; 4) 5-phenylpentanol; 5) 4-n-butylbenzoic acid; 6) toluene; 7) cis-chalcone; 8) trans-chalcone; 9) mefenamic acid. r^2 value is compared to the Zorbax StableBond C18 column.

Table 3.4 Summary of Extreme phases based on the four triangles [a.]

Labels	Stationary phases	Types	Extreme phases on triangle			
			S-B-C	**S-A-C**	**S-A-B**	**A-B-C**
a	Inertsil CN-3	Cyano	√	√	√	√
b	EC Nucleosil 100-5 Protect	EPG	√	√	√	√
c	Hypersil Prism C18 RP	EPG	√	√	√	√
d	Bonus RP	EPG	√	√	√	√
e	BetaMax Acid	EPG	√	√	√	√
f	Purospher RP-18	B-C18	√	√		√
g	Discovery HS PEG	EPG	√	√	√	√
h	Hypurity Advance	EPG	√	√	√	√
i	Vydac 218MS	A-C18	√		√	√
j	HC-OH	Special	√		√	
k	HC-C8	Special	√		√	
l	ZirChrom-PS	Special	√	√	√	√
m	Nova-Pak CN HP 60A	Cyano	√	√	√	
n	BioBasic Phenyl	Phenyl	√	√	√	√
o	$^{-}SO_3$-HC-C8	Special	√	√	√	
	Inertsil Ph-3	Phenyl			√	
	Prodigy Phenyl-3	Phenyl			√	
	Platinum EPS C8	B-C8			√	
	HC-T	Special			√	

ProntoSil CN	Cyano	√		√
Kromasil KR60-5CN	Cyano		√	√
Discovery CN	Cyano	√	√	√
Genesis CN 300A	Cyano	√	√	√
Genesis CN 120A	Cyano	√	√	√
Thermo CN	Cyano		√	√
ACE 5CN	Cyano	√	√	√
Inertsil ODS-EP	B-C18	√	√	√
Prontosil 120-5-C8 ace-EPS	EPG	√	√	√
BioBasic CN	Cyano	√	√	√
ZirChrom-EZ	Special	√	√	√
Precision CN	Cyano	√	√	
ZirChrom-PBD	Special		√	
Spherisorb S5 ODSB				√
Nucleosil 100-5-C18 Nautilus				√
Hypersil Prism C18 RPN				√
Alltima HP C18 Amide	EPG			√

[a]. All phases which we consider to lie well outside the main cluster in any of the four triangles are listed here. Many of the phases appear in several triangles. Some show up in all four triangles, very few are present in only a single triangle. Note these are not necessarily “unique” phases as they may well have close neighbors.

dimensional selectivity data in a two-dimensional space. It very clearly shows that the 366 RPLC columns studied here cover only a small fraction of the currently available phase selectivity space leaving a great deal of room for researchers to develop novel rather than more redundant phases. Moreover, this approach to selectivity characterization as applied to the non-alkysilica phases clearly shows that the same surface chemistry (functionality) does not guarantee the same phase selectivity. In contradistinction, the comparison of phases with different chemical functionalities just as clearly shows that different surface chemistry does not necessarily lead to different phase selectivity. Selection of columns of either equivalent or different selectivity is readily achievable with the application of the set of four "selectivity triangles" based on the Snyder-Dolan Hydrophobic-Subtraction approach. It provides an informative and universal approach to classifying the currently characterized set of reversed phases. The most different phases of the 366 phases are listed here.

Chapter 4

Optimization of the Synthesis of Hyper-Crosslinked Stationary Phases– A New Generation of Highly Efficient, Acid Stable Hyper-Crosslinked Materials for HPLC.

4.1 INTRODUCTION

Higher separation efficiency and faster speed have always been of great interest in HPLC and have become increasingly important in recent years mainly driven by the challenge of either more complex samples or growing numbers of samples [1]. Many approaches have been developed as potential solutions including sub-2 μm particles at ultra-high pressure [2,3], monolithic columns [4], the superficially porous stationary phases [5] and high temperature[6-8]. Among these techniques, the use of high temperature especially for fast analysis has recently drawn a lot of attention. In fact, the potential of high temperature liquid chromatography has been demonstrated by Chen and Horvath almost twenty years ago, where they successfully separated a mixture of four proteins within 10 seconds at 120 ºC [6]. The major improvement of this experiment was the substantial reduced total analysis time when compared to typical 30-minutes run. This is mainly achieved by the use of high temperature (120 degree). In particular, increasing the temperature can lead to a decrease in the viscosity of the mobile phase and concomitant reduction of system backpressure. The lower backpressure can then enable the use of higher flow rate (i.e. 5ml/min in Chen's work) for faster analyses [9]. In

addition, the reduced viscosity also allows faster diffusion of analytes, thereby improving the mass transfer of solutes in and out of stationary phases [9]. Consequently, ultra fast separation could be achieved without increasing the back pressure or losing efficiency [7,8]. With the high temperature ultra fast separations, the throughput and the efficiency of analysis could be dramatically improved [10-12]. Also with the ultra fast high temperature separation as the second dimension, a LC*LC system could provide a significantly improved resolving power than one-dimensional HPLC system in analyzing protein and peptide samples [13]. However, the use of high temperatures requires that stationary phases used in the second dimension separations be very stable, especially when a buffered eluent is required. Unfortunately, only a few of the very large number of commercially available silica-based stationary phases meet this requirement.

As a result, a novel type of acid stable, silica-based platform has been developed in our laboratory [14-17]. Orthogonal polymerization reactions are used to prepare a *very thin layer* of hyper-crosslinked (HC) aromatic network that is entirely confined to the silica surface. Outstanding stability has been achieved due to the formation of extensively *networked* polymers. At the same time, the excellent mass transfer properties of monomeric bonded phases were preserved and none of the adverse kinetic effects [18-20] of depositing a polymer have been observed. The stability and efficiency afforded by these novel phases make them good candidates for use as the stationary phase for the second dimension column of 2DLC. However, since the Friedel–Crafts (F-C) chemistry we use to synthesize the HC phases is complicated and involves many experimental variables (reaction temperatures, catalyst concentration, reaction times, catalyst types,

and crosslinker types), optimization of the synthesis is needed to effect further improvements in column efficiency and acid stability of the HC phases.

Previously, the effect of catalyst type and silica substrate were studied in this lab [15,17]. The very high silanophilicity of our first generation of HC phases evident in the poor plate numbers for basic solutes [15-17] synthesized by using aluminum trichloride as the F-C catalyst and a relatively active silica as the substrate, was primarily due to the activation of some silanol groups caused by contaminating the silica with traces of aluminum (III) and the intrinsic high activity of the type of silica used. The problem was essentially solved by replacing aluminum trichloride with tin tetrachloride (a less reactive but still effective F-C catalyst [15]), and by using a better grade of HPLC silica. The plate count of organic bases on a 5.0 cm × 0.46 cm column increased from 2100 to 3700 upon use of the tin catalyst, and from 3700 to 4600 upon the additional change to the less active silica substrate. The phase thus prepared is denoted as the second generation of HC phases. Although more than twice as many plate counts for basic drugs were achieved on these second generation of HC phases than were on the first generation of HC phases, studies in this lab suggested that tin(IV) contamination still took place during the synthesis[14,15]. This became evident when a mixture of peptide standards were separated on the HC phases, considerably wider peak widths (20-30%) and lower plate counts were observed on these phases when compared to conventional bonded C18 columns [21,22]. In addition, the positive charges due to the presence of metal ions also affect the performance of an ion exchange phases based on the HC platform [21], producing peak tailings and irreproducible retentions of analytes which could chelate metals (i.e. catecholamine). In this work, kinetic studies have been performed to

investigate each step of the F-C reactions to further optimize the 2nd HC phases. Effects of reaction times and crosslinking reagents were investigate to minimize the silanolphilicity of the HC phases by improving the synthesis conditions. The resulting third generation of HC phases will be denoted as the "HC-T" phase since in the last step it is derivatized with toluene in contrast to the second generation phase which is called the "HC-C_8" phase, derivatized with an octyl phenyl group. It should be point out that the purpose of this study is to identify a set of synthetic conditions that allows us to further reduce metal contamination during the development of HC phases. Thus the kinetics studies as well as the synthesis of the HC-T phase were mainly performed on Zorbax silica. Previous work in this lab had already demonstrated that this type of silica typically shows a relatively strong silanol activity and thus does not perform as well as some silicas made with lower activity [15]. This provides us with considerable additional potential for further improving the HC-T phase by simply choosing alternative underlying silica with lower silanol activity.

4.2 Experimental

4.2.1 Chemicals

All solvents used in this work were HPLC grade. Acetonitrile (MeCN) was obtained from Burdick and Jackson (Muskegon, MI). Dichloromethane was obtained from Mallinkrodt-Baker (Paris, KY). 1, 2-Dichloroethane was obtained from Sigma (St. Louis, MO). Tetrahydrofuran (THF) was obtained from EM Science (Gibbstown, NJ). Acetone, methanol (MeOH), and isopropanol (IPA) were obtained from PharmCo (Brookfield, CT). TFA, toluene, triphenylmethane (TPM), chloromethylmethyl ether

(CMME), 2, 4, 6-tris (bromomethyl) - mesitylene (TBM) and $SnCl_4$ (99%) was obtained from Aldrich (Milwaukee, WI). Dimethyl-chloromethylphenylethylchlorosilane (DMCMPES) was obtained from Gelest Inc. (Tullytown, PA). HPLC water was prepared by purifying house deionized water with a Barnstead Nanopure II deionizing system with an organic-free cartridge and run through an "organic-free" cartridge followed by a 0.45 μm Mini Capsule filter from PALL (East Hills, NY).

All chromatographic solutes were obtained from Aldrich or Sigma. Polystyrene standards were obtained from Polyscience, Inc. (Warrington, PA) and dissolved in pure THF at a concentration of approximately 0.5 to 2 mg/ml.

Type-B Zorbax silica particles and SB C_{18} particles were gifts from Agilent Technologies, Inc (Wilmington, DE). The particle diameter, surface area, and pore diameter of the particles are 5.0 microns, 180 m^2/g, and 80 Å respectively.

4.2.2 Kinetic Studies

Primary Crosslinking: 1-g of Type-B Zorbax silica that had been silylated with DMCMPES was slurried in 10 mL of fresh 1, 2-dichloroethane. The slurry was sonicated under vacuum in a 50 mL round bottom flask for 15 minutes to fully wet the pores. After sonication, 1.2 mmol styrene heptamer or 2.4 mmol TPM were added to the stirred slurry together with 0.1mmol nitrobenzene as an internal standard. The reaction mixture was then heated and refluxed at 80 °C. Before adding any catalyst, a small amount of sample was taken by syringe to serve as a blank before adding any catalyst. Then 5mmol of $SnCl_4$ were added to the slurry and served as the F-C catalyst. An activated alumina column was used to close the condenser to prevent water contamination from lab air.

After 0.5, 5, 15, 60 minutes, samples were taken and quenched with MeCN-water (70:30). The mixture was then filtered and analyzed by HPLC.

Secondary Crosslinking: 1-g of starting material (Type-B Zorbax silica first silylated with DMCMPES and then reacted with SH for 15 minutes) was slurried and sonicated in 10 mL of fresh 1, 2-dichloroethane as described above. 5mmol CMME or 1.8mmol TBM were added to serve as the secondary crosslinking reagent. The reaction vessels were the heated and refluxed at 50 °C. Before adding any catalyst, a small amount of sample was taken as blanks. Then 5mmol $SnCl_4$ were added to serve as the F-C catalyst. An activated alumina column was used to cap the condenser. After 15, 30, 45, 60 and 90 minutes, samples were taken and filtered. The silica particles were washed sequentially with 350 mL aliquots of dichloromethane, THF, MeOH, MeOH/water, and acetone. After washing, the silica was dried under vacuum at 60 °C. A small fraction (~0.1g) of the silica sample was sent for elemental analysis. It should be point out that CMME is a highly volatile, strong alkylating agent with known toxicity. Thus all the reactions were performed in a hood with great caution taken when handling this chemical.

Third Derivatization: 1-g of starting material (Type-B Zorbax silica that has been silylated with DMCMPES, reacted with TPM for 15 minutes and then TBM for 45 minutes) was slurried and sonicated in either 10 mL of 1,2-dichloroethane or toluene. Then 5mmol octylbenzene were added to the slurry. The reaction vessels were then heated and refluxed at 80 °C. Before adding 5mmol $SnCl_4$ as the catalyst, a blank sample was taken. An activated alumina column used to close the condenser during the reaction. Samples were taken and filtered at 10, 20 and 30 minutes. Before elemental analysis, the silica was washed and dried as describe above.

4.2.3 Stationary Phase Synthesis

Both HC phases were prepared by a series of three $SnCl_4$ catalyzed Friedel-Crafts alkylations on Type B Zorbax silica that has been silylated with DMCMPES. The detailed reaction conditions to prepare HC-C_8 are summarized in Table 4.1 and can also be found in our previous publications[15]. To synthesize the HC-T phase, the first reaction used TPM at a molar ratio of 6:1 TPM: initial surface DMCMPES groups (i.e. 18:1 phenyl rings:surface chloromethyl groups) to crosslink the surface bound chloromethyl groups on the silylated silica.. The reaction was stopped after 15-minutes of refluxing at 80 °C. In the second step, we used a four fold molar excess of TBM relative to the amount of surface chloromethyl groups to further crosslink the surface aromatic groups and simultaneously provide additional chloromethyl functionalities for further derivatization. This reaction was done at 50 °C for 45 minutes. In the last step, toluene was used as both solvent and alkylating reagent to react with the residual chloromethyl groups for 10 minutes at 80 °C.

Before each F-C reaction, the slurry was sonicated under vacuum for 15 minutes before each step to fully wet the particle pores. To prevent atmospheric water from deactivating the catalyst, we used an alumina column to close the condenser during the synthesis. After each Friedel-Crafts step, the particles were filtered and washed sequentially with 350 milliliters of fresh 1, 2-dichloroethane, tetrahydrofuran, tetrahydrofuran with 10% concentrated hydrochloride, tetrahydrofuran, MeOH, and acetone. At the end of the washing sequence, the stationary phase was air dried overnight at room temperature before the next step was performed.

4.2.4 Acid Pretreatment

After synthesis, the hyper-crosslinked phase HC-T, was pre-conditioned by gradient acid (5% TFA) washing at 150 °C as described in our previous publications[15,17]. The purpose of this aggressive gradient acid washing is to: 1) remove residual tin(IV) introduced during the Friedel-Crafts reactions, 2) hydrolyze residual chloromethyl groups and the labile Si-O-Si bonds to prevent their slow hydrolysis over time during use, and 3) to eliminate incompletely crosslinked organic surface moieties. After gradient washing, the column was flushed with 50/50 IPA/H_2O thoroughly and then unpacked to dry the particles inside.

4.2.5 Elemental Analysis

A small amount of stationary phases after each step was sent for carbon, hydrogen, bromine and chlorine analysis conducted by Atlantic Microlabs, Inc. (Norcross, GA).

4.2.6 Column Packing

HC particles were packed into a 5.0 × 0.46 cm column for further characterization. The particles were slurried in IPA (1.0 g/8.0 mL) and sonicated for 20 minutes prior to packing. Columns were packed by the downward slurry technique using He gas to drive a high pressure pump (Haskel 16501, Haskel International Inc.; Costa Mesa, CA) and push IPA through the column. The packing pressure was increased from 3000 psi to 6000 psi within the first 5 seconds and then kept at 6000 psi until about 90 mL of solvent were collected before the pressure was released.

4.2.7 Acid stability test

Dynamic stability tests were performed on a 5.0 cm × 0.21 cm HC-T column. A 50/50 (v/v) MeCN/H_2O with 5% trifluoroacetic acid (pH=0.5) mobile phase flowed

through the column at 150 °C for more than thousand column volumes. The relative retention of a neutral probe was monitored and used to evaluate the stability of the phase

4.2.8 Inverse size exclusion chromatography (ISEC)

ISEC were performed on a 5.0 cm × 0.46 cm HC-T column and a 5.0 cm × 0.46 cm column packed with bare Zorbax silica. A series of low polydispersity polystyrene standards (M_w = 300, 2727, 4000, 13.7×10^3, 18.7×10^3, 30×10^3, 50×10^3, $10\times10^6$and 20×10^6 Da) were tested on both columns with 100 % THF as the eluent. The columns were thermostated at 40 °C and the flow rate was at 1.0 ml/min. Toluene was injected as the marker to measure the void volumes of the two columns. The diameter of the polystyrene probes was calculated using the method of Halasz and Martin[23,24]

4.2.9 SEM Experiments

SEM analysis was performed on bare Zorbax silica, HC-T phase and HC-T phase after HF digestion. The last sample was prepared by adding 0.5 mL of 48% HF (ultra-high purity, 10-fold molar excess relative to the silica) into slurry of 0.1g of HC-T particles fully wetted by 10 mL of MeOH: water (50:50). The slurry was shaken and then allowed to settle for five minutes before 0.1 g of boric acid was added with 9.5 mL water. These treated particles were washed extensively with 50/50 (v/v) MeOH/water and pure MeOH before they were dried at 60 ºC under vacuum. 0.1 g of bare silica, untreated HC-T particles and HF treated particles were then evenly deposited onto carbon tape and coated with 100 Å of platinum. The SEM images were taken with JEOL 6500 (Characterization facility, University of Minnesota, MN) with 10.5 mm working distances (WD) and 5 kV accelerating voltages. Magnification was set to be 5000× for all samples.

4.2.10 Chromatographic Conditions

All chromatographic experiments were carried out on a Hewlett-Packard 1090 system, equipped with a binary pump, an autosampler, a temperature controller and a diode array detector (Hewlett Packard S.A., Wilmington, DE). Data were collected and processed using Hewlett Packard Chemstation software. The solutes were prepared in ca. 1 mM 50/50 MeCN/H_2O solutions and the injection volume was 0.5 μL.

4.3 Results and Discussion

Previous studies [15] in this lab suggest that the synthetic conditions of the three F-C steps are critical to the performance of final HC phases. In particular, the changes in the specific F-C catalyst used and the specific silica substrate used can significantly reduce the effect of the metal contamination on silica's surface and thus improve the separation efficiency of the HC phases as discussed above[15,17]. To further reduce tin(IV) contamination and optimize the synthesis conditions, a study of all permutation of other synthetic variables (e.g. reaction time, the concentration and the type of reagent) are clearly necessary to fully explore and understand all of the key experimental variables involved. As a result, a detailed kinetic study has been done to determine the effects of the crosslinking reagents and reaction time on the performance of final stationary phases while the catalyst amount was held constant. However, it is important to note that all optimizations must be done without sacrificing the crosslinking efficiency and acid stability of HC phases.

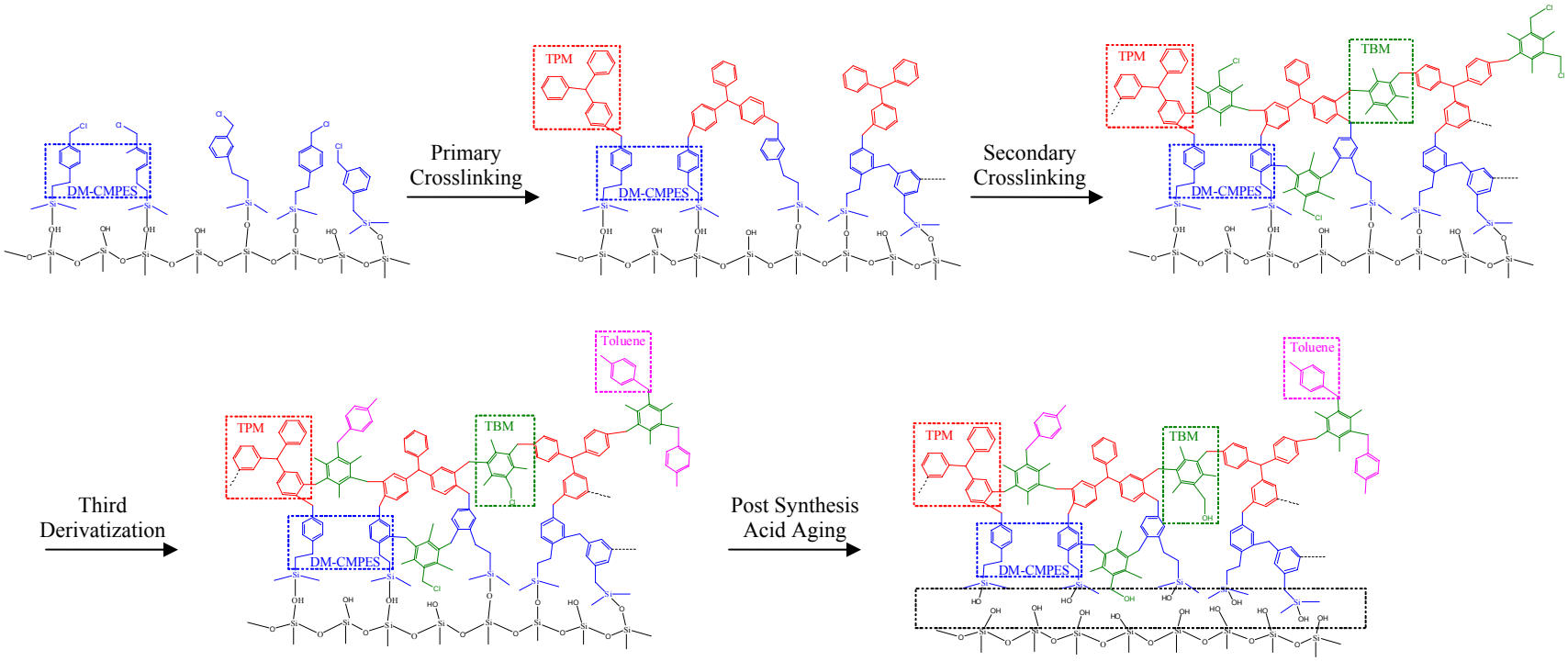

Figure 4.1 Synthesis scheme for the HC-T phase

Table 4.1 Summary of synthetic conditions and separation efficiencies of various HC phases.

Stationary phase[a]	catalyst	reaction reagent			reaction time (mins)			reaction temperature (ºC)			Efficiency[b] (plate count/meter)	
		step 1	step 2	step 3	step 1	step 2	step 3	step 1	step 2	step 3	Aceto-phenone[c]	Amitri-Ptyline[d]
SB-C_{18}	N/A	N/A	N/A	N/A	N/A	N/A	N/A	N/A	N/A	N/A	4500	2750
HC-C_8	$SnCl_4$	SH	CMM E	Octyl-benzene	180	90	30	80	50	80	5100	2980
HC-T	$SnCl_4$	TPM	TBM	Toluene[e]	15	45	10	80	50	80	5100	3940

a. For all crosslinking reactions, 10 fold $SnCl_4$ relative to surface DM-CMPES was used to catalyze all reactions. All reactions were done in 1, 2-dichloroethane.Detection limit is 0.25% (wt/wt). All of these columns are based on Zorbax silica.

b. Chromatographic conditions: All separations were performed at 40 ºC, F = 1.0 mL/min, 0.5 - 1.0 nanomole of nortriptyline was injected. However, %ACN was varied to make k' similar on two phases. For SB C18 phase, mobile phase: 0.1% formic acid in 38/62 ACN/water; For HC-C8 phase, mobile phase: 0.1% formic acid in 31/69 ACN/water; For HC-T phase, mobile phase: 0.1% formic acid in 29/71 ACN/water.

c. Acetophenone: neutral compound.

d. Amitriptyline: Basic compound.

e. Toluene was used as solvent.

4.3.1 Effect of Crosslinking and Derivatization Reagents

4.3.1.1 Optimization of New Crosslinking Reagents

As shown in Table 4.1, in the first F-C step, the styrene heptamer was initially used as the primary crosslinker based on its high reactivity and multiple reactive phenyl groups available for alkylation. However, one of our major concerns with this chemical is the fact that it is not a pure compound but rather a mixture of styrene oligomers with different chain lengths (n = 4, 5, 6, 7, 8…). This chemical complexity, together with batch–to–batch differences from the manufacture can lead to irreproducibility of the HC phases thus prepared. Moreover, the relatively low solubility associated with the higher molecular weight fractions limits the highest concentration that we could use and thus limits the overall speed of reaction. In an effort to solve these problems, an alternative crosslinkable aromatic compound, triphenyl methane (TPM) was proposed and tested based primarily on its chemical simplicity and high solubility. As shown in Figure 4.2, TPM is also a multi-valent reagent with the same reactive functionality, i.e. phenyl rings, as styrene heptamer. Therefore, we expected to see comparable reactivity with TPM as for the long chain oligomers. Indeed, very similar patterns were observed in both kinetic plots as shown in Figure 4.3a, suggesting that TPM is as good as styrene heptamer but with higher purity and better solubility.

Even though the secondary crosslinker CMME had shown exceptional alkylating activity and provided highly efficient crosslinking in the second step of FC reactions, it is a highly volatile reagent with known carcinogenicity. This strongly restricts the use of CMME in practice, especially at evaluated temperatures with high concentrations. In addition, when handling this type of chemical great caution needs to be taken due to its

toxicity and volatility. With all these concerns, we decided to test 2, 4, 6-tris(bromomethyl)-mesitylene (TBM) as an alternative secondary crosslinker. The major advantage of TBM over CMME is that it is a non-volatile thus less hazardous but still a strong alkylating reagent. As shown in Figure 4.3b, there are three reactive -CH_2Br groups in each molecule, thus we anticipated that TBM would be more effective as a crosslinker than CMME; it could provide a higher extent of crosslinking and thereby generate a more extensively crosslinked polymer network and perhaps better acid stability. In addition the higher reactivity of -Br vs. -Cl [25] makes it possible that a reasonable crosslinking degree would be achieved under milder reaction conditions (e.g. shorter reaction times), thereby reducing the effect of tin(IV) contaminations. However, to our surprise, considerably slower reaction kinetics were observed with TBM when compared to that of CMME (see Figure 4.3b). For example, after an hour of reaction with surface phenyl rings, there were only 1.0 ± 0.1 μmol/m^2 of TBM attached to the aromatic network based on carbon content analysis, which was 60% less than the loading density of CMME (i.e. 2.7 ± 0.1 μmol/m^2). One potential cause of this slow reaction kinetics is the low solubility of TBM in the solvent 1, 2- dichloroethane. In fact, the amount of TBM used in the kinetic study was only 1/3 compared to CMME. The dramatically decreased concentration of TBM vs. CMME can cause significantly lower reactivity for TBM as measured by the number of molecules reacted per unit time. Another possible reason is the size differences between two molecules. As shown in Figure 4.2, TBM is clearly bulkier with twelve carbons when compared to CMME. Such structure can generate steric problems in the reaction and thereby lead to slower kinetics on the silica surface. Nevertheless, we felt the reactivity of TBM was sufficient for the formation of a surface

polymer network; ultimately this was confirmed by the SEM images and will be discussed in detail later. Thus we decided to use TBM in place of CMME in our modified synthetic scheme.

4.3.1.2 Optimization of New Derivatization Reagents

For the last step of phase derivatization we also employed F-C chemistry mainly because it allows us to easily introduce different functionalities into the surface aromatic groups. Thus we can potentially produce a wide variety of stationary phases with diverse chromatographic selectivities. During the development of the second generation of HC phases, octylbenzene was attached to the surface polymer scaffold to produce a reversed type phase (i.e. the HC-C_8 phase). However, as noted above, a chemical reagent with higher reactivity is more favorable since it can facilitate the completion of reaction under a milder reaction conditions. Thus we decided to test toluene since not only it can be used as a reagent, but more importantly, it can also be used at very high concentration by taking it as the solvent for the third F-C step. The kinetics of the modified reaction are shown in Figure 4.3c, together with that of the original F-C reaction using octylbenzene. As expected, due to the dramatically increased concentration (at least an order of magnitude) of toluene vs. octylbenzene, the optimized reaction is much more effective as indicated by almost two fold increase in the number of molecules reacted.

4.3.2 Effect of Reaction Time

During the kinetic studies, we made a very important observation. Even with a mild Lewis acid such as tin (IV) chloride as the catalyst, to our surprise, the kinetics of the F-C reactions were much faster than we had expected. Specifically, for the primary F-C crosslinking and the tertiary F-C derivatization, the reactions were nearly complete

within the first 15-20 minutes; while for the secondary F-C crosslinking step, even though both CMME and TBM were still reacting at 90 minutes, the bulk the of carbon added (~80%) was loaded onto the surface within the first 45 minutes. This discovery allowed us to synthesize our HC phases using much shorter reaction times thereby greatly decreasing the exposure of the silica to metal ions without sacrificing degree of crosslinking, that is a network polymer was still formed, and acid stability (see below).

4.3.3 Synthesis and Elemental Analysis of the HC-T Phase

The synthesis scheme for the HC-T phases and the phase structure at each step are shown in Figure 4.1. In order to understand this complex, multi-step synthesis, the product of each stage in the reaction was characterized by elemental analysis and compared with that of the HC-C_8 phase (see Table 4.2). Since the chemicals and reaction time in each step are now different, consequently the absolute carbon loading on these two HC phases are different. In order to make a fair comparison of the relative success of each step of the synthesis for both the HC-C_8 and HC-T phases, "loading density" was calculated based upon the number of moles of carbon added during the reaction[15],

$$\mu mol/m^2 = \frac{(\%^2C - \%^1C) \times 10^6}{12 \times Nc \times (100 - \%^2C - \%^2H - \%^2Cl)} \times \frac{1}{S} \qquad (2)$$

$\%^1$C: the percentage of carbon before crosslinking.
$\%^2$C: the percentage of carbon after crosslinking.
$\%^2$H: the percentage of hydrogen after crosslinking.
$\%^2$Cl: the percentage of chlorine after crosslinking.
N_C: number of carbon atoms per crosslinker molecule.

The results are summarized in Table 4.3. After primary crosslinking, there were 0.25 μmoles/m^2 of TPM loaded onto silica on the HC-T phase while 0.20 μmoles/m^2 of SH groups were added to the HC-C_8 phase. The result obtained here agrees very well

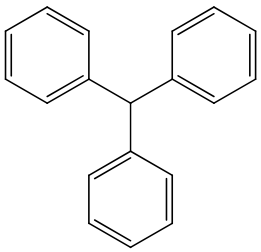

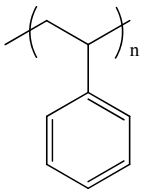

n=4, 5, 6, 7, 8 ….

Triphenyl methane (TPM)

Styrene heptamer (SH)

(a)

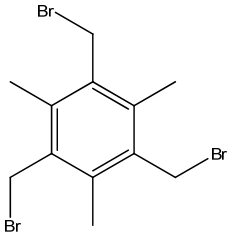

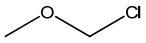

2, 4, 6-tris(bromomethyl)-mesitylene (TBM)

chloromethylmethyl ether (CMME)

(b)

Figure 4.2 Molecular structures of crosslinking reagents in F-C reactions and kinetic studies.
a) Primary crosslinker; b) Secondary crosslinker

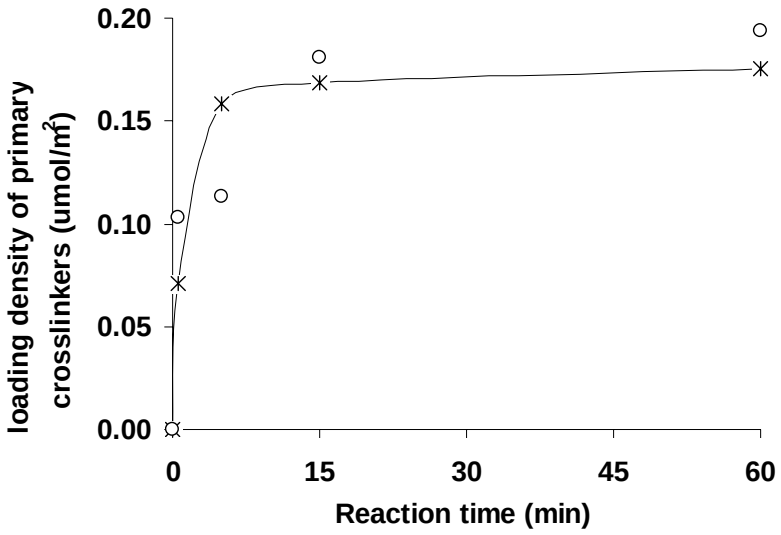
0.20
0.15
0.10
0.05
0.00
loading density of primary crosslinkers (umol/m2)
0
15
30
45
60
Reaction time (min)

(A)

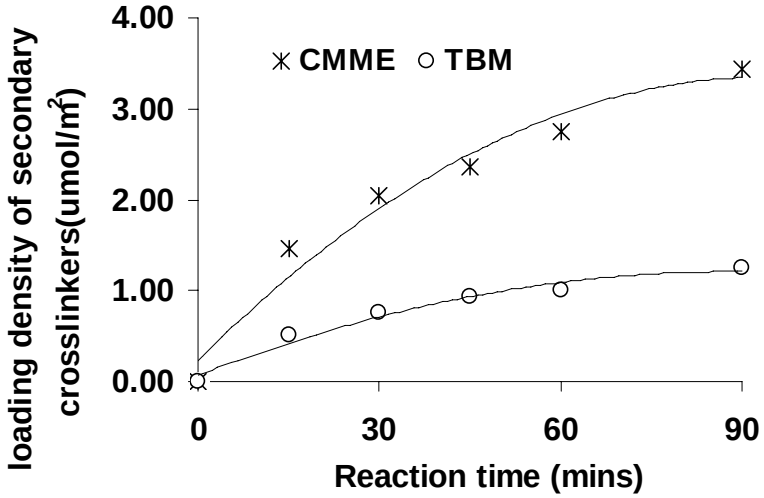
4.00
3.00
2.00
1.00
0.00
CMME
TBM
loading density of secondary crosslinkers(umol/m2)
0
30
60
90
Reaction time (mins)

(B)

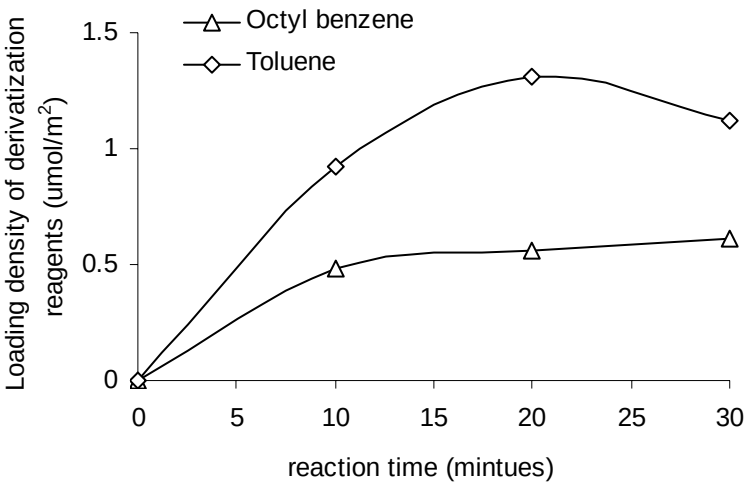

(C)

Figure 4.3 Plots of loading density (μmol/m^2) of reagents vs. reaction time (minutes) based on kinetic studies of F-C crosslinking and derivatization reactions. The experimental conditions are described in Section 4.2.
A). primary crosslinking: TPM vs. Styrene Heptamer;
B). secondary crosslinking: TBM vs. CMME;
C). third derivatization: Toluene vs. Octyl Benzene

Table 4.2 Summary of elemental analysis at each stage in the synthesis of the HC-T and the HC-C8 phases.

	HC-T			HC-C_8		
Silica substrate	C %[a]	H %[b]	Cl %[c]	C %[a]	H %[b]	Cl %[c]
DM-CMPES	6.61	0.92	1.51	6.30	0.79	1.53
Primary Crosslinking	7.53	0.94	0.35	8.27	0.91	<0.25
Secondary Crosslinking	8.73	1.04	0.77	8.94	1	1.61
Derivatization	9.32	1.07	<0.25	11.49	1.27	0.61
after gradient washing	9.72	1.24	<0.25	11.31	1.25	0.27

a. Detection limit is 0.10% (wt/wt).
b. Detection limit is 0.10% (wt/wt).
c. Detection limit is 0.25% (wt/wt).

Table 4.3 Summary of loading density at each stage in the synthesis of the HC-T and HC-C_8 phase based upon elemental analysis.

	Loading density[a] (μmol/m^2)	
Reagents	HC-T	HC-C_8
TPM / Styrene heptamer	0.25	0.18
TBM / CMME	0.52	3.51
Toluene / Octylbenzene	0.44	0.97

[a] Calculated based upon carbon content(w/w) from elemental analysis.

with observations from the kinetic study, suggesting TPM is indeed a highly efficient crosslinker. Note that even though the reaction time was now greatly reduced from 180 minutes to 15 minutes, no loss in crosslinking efficiency was seen since the reaction was essentially completed within the first 15 minutes.

On the other hand, less TBM was reacted compared to CMME in the secondary crosslinking reaction. This was anticipated and could be attributed to the lower reactivity observed for TBM in the kinetic studies as well as the shortened reaction time used in modified synthetic scheme. Nevertheless, the amount of TBM loaded on the surface was adequate to ensure the formation of a network polymer on the silica surface; this was verified by the SEM images as will be discussed in the next section.

For the third derivatization, to our surprise, the loading density of toluene is only 0.44 μmoles/m^2, approximately 50% less than the loading of octylbenzene seen in our previous work [15]. Based upon the results of the kinetic studies shown in Figure 4.3, we expected to see more toluene loaded on to the surface of silica than octylbenzene in the earlier work. However, the toluene loading results in the large scale derivatization process (0.44 umol/m^2) in 10 minutes do not agree well with the results seen in the kinetic study (see Figure 4.3) where almost 0.80 μmoles/ m^2 were loaded in 10 minutes. The large scale derivatization was repeated twice with nearly the same result. As far as we can tell all conditions (i.e. reaction time, temperature, relative amount of reagents) are the same; the only difference is the scale of the reaction – one gram of silica was used in the kinetic study and 10 grams of silica was used in the large scale derivatization. We have no explanation for this difference other than reaction scale.

4.3.4 Characterization of the stability of HC-T polymer network by SEM

To verify that a hyper-crosslinked network polymer had been formed on the interior surface of the silica particle by the new synthetic scheme, we took SEM pictures of the coated silica particles before and after removal of the silica skeleton by exhaustive dissolution of the silica substrate by treatment with hydrofluoric acid. This treatment is called "HF digestion" and the detailed procedure for doing this are in our previous publications [15,17]. The resulting micrographs together with the images of bare Zorbax particles are shown in Figure 4.4. If we first compare the particles before and after the hyper-crosslinking modifications, the morphologies of the two cases are essentially the same, both of which are spherical particles with an average diameter of 5 μm. Overall, it is very important to know that the two steps of F-C reactions did not compromise the mesoporous structure of the HC-T phase. This is the basis for the excellent chromatographic efficiency of the phase thus prepared.

Since silica can be totally dissolved in hydrofluoric acid, there was nothing left when we treated the bare Zorbax particle by hydrofluoric acid digestion. However, the result is clearly different for the HC-T particles as indicated by the residual micro-sphere of polymer beads shown in Figure 4.4c. This is because, even after the silica substrate was fully removed by HF digestion, the polymer networks remains intact due to the extensive crosslinking and network formation. These results confirm the formation of hypercrosslinked network polymers on the interior surface of the HC-T phase. The existence of such a network will prevent phase loss even under very aggressive conditions [15,17]; thus the HC-T phase is expected to have high acid stability when compared to conventional ODS phases. Note that the size of the polymer beads is significantly smaller than the HC-T phase before HF digestion. We believe that

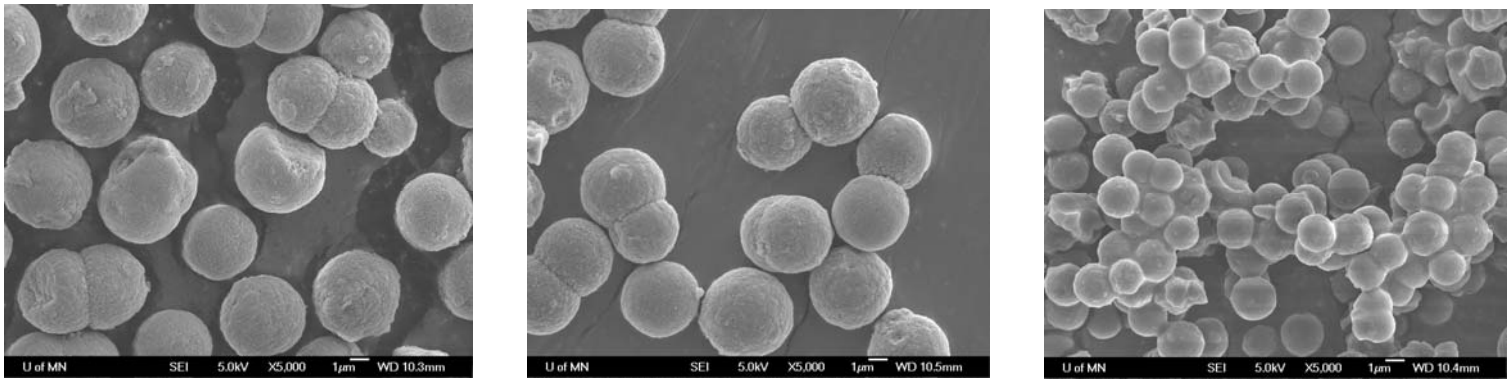

(A) (B) (C)

Figure 4.4 SEM images of the bare Zorbax particle, HC-T phases before and after removal of the silica substrate by HF digestion. A) Bare Zorbax particles; B) HC-T coated silica particles before HF treatment; C) HC-T coated silica particles after HF removal of the silica substrate.

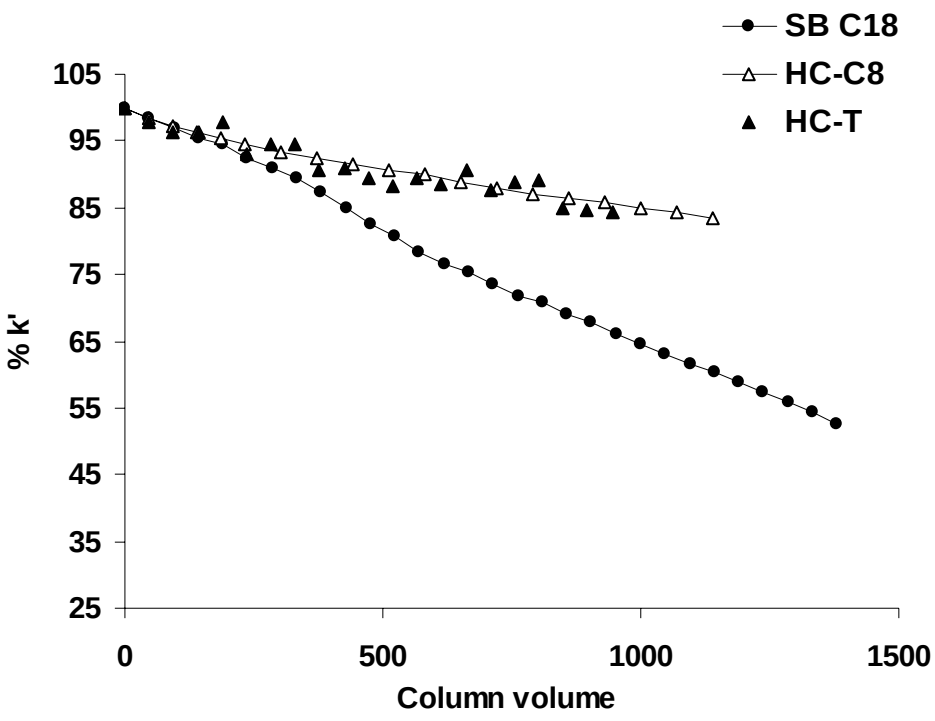

Figure 4.5 Stability comparisons of the HC-T phase, the HC-C_8 phase and the SB C_{18} phase. The stability test conditions are 5% trifluoroacetic acid in 50/50 ACN/water (v/v), T = 150 °C. Data of SB C_{18} and HC-C_8 adapted from Lianjia Ma's work [12].

the decrease in image size is mainly due to the removal of the silica support and the drying process during sample preparation before SEM.

4.3.5 Characterization of the stability of HC-T phase by dynamic aging

The acid stability of the HC-T phase was further tested and compared with the second HC-C_8 phase and the sterically protected C_{18} phases under more chromatographic relevant conditions We used the same acid aging conditions as in our previous work [15,17]. The results are shown in Fig. 4.5, wherein the relative retentions of a neutral probe (i.e. hexadecanophenone) were plotted against the volume of mobile phases flushed though the columns. As can be seen from Figure 4.5, all of the plots followed the same pattern with normalized retention factors decreasing over time. However, it is evident that the decrease of retention is more rapidly on the sterically protected C_{18} phase, which is the one of the best acid stable commercial phases; while the two HC phases showed much less tendency to change. For example, after 1000 column volumes, the retention factor of hexadecanophenone dropped by 35% on the sterically protected C_{18} phase; while it only dropped 15% on the two hyper-crosslinked phases. It is clear that the two HC phases possess outstanding stability even compared to sterically protected C_{18} phases. More importantly, the new HC-T phase is just as stable as the second generation of HC-C_8 phase, suggesting the improvement in synthetic scheme was not achieved at the price of diminished acid stability.

4.3.6 Characterization of pore size distributions of HC-T phase

It is very important to point out that, the two sequential F-C coupling reactions did not compromise the pore accessibility of the underlying silica substrate. This was confirmed by inverse size exclusion chromatography (ISEC). The results of the ISEC

study are shown in Figure 4.6. It is clearly that the pore accessibility of the HC-T phase is even better than that of the monomeric silanized Extend C_{18} phase, which is also based on the Zorbax silica. This suggests the F-C polymer forming reactions are confined to the surface and there is no pore blockage which is believed to be the primary cause for poor chromatographic efficiency of many polymer coated stationary phases [18-20]. The results here agree well with the previous conclusions based on our earlier HC phases [15,17].

4.3.7 Separation efficiency for basic analytes

The silanolphilicity of different HC phases were studied and compared by testing the phases with several representative basic drugs as probes; the resulting chromatogram is shown in Figure 4.7. The observed plate counts, retentions and peak shapes of the basic analytes on the two HC phases are compared in Table 4.4. As can be seen, the observed plate counts and peak shapes for all three basic analytes are much better on the HC-T phase than on the HC-C_8 phase; while these two phases gave similar plate counts for neutral compounds such as acetophenone. These results strongly suggest that the effect of the metal contamination was reduced significantly when the reaction times during phase preparation were properly optimized.

Next the separation efficiency of the HC-T phase was compared to that of three commercial stationary phases. One of them is the sterically protected C_{18} phase, which is also based on the same silica used to make the HC phase (Zorbax silica). The other two are the ACE C_{18} and the Inertsil ODS 3 phase, both of which are made on high quality silica substrates with endcapping and thus provide high efficiencies for basic solutes as long as the columns are not overloaded [26-29]. Small amount of solutes were injected in

all cases and the resulting chromatograms are shown in Figure 4.8. As clearly shown, the new HC-T phase gave the highest plate counts for all three basic analytes using formic acid buffered mobile phase, which was deliberately chosen. Formic acid is a very weak ion-pairing agent [26,28,30] and thus constitutes a more strenuous test media as compared to trifluoroacetic acid or perchloric acid buffers [31,32]. It is very important to note that the HC-T phase was in fact prepared from Zorbax silica. Previous work in this lab had already demonstrated that this type of silica typically shows a relatively strong silanol activity and thus it did not perform as well as did the other lower activity silica when used as the substrate on which to form a hyper-crosslinked phase[15]. Thus the excellent peak shapes observed in this study support our view that the decreased period of exposure to the F-C metal catalyst (Sn(IV)) in the present work decreased the contamination of the surface with metal and gave a less silanophilic product.

4.3.8 Separation efficiency for peptide standards

Previously when a mixture of peptide standards were separated on the second generation of HC phases, considerably wider peak widths (20-30%) and lower plate counts were observed on these phases when compared to conventional bonded C18 columns[22]. We believe this is mainly due to the strong silanophilicity caused by tin (IV) contamination during the three steps of F-C reactions. Since our newly developed HC-T phases showed significantly improved efficiency for basic analytes in acidic conditions, it is of great interest to evaluate the separations of those peptides on the new HC-T phases, to find out the effects of synthesis optimization on the separation of peptides on HC phases.

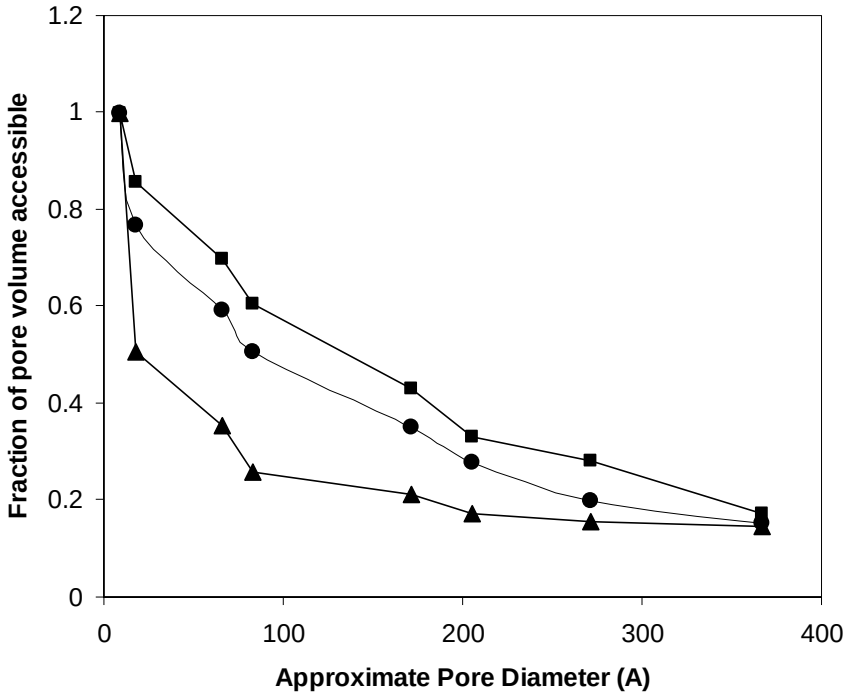

Figure 4.6 Pore accessibility study by inverse size exclusion chromatography. Mobile phase: 100% THF; T= 40 ºC; F = 1.0 mL/min, λ = 254 nm. ■ Bare Zorbax silica; ▲ Extend C_{18}; ● HC-T.

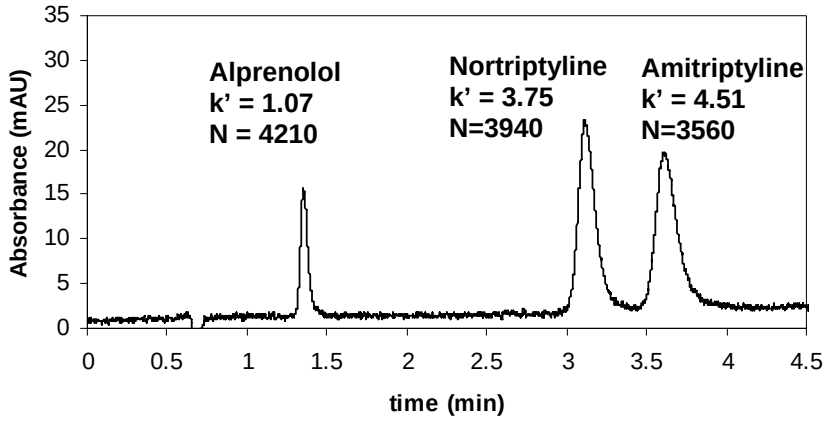

(a)

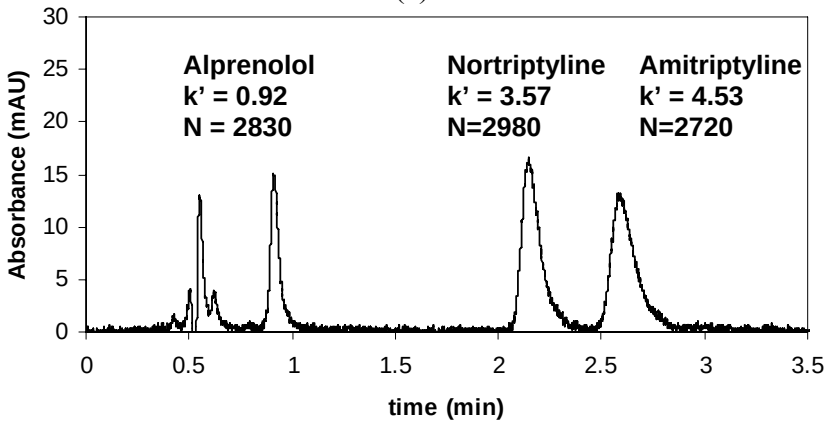

(b)

Figure 4.7 Silanophilicity comparison of HC-T and HC-C_8 phase. A mixture of alprenolol, nortriptyline, and amitriptyline was separated on: (a) HC-T ($N_{acetophenone}$= 5100) and (b) HC-C_8 phase ($N_{acetophenone}$= 5100) in 0.1%(v/v)formic acid buffered mobile phases, %ACN was varied to make k' similar on both phases. For HC-T ϕ_{ACN} =29%; for HC-C8 ϕ_{ACN}=31%. Both columns have the same dimension of 5×0.46 cm. T = 40 °C, F = 1mL/min, λ = 254 nm. 0.1-0.2 nanomole of samples were injected.

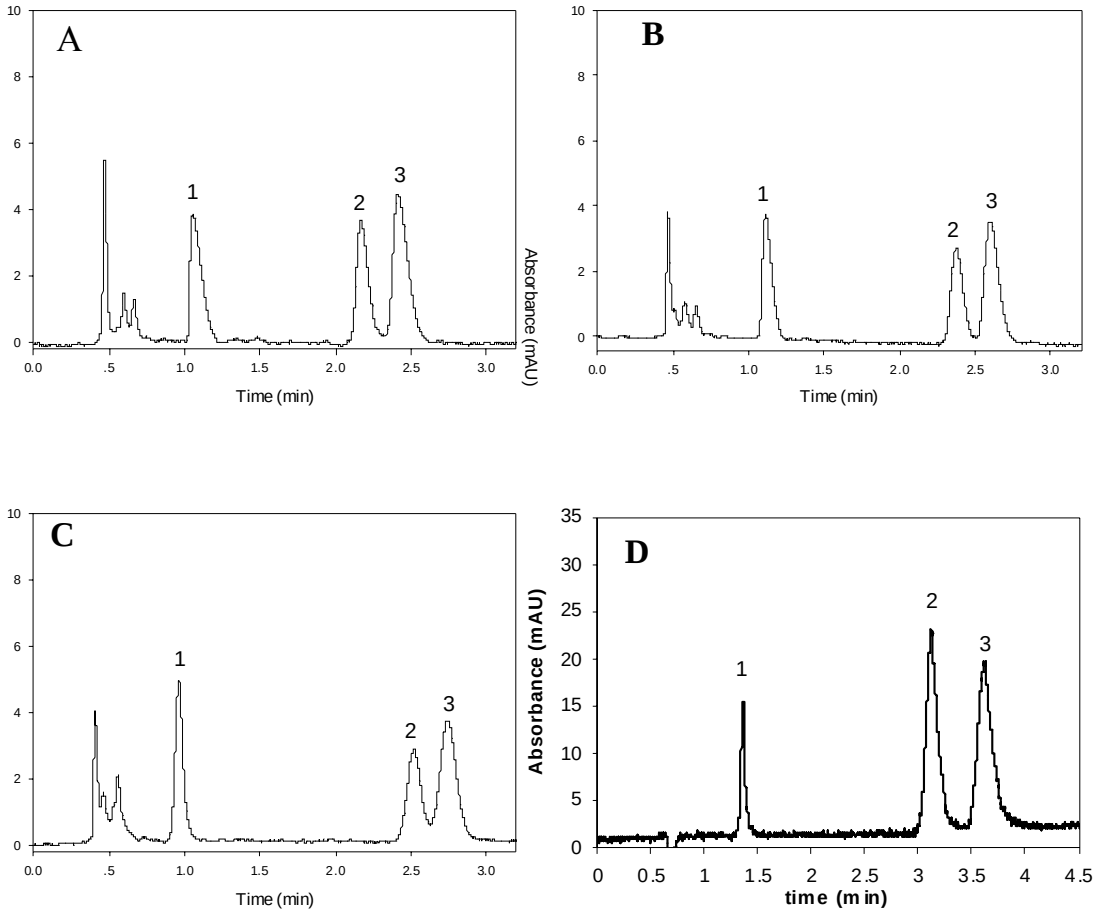

Figure 4.8 Separations of three basic analytes on four RPLC phases. Separation of alprenolol, nortriptyline, and amitriptyline were done on (A) SB C_{18} ($N_{acetophenone}$=4500); (B) ACE C_{18}($N_{acetophenone}$=4500); (C) Inertsil ODS3($N_{acetophenone}$=4000); (D) HC-T ($N_{acetophenone}$=5100) in 0.1%(v/v)formic acid buffered mobile phases, %ACN was varied to make k' similar on all phases. For SB C_{18} φ_{ACN} = 38%; for ACE C_{18} φ_{ACN} = 34%; for Inertsil ODS 3 φ_{ACN} = 16.3%; for HC-T ϕ_{ACN} =29%. All columns have the same dimension of 5×0.46 cm. T = 40 °C, F = 1mL/min, λ = 254 nm. 0.1-0.2 nanomole of samples were injected. (1) Alprenolol, (2) nortriptyline, and (3) amitriptyline. SB C_{18}, ACE C_{18}, and Inertsil ODS 3 data adapted from Lianjia Ma's work [12].

Table 4.4 Efficiency comparison of three basic drugs in formic acid buffered mobile phase[a].

	alprenolol		nortriptyline		amitriptyline	
Stationary phase	**k'**	**N**	**k'**	**N**	**k'**	**N**
HC-T [a]	1.07	4210	3.75	3940	4.51	3560
HC-C_8 [a]	0.92	2830	3.57	2980	4.53	2720
SB C_{18} [b]	1.31	900	3.74	3550	4.28	2750
ACE C_{18} [b]	1.16	1450	3.62	3750	4.06	3400
Inertsil ODS_3 [b]	0.83	1650	3.8	3500	4.22	3000

a. The chromatographic conditions are the same as Figure 4.8. Efficiencies are reported for columns of 4.6mm × 50mm dimension.

b. Data were obtained from reference [12].

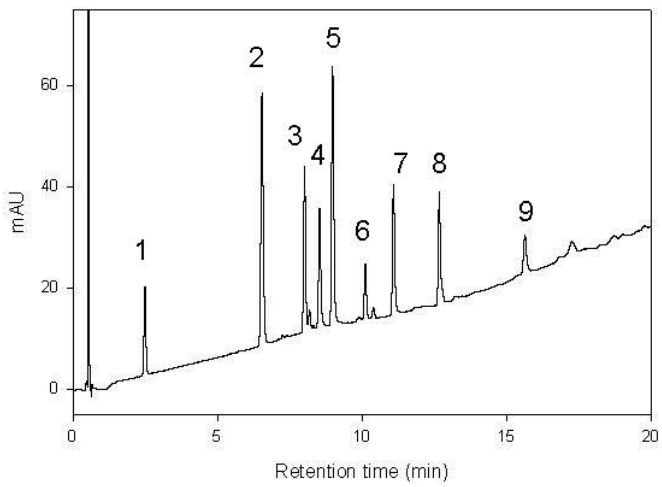
1
2
3
4
5
6
7
8
9
mAU
Retention time (min)

(A)

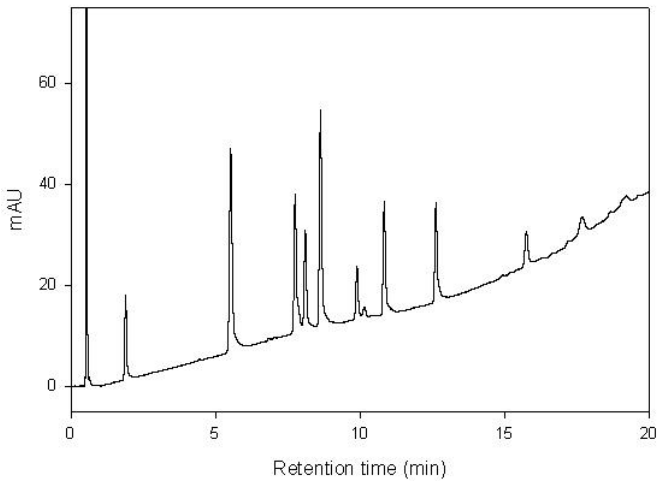
mAU
Retention time (min)

(B)

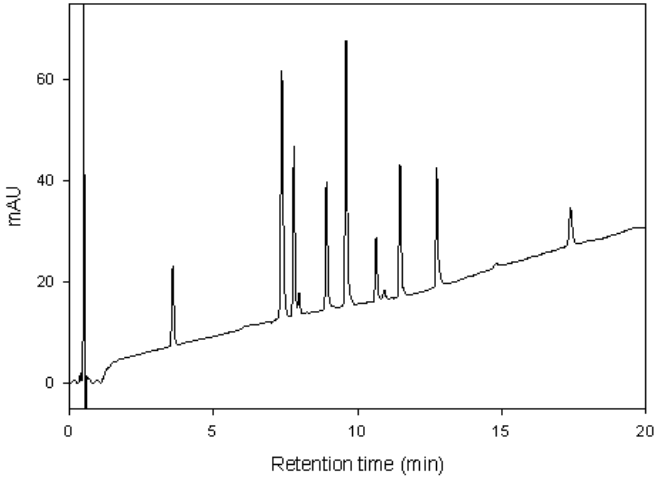
mAU
Retention time (min)

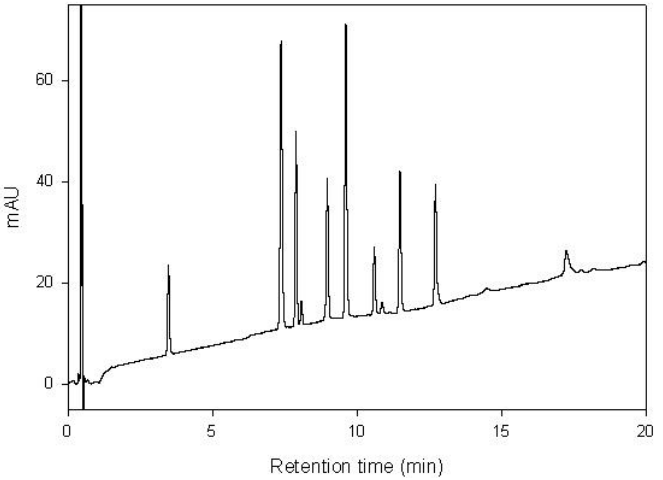
mAU
Retention time (min)

(C) (D)

Figure 4.9 Separations of nine peptides on four RPLC stationary phases. Chromatographic conditions: All columns (5.0×0.46cm) are packed with 5 μm particles. Mobile phases: solvent A: 0.1% formic acid in 5/95 (v/v) ACN/water, solvent B: 0.1% formic acid in 55/45 (v/v) ACN/water. Gradient profile: 0.00-10.00 min 0-80% B, 15.00-15.01min 80-0% B, 15.01-22.00 min 10% B. F = 1.4 mL/min, Temp = 40 °C, λ=214 nm. Nine peptides mixture (0.01-0.08 mg/mL) 5 μL injection. Solutes: 1. Gly-Phe; 2. Phen-Phe; 3. LHRH Human; 4. Angiotensin II; 5. [Val^5]-Angiotensin; 6. Substance P; 7. Renin Substrate; 8. Insulin Chain B; 9. Melittin; A). HC-T; B). HC-C_8; C). ACE C_{18}; D). SB C_{18}.

Table 4.5 Separations of nine peptides on various stationary phases in TFA buffered mobile phases. [a]

	Retention time (min)				Peak width $W_{1/2}$ (min)			
Samples	HC-T	HC-C_8	SB C_{18}	ACE C_{18}	HC-T	HC-C_8	SB C_{18}	ACE C_{18}
Gly-Phe	2.47	1.88	3.46	3.59	0.069	0.065	0.069	0.077
Phe-Phe	6.52	5.52	7.36	7.37	0.086	0.097	0.079	0.088
LHRH Human	8.00	7.75	7.87	7.78	0.072	0.082	0.064	0.069
Angiotensin II	8.52	8.10	8.96	8.91	0.076	0.086	0.069	0.073
[Val^5]-Angiotensin I	8.97	8.62	9.60	9.59	0.080	0.086	0.073	0.076
Substance P	10.10	9.88	10.58	10.64	0.075	0.084	0.073	0.076
Renin Substrate	11.08	10.83	11.47	11.46	0.080	0.084	0.076	0.077
Insulin Chain B	12.66	12.62	12.70	12.74	0.075	0.081	0.073	0.070
Melittin	15.62	15.75	17.22	17.37	0.104	0.109	0.155	0.110
Average					0.074	0.080	0.075	0.074
Standard deviation					0.010	0.012	0.028	0.013

[a] The chromatographic conditions are the same as Figure 4.9

The sample chromatograms are shown in Figure 4.9. The measured retentions and peak widths of the nine peptides on the two HC phases together with the results of the sterically protected C_{18} phase and the ACE C_{18} are listed and compared in Table 4.5. Under gradient elution conditions, the quality of separation is usually evaluated by the half peak width in time unit, $W_{1/2}$. As can be see, among the stationary phases tested the peptide standards clearly showed the widest peaks on the HC-C_8 phase. On the other hand, all nine peptides have similar if not exactly the same observed $W_{1/2}$ values on the HC-T phase when compared to the other two C_{18} phases. This result agrees very well with observations from the separations of basic analytes, suggesting the surface silanols were indeed involved in the poor peak shape of the bases and peptides. The silanolphilicty of the HC-T phase was greatly reduced by optimizing the phase synthesis conditions. As a result, the separation efficiency of basic drugs and peptides on the HC-T phase were significantly improved and are now comparable if not actually superior to the SB C_{18} and ACE C_{18} phases.

4.4 Conclusions

Kinetic studies have been carried out on the effect of reaction time and crosslinking reagents used in preparing HC phases. We concluded that:

1) The Friedel-Crafts chemistry used to prepare HC phases is nearly complete within about 15 minutes. Thus a new generation of Hyper-Crosslinked materials for HPLC was developed by greatly reducing the reaction time for each step of the synthesis from the multi-hour reactions used previously.

2) The acid stability of the new HC phase is not compromised by these synthetic changes. Stability tests at 150 ^{o}C in 5% TFA indicate that the new phase is just as stable as the previously developed HC phases, both are more than an order of magnitude more stable than the benchmark conventional-type C_{18} phase.

3) Preliminary results also showed a much better efficiency for both small basic analytes and peptides on the new HC-T phase compared to both the HC-C8 phase and commercial stationary phases.

4) Given its superb acid stability and outstanding chromatographic efficiency, this phase will be useful for ultra fast high temperature chromatography[33] or as the second dimension separation media in high temperature fast 2DLC[13]. The excellent peak shapes indicate that it should be useful for LC-MS analysis of bases in acidic media.

Chapter 5

Critical Comparison of Performances of Superficially Porous Particles and Sub-2 μm Particles under Optimized Ultra-high Pressure Conditions

5.1 Introduction

Higher separation efficiency and faster speed have always been of great interest in HPLC and have become increasingly important in recent years mainly driven by the challenge of either more complex samples or growing numbers of samples [1]. Many approaches have been developed as potential solutions including high temperature [2,3], sub-2 μm particles at ultra-high pressure [4,5], monolithic columns [6] and the superficially porous stationary phases [7]. Among these techniques, superficially porous stationary phases have recently drawn a lot of attention. In fact, 5 μm superficially porous particles were developed more than a decade ago [8] and have been shown to provide excellent performance in various applications especially for peptides [9]. Interest in this type of particle design was greatly enhanced by the recent introduction of 2.7 μm particles with a 0.5 μm outer porous shell [7]. Due to the reduced diffusion length for analytes, superficially porous particles are expected to have superior mass transfer properties compared to the fully porous particles and therefore provide similar separation efficiencies compared to sub-2 μm particles but at much lower pressure. However, this is

contingent upon the extent to which mass transfer resistance comes from inside the particle vs. the degree of external or film mass transfer resistance [10,11].

Attempts have been made to compare 2.7 μm superficially porous particles and the sub-2 μm fully porous particles [7,12]. Most studies focused on the mass transfer properties, backpressure of the columns and the separation efficiency under certain experimental conditions (mostly in isocratic elution). For instance, Maloney compared the 2.7 μm superficially porous particles to several sub-2 μm fully porous particles under isocratic conditions and found that superficially porous particles give slightly lower plate counts (~20%) but at much lower pressure (~50%). This feature allowed them to couple columns in series to obtain very high plate counts great than 90,000. Guiochon and coworkers also showed that high peak capacities can be achieved with 2.7 μm superficially porous particles for biological separations [13].

Traditionally, the kinetic characteristics of different stationary phases and columns have been compared in terms of their van Deemter flow curves [14]. However, permeability considerations are missing from such plots and they do not tell one which particle design and what column format to choose for a particular separation[15]. To address this issue, Poppe proposed the "Poppe plot" wherein the plate time (t_0/N) is plotted against the plate count (N). This is an elegant tool for visualizing the compromise between separation efficiency and speed [16]. This concept was extended by Desmet and a family of "kinetic plots" was developed to meet the need of different applications[15]. We have also extended the isocratic Poppe plot to gradient elution [17]. The biggest advantage of the "Poppe plot" or "kinetic plot" technique is that these plots allow one to find the optimal conditions (e.g. optimal column length and flow rate) under given

separation conditions (e.g. fixed analysis time and maximum pressure). Therefore, different particle designs and columns can be compared under optimized conditions as opposed to some arbitrary conditions. This approach has provided many invaluable insights for the future development of chromatographic columns [16,18].

Poppe or kinetic plots are usually constructed by first measuring the flow curve of a stationary phase on a given column length. By assuming that the kinetic characteristics are independent of length, one can calculate the best achievable plate count for any column length. The accuracy of these methods was recently verified by measuring plate counts on a series of coupled columns under predicted conditions in the studies of Sandra et al. for Poppe plot [19] and of Desmet et al. for kinetic plot [20]. Most recently Cabooter et al. applied the kinetic plot method to design coupled column systems that can generate 100,000 plates in the shortest possible time on 1.7 μm fully porous particles at 1000 bar and 2.7 μm superficially porous particles at 600 bar. They found that both systems were able to produce theoretical plates close to 100,000 within approximately the same time [21]. They also achieved faster separations by elevating the column temperature from 30 to 80 °C.

The goal of the present study is to use the Poppe plot as a tool to make a critical comparison of the 2.7 μm superficially porous particles at pressure less than 600 bar (i.e. maximum pressure of the column hardware) and sub-2 μm fully porous particles at pressure less than 1000 bar (i.e. maximum pressure of the instrument). 2.7 μm Halo C18 and 1.7 μm BEH C18 were chosen in this study. Both theoretical calculation and experimental measurement were conducted in isocratic elution. The comparison was then extended to gradient separation of a pharmaceutical mixture.

5.2 Theory

5.2.1 Isocratic Poppe plots

With isocratic Poppe plots, the key is to calculate the best plate count that can be achieved at a certain maximum pressure. At a given column dead time (t_0), one computes the column length (L) and flow rate (F) so that the plate count (N) is maximized by simultaneously satisfying two constraints. First, the combination of column length and flow rate should give the desired column dead time:

$$L = u \cdot t_o = (\varepsilon_e / \varepsilon_{tot}) u_e t_o \qquad (5.1)$$

where u is the chromatographic linear velocity of an unretained solute, u_e is the interstitial linear velocity, ε_e and ε_{tot} are the interstitial porosity and total porosity respectively. Secondly, the column is operated at the desired pressure drop:

$$\Delta P = \Phi \eta \frac{u_e L}{d_p^2} \qquad (5.2)$$

where ΔP is the pressure drop, Φ is the column flow resistance, η is the mobile phase viscosity, and d_p is the particle size. At any given t_0 and ΔP, flow rate and column length can be solved from eqns. 5.1 and 5.2 and thus the optimal plate count (N) and plate count production (N/t_0) can be calculated. The value of t_0 is incremented from fast separation to long analysis to complete the Poppe plot and the calculation was done in Microsoft Excel.

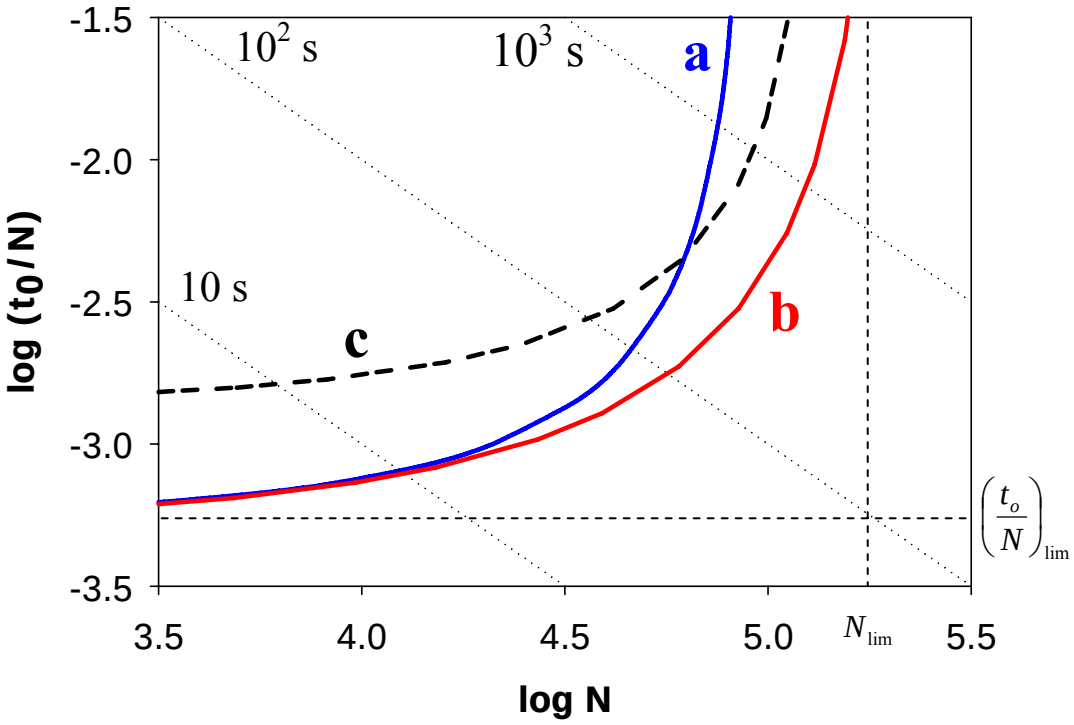

Figure 5.1 Theoretical isocratic Poppe plots for packed bed columns. Each dotted line represents a constant column dead time.
Case a: 1.7 µm BEH C_{18} at ΔP_{max} = 950 bar.
Case b: 2.7 µm Halo C_{18} at ΔP_{max} = 570 bar.
Case c (hypothetical): 2.7 µm BEH C_{18} at ΔP_{max} = 570 bar.
Reduced van Deemter coefficients are listed in Table 5.1. Porosity and flow resistance are listed in Table 5.2. Other conditions: 21 ^{o}C; η = 0.64 cPoise; $D_m = 1.14 \times 10^{-5}$ cm^2/sec.

An important aspect of isocratic Poppe plots is the asymptote of each curve (see Figure 5.1). The vertical asymptote on the right represents the limiting plate count (Nlim) at very long analysis time. The horizontal asymptote at the bottom represents the limiting speed $(t_0/N)_{lim}$ at very short analysis time. The values of the two asymptotes can be calculated through the following two equations [22]:

$$N_{\lim} = \frac{\psi^2 \lambda d_p^2}{BD_m} \qquad (5.3)$$

$$\left(\frac{t_o}{N}\right)_{\lim} = \frac{Cd_p^2}{\lambda D_m} \qquad (5.4)$$

where ψ and λ are column property related constants, and B and C are the van Deemter flow curve coefficients. It is clear from eqn. 5.3 that a stationary phase of larger particle size and smaller B term (i.e. less longitudinal diffusion) can provide higher maximum plate count. On the other hand, eqn. 5.4 suggests that a phase of smaller particle size and smaller C term (i.e. faster mass transfer) can provide faster separation.

To calculate isocratic Poppe plot, the mobile phase viscosity was estimated by Chen-Horvath equation [23]. The solute diffusion coefficient was calculated using the Li-Carr correlation [24]. The interstitial porosity (ε_e) of the Halo C18 was taken to be 0.423 from a study of Gritti et al [10]. The interstitial porosity (ε_e) of the BEH C18 was taken to be 0.353 from a study of Desmet et al [25]. The total porosities (ε_{tot}) of both particles were measured by injecting uracil in 50/50 mixture of acetonitrile (ACN) and water. This in turn allowed the estimation of intraparticle porosity (ε_{in}) of both particles by:

$$\varepsilon_{in} = \frac{\varepsilon_{tot} - \varepsilon_e}{1 - \varepsilon_e} \qquad (5.5)$$

Another important parameter needed for isocratic Poppe plots is the flow resistance of the column. Column backpressures were collected on both Halo C18 and BEH C18 at different flow rates during the flow studies. The value of flow resistance was calculated from the slope of the plot of column backpressure against interstitial linear velocity according to eqn. 5.2.

5.2.2 Gradient peak capacity Poppe plots

Since many practical separations are conducted by gradient elution, it is important to ensure that the conclusions from the isocratic Poppe plot comparison are applicable to gradient elution. Under gradient conditions, peak capacity is the most relevant measure of separation efficiency and it is of great interest to maximize the peak capacity and separation speed (i.e. peak capacity per unit time) [26,27]. We have previously extended the concept of isocratic Poppe plot to gradient elution and developed gradient peak capacity Poppe plot by plotting peak capacity time (t_G/n_c) against peak capacity (n_c) [17]. Comparing the two stationary phases in such plot can provide interesting and useful insights.

One of the key factors that affects peak capacity in gradient elution is the gradient steepness [28]:

$$b = \frac{S \cdot \Delta\phi \cdot V_m}{F \cdot t_G} \qquad (5.6)$$

where S is the sensitivity of the solute's retention to a change in mobile phase composition as based on Linear Solvent Strength Theory (LSST) [29]. To make a fair

comparison between Halo C18 and BEH C18, it is *critical* to ensure both columns were operated at similar gradient steepness. This was done by first determining the following four operational parameters: column dead volume (V_m), mobile phase composition change during the gradient ($\Delta\phi$), S values of the solutes, and the flow rate (F). Then gradient time (t_G) was adjusted on both stationary phases to achieve the same gradient steepness. Details of these determinations are described below.

First, V_m was measured by the retention time of uracil and $\Delta\phi$ was determined by the initial and final mobile phase compositions that were adjusted on each stationary phase so that retention window between the first and last solute was maximized to optimize the peak capacity [28]. Second, the S values (along with lnk'_w) of the solutes were measured by a method described in an earlier study and are listed in Table 5.5 [28]. The average S value of the seven compounds was used in eqn. 5.6 to calculate the gradient steepness. Next, the flow rates were set so that each column was operated at the maximum pressure. This maximizes the isocratic plate count (see eqn. 5.2) and thus the gradient peak capacity since peak capacity is approximately proportional to the square root of plate count [9,30]. It should be noted that the flow rates used in the gradient elution study were different from those in the isocratic study due to the difference in mobile phase viscosity. Finally gradient time (t_G) on each column was adjusted so that the same gradient steepness was obtained. The detailed experimental conditions are given in Table 5.6. Peak capacities were calculated by [28]:

$$n_c = (t_{R,n} - t_{R,1}) / w \qquad (5.7)$$

where $t_{R,n}$ and $t_{R,1}$ are the retention time of the last and first eluting sample peak; w is the average 4σ peak width of all peaks.

5.3 Experimental

5.3.1 Materials and reagents

All solvents used in this work were HPLC grade. Acetonitrile (ACN) was purchased from Mallinkrodt-Baker (Paris, KY). Trifluoroacetic acid (TFA) was obtained from Fisher Scientific. HPLC water was obtained from a Millipore system.

Solutes used in the isocratic elution study were obtained from Aldrich. The sample mixture contained acetophenone (0.2 mg/mL), propiophenone (0.4 mg/mL), butyrophenone (0.9 mg/mL), valerophenone (1.1 mg/mL) and was prepared by diluting their individual stock solutions in acetonitrile with 43/57 ACN/H_2O. Uracil was purchased from Sigma and dissolved in pure water at a concentration that gives adequate signal to determine the column dead volume.

A mixture consisting of an AstraZeneca development compound and several of its synthetic impurities was used in the gradient study. Their molecular weights are about 500. Due to their basic nature, an overloading study was first conducted (data not shown) and a very low sample concentration was chosen to ensure the measured peak capacities were not compromised on both BEH C18 and Halo C18.

5.3.2 Instrumentation and columns

The chromatographic experiments were conducted using a Waters Acquity UPLC system equipped with a single column heating compartment and a photodiode-array

detector. Detection was made at 254 nm for the alkylphenones and 260 nm for the pharmaceutical mixture with a collection rate of 20 Hz. The UPLC system had a 5 μL injection loop and a 500 nL flow cell (path length = 10 mm). The overall system void volume, from the injection valve to the detector, was measured to be 0.14 mL. For all experiments, instrument control was performed using Empower (Waters) and data were collected and analyzed by Atlas (Thermo).

Two types of stationary phases were used in this study. Columns packed with 1.7 μm BEH C18 (2.1 mm i.d.) were purchased from Waters (Milford, MA). Columns packed with 2.7 μm Halo C18 (2.1 mm i.d.) were the generous gifts from Mac-Mod (Chadds Ford, PA). Three different column lengths (5, 10 and 15 cm) were obtained for each stationary phase. Since the goal of the study is to compare the efficiency of the two different particle types, C18 bonding was chosen for both particles to minimize the difference in selectivity.

The maximum pressure the Acquity UPLC instrument can deliver is 1000 bar and the maximum pressure the Halo C18 column hardware can withstand is 600 bar. To avoid operating at the absolute maximum of either the instrument or the column hardware, we operated the columns at 95% of the maximum pressure, i.e. 950 bar for the BEH C18 and 570 bar for the Halo C18.

5.3.3 Flow study

The flow studies were performed on a 100 × 2.1 mm Halo C18 column and a 50 × 2.1 mm BEH C18 column with alkylphenones. Both columns were brand new. Column efficiency (i.e. plate count) was measured at a series of flow rates between 0.05 and 1.10 mL/min. The columns were thermostated at 40 °C and the detection was at 254 nm. The

mobile phases were 0.1% TFA in 42/58 ACN/H_2O (v/v) for the BEH column and 0.1% TFA in 43/57 ACN/H_2O (v/v) for the Halo column. These mobile phases gave a range of retention factors between 1 and 10 for the alkylphenones on both phases.

The measured plate counts were corrected for extra-column volume and broadening, which was measured by injecting butyrophenone with a zero-dead-volume connector in place of the column. The plate heights for the flow curves were calculated using the corrected plate counts.

5.4 Results and discussion

5.4.1 Flow study

The kinetic properties of BEH C18 and Halo C18 were first assessed in a flow study. The plate counts of each stationary phase were measured at a series of different flow rates to generate the reduced plate height (h) vs. reduced linear velocity (ν) plot. The reduced linear velocity was calculated from the interstitial linear velocity according to Horvath [31]:

$$\nu = \frac{u_e d_p}{D_m} \qquad (5.8)$$

where D_m is the diffusion coefficient of the analyte in the mobile phase. The h vs. ν curves were fitted into both the van Deemter and Knox equations to obtain the A, B and C coefficients. Clearly the A, B and C terms in eqn. 9 are different from those in eqn. 10.

$$h = A + B/\nu + C\nu \qquad (5.9)$$

$$h = A\nu^{1/3} + B/\nu + C\nu \qquad (5.10)$$

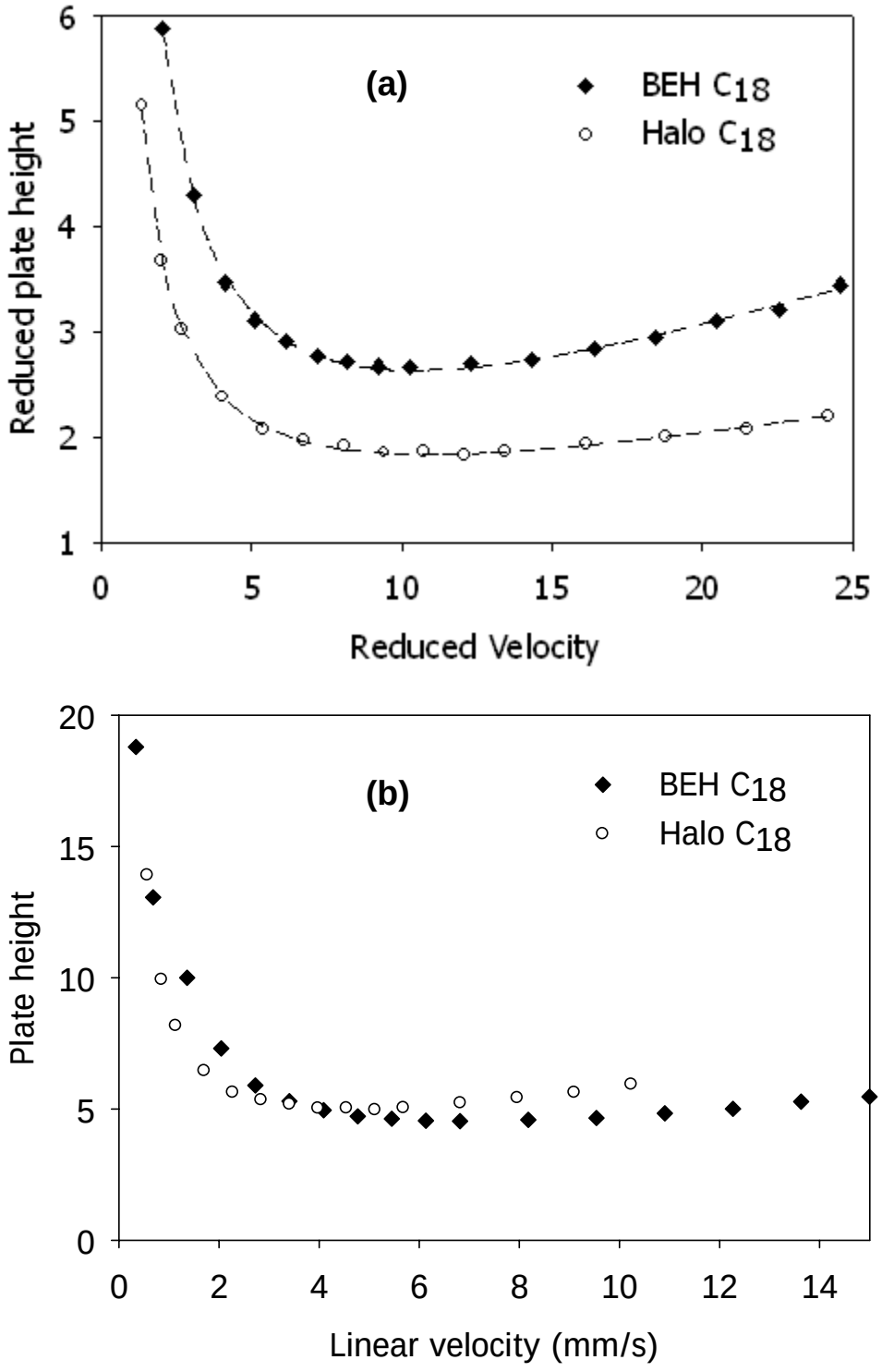

Figure 5.2 Flow curve comparison of Halo C18 (-○-) and BEH C18 (-♦-). (a) reduced coordinates; (b) non-reduced coordinates. The diamonds and circles are experimental data points. The dashed lines correspond to the best-fitted curves calculated by van-Deemter equation. Chromatographic conditions are the same as described in Table 5.1.

Table 5.1 Summary of van Deemter flow curve study on the Halo C_{18} phase and the BEH C_{18} phase

Solute	k' (Butyrophenone)	Equations	A[c]	B[c]	C[c]	h_{min}	N[e]	S.E.[f]
BEH C_{18}[a]	6.3	Van Deemter[c]	0.66 ± 0.04	10.2 ± 0.1	0.095 ± 0.002	2.6	16	0.04
		Knox[d]	0.38 ± 0.02	10.7 ± 0.1	0.076 ± 0.003			0.03
Halo C_{18}[b]	6.2	Van Deemter[c]	0.78 ± 0.02	5.73 ± 0.05	0.049 ± 0.001	1.8	15	0.02
		Knox[d]	0.47 ± 0.01	6.17 ± 0.03	0.023 ± 0.002			0.02

[a] Experiments were conducted on a 50 × 2.1 mm 1.7 μm BEH C_{18} column in 42/58 ACN/H_2O at 40 °C.
[b] Experiments were conducted on a 100 × 2.1 mm 2.7 μm Halo C_{18} column in 43/57 ACN/H_2O at 40 °C.
[c] Dimensionless van Deemter coefficients of *h* vs. *v* by the van Deemter equation (eqn. 5.9)
[d] Dimensionless Knox coefficients of *h* vs. *v* by the Knox equation (eqn. 5.10)
[e] Number of data points
[f] Standard error of the fit

Figure 5.2 shows the flow curves for butyrophenone (k' ~ 6) on the two columns in both reduced and non-reduced coordinates. The minimum reduced plate height is markedly smaller on the Halo C18 than on the BEH C18. This suggests that the Halo column has a more ideal packing. It is, however, evident in Figure 5.2b that both phases gave similar minimum plate heights (4.9 μm for Halo and 4.4 μm for BEH) and that the BEH C18 produced 10-20% higher efficiency at high flow rate. The very low plate height ($h_{min} < 2$) of the Halo C18 has been previously reported on 4.6 mm i.d. columns [7] and was attributed to the narrower particle size distribution and higher particle density of the Halo phase, which potentially lead to a more homogeneous packed column bed.

The h vs. ν data fit very well to both van Deemter and Knox equations as shown in Table 5.1. It is convincing from both fits that there are two main differences between the two columns. First, the B term of the Halo phase is substantially smaller compared to that of the BEH phase. This is consistent with the less porous structure of the Halo particles (see intraparticle porosity in Table 5.2) and agrees with previous reports [9]. The smaller B term is particularly important in the low velocity range, where axial diffusion dominates the band broadening process. This result in combination with the larger particle size leads to a much larger value of the maximum achievable plate count on the Halo phase at very long analysis times (see eqn. 5.3). Secondly, the C term of the Halo phase is much smaller compared to that of the BEH phase in the reduced van Deemter and Knox plots. Recently, it was reported that the C term actually increases from fully porous silica to superficially porous particles of comparable sizes[30,32]. However, this trend was not observed in this study, suggesting that at high velocities, the Halo column can maintain low plate heights, enabling fast analysis without

compromising efficiency (see eqn. 5.4). Because the flow curves fit equally well to both equations, we chose to use van Deemter equation in the calculation of isocratic Poppe plot.

5.4.2 Flow resistance

The column backpressures were also measured and are shown in Figure 5.3. As expected, the 50 mm BEH column had higher backpressures compared to the 100 mm Halo column. If we assume a 50 mm Halo column, the backpressure would be approximately 130 bar at 0.50 mL/min, which is almost 60% lower compared to the BEH column (ΔP = 320 bar). The values of the flow resistance for each phase were calculated from the slope of the lines in Figure 5.3 using the nominal particle sizes and the external porosities shown in Table 5.2. The flow resistance of the Halo phase is about 20% higher than that of the BEH phase and this agrees with the results of Gritti et al [10]. However, this result is based on the assumption that both nominal particle sizes are accurate.

5.4.3 Theoretical isocratic Poppe plots

Figure 5.1 shows the calculated isocratic Poppe plots for butyrophenone on the BEH C18 and the Halo C18 at a maximum pressure of 950 bar and 570 bar respectively. Experimentally determined van Deemter coefficients listed in Table 5.1 were used in the calculation. The mobile phase viscosities were calculated at 42% ACN for BEH and 43% ACN for Halo to ensure similar retention of the alkylphenones on both phases. As experiments will be performed to verify the theory and the instrument thermostat compartment cannot accommodate columns longer than 15 cm, the isocratic Poppe plots were calculated at typical laboratory temperature of 21 ^{o}C.

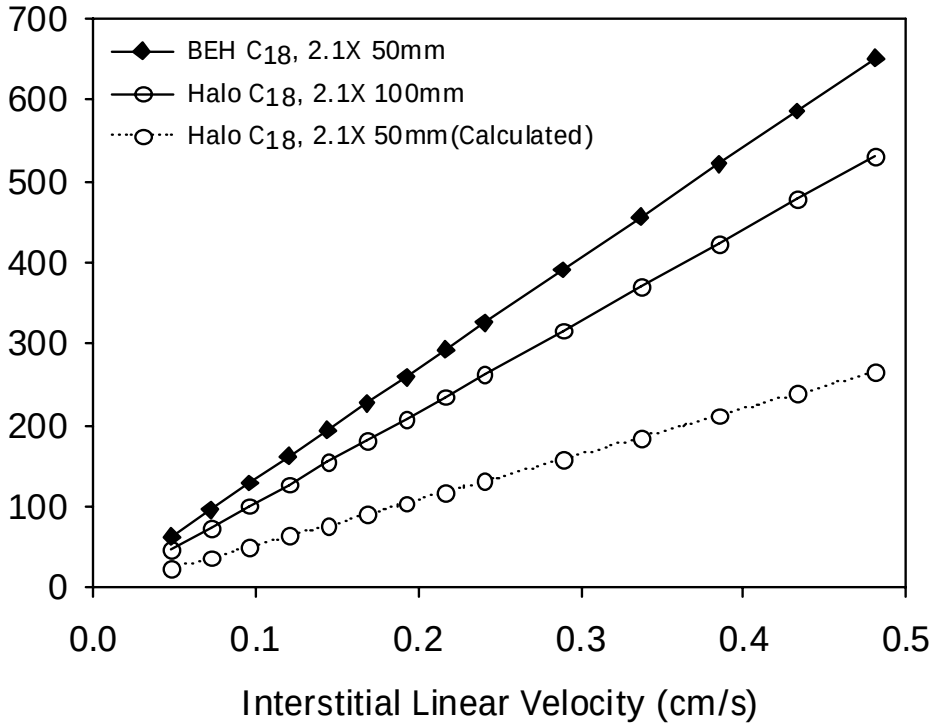

Figure 5.3 Column backpressures at a function of flow rate. The chromatographic conditions are the same as described in Table 5.1. Pressures on the 5 cm Halo C18 are calculated based upon experimental data on a 10 cm Halo C18 column.

Table 5.2 Physico-chemical Properties of Halo C_{18} particles and BEH C_{18} particles

Stationary phase	Particles size (μm)	Pore diameter (Å)	Surface Area (m^2/g)	Interstitial porosity (ε_e)	Total porosity (ε_t)[c]	Intra-particle porosity (ε_i)[d]	Flow resistance ϕ[e]
Halo C_{18}	2.7	90	150	0.423[a]	0.469	0.08	541
BEH C_{18}	1.7	130	185	0.353[b]	0.537	0.284	431

[a] Results report by Guiochon et al. [18].
[b] Results report by Desmet et al. [19].
[c] Total porosity is based on equation: $\varepsilon_{tot} = V_m / \pi R^2 L$. Here, V_m is the dead volume measured by uracil; R is the diameter of the column; L is the column length. Chromatographic conditions are the same as described in Table 5.1.
[d] Interstitial porosity is calculated based upon eqn. 5.5.
[e] Flow resistance is based on interstitial velocity according to eqn. 5.2.

The plots here clearly resemble the Poppe plots shown by others for conventional packed bed columns [16,33]. Case a is for the 1.7 μm BEH C18 phase at 950 bar. Case b is for the 2.7 μm Halo C18 phase under 570 bar pressure. Case c is a hypothetical situation where we assume a BEH C18 phase with a 2.7 μm particle size at 570 bar. Since we assumed the same particle type (i.e. same fully porous BEH particle with C18 bonding) and that the reduced van Deemter coefficients are independent of particle size, the same A, B and C values as those for the 1.7 μm BEH C18 were used. By comparing case a to case c, one can see the effect of increasing particle size and decreasing pressure. By comparing case c to case b, one can see the effect of different van Deemter coefficients while everything else is held constant.

First, the two curves for case a and c cross over at a column dead time of about 300 seconds and a plate count of around 50,000. On the right side of this cross over point (i.e. $t_0 > 300$ sec), hypothetical 2.7 μm BEH C18 phase at 570 bar provides higher plate counts. On the left side, the 1.7 μm BEH C18 phase at 950 bar generates faster separations. This is in complete agreement with eqn. 5.3 and 5.4 and the conclusions obtained from other studies [16,17,20]. On the other hand, the two curves for case b and case c do not cross over and curve b is always below curve c. This suggests that the 2.7 μm Halo C18 phase operated at 570 bar pressure can always outperform the hypothetical 2.7 μm BEH C18 phase at 950 bar, that is, it will give higher plate counts and faster separations. This behavior is obviously caused by the smaller B and C terms of the Halo phase (see eqn. 5.3 and 5.4).

If we compare the two real stationary phases (case a and b), it is clear that the two curves almost converge on the left side of the plot and this suggests they can generate

similar plate count when the analysis is very fast (t_0 < 10 sec). As we move toward the right side of the plot, the two curves start to separate and curve b drops below curve a, that is, the column corresponding to curve b performs better. This suggests that the 2.7 μm Halo phase increasingly outperforms the 1.7 μm BEH phase at longer analysis times. At extremely long analysis times (e.g. t_0 > 1000 sec), more than two-fold higher plate counts can be obtained on the Halo phase. Overall, the calculation predicts that *the use of 2.7μm superficially porous particles under 600 bar has the potential of generating comparable or even better performance compared to sub-2μm fully porous particles under 1000 bar, with greater advantage at long analysis/high efficiency region.* It should be noted that extra-column broadening is not included in our calculation but it should be more detrimental for smaller particles as their optimum performance requires that shorter columns (i.e. smaller column volumes) be used [2,34].

5.4.4 Experimental verification of isocratic Poppe plots

The accuracy of the theory was confirmed by conducting measurements of isocratic plate counts (N) and column dead time (t_0) on a series of commercially available columns. The experiments with 3 cm columns could not be conducted since for such length on both phases, the calculated optimal flow rate would be above the limit allowed by the instrument (e.g. > 1.50 mL/min). Therefore, experiments were conducted with column lengths of 5, 10, 15, 30 and 45 cm. The measured values of N and t_0/N at each length are placed on the calculated isocratic Poppe plot to verify the accuracy of the theory. Column lengths of 30 and 45 cm were achieved by coupling two or three 15 cm columns in series.

The results are shown in Figure 5.4 and also listed in Table 5.3. In general the experimental data points fell close to the calculated curves, suggesting the theory was reasonably accurate. Representative sample chromatograms obtained are shown in Figure 5.5 and 5.6 for Halo C18 and BEH C18 respectively. For the very fast separations obtained on two 5 cm columns, the BEH phase gave slightly higher plate count while the total analysis time is 40% shorter on the Halo phase. Similar results were observed for a column length of 10 or 15 cm, suggesting substantial savings in analysis times can be achieved on the superficially porous particles in practice. As discussed above, the reason here is mainly due to larger particle size, which enabled higher flow rate without exceeding the pressure limit. For a column length of 45 cm, however, both higher plate count and shorter analysis time were obtained on the Halo phase, which is in close agreement with the calculated Poppe plot.

It is very important to understand that, the comparison above is between separations on columns of the same length. If we were to compare the separations between the two phases at the same analysis time, a longer Halo column should be used due to its lower pressure drop and this would mean that higher efficiency will be obtained on the Halo phase compared to the BEH phase at the same analysis time. This approach is presented in Figure 5.4 by looking at the diagonal lines of the same t0 value. As an example, for a t0 of 100 sec, points 1 and 2 represent the best separations on BEH and Halo particles respectively. For the BEH C18, a 22 cm column is needed at 0.24 mL/min to generate maximum plate count around 46,400; whereas a longer column (28 cm) should be used for the Halo C18 at higher flow rate (0.28 mL/min) to ensure the same analysis time but producing 20% higher efficiency (N=56,800). Therefore, these results

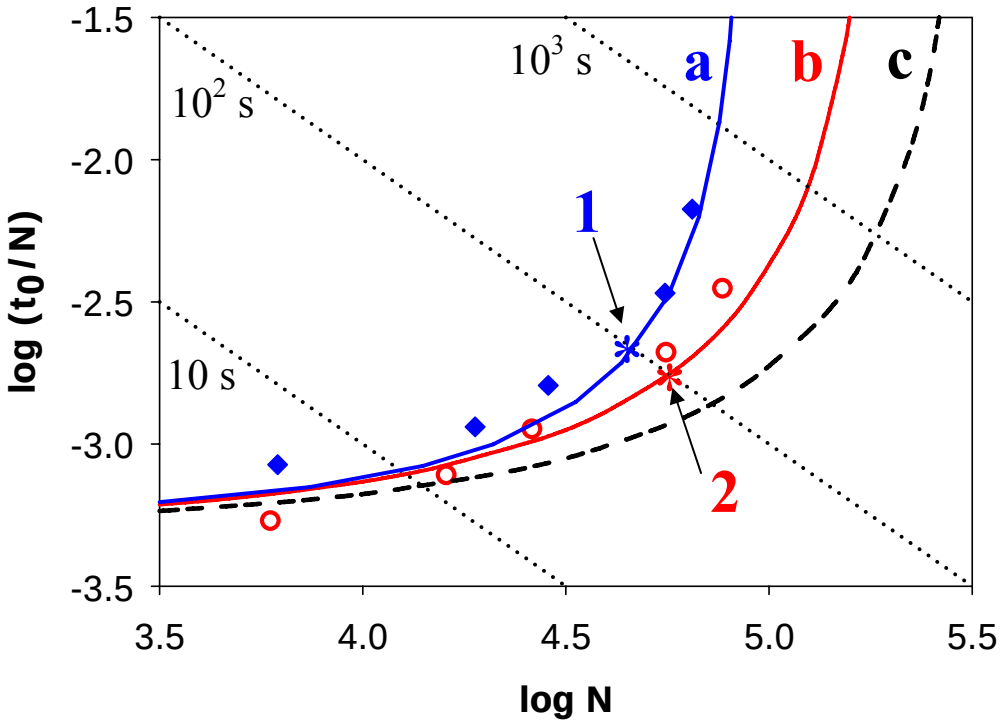

Figure 5.4 Isocratic Poppe plots with experimentally measured points for Halo C18 and BEH C18. Each dotted line represents a constant column dead time.
Curve a: 1.7 µm BEH C_{18} at ΔP_{max} = 950 bar; (♦) Experimental data points on BEH C_{18}.
Curve b: 2.7 µm Halo C_{18} at ΔP_{max} = 570 bar; (○) Experimental data points on Halo C_{18}.
Curve c (hypothetical): 2.7 µm Halo C_{18} at ΔP_{max} = 950 bar.
Point 1 and 2 (asterisks) are the points on each phase that give a dead time of 100 seconds.
All parameters used in calculations are the same as described in Figure 5.1.

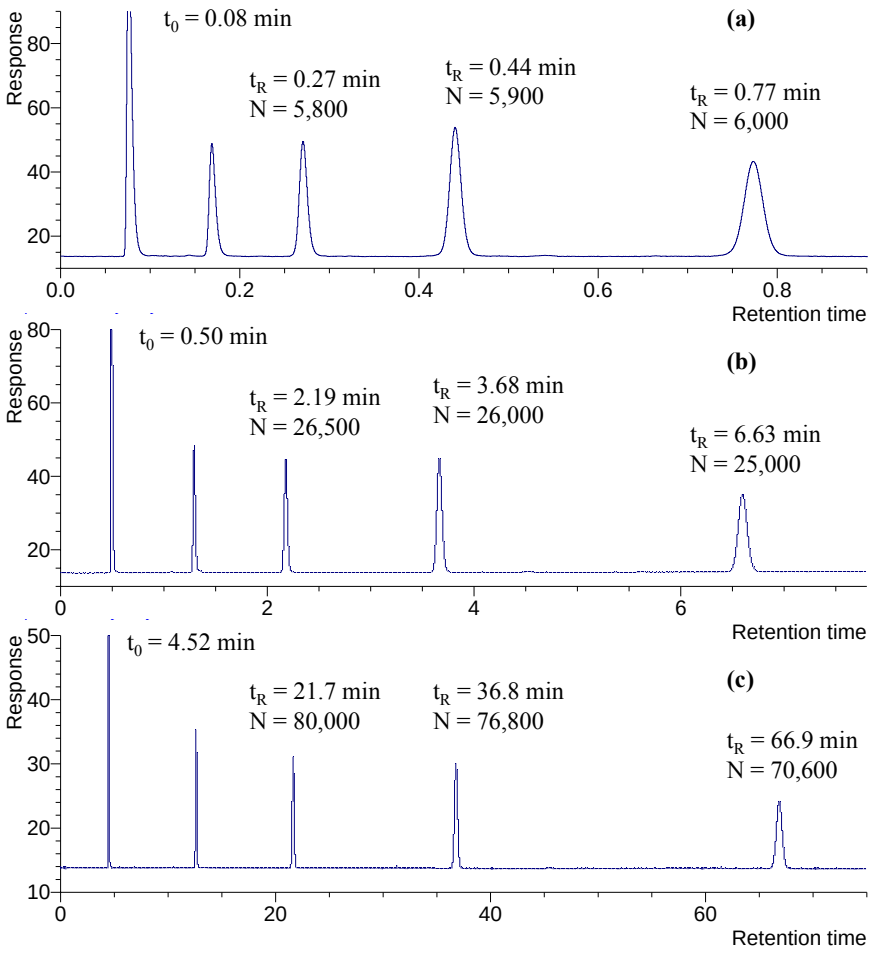

Figure 5.5 Sample chromatograms of an alkylphenone mixture on Halo C18 columns in isocratic elution. Column length: (a) 5 cm, (b) 10 cm, (c) 45 cm. Chromatographic conditions are listed in Table 5.3. Solutes from left to right: uracil, acetophenone, propiophenone, butyrophene and valerophenone.

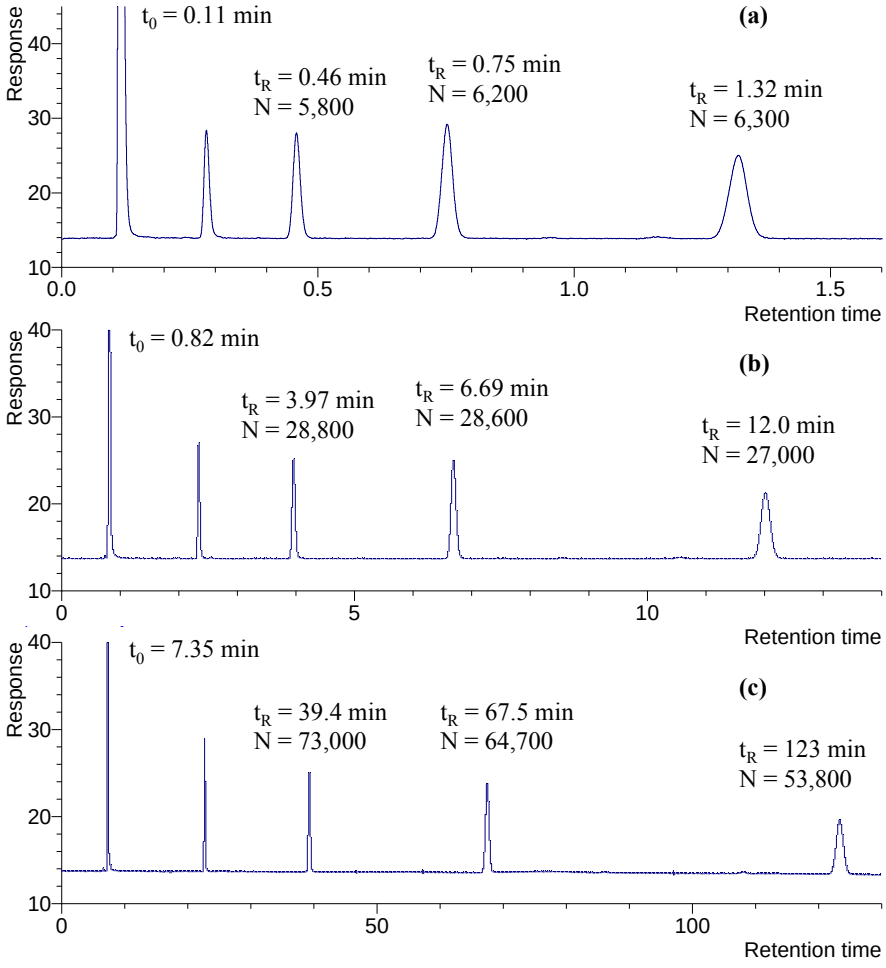

Figure 5.6 Sample chromatograms of an alkylphenone mixture on BEH C18 columns in isocratic elution. Column length: (a) 5 cm, (b) 10 cm, (c) 45 cm. Chromatographic conditions are listed in Table 5.3. Solutes from left to right: uracil, acetophenone, propiophenone, butyrophene and valerophenone.

Table 5.3 Comparison of the calculated and experimental column dead time, plate count and backpressure on Halo C_{18} phase and BEH C_{18} phase at various column lengths.

BEH C_{18}	Calculated F	Calculated			Experimental			T_{inlet} (°C)	T_{outlet} (°C)
L (cm)	(mL/min)	t_0 (sec)	N_{max}	ΔP (bar)	t_0 (sec)	N	ΔP (bar)		
5.0	1.07	5.2	7400	950	5.2	6200	917	22.3	31.3
10	0.53	20.9	20900	950	21.7	18900	823	22.0	27.2
15	0.36	47.0	33400	950	46.0	28600	914	21.4	25.5
30	0.18	188.2	56500	950	188.3	55400	986	21.3	22.0
45	0.12	423.4	67200	950	433.3	64700	976	21.0	21.7

Halo C_{18}	Calculated F	Calculated			Experimental			T_{inlet} (°C)	T_{outlet} (°C)
L (cm)	(mL/min)	t_0 (sec)	N_{max}	ΔP (bar)	t_0 (sec)	N	ΔP (bar)		
5.0	1.55 (1.50[a])	3.1	4800	570	3.2[a]	5900[a]	595[a]	22.6	28.3
10	0.78	12.5	15100	570	12.5	16000	573	22.2	26.5
15	0.52	28.2	27100	570	29.5	26000	551	22.3	25.3
30	0.26	112.9	60300	570	117.4	55800	565	21.9	23.6
45	0.17	254.0	84700	570	270.8	76800	563	21.1	22.0

[a]. Experiment on the 5 cm Halo C18 column was conducted at 1.50 mL/min due to its higher pressure.

suggests that *one can achieve comparable or better performance with the 2.7μm Halo C18 compared to 1.7μm BEH C18 at the same analysis time under appropriately optimized conditions*.

5.4.5 Accuracy of the theory

Despite the fact that the experimental results agree with the theoretical prediction in general, there were some errors. For BEH columns, the experimental plate counts agreed very well with calculated values for long columns but were up to 20% lower than calculation for short columns that were operated at high linear velocities. One potential cause of this deviation is the effect of frictional heating, especially for small particles at high pressure. The radial temperature gradient due to the heat dissipation at the column wall can cause significant loss in plate count. This has been shown in several reports [35,36]. Unfortunately the radial temperature gradient is very difficult to measure. On the other hand, the longitudinal temperature gradient was readily measured on all column lengths used in this study by applying thermocouples at the inlet and the outlet of the columns. The measured temperatures are listed in Table 5.3 and it is clear that shorter columns had larger longitudinal temperature gradients (up to 9 °C). This is in complete agreement with a recent theoretical study of Gritti et al. where they concluded that both longitudinal and radial temperature gradients increase as the column length decreases [37]. This could have significant contribution to the larger prediction errors for the shorter columns.

We also observed some prediction errors for the Halo columns. In particular, plate counts smaller than predicted values were obtained on long coupled columns. Since it is not uncommon that columns with different lengths are packed differently, we

assessed the packing quality of each column by measuring their individual plate counts as listed in Table 5.4. It is clear that the shorter Halo columns were better packed due to their higher values of plate count per meter. This observation agrees with similar results reported by Desmet et al [21]. We believe this is the main reason we saw larger prediction errors for longer Halo columns. In contrast, the five BEH columns were packed quite consistently.

Other possible contributions to the prediction errors include the uncertainty in the particle size values used in the calculation and the fact that the Poppe plot calculations were based on the van Deetmer coefficient measurement on a single column. As shown in Table 5.4, each column is packed slightly differently thus might have slightly different flow curves, flow resistance and total porosity. Thus the accuracy of the calculation can be improved if average properties of several columns are used in the calculation as suggested by Desmet [21].

Despite these sources of error, our experimental results agreed with our prediction. In fact, if the experimental points were connected to produce experimental Poppe curves, the curve of the Halo phase would be underneath that of the BEH phase, suggesting that the Halo phase can provide better performance across the range of analysis times studied here. Because an increase in maximum operating pressure will certainly result in higher plate counts at long analysis it is self-evident that the performance of Halo columns could be further improved if they could be operated at even higher pressures. The benefit provided by a higher pressure limit (i.e. 1000 bar) is clearly demonstrated by curve c in Figure 5.4.Approximately 60% higher plate counts can be achieved at 950 bar than at 570 bar when analysis time is long (e.g. $t_0 > 1000$ sec). However, if one needs an ultra-fast

Table 5.4 Column efficiency of individual Halo C_{18} and BEH C_{18} columns

Stationary phase	Column #	L(cm)	k'	Plate count (N)	Normalized plate count (N/m)
Halo C_{18}[a]	1	5	7.1	10300	206000
	2	10	7.3	19500	195000
	3	15	7.3	24200	161300
	4	15	7.2	24700	164700
	5	15	7.2	25000	166700
BEH C_{18}[b]	1	5	6.9	9900	198000
	2	10	7.1	20700	207000
	3	15	7.0	27200	181300
	4	15	7.3	34400	229300
	5	15	7.1	28600	190700

[a] Column efficiency was measured at 0.50mL/min in 43/57 ACN/H_2O at room temperature by butyrophenone.
[b] Column efficiency was measured at 0.35mL/min in 42/58 ACN/H_2O at room temperature by butyrophenone.

separation (e.g. t_0 < 10 sec), the gain in plate count by going to higher pressures is very small. This is in complete agreement with previous reports [17].

5.4.6 Gradient peak capacity Poppe plots

The comparison between Halo C18 and BEH C18 was extended to gradient conditions by measuring peak capacities of a pharmaceutical sample. Although peak capacity can be calculated through theory as previously reported [28], we only measured experimental peak capacities and plotted them on gradient peak capacity Poppe plot coordinates to compare the two particles. As discussed earlier, it is critical to compare the peak capacities of the two stationary phases at the same gradient steepness. The experimental conditions used in this comparison are listed in Table 5.6. It should be stressed that these conditions are not meant to maximize the peak capacity for each column length as higher peak capacity can be achieved by choosing longer gradient times. Instead, we merely wanted to identify a set of conditions that allows fair comparison within practically acceptable time frame, especially for long columns.

Peak capacities were measured by operating the BEH C18 and Halo C18 columns of different lengths under the conditions given in Table 5.6. The experimental results were plotted in a gradient peak capacity Poppe plot of t_G/n_c vs. n_c as shown in Figure 5.7. In this plot, case a is the 1.7 μm BEH C18 phase at 950 bar, while case b is the 2.7 μm Halo C18 phase under 570 bar. Each data point represents an analysis on commercially available columns between 5 and 45 cm. Representative chromatograms are shown in Figure 5.8 and 5.9 for Halo C18 and BEH C18 respectively.

Table 5.5 Linear Solvent Strength Theory (LSST) parameters of seven pharmaceutical compounds on Halo C_{18} phase and BEH C_{18} phase

	Best fitted LSST coefficients[a]							
	BEH C18				Halo C18			
Peak#	ln k'$_w$	S	R^2	S.E.	ln k'$_w$	S	R^2	S.E.
1	1.71	18.12	1.0000	0.0001	3.57	20.54	1.0000	0.0001
2	5.35	37.47	1.0000	0.0100	9.40	42.09	1.0000	0.0047
3	5.42	32.91	1.0000	0.0084	8.99	37.58	1.0000	0.0037
4	5.47	31.77	1.0000	0.0130	8.93	36.30	1.0000	0.0063
5	3.92	17.38	0.9998	0.0416	5.70	18.59	1.0000	0.0141
6	5.38	20.96	0.9999	0.0371	7.65	23.36	1.0000	0.0310
7	5.77	22.82	1.0000	0.0310	8.28	25.61	1.0000	0.0272
Average	**4.72**	**25.92**			**7.50**	**29.15**		

a. LSST parameters were measured according to a method described in Ref. [23]. Retention times of the seven compounds were measured at three gradient times (5, 10 and 20 min) under the following conditions: a 100 × 2.1 mm2.7 μm Halo C_{18} column and a 100 × 2.1 mm 1.7 μm BEH C_{18} column, 0.60 mL/min, 40 ^{o}C, 0.1% TFA in the mobile phase (v/v), gradient from 10% ACN to 35% ACN.

Table 5.6 Comparison of peak capacity and peak capacity production on Halo C_{18} phase and BEH C_{18} phase at various column lengths.[a]

BEH C_{18}[b]	Experimental Conditions			Measurement				
L (cm)	F (mL/min)[d]	t_G (min)	b[e]	t_0 (min)	Δt_R[f] (min)	$W_{1/2,\,ave}$[g] (sec)	n_c[h]	n_c/t_G (min^{-1})
5.0	0.98	3	0.23	0.14	2.78	1.30	76	25
10	0.49	11	0.23	0.50	10.49	2.70	137	12
15	0.33	23	0.22	1.04	22.30	4.38	180	7.8
30	0.16	97	0.22	4.40	95.45	11.23	300	3.1
45	0.11	210	0.22	9.51	206.47	20.81	350	1.7

Halo C_{18}[c]	Experimental Conditions			Measurement				
L (cm)	F (mL/min)[d]	t_G (min)	b[e]	t_0 (min)	Δt_R[f] (min)	$W_{1/2,\,ave}$[g] (sec)	n_c[h]	n_c/t_G (min^{-1})
5.0	1.35	2	0.25	0.094	1.83	0.93	69	35
10	0.71	7	0.23	0.30	6.53	1.88	123	18
15	0.47	16	0.22	0.68	15.10	3.20	167	10
30	0.24	58	0.23	2.50	55.01	7.51	259	4.5
45	0.16	128	0.23	5.60	122.16	13.51	319	2.5

a. Chromatographic conditions: room temperature, 0.1% TFA present in the mobile phase (v/v), 1.0 μL injection for column length between 5 and 30 cm, 2.0 μL injection for columns of 45 cm.
b. Gradient from 11% ACN to 30% ACN on BEH C_{18} phase
c. Gradient from 11% ACN to 29% ACN on Halo C_{18} phase
d. Flow rate were calculated based upon the viscosity of a 21/79 ACN/H_2O mobile phase at 21 ^oC (i.e. maximum viscosity composition).
e. Gradient steepness calculated using eqn. 5.7. Average S value of the seven compounds were used as shown in Table 5.5.
f. Retention window between the last and first eluting peaks
g. Average peak width at the half height
h. Peak capacity calculated using eqn. 5.7

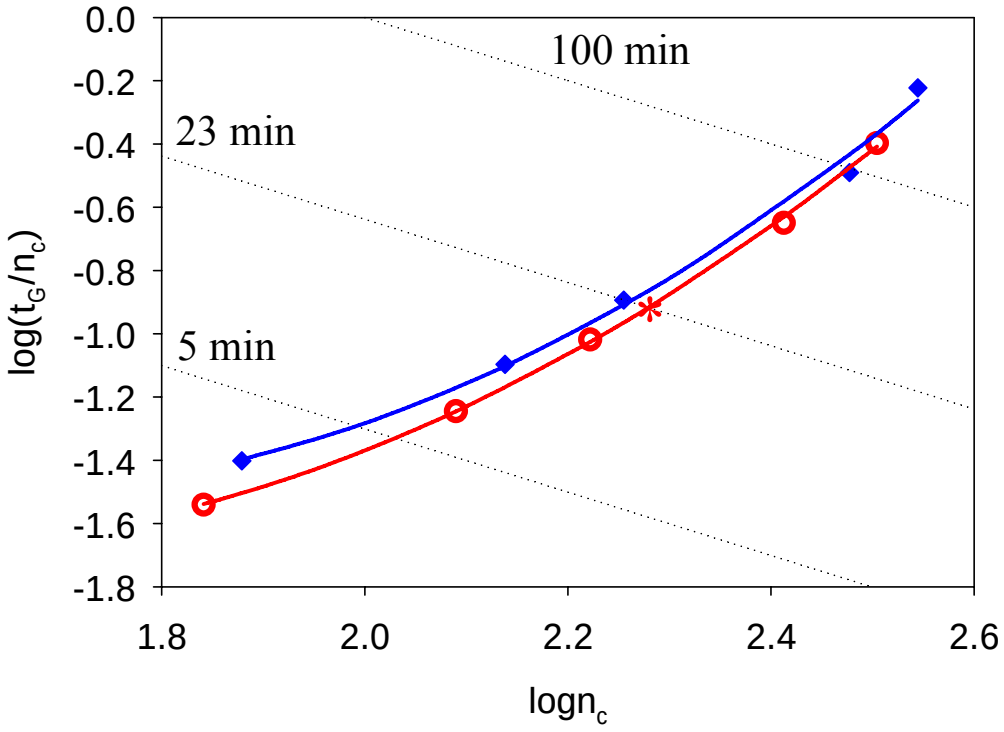

Figure 5.7 Experimental gradient peak capacity Poppe plot for Halo C18 and BEH C18. Each dotted line represents a constant gradient time (t_G). (♦) Experimental data points on 1.7 µm BEH C_{18} at ΔP_{max} = 950 bar. (○) Experimental data points on 2.7 µm Halo C_{18} at ΔP_{max} = 570 bar. The asterisk represents a point when a 23-minute gradient is run on the Halo C18. All chromatographic conditions are the same as described in Table 5.6.

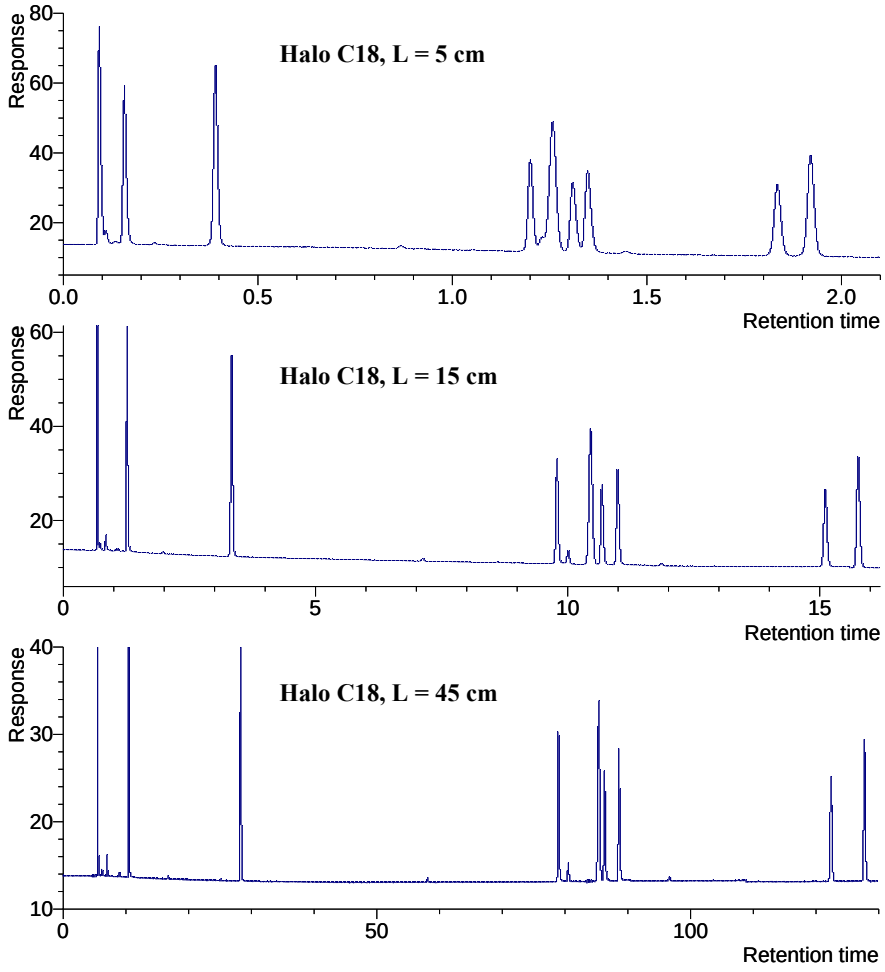

Figure 5.8 Representative chromatograms of a pharmaceutical mixture on Halo C18 columns with various column lengths in gradient elution. Chromatographic conditions are listed in Table 5.6.

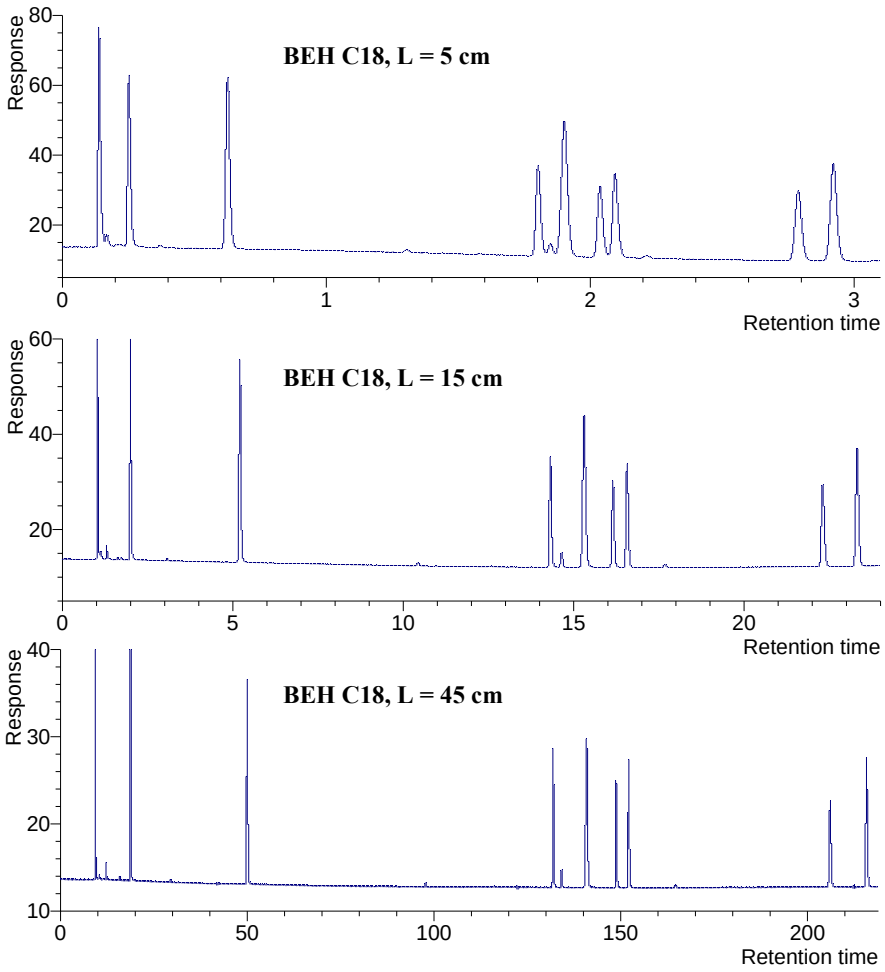

Figure 5.9 Representative chromatograms of a pharmaceutical mixture on BEH C18 columns with various column lengths in gradient elution. Chromatographic conditions are listed in Table 5.6.

For all chromatographic runs, similar results were observed: The 2.7 μm Halo columns were 86-93% as efficient as the 1.7 μm BEH columns of the same length, but at only 65% of the time. The results here are in close agreement with our findings with neutral compounds under isocratic conditions, suggesting that in practice, substantial savings in analysis times can be achieved with superficially porous particles under gradient conditions. One the other hand, if we were to compare the separations between the two phases at the same gradient time, a longer Halo column should be used at a higher flow rate (see each diagonal line); this would mean that higher peak capacities will be obtained on the Halo phase compared to the BEH phase. As an example, when $t_G = 23$ min, a 15 cm BEH column should be used at 0.33 mL/min, as shown in Table 5.6, to generate a peak capacity of 180; whereas a longer Halo column (18 cm) should be used at a higher flow rate (0.39 mL/min) to ensure the same gradient steepness and the same analysis time, but producing 6% higher peak capacity ($n_c = 190$) and thereby 6% increase in average resolution. Overall, the curve of the Halo phase is always underneath that of the BEH phase, suggesting that the Halo phase can provide slightly better peak capacities within the studied range of gradient times. This result is consistent with our previous observation that 5 μm Poroshell particles provide higher peak capacities compared to fully porous particles with the same size [9]. It is worth noting that the difference between the two curves in Figure 5.7 appeared to be smaller than that in Figure 5.4. This is due to the fact that peak capacity is roughly proportional to the square root of plate count.

5.5 Conclusions

The performance of sub-2 μm fully porous particles at ultra-high pressure and 2.7 μm superficially porous particles at lower pressure were compared by the Poppe plot technique. We concluded that:

1) For ultra-fast analysis (i.e. $t_0 < 10$ sec), the Halo phase can provide similar efficiency (i.e. plate count) and speed (i.e. plate count production) compared to the BEH phase.

2) As analysis time increases, the Halo phase starts to outperform the BEH phase and the advantage becomes larger at longer analysis time (e.g. > 2 times larger plate counts at $t_0 > 1000$ sec).

3) The main reason that the Halo phase gives much higher plate counts at long analysis time is its smaller B term (less longitudinal diffusion) and larger particle size.

4) The fact that the larger Halo phase generates similar performance compared to the smaller BEH phase for ultra-fast separation can be partially attributed to the difference in their C terms but carefully designed study is needed to reconcile the different observations in the literature.

5) Performance of the 2.7 μm Halo phase can be further improved by extending its maximum operating pressure to ultra-high pressure conditions (i.e. 1000 bar). This would be particularly beneficial for high efficiency separations and a low dispersion system would be necessary to avoid any loss in separation efficiency.

The comparison was extended to the study of gradient elution of a pharmaceutical mixture. This was achieved by constructing gradient peak capacity Poppe plots from experimentally measured peak capacities on a series of columns of different lengths. The

results were similar to those found in the isocratic study and confirm the great potential of applying superficially porous phases in real world separations.

Chapter 6

Summary of Chromatographic Selectivity and Hyper-Crosslinked Liquid Chromatography Stationary Phases and Future Work

6.1 Summary

This chapter contains a summary of the main results and conclusions of this thesis. An overview of potential future directions will also be presented.

6.1.1 The synthesis and characterization of the HC-COOH phase

1) A novel type of silica-based carboxylate modified reversed phase HC-COOH has been synthesized by introducing a small amount of carboxylate functionality into a aromatic *hyper-crosslinked* (HC) networks of a previously developed acid stable materials.
2) Based upon the free energy of transfer per methylene unit, $\Delta G°_{CH_2}$, the H coefficient in Snyder-Dolan HSM characterization method, and ν coefficient in the LSER study, it is clear that the hydrophobicity of HC-COOH is reduced mainly due to the absence of the hydrophobic octyl chain. However, there is still ~80% of the hydrophobicity of the HC-C8 phase reserved on the new HC-COOH phase.
3) Based upon the elemental analysis, the C coefficient in Snyder-Dolan HSM characterization method at pH 2.8 and pH 7.0, and the inversely correlated relationship between the retention of basic probes and the eluent concentration of counterion, it is clear that the HC-COOH phase offers a very unique hydrophobic assisted weak cation exchange activity, wherein cation exchange interaction between cationic solutes and HC-COOH phase was closely related with the hydrophobic interaction between the solutes and the stationary phase.

4) The phase thus prepared showed a mixed-mode reversed-phase/weak cation exchange (RP/WCE) retention mechanism, which clearly distinguished the carboxylic phase from conventional reversed phases.
5) The novel retention mechanism can also greatly benefit the separation of highly hydrophilic basic compounds, which are very hard to separate by the most frequently used conventional RPLC phases.
6) Excellent separation efficiency and enhanced sample loading capacity for basic compounds is also demonstrated in the successful application of the HC-COOH phase to the separation of drugs of abuses.

6.1.2 Stationary phase selectivity "triangles" based on Snyder-Dolan HSM method

1) A set of four phase selectivity classification "triangle" plots have been developed based on the Snyder-Dolan Hydrophobic-Subtraction Model, wherein the apices of the triangles represent the relative contributions of steric hindrance (χ_S), hydrogen bonding acidity (χ_A), hydrogen bonding basicity (χ_B), coulombic interactions (χ_C) to phase selectivity.
2) It allows the visualization of column selectivity for a large number of phases by plotting three-dimensional selectivity data in a two-dimensional space. It very clearly shows that the 366 RPLC columns studied here cover only a small fraction of the currently available phase selectivity space leaving a great deal of room for researchers to develop novel rather than more redundant phases.
3) This approach to selectivity characterization as applied to the non-alkysilica phases clearly shows that the same surface chemistry (functionality) does not guarantee the same phase selectivity. In contradistinction, the comparison of phases with different

chemical functionalities just as clearly shows that different surface chemistry does not necessarily lead to different phase selectivity.

4) Selection of columns of either equivalent or different selectivity is readily achievable with the application of the set of four "selectivity triangles" based on the Snyder-Dolan Hydrophobic-Subtraction approach.
5) It provides an informative and universal approach to classifying the currently characterized set of reversed phases.
6) The most different phases of the 366 phases are summarized.

6.1.3 Optimization of the Synthesis of a Hyper-Crosslinked Stationary Phases

1) Kinetic studies have been carried out on the effect of reaction time and crosslinking reagents used in preparing HC phases.
2) We have determined that the Friedel-Crafts chemistry used to prepare HC phases is nearly complete within about 15 minutes. Thus reaction time for each step of the synthesis was greatly reduced from the multi-hour reactions used previously without sacrificing the stationary phases' acid stability and separation performance.
3) A new generation of Hyper-Crosslinked materials for HPLC was developed based upon the optimized synthetic scheme.
4) The acid stability of the new HC phase is not compromised by these synthetic changes. Stability tests at 150 ^{o}C in 5% trifluoroacetic acid indicate that the new phase is just as stable as the previously developed HC phases, both are more than an order of magnitude more stable than the benchmark conventional-type C18 phase.

5) Preliminary results also showed a much better efficiency for both small basic analytes and peptides on the new HC-T phase compared to both the HC-C8 phase and commercial stationary phases.
6) Given its superb acid stability and outstanding chromatographic efficiency, we believe this phase will be useful for ultra fast high temperature chromatography [1] or as the second dimension separation media in high temperature fast 2DLC [2]. The excellent peak shapes indicate that it should be useful for LC-MS analysis of bases in acidic media.

6.1.4 Critical Comparison of Performances of Superficially Porous Particles and Sub-2 μm Particles under Optimized Ultra-high Pressure Conditions

The performance of sub-2 μm fully porous particles at ultra-high pressure and 2.7 μm superficially porous particles at lower pressure were compared by the Poppe plot technique. We concluded that:

1) For ultra-fast analysis (i.e. $t0 < 10$ sec), the Halo phase can provide similar efficiency (i.e. plate count) and speed (i.e. plate count production) compared to the BEH phase.
2) As analysis time increases, the Halo phase starts to outperform the BEH phase and the advantage becomes larger at longer analysis time (e.g. > 2 times larger plate counts at $t0 > 1000$ sec).
3) The main reason that the Halo phase gives much higher plate counts at long analysis time is its smaller B term (less longitudinal diffusion) and larger particle size.

4) The fact that the larger Halo phase generates similar performance compared to the smaller BEH phase for ultra-fast separation can be explained by its smaller C term (better mass transfer).
5) Performance of the 2.7 μm Halo phase can be further improved by operating at ultra-high pressure conditions (i.e. 1000 bar). This will be particularly beneficial for high efficiency separations and a low dispersion system would be necessary to avoid any loss in separation efficiency.
6) The comparison was extended to the study of gradient elution of a pharmaceutical mixture. This was achieved by constructing gradient peak capacity Poppe plots from experimentally measured peak capacities on a series of columns of different length. The results were similar to those found in the isocratic study and confirm the great potential of applying micro superficially porous phases in real world applications.

6.2 Future work

6.2.1 Chromatographic Applications of the new generation HC-COOH Phase

Highly hydrophilic basic compounds are of great importance in many fields including clinical and biological research, pharmaceutical development and forensic analysis. However, their retention and separation are an on-going challenge for the most widely used RPLC stationary phases. A highly aqueous mobile phase (e.g.10~15% ACN) or ion-paring reagents (e.g. $^{-}ClO_4$) is often required to achieve retention of these polar analytes, which can then cause de-wetting of the hydrophobic alkyl-bonded phase [3,4] or decreased sensitivity in electrospray ionization mass spectrometry [5], the method of

choice for majority of quantitative and qualitative analyses of compounds in biological matrices.

Our previous work [6] has demonstrated the feasibility of separating these highly hydrophilic compounds using a mixed mode reversed phase/strong cation exchange phase $^{-}SO_3$-HC-C_8 phase under much stronger mobile phase conditions (i.e. 40%~80% ACN). However, the strong ionic interaction between the solutes and the sulfonyl groups on silica surface often requires the use of non-volatile additives such as strong amine modifiers (e.g. Triethylamine) or salt (e.g. NaCl) to elute basic solutes from the strong cation exchange phases [6-8]. With the weak cation exchange groups introduced, preliminary results showed that sufficient retention and resolution of these highly hydrophilic drugs can be achieved the newly developed HC-COOH phase, under the same mobile phase strength (i.e. 40%~80% ACN) but by a weak acid pH gradient using formic or acetic acid. The high volatility of the additives together with the substantial higher mobile phase strength (i.e. higher percentage of organic) clearly make separations on HC-COOH phase more LC-MS compatible when compared to the $^{-}SO_3$-HC-C_8 phase and conventional reversed phases. Thus the newly developed HC-COOH phase should be able to perform well in chromatographic separations where MS or MS/MS detection is required or advantageous. The performance of the HC-COOH phase, especially for the electrospray ionization mass spectrometry, should be further investigated and compared with that of the $^{-}SO_3$-HC-C_8 phase and conventional reversed phases. This will require a selection of model compounds and optimized LC-MS conditions for critical comparisons of stationary phase of interests. We believe the application of the HC-COOH phase will significantly improve the signal to noise ratio and hence enhancing sensitivity of LC-MS.

The result can benefit the analysis of highly hydrophilic basic compounds importance in many fields including clinical and biological research, pharmaceutical development and forensic analysis.

6.2.2 Further optimization and derivatization of HC phases

a) Hyper-Crosslinked Stationary Phases for Ultra-Fast High Performance Liquid Chromatography (UF-HPLC)

Although we have produced highly efficient acid stable HC phases, further improvement in separation performance of the HC phases, especially in terms of separation speed, are absolutely necessary. Sample throughput of current LC techniques has become increasingly important in recent years mainly driven by the challenge of the rapidly growing numbers of samples need to be analyzed everyday [9]. The key to speed up the separations in LC is to increase the flow rate. However, for the conventionally used 5 μm totally porous silica packings, their application at high flow rate were greatly limited due to its significant loss in efficiency [5,9-11]. For example, for a well packed HC phase, more than 30% of efficiency will be sacrificed when the separation is done at 3ml/min instead of 1ml/min; while nearly half of efficiency will be lost at 5ml/min. The problem here is slow mass transfer of the underlying 5-μm fully porous silica particles [5,10,11]. Due to its embedded long diffusion path, solutes have to spend long time in the micropores of silica undergoing dispersions which eventually leads to the broadening of the peak and thus low efficiency [5,10,11].

The mass transfer properties of the HC phases can be greatly improved by reducing particle diameter or using superficially porous particles with a solid central core

and a very thin porous outer skin [12,13]. We believe the high temperature chromatography using these new HC phases will not only increase sample throughput and thus benefit the development of Fast Liquid Chromatography (LC) technique, but it will also facilitate the application of comprehensive two dimensional LC through the development of hyper-fast separation techniques [2].

b) Hyper-Crosslinked Stationary Phases for Intermediate and High pH

Even though we have produced highly efficient acid stable HC phases, it is of critical importance to extend the pH operating range into intermediate and high pH. As discussed before [14,15], raising mobile phase pH can also "turn off" these electrostatic interactions by deprotonating the solutes, leading to significant improvement in both peak shape and efficiency. In addition, it can also enhance the sample loading capacity of the basic compounds since the loadability of the uncharged analytes is much high than that of the charged ones [16,17]. However, when the mobile phase pH is greater than 9, the incompletely shielded silica supports begin to dissolve leading to the cleavage of bonded phase from the support [15,18-20]. This can be more severe for the HC phases with additional free silanols and more exposed silica surface after the strong acid conditioning.

To improve the basic stability of the HC phases without compromising their efficiency and low pH stability, development of new generation of hyper-crosslinked phase by using a novel type of hybrid organic-inorganic particles [21] should reduce the unshielded, underivatized silica surface and thus lead to better high pH stability. This type of particles is synthesized by the reaction of a tetraalkoxysilane and an alkyl trialkoxysilane (or 1,2-bis(triethoxysilyl)ethane) [22-24], with organic moiety presented in both the internal structure and on the surface of the particle. Many studies have shown

that C18 derivatized inorganic-organic hybrid stationary phases are more stable at pH 10 compared to several conventional C18 bonded phases [25,26]. More importantly, it also preserves the advantages of silica with rigidity, high efficiency and ease of modification [27]. Thus we believe the new HC phases would combine the acid stability afforded by the hyper-crosslinked" (HC) chemistry and the basic stability of "hybrid organic-inorganic" technology. The resulting materials with an extended pH (0.5-12) and thermal (up to 150 °C) stability, excellent separation efficiency and novel selectivity will be a quantum leap forward for silica-based column technology.

c) Derivatization of HC phases with other functional groups

One of the most important features of the HC platform is the rich chemistry of surface aromatic and benzyl chloride moieties, hence allowing for further derivatization with various functional groups. These potential new stationary phases should maintain the excellent chemical, thermal stability and separation efficiency but with a wide variety of chromatographic selectivities. For example, synthesis of an ultra-stable highly fluorinated phase or a zwitterionic phase and characterization of their selectivity may lead to distinct selectivity from not just the HC-phases developed previously but all the other reversed phases currently available. Specifically:

1) A highly fluorinated phase: Previous studies [2] showed that a commercial phase of this type had interesting selectivity but was not very stable as shown by serious retention drift and clear baseline issues with UV detectors even at moderate temperatures (40 °C). Route 1 (see Fig. 1) shows the how such a stable phase could be prepared by forming much stronger carbon-carbon bond through Friedel-Crafts alkylation. The phase thus prepared is expected to show both novel selectivity and excellent stability.

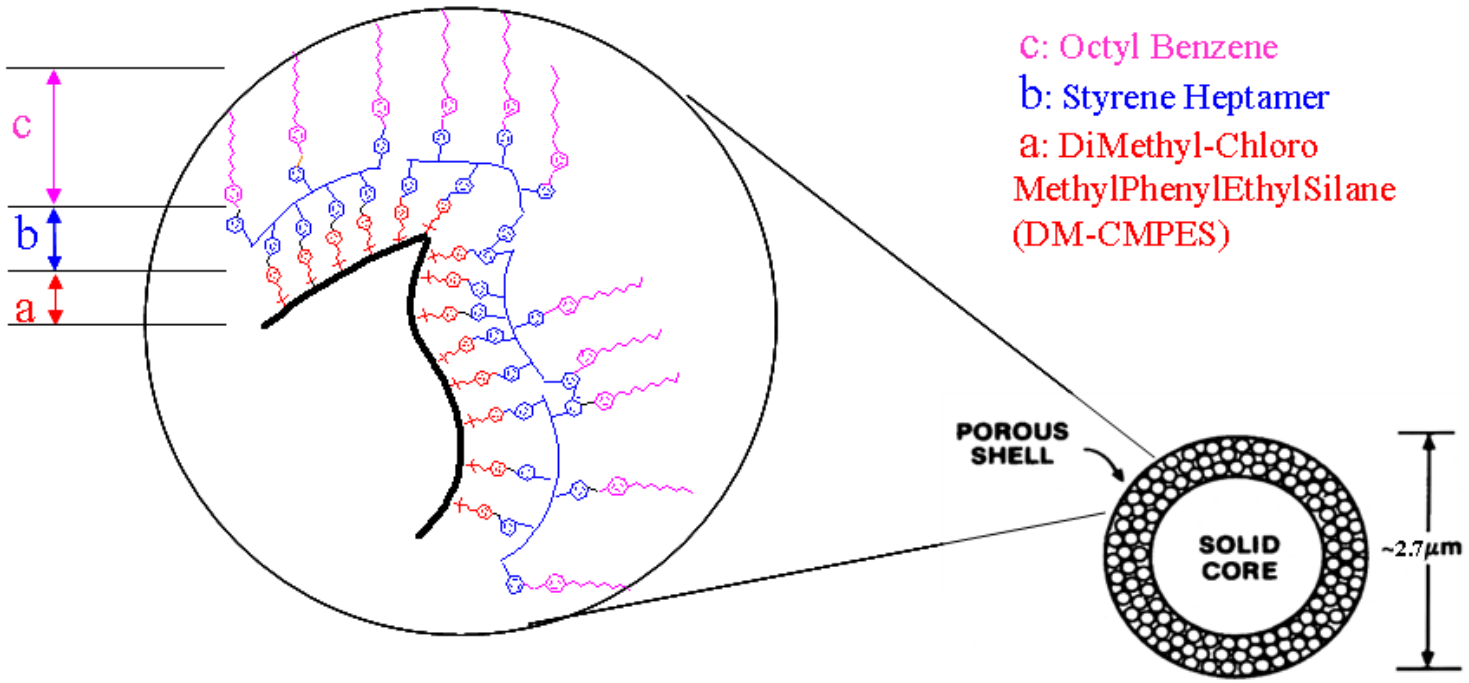

Figure 6.1 The proposed surface structure of new HC phases based on the new superficially porous particles

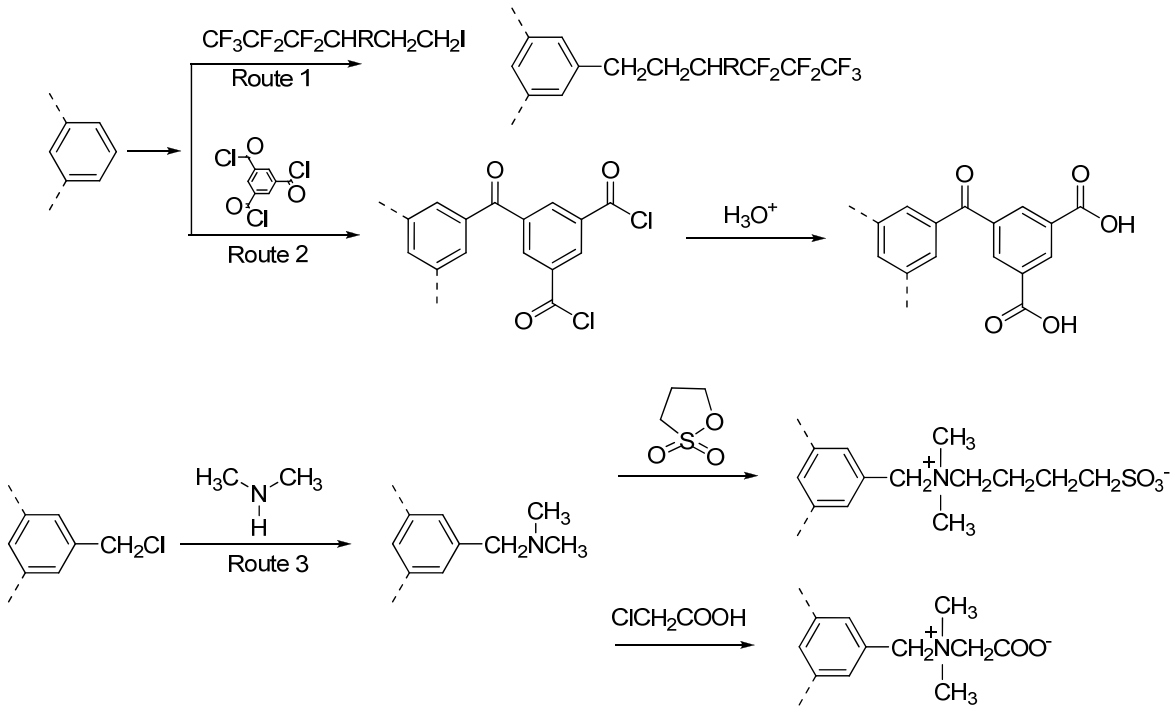

Figure 6.2 The proposed synthesis schemes for different types of new HC phases

2) A zwitterionic phase is proposed as a more "universal" phase able to handle neutral, cationic and anionic solutes and be compatible with a second dimension RPLC phase. The diversity of chemicals faced in multi-component samples frequently entails mixtures containing carboxylic acids, neutrals, and basic (e.g. amine) compounds in a single sample. Clearly neither anion-exchange nor cation-exchange chromatography alone suffice for the first dimension. Zwitterionic phases were pioneered in the early 90s by e.g. Weber [28] and Hartwick [29,30].

Bibliography

Chapter 1

[1] H. Elgass, H. Engelhardt, I. Halasz, Fresenius Zeitschrift Fur Analytische Chemie 294 (1979) 97.
[2] G. Schomburg, Lc Gc-Magazine of Separation Science 6 (1988) 36.
[3] K.K. Unger, Journal of Chromatography Library, Vol. 16: Porous Silica, Its Properties and Use as Support in Column Liquid Chromatography, Elsevier Scientific Pub. Co., New York, 1979.
[4] W. Melander, J. Stoveken, C. Horvath, J. Chromatogr. A 199 (1980) 35.
[5] H. Engelhardt, G. Ahr, Chromatographia 14 (1981) 227.
[6] U.D. Neue, in R.A. Meyers (Editor), Encyclopedia of Analytical Chemistry, John Wiley and Sons, New York, 2000.
[7] L.C. Sander, S.A. Wise, in CRC Critical Reviews in Analytical Chemistry, CRC Press, Boca Raton, 1987.
[8] K.K. Unger, Packings and Stationary Phases in Chromatographic Techniques, M. Dekker, New York, 1989.
[9] D.V. McCalley, LC-GC 17 (1999) 440.
[10] D.V. McCalley, J. Chromatogr. 902 (2000) 311.
[11] J. Nawrocki, Chromatographia 31 (1991) 193.
[12] L.J. Ma, P.W. Carr, Analytical Chemistry 79 (2007) 4681.
[13] J. Nawrocki, Chromatographia 31 (1991) 177.
[14] J. Nawrocki, J. Chromatogr. A 779 (1997) 29.
[15] H.A. Claessens, M.A.v. Straten, J.J. Kirkland, J. Chromatogr. A 728 (1996) 259.
[16] J.J. Kirkland, LC-GC 14 (1996) 486.
[17] H. Luo, P.W. Carr, Analytical and Bioanalytical Chemistry 391 (2008) 919.
[18] J.J. Kirkland, J.W. Henderson, J.J. DeStefano, M.A.v. Straten, H.A. Claessens, J. Chromatogr. A 762 (1997) 97.
[19] L.R. Snyder, J.L. Glajch, J.J. Kirkland, Practical HPLC Method Development, Wiley-Interscience, New York, 1996.
[20] Y. Mao, P.W. Carr, Anal. Chem. 72 (2000) 110.
[21] Y. Mao, P.W. Carr, Anal. Chem. 72 (2000) 2788.
[22] Y. Mao, P.W. Carr, Anal. Chem. 73 (2001) 1821.
[23] Y. Mao, P.W. Carr, Anal. Chem. 73 (2001) 4478.
[24] F.D. Antia, C. Horvath, J. Chromatogr. 435 (1988) 1.
[25] B. Yan, J. Zhao, J.S. Brown, J. Blackwell, P.W. Carr, Anal. Chem. 72 (2000) 1253.
[26] D.R. Stoll, X.P. Li, X.O. Wang, P.W. Carr, S.E.G. Porter, S.C. Rutan, Journal of Chromatography A 1168 (2007) 3.
[27] H. Luo, Chemistry, University of Minnesota, Minneapolis, 2006.
[28] J. Nawrocki, C. Dunlap, A. McCormick, P.W. Carr, Journal of chromatography A 1028 (2004) 1.
[29] M.J.J. Hetem, J.W. De Haan, H.A. Claessens, L.J.M. Van de Ven, C.A. Cramers, J.N. Kinkel, Analytical Chemistry 62 (1990) 2288.
[30] J.J. Kirkland, J.L. Glajch, R.D. Farlee, Anal. Chem. 61 (1989) 2.

[31] J.L. Glajch, J.J. Kirkland, U.S. Patent # 4,705,725, 1987.
[32] M.J. Wirth, R.W.P. Fairbank, H.O. Fatunmbi, Science 275 (1997) 44.
[33] M.J. Wirth, H.O. Fatunmbi, Analytical Chemistry 64 (1992) 2783.
[34] M.J. Wirth, H.O. Fatunmbi, Anal. Chem. 65 (1993) 822.
[35] M.J. Wirth, H.O. Fatunmbi, U.S. Patent # 5,599,625, 1997.
[36] M.J. Wirth, H.O. Fatunmbi, U.S. Patent # 5,716,705, 1998.
[37] B.C. Trammell, L. Ma, H. Luo, D. Jin, M.A. Hillmyer, P.W. Carr, Anal. Chem. 74 (2002) 4634.
[38] J.J. Pesek, W. Rashet, Chromatographia 30 (1990) 442.
[39] H.O. Fatunmbi, M.D. Bruch, M.J. Wirth, Anal. Chem. 65 (1993) 2048.
[40] M.R. Buchmeiser, J. of Chromatography, A 918 (2001) 233.
[41] J.J. Pesek, M.T. Matyska, Journal of Chromatography, A 952 (2002) 1.
[42] R.A. Henry, American Laboratory (Shelton, CT, United States) 34 (2002) 18.
[43] R.E. Majors, LC-GC 4 (1986) 872.
[44] M. Hanson, B. Eray, K. Unger, A.V. Neimark, J. Schmid, K. Albert, E. Bayer, Chromatographia 35 (1993) 403.
[45] C.G. Horvath, S.R. Lipsky, Nature 211 (1966) 748.
[46] B.B. Wheals, Journal of Chromatography 107 (1975) 402.
[47] D.H. Reeder, J. Li, P.W. Carr, M.C. Flickinger, A.V. McCormick, J. Chromatogr. A 760 (1997) 71.
[48] T.P. Weber, P.W. Carr, E.F. Funkenbusch, J. Chromatogr. 519 (1990) 31.
[49] T.P. Weber, P.T. Jackson, P.W. Carr, Anal. Chem. 67 (1995) 3042.
[50] J. Li, P.W. Carr, Anal. Chim. Acta 334 (1996) 239.
[51] J. Li, P.W. Carr, Anal. Chem. 68 (1996) 2857.
[52] J. Li, P.W. Carr, Anal. Chem. 69 (1997) 2193.
[53] J. Li, D.H. Reeder, A.V. McCormick, P.W. Carr, J. Chromatogr. A 791 (1997) 45.
[54] J.L. Glajch, J.J. Kirkland, U.S. Patent # 4,847,159, 1989.
[55] Agilent Zorbax Column Selection Guide, Agilent Technologies, 2001.
[56] B.C. Trammell, L.J. Ma, H. Luo, M.A. Hillmyer, P.W. Carr, Journal of Chromatography A 1060 (2004) 61.
[57] L.J. Ma, H. Luo, J. Dai, P.W. Carr, Journal of Chromatography A 1114 (2006) 21.
[58] H. Luo, L.J. Ma, Y. Zhang, P.W. Carr, Journal of Chromatography A 1182 (2008) 41.
[59] G.I. Rosenberg, A.S. Shabaeva, V.S. Moryakov, T.G. Musin, M.P. Tsyurupa, V.A. Davankov, Reactive Polymers, Ion Exchangers, Sorbents 1 (1983) 175.
[60] J.C. Giddings, Unified Separation Science, Wiley-Interscience, New York, 1991.
[61] J.J. Gilroy, J.W. Dolan, L.R. Snyder, Journal of Chromatography A 1000 (2003) 757.
[62] J.J. Gilroy, J.W. Dolan, P.W. Carr, L.R. Snyder, Journal of Chromatography A 1026 (2004) 77.
[63] N.S. Wilson, J. Gilroy, J.W. Dolan, L.R. Snyder, Journal of Chromatography A 1026 (2004) 91.
[64] D.H. Marchand, K. Croes, J.W. Dolan, L.R. Snyder, Journal of Chromatography A 1062 (2005) 57.
[65] D.H. Marchand, K. Croes, J.W. Dolan, L.R. Snyder, R.A. Henry, K.M.R. Kallury, S. Waite, P.W. Carr, Journal of Chromatography A 1062 (2005) 65.

[66] N.S. Wilson, M.D. Nelson, J.W. Dolan, L.R. Snyder, R.G. Wolcott, P.W. Carr, J. Chromatogr. A 961 (2002) 171.
[67] N.S. Wilson, M.D. Nelson, J.W. Dolan, L.R. Snyder, P.W. Carr, J. Chromatogr. A 961 (2002) 195.
[68] N.S. Wilson, J.W. Dolan, L.R. Snyder, P.W. Carr, L.C. Sander, J. Chromatogr. A 961 (2002) 217.
[69] L.R. Snyder, J.W. Dolan, P.W. Carr, J. Chromatogr. A 1060 (2004) 77.
[70] J. Nawrocki, B. Buszewski, J. Chromatogr. 449 (1989) 1.
[71] M. Verzele, M. Depotter, Journal of Chromatography 166 (1978) 320.
[72] P.C. Sadek, C.J. Koester, L.D. Bowers, Journal of Chromatographic Science 25 (1987) 489.
[73] U.D. Neue, E. Serowik, P. Iraneta, B.A. Alden, T.H. Walter, Journal of chromatography A 849 (1999) 87.
[74] U.D. Neue, Y.F. Cheng, Z. Lu, B.A. Alden, P.C. Iraneta, C.H. Phoebe, K. Van Tran, Chromatographia 54 (2001) 169.
[75] D.V. Mccalley, Journal of Chromatography A 664 (1994) 139.
[76] T.L. Ascah, B. Feibush, Journal of Chromatography 506 (1990) 357.
[77] B. Buszewski, J. Schmid, K. Albert, E. Bayer, Journal of Chromatography 552 (1991) 415.
[78] T. Czajkowska, I. Hrabovsky, B. Buszewski, R.K. Gilpin, M. Jaroniec, Journal of chromatography A 691 (1995) 217.
[79] J.E. O'Gara, D.P. Walsh, C.H. Phoebe, B.A. Alden, I.S.P. Bouvier, P.C. Iraneta, M. Capparella, T.H. Walter, Lc Gc North America 19 (2001) 632.
[80] J. Schmid, K. Albert, E. Bayer, Journal of chromatography A 694 (1995) 333.
[81] A. Sandi, L. Szepesy, Journal of chromatography A 818 (1998) 1.
[82] U.D. Neue, B.A. Alden, T.H. Walter, Journal of chromatography A 849 (1999) 101.
[83] R. Nasuto, L. Kwietniewski, Chromatographia 29 (1990) 597.
[84] A. Kaibara, M. Hirose, T. Nakagawa, Chromatographia 30 (1990) 99.
[85] T. Hanai, J. Hubert, Journal of Chromatography 291 (1984) 81.
[86] T. Hanai, F. Ahmed, I. Rustamov, D. Babusis, Journal of Liquid Chromatography & Related Technologies 22 (1999) 501.
[87] N. Tanaka, Y. Tokuda, K. Iwaguchi, M. Araki, Journal of Chromatography 239 (1982) 761.
[88] S.H.Y. Wong, S.L. Mchugh, J. Dolan, K.A. Cohen, Journal of Liquid Chromatography 9 (1986) 2511.
[89] C. Stella, S. Heinisch, X.L. Liu, P.A. Carrupt, G. Cazorla, J.Y. Gauvrit, P. Lanteri, K. Le Mapihan, J. Vial, S. Heron, A. Tchapla, J.L. Rocca, J.L. Veuthey, S. Rudaz, Journal of Pharmaceutical and Biomedical Analysis 39 (2005) 104.
[90] G.E. Berendsen, K.A. Pikaart, L.D. Galan, C. Olieman, Analytical Chemistry 52 (1980) 1990.
[91] H.A.H. Billiet, P.J. Schoenmakers, L. Degalan, Journal of Chromatography 218 (1981) 443.
[92] K. Jinno, H. Nakamura, Chromatographia 39 (1994) 285.
[93] T. Monde, T. Kamiusuki, T. Kuroda, K. Mikumo, T. Ohkawa, H. Fukube, Journal of chromatography A 722 (1996) 273.

[94] F.M. Rabel, D.A. Martin, Journal of Liquid Chromatography 6 (1983) 2465.
[95] P.C. Sadek, P.W. Carr, Journal of Chromatography 288 (1984) 25.
[96] E. Csato, N. Fulop, G. Szabo, Journal of Chromatography 511 (1990) 79.
[97] M.R. Euerby, A.P. McKeown, P. Petersson, Journal of Separation Science 26 (2003) 295.
[98] J.J. Hetem, Chemically Modified Silica Surfaces in Chromatography: A Fundamental Study, Huthig Buch Verlag, Heidelberg, 1993.
[99] E. Lesellier, C. West, Journal of chromatography A 1158 (2007) 329.
[100] M. Vitha, P.W. Carr, Journal of Chromatography A 1126 (2006) 143.
[101] K. Kimata, K. Iwaguchi, S. Onishi, K. Jinno, R. Eksteen, K. Hosoya, M. Araki, N. Tanaka, Journal of Chromatographic Science 27 (1989) 721.
[102] H. Engelhardt, M. Arangio, T. Lobert, LC-GC 15 (1997) 856.
[103] L.C. Sander, S.A. Wise, Anal. Chem. 59 (1987) 2309.
[104] A. Sandi, A. Bede, L. Szepesy, G. Rippel, Chromatographia 45 (1997) 206.
[105] M.J. Kamlet, R.W. Taft, Acta. Chem. Scand., Ser. B 39 (1985) 611.
[106] M.J. Kamlet, M.H. Abraham, P.W. Carr, R.M. Doherty, R.W. Taft, J. Chem. Soc. Perkin Trans. II 12 (1988) 2087.
[107] H.A. Claessens, M.A. van Straten, C.A. Cramers, M. Jezierska, B. Buszewski, Journal of chromatography A 826 (1998) 135.
[108] T. Baczek, R. Kaliszan, K. Novotn, P. Jandera, Journal of chromatography A 1075 (2005) 109.
[109] C.M. John, Journal of chemical technology and biotechnology. Chemical technology 34 (1984) 38.
[110] J.W. Dolan, L.R. Snyder, Journal of Chromatography A 1216 (2009) 3467.

Chapter 2

[1] J.W. Dolan, L.R. Snyder, N.M. Djordjevic, D.W. Hill, D.L. Saunders, L. Van Heukelem, T.J. Waeghe, J. Chromatogr. A 803 (1998) 1.
[2] P.L. Zhu, L.R. Snyder, J.W. Dolan, N.M. Djordjevic, D.W. Hill, L.C. Sander, T.J. Waeghe, J. Chromatogr. A 756 (1996) 21.
[3] W.S. Hancock, R.C. Chloupek, J.J. Kirkland, L.R. Snyder, J. Chromatogr. A 686 (1994) 31.
[4] A. Marin, C. Barbas, Journal of Pharmaceutical and Biomedical Analysis 40 (2006) 262.
[5] J. Pellett, P. Lukulay, Y. Mao, W. Bowen, R. Reed, M. Ma, R.C. Munger, J.W. Dolan, L. Wrisley, K. Medwid, N.P. Toltl, C.C. Chan, M. Skibic, K. Biswas, K.A. Wells, L.R. Snyder, Journal of Chromatography A 1101 (2006) 122.
[6] R.M. Krisko, K. McLaughlin, M.J. Koenigbauer, C.E. Lunte, Journal of Chromatography A 1122 (2006) 186.
[7] J.W. Dolan, A. Maule, D. Bingley, L. Wrisley, C.C. Chan, M. Angod, C. Lunte, R. Krisko, J.M. Winston, B.A. Homeier, D.V. McCalley, L.R. Snyder, Journal of Chromatography A 1057 (2004) 59.
[8] A. Makarov, R. LoBrutto, Y. Kazakevich, Journal of Liquid Chromatography & Related Technologies 31 (2008) 1533.

[9] D.M. Diehl, E.S. Grumbach, J.R. Mazzeo, U.D. Neue, Abstracts of Papers of the American Chemical Society 227 (2004) U58.
[10] W. Melander, J. Stoveken, C. Horvath, J. Chromatogr. A 199 (1980) 35.
[11] J.F. Wheeler, T.L. Beck, S.J. Klatte, L.A. Cole, J.G. Dorsey, Journal of chromatography A 656 (1993) 317.
[12] N. Tanaka, K. Kimata, K. Hosoya, H. Miyanishi, T. Araki, Journal of chromatography A 656 (1993) 265.
[13] L.C. Tan, P.W. Carr, M.H. Abraham, Journal of chromatography A 752 (1996) 1.
[14] J.J. Destefano, J.A. Lewis, L.R. Snyder, Lc Gc-Magazine of Separation Science 10 (1992) 130.
[15] D.H. Marchand, L.R. Snyder, J.W. Dolan, Journal of Chromatography A 1191 (2008) 2.
[16] J.J. Gilroy, J.W. Dolan, L.R. Snyder, Journal of Chromatography A 1000 (2003) 757.
[17] J.J. Gilroy, J.W. Dolan, P.W. Carr, L.R. Snyder, Journal of Chromatography A 1026 (2004) 77.
[18] N.S. Wilson, J. Gilroy, J.W. Dolan, L.R. Snyder, Journal of Chromatography A 1026 (2004) 91.
[19] D.H. Marchand, K. Croes, J.W. Dolan, L.R. Snyder, Journal of Chromatography A 1062 (2005) 57.
[20] D.H. Marchand, K. Croes, J.W. Dolan, L.R. Snyder, R.A. Henry, K.M.R. Kallury, S. Waite, P.W. Carr, Journal of Chromatography A 1062 (2005) 65.
[21] R. Nogueira, D. Lubda, A. Leitner, W. Bicker, N.M. Maier, M. Lammerhofer, W. Lindner, Journal of Separation Science 29 (2006) 966.
[22] W. Bicker, M. Lammerhofer, W. Lindner, Journal of Chromatography B-Analytical Technologies in the Biomedical and Life Sciences 822 (2005) 160.
[23] W. Bicker, M. Lammerhofer, T. Keller, R. Schuhmacher, R. Krska, W. Lindner, Analytical Chemistry 78 (2006) 5884.
[24] R. Nogueira, M. Lammerhofer, W. Lindner, Journal of Chromatography A 1089 (2005) 158.
[25] K. Ohyama, Y. Shirasawa, M. Wada, N. Kishikawa, Y. Ohba, K. Nakashima, N. Kuroda, Journal of chromatography A 1042 (2004) 189.
[26] E. Apfelthaler, W. Bicker, M. Lammerhofer, M. Sulyok, R. Krska, W. Lindner, R. Schuhmacher, Journal of chromatography A 1191 (2008) 171.
[27] H. Luo, L.J. Ma, C. Paek, P.W. Carr, Journal of Chromatography A 1202 (2008) 8.
[28] W. Bicker, M. Lammerhofer, W. Lindner, Analytical and Bioanalytical Chemistry 390 (2008) 263.
[29] M. Lammerhofer, M. Richter, J.Y. Wu, R. Nogueira, W. Bicker, W. Lindner, Journal of Separation Science 31 (2008) 2572.
[30] L.R. Snyder, J.W. Dolan, P.W. Carr, J. Chromatogr. A 1060 (2004) 77.
[31] K. Koczian, E. Haghedooren, S. Dragovic, B. Noszal, J. Hoogmartens, E. Adams, Journal of Pharmaceutical and Biomedical Analysis 44 (2007) 894.
[32] C. West, E. Lesellier, Journal of Chromatography A 1203 (2008) 105.
[33] E. Haghedooren, D. Visky, P. Dehouck, K. Koczian, J. Diana, Z. Kovacs, B. Noszal, J. Hoogmartens, E. Adams, Lc Gc Europe 20 (2007) 82.

[34] E. Haghedooren, J. Diana, B. Noszal, J. Hoogmartens, E. Adams, Talanta 71 (2007) 31.
[35] D.R. Stoll, X.P. Li, X.O. Wang, P.W. Carr, S.E.G. Porter, S.C. Rutan, Journal of Chromatography A 1168 (2007) 3.
[36] N. Fontanals, R.M. Marce, F. Borrull, Journal of Chromatography A 1152 (2007) 14.
[37] S.H. Zhang, J. Zhang, C. Horvath, Journal of Chromatography A 914 (2001) 189.
[38] B. Scherer, F. Steiner, Journal of Chromatography A 924 (2001) 197.
[39] C.W. Klampfl, W. Buchberger, P.R. Haddad, Journal of Chromatography A 911 (2001) 277.
[40] P.Q. Huang, X.Y. Jin, Y.J. Chen, J.R. Srinivasan, D.M. Lubman, Analytical Chemistry 71 (1999) 1786.
[41] Z. Deyl, F. Svec, Capillary electrochromatography, Elsevier, Amsterdam, 2001.
[42] K. Ohyama, Y. Shirasawa, M. Wada, N. Kishikawa, Y. Ohba, K. Nakashima, N. Kuroda, Electrophoresis 25 (2004) 3224.
[43] C.G. Huber, E. Stimpf, P.J. Oefner, G.K. Bonn, Lc Gc-Magazine of Separation Science 14 (1996) 114.
[44] L.R. Snyder, J.L. Glajch, J.J. Kirkland, Practical HPLC Method Development, Wiley-Interscience, New York, 1996.
[45] R.E. Majors, LC-GC 4 (1986) 872.
[46] F. Progent, M.Taverna, A. Banco, A.Tchapla, C.Smadja, Journal of chromatography A 1136 (2006) 221.
[47] B.G. Keevil, S. Thornton, Clinical Chemistry 52 (2006) A180.
[48] H. Luo, P.W. Carr, Analytical and Bioanalytical Chemistry 391 (2008) 919.
[49] L.J. Ma, P.W. Carr, Analytical Chemistry 79 (2007) 4681.
[50] L.J. Ma, H. Luo, J. Dai, P.W. Carr, Journal of Chromatography A 1114 (2006) 21.
[51] B.C. Trammell, L.J. Ma, H. Luo, M.A. Hillmyer, P.W. Carr, Journal of Chromatography A 1060 (2004) 61.
[52] B.C. Trammell, L.J. Ma, H. Luo, D.H. Jin, M.A. Hillmyer, P.W. Carr, Analytical Chemistry 74 (2002) 4634.
[53] H. Luo, L.J. Ma, Y. Zhang, P.W. Carr, Journal of Chromatography A 1182 (2008) 41.
[54] W. Kopaciewicz, S. Fulton, S.Y. Lee, Journal of Chromatography 409 (1987) 111.
[55] L.G. Gagliardi, C.B. Castells, C. Rafols, M. Roses, E. Bosch, Analytical Chemistry 79 (2007) 3180.
[56] X.Q. Yang, L.J. Ma, P.W. Carr, Journal of Chromatography A 1079 (2005) 213.
[57] Q. Xing, Y. X., R. Q.;, Z. Zhou, W.W. Pei, Basic Organic Chemistry, Advanced Education Press, Beijing, 2000.
[58] K.E. Bij, C. Horvath, W.R. Melander, A. Nahum, Journal of Chromatography 203 (1981) 65.
[59] S.A. Carr, M.J. Huddleston, M.F. Bean, Protein Sci. 2 (1993) 183.
[60] X.Q. Yang, J. Dai, P.W. Carr, Analytical Chemistry 75 (2003) 3153.
[61] M.A. Stadalius, J.S. Berus, L.R. Snyder, Lc Gc-Magazine of Separation Science 6 (1988) 494.

[62] J.S. Kiel, S.L. Morgan, R.K. Abramson, Journal of Chromatography 320 (1985) 313.
[63] R. Gill, S.P. Alexander, A.C. Moffat, Journal of Chromatography 247 (1982) 39.
[64] X.Q. Yang, J. Dai, P.W. Carr, Journal of Chromatography A 996 (2003) 13.
[65] J. Dai, X.Q. Yang, P.W. Carr, Journal of Chromatography A 1005 (2003) 63.
[66] N.S. Wilson, M.D. Nelson, J.W. Dolan, L.R. Snyder, R.G. Wolcott, P.W. Carr, J. Chromatogr. A 961 (2002) 171.
[67] N.S. Wilson, M.D. Nelson, J.W. Dolan, L.R. Snyder, P.W. Carr, J. Chromatogr. A 961 (2002) 195.
[68] N.S. Wilson, J.W. Dolan, L.R. Snyder, P.W. Carr, L.C. Sander, J. Chromatogr. A 961 (2002) 217.
[69] J.W. Dolan, L.R. Snyder, Journal of Chromatography A 1216 (2009) 3467.
[70] W. Melander, J. Stoveken, C. Horvath, Journal of Chromatography 199 (1980) 35.
[71] J.H. Zhao, P.W. Carr, Analytical Chemistry 70 (1998) 3619.
[72] A.S. Wang, L.C. Tan, P.W. Carr, Journal of chromatography A 848 (1999) 21.
[73] P.W. Carr, M. Vitha, J. Weckwerth, L.C. Tan, J. Li, Abstracts of Papers of the American Chemical Society 216 (1998) U190.
[74] J.A. Blackwell, P.W. Carr, Hrc-Journal of High Resolution Chromatography 21 (1998) 427.
[75] M.J. Kamlet, M.H. Abraham, P.W. Carr, R.M. Doherty, R.W. Taft, J. Chem. Soc. Perkin Trans. II 12 (1988) 2087.
[76] M.J. Kamlet, R.W. Taft, Acta. Chem. Scand., Ser. B 39 (1985) 611.
[77] C.M. John, Journal of chemical technology and biotechnology. Chemical technology 34 (1984) 38.
[78] M. Vitha, P.W. Carr, Journal of Chromatography A 1126 (2006) 143.
[79] J. Dai, P.W. Carr, D.V. McCalley, Journal of Chromatography A 1216 (2009) 2474.
[80] J.L. Wade, A.F. Bergold, P.W. Carr, Analytical Chemistry 59 (1987) 1286.
[81] C.A. Lucy, J.L. Wade, P.W. Carr, Journal of Chromatography 484 (1989) 61.
[82] N.H. Davies, M.R. Euerby, D.V. McCalley, Journal of chromatography A 1138 (2007) 65.
[83] B. Paull, P.N. Nesterenko, Analyst 130 (2005) 134.
[84] A. Klingenberg, A. Seubert, Journal of chromatography A 946 (2002) 91.
[85] A. Klingenberg, A. Seubert, Journal of Chromatography 640 (1993) 167.
[86] D.V. McCalley, Journal of chromatography A 793 (1998) 31.
[87] S.M.C. Buckenmaier, D.V. McCalley, M.R. Euerby, Analytical Chemistry 74 (2002) 4672.
[88] J.E. Eble, R.L. Grob, P.E. Antle, L.R. Snyder, Journal of Chromatography 384 (1987) 45.
[89] D.V. McCalley, Analytical Chemistry 75 (2003) 3404.

Chapter 3

[1] J.W. Dolan, L.R. Snyder, N.M. Djordjevic, D.W. Hill, D.L. Saunders, L. Van Heukelem, T.J. Waeghe, J. Chromatogr. A 803 (1998) 1.
[2] P.L. Zhu, L.R. Snyder, J.W. Dolan, N.M. Djordjevic, D.W. Hill, L.C. Sander, T.J. Waeghe, J. Chromatogr. A 756 (1996) 21.
[3] W.S. Hancock, R.C. Chloupek, J.J. Kirkland, L.R. Snyder, J. Chromatogr. A 686 (1994) 31.
[4] L.R. Snyder, J. Chromatogr. A 92 (1974) 223.
[5] C. Horvath, W. Melander, I. Molnar, J. Chromatogr. 125 (1976) 129.
[6] A. Vailaya, C. Horvath, J. Phys. Chem. B 102 (1998) 701.
[7] F.D. Antia, C. Horvath, J. Chromatogr. 550 (1991) 411.
[8] W. Melander, J. Stoveken, C. Horvath, J. Chromatogr. 199 (1980) 35.
[9] W. Melander, D.E. Campbell, C. Horvath, J. Chromatogr. 158 (1978) 215.
[10] B.K. Chen, C. Horvath, J. Chromatogr. 171 (1979) 15.
[11] A. Nahum, C. Horvath, J. Chromatogr. 203 (1981) 53.
[12] D.E. Martire, R.E. Boehm, J. Liq. Chromatogr. 3 (1980) 753.
[13] D.E. Martire, R.E. Boehm, J. Phys. Chem. 91 (1987) 2433.
[14] D.E. Martire, J. Chromatogr. 471 (1989) 71.
[15] L.R. Snyder, J.W. Dolan, P.W. Carr, J. Chromatogr. A 1060 (2004) 77.
[16] N.S. Wilson, M.D. Nelson, J.W. Dolan, L.R. Snyder, R.G. Wolcott, P.W. Carr, J. Chromatogr. A 961 (2002) 171.
[17] H. Colin, A.M. Krstulovic, M.F. Gonnord, G. Guiochon, Z. Yun, P. Jandera, Chromatographia 17 (1983) 9.
[18] M. Vitha, P.W. Carr, J. Chromatogr. A 1126 (2006) 143.
[19] A. Tchapla, S. Heron, H. Colin, G. Guiochon, Anal. Chem. 60 (1988) 1443.
[20] L. Limsavarn, J.G. Dorsey, J. Chromatogr. A 1102 (2006) 143.
[21] S.R. Cole, J.G. Dorsey, J. Chromatogr. A 635 (1993) 177.
[22] K.B. Sentell, J.G. Dorsey, J. Chromatogr. A 461 (1989) 193.
[23] L.C. Tan, P.W. Carr, M.H. Abraham, J. Chromatogr. A 752 (1996) 1.
[24] D. Bolliet, C.F. Poole, M. Roses, Anal. Chim. Acta. 368 (1998) 129.
[25] M.H. Abraham, M. Roses, C.F. Poole, S.K. Poole, J. Phys. Org. Chem. 10 (1997) 358.
[26] L.A. Lopez, S.C. Rutan, J. Chromatogr. A 965 (2002) 301.
[27] M.F. Delaney, A.N. Papas, M.J. Walters, J. Chromatogr. 410 (1987) 31.
[28] L.C. Sander, S.A. Wise, Anal. Chem. 67 (1995) 3284.
[29] K.J. Schostack, E.R. Malinowski, Chemom. Intell. Lab. Syst. 6 (1989) 21.
[30] H. Engelhardt, M. Jungheim, Chromatographia 29 (1990) 59.
[31] L.R. Snyder, P.W. Carr, S.C. Rutan, J. Chromatogr. A 656 (1993) 537.
[32] P.C. Sadek, P.W. Carr, R.M. Doherty, M.J. Kamlet, R.W. Taft, M.H. Abraham, Anal. Chem. 57 (1985) 2971.
[33] U.D. Neue, B.A. Alden, T.H. Walter, J. Chromatogr. A 849 (1999) 101.
[34] R. Kaliszan, Structure and Retention in Chromatography: A Chemometric Approach, Harwood Acad. Publ., Amsterdam, 1997.
[35] D.H. Marchand, L.R. Snyder, J.W. Dolan, J. Chromatogr. A 1191 (2008) 2.
[36] J.W. Dolan, L.R. Snyder, J. Chromatogr. A 1216 (2009) 3467.
[37] L.C. Sander, S.A. Wise, CRC Crit. Rev. Anal. Chem. 18 (1987) 299.
[38] L.C. Sander, S.A. Wise, J. High. Resolut. Chrom. Chrom. Comm. 11 (1988) 383.

[39] K. Kimata, K. Iwaguchi, S. Onishi, K. Jinno, R. Eksteen, K. Hosoya, M. Araki, N. Tanaka, J. Chromatogr. Sci. 27 (1989) 721.
[40] E. Cruz, M.R. Euerby, C.M. Johnson, C.A. Hackett, Chromatographia 44 (1997) 151.
[41] J. Layne, J. Chromatogr. A 957 (2002) 149.
[42] L.C. Sander, S.A. Wise, J. Sep. Sci. 26 (2003) 283.
[43] C.F. Poole, S.K. Poole, J. Chromatogr. A 965 (2002) 263.
[44] L. Szepesy, J. Sep. Sci. 26 (2003) 201.
[45] D. Visky, Y. Vander Heyden, T. Ivanyi, P. Baten, J. De Beer, Z. Kovacs, B. Noszal, E. Roets, D.L. Massart, J. Hoogmartens, J. Chromatogr. A 977 (2002) 39.
[46] D.H. Marchand, K. Croes, J.W. Dolan, L.R. Snyder, R.A. Henry, K.M.R. Kallury, S. Waite, P.W. Carr, J. Chromatogr. A 1062 (2005) 65.
[47] D.H. Marchand, K. Croes, J.W. Dolan, L.R. Snyder, J. Chromatogr. A 1062 (2005) 57.
[48] N.S. Wilson, J. Gilroy, J.W. Dolan, L.R. Snyder, J. Chromatogr. A 1026 (2004) 91.
[49] J.J. Gilroy, J.W. Dolan, P.W. Carr, L.R. Snyder, J. Chromatogr. A 1026 (2004) 77.
[50] J.J. Gilroy, J.W. Dolan, L.R. Snyder, J. Chromatogr. A 1000 (2003) 757.
[51] N.S. Wilson, M.D. Nelson, J.W. Dolan, L.R. Snyder, P.W. Carr, J. Chromatogr. A 961 (2002) 195.
[52] N.S. Wilson, J.W. Dolan, L.R. Snyder, P.W. Carr, L.C. Sander, J. Chromatogr. A 961 (2002) 217.
[53] R.M. Smith, Retention and selectivity in liquid chromatography Elsevier Science; 1st edition Amsterdam, 1995.
[54] D.E. Martire, R.E. Boehm, J. Phys. Chem. 87 (1983) 1045.
[55] S. Dragovic, E. Haghedooren, T. Nemeth, I.M. Palabiyik, J. Hoogmartens, E. Adams, J. Chromatogr. A 1216 (2009) 3210.
[56] T. Baczek, R. Kaliszan, K. Novotn, P. Jandera, J. Chromatogr. A 1075 (2005) 109.
[57] J. Pellett, P. Lukulay, Y. Mao, W. Bowen, R. Reed, M. Ma, R.C. Munger, J.W. Dolan, L. Wrisley, K. Medwid, N.P. Toltl, C.C. Chan, M. Skibic, K. Biswas, K.A. Wells, L.R. Snyder, J. Chromatogr. A 1101 (2006) 122.
[58] J. Zhao, P.W. Carr, Anal. Chem. 71 (1999) 2623.
[59] M.H. Abraham, H.S. Chadha, A.R.E. Leitao, R.C. Mitchell, W.J. Lambert, R. Kaliszan, A. Nasal, P. Haber, J. Chromatogr. A 766 (1997) 35.
[60] A. Sandi, M. Nagy, L. Szepesy, J. Chromatogr. A 893 (2000) 215.
[61] A. Sandi, L. Szepesy, J. Chromatogr. A 818 (1998) 1.
[62] S.C. Rutan, P.W. Carr, W.J. Cheong, J.H. Park, L.R. Snyder, J. Chromatogr. A 463 (1989) 21.
[63] M. Gilar, P. Olivova, A.E. Daly, J.C. Gebler, Anal. Chem. 77 (2005) 6426.
[64] E. Lesellier, C. West, J. Chromatogr. A 1158 (2007) 329.
[65] L.R. Snyder, Column Match Database(personal communication with Dr. L. R. Snyder).
[66] H. Luo, L.J. Ma, Y. Zhang, P.W. Carr, J. Chromatogr. A 1182 (2008) 41.
[67] H. Luo, L.J. Ma, C. Paek, P.W. Carr, J. Chromatogr. A 1202 (2008) 8.

[68] L.J. Ma, H. Luo, J. Dai, P.W. Carr, J. Chromatogr. A 1114 (2006) 21.
[69] B.C. Trammell, L.J. Ma, H. Luo, M.A. Hillmyer, P.W. Carr, J. Chromatogr. A 1060 (2004) 61.
[70] C. West, E. Lesellier, J. Chromatogr. A 1203 (2008) 105.
[71] U.D. Neue, K. VanTran, P.C. Iraneta, B.A. Alden, J. Sep. Sci. 26 (2003) 174.
[72] M. Euerby, P. Petersson, J. Chromatogr. A 994 (2003) 13.
[73] M.R. Schure, Multidimensional Liquid Chromatography: Theory, Instrumentation and Applications, Wiley, New York, 2008.
[74] D.R. Stoll, X.P. Li, X.O. Wang, P.W. Carr, S.E.G. Porter, S.C. Rutan, J. Chromatogr. A 1168 (2007) 3.
[75] J.C. Giddings, Anal. Chem. 56 (1984) 1258.

Chapter 4

[1] R.E. Majors, LC-GC North America 26 (2008) 16.
[2] J.E. MacNair, K.C. Lewis, J.W. Jorgenson, Analytical Chemistry 69 (1997) 983.
[3] J.R. Mazzeo, U.D. Neue, M. Kele, R.S. Plumb, Analytical Chemistry 77 (2005) 460a.
[4] W. Naijun, R. Thompson, in Journal of Liquid Chromatography & Related Technologies, Taylor & Francis Ltd, 2006, p. 949.
[5] J.J. DeStefano, T.J. Langlois, J.J. Kirkland, J. Chromatogr. Sci. 46 (2008) 254.
[6] H. Chen, C. Horvath, Anal. Methods Instrum. 1 (1994) 213.
[7] J.D. Thompson, P.W. Carr, Anal. Chem. 74 (2002) 4150.
[8] B. Yan, J. Zhao, J.S. Brown, J. Blackwell, P.W. Carr, Anal. Chem. 72 (2000) 1253.
[9] F.D. Antia, C. Horvath, J. Chromatogr. 435 (1988) 1.
[10] T. Greibrokk, Journal of Separation Science 24 (2001) 897.
[11] T. Greibrokk, Analytical Chemistry 74 (2002) 374a.
[12] C.J. Dunlap, C.V. McNeff, D.R. Stoll, P.W. Carr, Anal. Chem. 73 (2001) 599A.
[13] D.R. Stoll, X. Li, X. Wang, P.W. Carr, S.E.G. Porter, S.C. Rutan, J. Chromatogr. A 1168 (2007) 3.
[14] H. Luo, L. Ma, Y. Zhang, P.W. Carr, J. Chromatogr. A 1182 (2008) 41.
[15] L. Ma, H. Luo, J. Dai, W. Carr Peter, J. Chromatogr. A 1114 (2006) 21.
[16] B.C. Trammell, L. Ma, H. Luo, M.A. Hillmyer, P.W. Carr, J. Am. Chem. Soc. 125 (2003) 10504.
[17] B.C. Trammell, L. Ma, H. Luo, M.A. Hillmyer, P.W. Carr, J. Chromatogr. A 1060 (2004) 61.
[18] G. Schomburg, Lc Gc-Magazine of Separation Science 6 (1988) 36.
[19] C.G. Horvath, S.R. Lipsky, Nature 211 (1966) 748.
[20] B.B. Wheals, Journal of Chromatography 107 (1975) 402.
[21] H. Luo, in Chemistry, University of Minnesota, Minneapolis, 2006.
[22] L. Ma, in Chemistry, University of Minnesota, Minneapolis, 2005.
[23] I.M. Halasz, K., Angewandte Chemie 90 (1978) 954.
[24] I.M. Halasz, K., Ber. Busenges Phys. Chem 79 (1975) 731.

[25] B.E. Boyes, A. Gratzfeld-Husgen, R. Weber, Chimia 55 (2001) 48.
[26] J. Dai, P.W. Carr, Journal of Chromatography A 1072 (2005) 169.
[27] J. Dai, P.W. Carr, D.V. McCalley, Journal of Chromatography A 1216 (2009) 2474.
[28] J. Dai, S.D. Mendonsa, M.T. Bowser, C.A. Lucy, P.W. Carr, Journal of Chromatography A 1069 (2005) 225.
[29] J. Dai, X.Q. Yang, P.W. Carr, Journal of Chromatography A 1005 (2003) 63.
[30] D.V. McCalley, Journal of chromatography A 793 (1998) 31.
[31] J. Dai, P.W. Carr, J. Chromatogr. A 1072 (2005) 169.
[32] D.V. McCalley, J. Chromatogr. A 987 (2003) 17.
[33] X. Yang, L. Ma, P.W. Carr, J. Chromatogr. A 1079 (2005) 213.

Chapter 5

[1] R.E. Majors, LC-GC N AM 26 (2008) 16.
[2] J.D. Thompson, P.W. Carr, Anal. Chem. 74 (2002) 4150.
[3] B.W. Yan, J.H. Zhao, J.S. Brown, J. Blackwell, P.W. Carr, Anal. Chem. 72 (2000) 1253.
[4] J.E. MacNair, K.C. Lewis, J.W. Jorgenson, Anal. Chem. 69 (1997) 983.
[5] J.R. Mazzeo, U. D.Neue, M. Kele, R.S. Plumb, Anal. Chem. 77 (2005) 460 A.
[6] N. Wu, R. Thompson, J. Liq. Chromatogr. Relat. Technol. 29 (2006) 949.
[7] J.J. DeStefano, T.J. Langlois, J.J. Kirkland, J. Chromatogr. Sci. 46 (2008).
[8] J.J. Kirkland, Anal. Chem. 64 (1992) 1239.
[9] X. Wang, W.E. Barber, P.W. Carr, J. Chromatogr. A 1107 (2006) 139.
[10] F. Gritti, G. Guiochon, J. Chromatogr. A 1166 (2007) 30.
[11] K. Kaczmarski, G. Guiochon, Anal. Chem. 79 (2007) 4648.
[12] J.M. Cunliffe, T.D. Maloney, J. Sep. Sci. 30 (2007) 3104.
[13] N. Marchetti, G. Guiochon, J. Chromatogr. A 1176 (2007) 206.
[14] J.J. van Deemter, F.J. Zuiderweg, A. Klinkenberg, Chem. Eng. Sci. 5 (1956) 271.
[15] G. Desmet, LC-GC Europe 21 (2008) 310.
[16] H. Poppe, J. Chromatogr. A 778 (1997) 3.
[17] X. Wang, D.R. Stoll, P.W. Carr, P.J. Schoenmakers, J. Chromatogr. A 1125 (2006) 177.
[18] P. Gzil, N. Vervoort, G.V. Baron, G. Desmet, Anal. Chem. 76 (2004) 6707.
[19] F. Lestremau, A. de Villiers, F. Lynen, A. Cooper, R. Szucs, P. Sandra, J. Chromatogr. A 1138 (2007) 120.
[20] D. Cabooter, A. de Villiers, D. Clicq, R. Szucs, P. Sandra, G. Desmet, J. Chromatogr. A 1147 (2007) 183.
[21] D. Cabooter, F. Lestremau, F. Lynen, P. Sandra, G. Desmet, J. Chromatogr. A 1212 (2008) 23.
[22] P.W. Carr, X. Wang, D.R. Stoll, In submission.
[23] H. Chen, C. Horvath, Anal. Methods & Instrum. 1 (1993) 213.
[24] J. Li, P.W. Carr, Anal. Chem. 69 (1997) 2550.
[25] D. Cabooter, J. Billen, H. Terryn, F. Lynen, P. Sandra, G. Desmet, J. Chromatogr. A 1178 (2008) 108.

[26] P. Petersson, A. Frank, J. Heaton, M.R. Euerby, J. Sep. Sci. 31 (2008) 2346.
[27] S.A.C. Wren, J. Pharm. Biomed. Anal. 38 (2005) 337.
[28] X. Wang, D.R. Stoll, A.P. Schellinger, P.W. Carr, Anal. Chem. 78 (2006) 3406.
[29] L.R. Snyder, J.W. Dolan, J.R. Gant, J. Chromatogr. A 165 (1979) 3.
[30] G. Guiochon, J. Chromatogr. A 1126 (2006) 6.
[31] C. Horvath, H.-J. Lin, J. Chromatogr. A 149 (1978) 43.
[32] M.J. Wirth, J. Chromatogr. A 1148 (2007) 128.
[33] S.-T. Popovici, P.J. Schoenmakers, J. Chromatogr. A 1073 (2005) 87.
[34] S. Heinisch, G. Desmet, D. Clicq, J.L. Rocca, J. Chromatogr. A 1203 (2008) 124.
[35] A. de Villiers, H. Lauer, R. Szucs, S. Goodall, P. Sandra, J. Chromatogr. A 1113 (2006) 84.
[36] F. Gritti, G. Guiochon, J. Chromatogr. A 1138 (2007) 141.
[37] F. Gritti, G. Guiochon, Anal. Chem. 80 (2008) 5009.

Chapter 6

[1] X.Q. Yang, L.J. Ma, P.W. Carr, Journal of Chromatography A 1079 (2005) 213.
[2] D.R. Stoll, X.P. Li, X.O. Wang, P.W. Carr, S.E.G. Porter, S.C. Rutan, Journal of Chromatography A 1168 (2007) 3.
[3] C. Poole, H. Ahmed, W. Kiridena, C. DeKay, W. Koziol, Chromatographia 65 (2007) 127.
[4] T.H. Walter, P. Iraneta, M. Capparella, Journal of chromatography A 1075 (2005) 177.
[5] W. Bicker, M. Lammerhofer, W. Lindner, Analytical and Bioanalytical Chemistry 390 (2008) 263.
[6] H. Luo, L.J. Ma, Y. Zhang, P.W. Carr, Journal of Chromatography A 1182 (2008) 41.
[7] H. Luo, in Chemistry, University of Minnesota, Minneapolis, 2006.
[8] H. Luo, L.J. Ma, C. Paek, P.W. Carr, Journal of Chromatography A 1202 (2008) 8.
[9] R.E. Majors, LC-GC North America 26 (2008) 16.
[10] H. Engelhardt, G. Ahr, Chromatographia 14 (1981) 227.
[11] K.K. Unger, Packings and Stationary Phases in Chromatographic Techniques, M. Dekker, New York, 1989.
[12] W. Naijun, R. Thompson, in Journal of Liquid Chromatography & Related Technologies, Taylor & Francis Ltd, 2006, p. 949.
[13] J.J. DeStefano, T.J. Langlois, J.J. Kirkland, Journal of Chromatographic Science 46 (2008) 254.
[14] J. Nawrocki, C. Dunlap, A. McCormick, P.W. Carr, Journal of chromatography A 1028 (2004) 1.
[15] L.R. Snyder, J.L. Glajch, J.J. Kirkland, Practical HPLC Method Development, Wiley-Interscience, New York, 1996.
[16] D.V. McCalley, Journal of chromatography A 793 (1998) 31.
[17] D.V. McCalley, Analytical Chemistry 75 (2003) 3404.
[18] A. Berthod, J. Chromatogr. 549 (1991) 1.

[19] H.A. Claessens, M.A.v. Straten, J.J. Kirkland, J. Chromatogr. A 728 (1996) 259.
[20] J. Nawrocki, J. Chromatogr. A 779 (1997) 29.
[21] K.K. Unger, N. Becker, P. Roumeliotis, J. Chromatogr. 125 (1976) 115.
[22] Z. Jiang, R.P. Fisk, J. O'Gara, T.H. Walter, K.D. Wyndham, in, US 2002070168, 2002, p. 21.
[23] Z. Jiang, J.E. O'Gara, R.P. Fisk, K.D. Wyndham, D.W. Brousmiche, in, WO 2004041398, 2004, p. 62.
[24] R.P. Fisk, T.H. Walter, Z. Jiang, in, WO 2000045951, 2000, p. 37.
[25] K.D. Wyndham, J.E. O'Gara, T.H. Walter, K.H. Glose, N.L. Lawrence, B.A. Alden, G.S. Izzo, C.J. Hudalla, P.C. Iraneta, Analytical Chemistry 75 (2003) 6781.
[26] A Review of Waters' New Hybrid Particle Technology and its Use in HPLC, Waters, 1999.
[27] Y.-F. Cheng, T.H. Walter, Z. Lu, P. Iraneta, B.A. Alden, C. Gendreau, U.D. Neue, J.M. Grassi, J.L. Carmody, J.E. O'Gara, R.P. Fisk, LC-GC 18 (2000) 1162.
[28] W.G. Tramposch, S.G. Weber, Journal of Chromatography A 544 (1991) 113.
[29] L.W. Yu, T.R. Floyd, R.A. Hartwick, Journal of Chromatographic Science 24 (1986) 177.
[30] L.W. Yu, R.A. Hartwick, Journal of Chromatographic Science 27 (1989) 176.